



HAL
open science

Cerebral plasticity following central and peripheral visual field loss : investigated through morphological and functional MRI

Nicolae Sanda

► **To cite this version:**

Nicolae Sanda. Cerebral plasticity following central and peripheral visual field loss : investigated through morphological and functional MRI. *Neurons and Cognition [q-bio.NC]*. Université Pierre et Marie Curie - Paris VI, 2017. English. NNT : 2017PA066584 . tel-01919424

HAL Id: tel-01919424

<https://theses.hal.science/tel-01919424>

Submitted on 12 Nov 2018

HAL is a multi-disciplinary open access archive for the deposit and dissemination of scientific research documents, whether they are published or not. The documents may come from teaching and research institutions in France or abroad, or from public or private research centers.

L'archive ouverte pluridisciplinaire **HAL**, est destinée au dépôt et à la diffusion de documents scientifiques de niveau recherche, publiés ou non, émanant des établissements d'enseignement et de recherche français ou étrangers, des laboratoires publics ou privés.

Thesis submitted for the degree of Doctor of
Philosophy
Sorbonne Universités - Université Pierre et Marie Curie



Institut de la vision / UMR S968
École doctorale "Cerveau, comportement, cognition"

Specialty: Neurosciences

Cerebral plasticity following central and peripheral visual field loss

- investigated through morphological and functional MRI -

BY : Nicolae SANDA, MD

Directed by : PROFESSOR AVINOAM B. SAFRAN, MD

MEMBERS OF THE JURY:

President : Prof. Bechir JARRAYA, MD, PhD, UVSQ, France

Reviewer : Prof. Dominic FFYTICHE, MD, PhD, KCL, United Kingdom

Reviewer : Prof. Olaf BLANKE, MD, PhD, EPFL, Switzerland

Member : Prof. Valérie BODAGHI, MD, PhD, Salpêtrière/UPMC, France

Member : Prof. Cameron PARSA, MD, UW-Madison, United States of America

Invited member : Prof. Michel THIBAUT DE SCHOTTEN, PhD, ICM, France

Thesis director : Prof. Avinoam B. SAFRAN, MD, Institut de la Vision, France

Publicly presented and defended on : 03 May 2017

Thèse présentée pour obtenir le grade de docteur
Sorbonne Universités - Université Pierre et Marie Curie



Institut de la vision / UMR S968
École doctorale "Cerveau, comportement, cognition"

Discipline : Neurosciences

Plasticité cérébrale induite par la perte du champ visuel central ou périphérique

- *approche par IRM morphologique et fonctionnelle* -

PAR : Nicolae SANDA

Sous la direction de AVINOAM B. SAFRAN, Prof. des Universités

MEMBRES DU JURY:

President : Bechir JARRAYA, Prof. des Universités, UVSQ, France

Rapporteur : Dominic FFYTICHE, Prof. des Universités, KCL, Royaume-Uni

Rapporteur : Olaf, BLANKE, Prof. des Universités, UPFL, Suisse

Membre : Valérie, BODAGHI, Prof. des Universités, Salpêtrière/UPMC, France

Membre : Cameron PARSA, Prof. des Universités, UW-Madison, Etats-Unis

Membre invité : Michel THIBAUT DE SCHOTTEN, Prof. des Universités, ICM,
France

Directeur de thèse : Avinoam B. SAFRAN, Prof. des Universités, Institut de la
Vision, France

Date de soutenance : 03 mai 2017

Remerciements

Je souhaiterais tout d'abord remercier le **Pr Avinoam SAFRAN**, à qui je ne dois non seulement son soutien crucial dans la réalisation de cette thèse mais également de m'avoir ouvert les portes de la neuro-ophtalmologie, de m'avoir transmis ce savoir clinique, qu'on ne trouve pas dans les livres, mais que l'on reçoit seulement d'un maître tel que lui. Je le remercie également pour l'enthousiasme avec lequel il m'a incité à observer et explorer les facettes méconnues de la vision.

Je voudrais également remercier le **Pr Michel THIEBAUT de SCHOTTEN** pour son aide essentielle dans la réalisation de cette thèse de même que pour avoir partagé sa grande érudition et sa perspective unique sur le fonctionnement et la structure du cerveau.

J'aimerais remercier le **Pr José-Alain SAHEL**, tout d'abord pour avoir créé l'Institut de la Vision et réuni sous un seul toit tant d'esprits exceptionnels, et ensuite pour la confiance qu'il m'a accordée au cours de la réalisation de cette thèse.

Je remercie aussi le **Dr Leonardo CERLIANI**, qui m'a été d'une aide précieuse dans le cadre de l'un des travaux présentés dans cette thèse.

Je voudrais aussi remercier le **Dr Christophe HABAS** et le *Service de neuroimagerie du Centre Hospitalier National d'Ophtalmologie des Quinze-Vingts*, le **Dr Saddek MOHAND-SAÏD** et le *Centre d'Investigation clinique* (en particulier **Dr Céline DEVISME**), qui ont été d'une aide précieuse dans la conduite des études en IRM et la difficile sélection des patients selon les critères stricts des exigences que nous avons énoncées.

J'aimerais aussi remercier le **Dr Colas AUTHIE**, pour les innombrables fois où il nous a aidé et sans lequel les travaux présentés dans cette thèse n'auraient pas été possibles.

Je voudrais également remercier le **Dr Norman SABBAH**, avec lequel nous avons eu de multiples et fructueuses collaborations, dont une fut essentielle pour l'une des études présentées dans cette thèse.

Je remercie aussi le **Pr Amir AMEDI** et le **Dr Sami ABOUD** pour leur contribution dans la mise en place de certains protocoles utilisés dans l'un des travaux présentés dans cette thèse.

J'aimerais également remercier l'ancienne équipe *Descartes*, pour son aide et ses encouragements tout au long de mon activité à l'Institut de la Vision.

Par ailleurs, je remercie chaleureusement le **Pr B. JARRAYA**, le **Pr D. FFYTICHE**, le **Pr O. BLANKE**, le **Pr V. BODAGHI**, le **Pr C. PARSÀ**, le **Pr M. THIBAUT DE SCHOTTEN**, et le **Dr C. HABAS** qui m'ont fait l'honneur d'accepter de faire

partie du jury de cette thèse.

Enfin, je remercie le **Pr Elena SANDA** et le **Dr Nicolae SANDA**, mes parents à qui je dois tout.

Abstract

Cerebral plasticity induced by visual loss represents a poorly understood field of neuroscience, with numerous questions that don't yet have an answer. Central and peripheral vision, the evolutionary compromise between spatial resolution and the sampled space volume, are processed in distinct areas of the brain. Understanding the impact of vision loss in these regions, is of utmost interest for the study of visual brain. Herein, in two models of retinal disorders affecting central and peripheral vision (namely *Stargardt macular dystrophy* and *retinitis pigmentosa*), we specifically investigated the effects of the central and peripheral visual loss on brain morphology and its functional connectivity.

1. Morphological plastic changes induced by central and peripheral visual loss

We explored the effects of visual loss on cortical thickness (CoTks) and cortical entropy (CoEn, marker of synaptic complexity) in the cytoarchitectonic regions of the occipital lobe. Central visual loss associated thinning in dorsal stream regions, while peripheral visual loss in early visual cortex (EVC) and regions belonging both to dorsal and ventral stream. These effects were unpredicted by the canonical view “*central vision – ventral stream*”, “*peripheral vision – dorsal stream*”. Normal CoEn in these areas suggests that synaptic complexity is preserved in the remaining networks. Only central visual field loss presented CoEn alterations, namely an increase in areas involved in object recognition, that likely reflects a synaptic complexity enhancement in response to the loss of the high spatial resolution of central vision. The gain in synaptic complexity could mask neuronal loss due to deafferentation and may account for the CoTks normality.

2. Plastic changes in the functional connectivity of central and peripheral EVC

We explored and compared to normally afferented EVC, the functional connectivity of afferented and deafferented parts of EVC and found that central and peripheral visual loss induce different patterns of reorganization. Residually afferented early visual cortex reinforce local connections presumably to enhance the processing of altered visual input, while deafferented EVC strengthen long-range connections presumably to assist high-order functions.

Combined structural and functional data indicate that areas with reduced CoTks superpose with several areas presenting reduced functional connectivity with the peripheral

EVC and that areas with increased CoEn superpose with several areas presenting increased functional connectivity with afferented peripheral EVC. These data point that alterations of the sensory input to the peripheral field are more prone to induce plastic changes.

Overview

Data in the current work provide an interesting perspective about the plasticity following central or peripheral visual field loss and show that it is more complex than the canonical model would have let to presume. These observations pave the way for further studies that could explain the exact functional role of the plastic changes and help revisiting the current, insufficient model of visual information processing.

[Résumé]

Les processus de plasticité cérébrale entraînés par la perte visuelle restent un domaine méconnu dans le champ des neurosciences. La vision centrale et périphérique, le meilleur compromis évolutionniste entre une bonne résolution spatiale et un volume d'espace échantillonné maximal, sont traitées par des régions différentes du cerveau. Par conséquent, étudier et comprendre l'impact de la perte visuelle centrale ou périphérique dans ces régions constitue une étape cruciale dans l'étude du *cerveau visuel*. Afin d'étudier ces processus, nous avons utilisé deux modèles de perte visuelle sélective de la vision centrale (*la dystrophie maculaire de Stargardt*) et périphérique (*la rétinopathie pigmentaire*), et nous avons évalué l'impact à terme de ces deux types de désafférentation sur la structure et la connectivité fonctionnelle du cerveau.

1. Plasticité structurelle induite par la perte sélective de la vision centrale ou périphérique

Nous avons étudié l'épaisseur corticale (EpCo) et de l'entropie corticale (EnCo, marqueur de complexité synaptique) du lobe occipital, région pour laquelle nous disposons d'une cartographie complète des régions cytoarchitectoniques. Nous avons constaté que la perte de la vision centrale induit un amincissement des régions appartenant au flux dorsal, tandis que la perte de la vision périphérique occasionne un amincissement du cortex visuel primaire (CVP), ainsi que des régions du flux ventral et dorsal. Ces effets étaient inattendus si on se rapporte au modèle canonique qui associe la vision centrale au flux ventral et la vision périphérique au flux dorsal. La normalité de l'EnCo dans ces régions, suggère que la complexité synaptique est préservée dans les réseaux neuronaux résiduels. Nous avons identifié des modifications de l'EnCo seulement en cas de perte de la vision centrale, où l'augmentation de l'EnCo dans des régions impliquées dans la reconnaissance des objets pourrait traduire une réponse adaptative à la perte de la haute résolution spatiale de cette partie du champ visuel. Cette augmentation de la complexité synaptique pourrait compenser une éventuelle perte neuronale et être responsable de la normalité de l'EpCo dans ces régions.

2. Plasticité de la connectivité fonctionnelle des régions du cortex visuel primaire recevant les projections de la partie *centrale* » et *périphérique* champ visuel

Dans cette étude, nous avons exploré et comparé la connectivité fonctionnelle des régions afférentées et desafférentées du CVP de sujets msouffrant de *dystrophie maculaire de Stargardt* et *retinitis pigmentosa*, avec les régions afférentées correspondantes du CVP de sujets avec une vision normale. Cette étude a révélé une réorganisation fonctionnelle distincte du CVP afférenté et désafférenté. Ainsi, le CVP qui reçoit les afférences visuelles résiduelles présente une connectivité fonctionnelle accrue avec des régions voisines, probablement afin de favoriser le traitement de l'information visuelle, tandis que le CVP désafférenté augmente sa connectivité fonctionnelle avec des régions plus éloignées, vraisemblablement pour contribuer aux fonctions supérieures et à des processus de type *top-down*.

L'analyse comparative des données morphologiques et fonctionnelles suggère une correspondance des régions amincies du cortex visuel associatif avec des régions qui montrent une diminution de la connectivité fonctionnelle avec le CVP périphérique, et des régions présentant une augmentation de la complexité synaptique avec des régions qui montrent une connectivité fonctionnelle accrue avec le CVP périphérique. Ces données suggèrent que la désafférentation sensorielle du CVP périphérique est plus propice au développement d'une réorganisation cérébrale.

Synoptique

Ces travaux révèlent un aspect inattendu de la plasticité cérébrale induite une perte isolée de la vision centrale ou périphérique. La réorganisation s'avère plus complexe que le laisser présager le modèle canonique actuel, vraisemblablement trop simple. Ils ouvrent la voie à de nouvelles études permettant de clarifier la fonction spécifique des changements plastiques observés et contribuer à réactualiser le modèle canonique du traitement de l'information visuelle.

Contents

Abstract	7
[Résumé]	9
I General Information	1
1 A brief history of vision	3
1.1 The beginning	3
1.2 The evolution	5
1.2.1 Photoreceptors	5
1.2.2 Eyes	13
1.2.3 Brains	18
2 Visual processing	25
2.1 Retinal processing	25
2.1.1 General organization and photoreceptor distribution	25
2.1.2 Cones neural circuitry.	28
2.1.3 Rod neural circuitry	33
2.2 Cerebral visual processing	36
2.2.1 General view on the central nervous system organization	36
2.2.2 Lemnothalamic pathway	39
2.2.3 Collothalamic pathway	44
2.2.4 Associative visual cortex	46
2.2.5 Brain's non-perceptual light processing	50
2.2.6 Action and the evolution of visual processing	51
3 Visual loss	55
3.1 Models of visual loss	55
3.1.1 Central visual field loss – Stargardt macular dystrophy	55
3.1.2 Peripheral visual field loss – pigmentary retinopathy (retinitis pigmentosa)	56
3.2 Plasticity induced by visual loss	58
3.2.1 Retinal plasticity following photoreceptor loss	58
3.2.2 Cerebral plasticity following visual loss	60

3.2.3	Cerebral plasticity and MRI	61
3.2.4	Cerebral plasticity in early blindness	63
3.2.5	Cerebral plasticity in late blindness	67
3.2.6	Plasticity in partial visual loss	70
3.2.7	Visual input and peculiar perceptive phenomena	71
II	Experimental contributions	73
1	Morphological changes: “ <i>Visual brain plasticity induced by central and peripheral visual field loss</i> ”	75
2	Functional changes: “ <i>Reorganization of early visual cortex functional connectivity following selective peripheral and central visual loss</i> ”*	97
III	General discussion	131
1	Synthesis of the principal results	133
2	Insight on visual brain plasticity from combined structural and functional data	137
3	Limitations	141
3.1	Study design	141
3.2	MRI protocol	141
3.3	Visual loss models	143
IV	Conclusion and perspectives	145
V	References	149
VI	Annexes	179
	Annexe I: “ <i>Increased optic nerve radiosensitivity following optic neuritis</i> ”	181
	Annexe II: “ <i>A neurological disorder presumably underlies painter Francis Bacon distorted world depiction</i> ”	185

Annexe III: <i>"Importance of eye position on spatial localization in blind subjects wearing an Argus II retinal prosthesis"</i>	189
Annexe IV: <i>"Color synesthesia. Insight into perception, emotion and consciousness"</i>	199
Annexe V: <i>"Impact of thrombolysis in acute stroke without occlusion: an observational comparative study"</i>	209
Annexe VI: <i>"Increased functional connectivity between language and visually deprived areas in late and partial blindness"</i>	217

PART I

General Information

A brief history of vision

Vision is the long distance sense that allowed *homo sapiens*, a physically delicate ape, to explore the universe. It provided him with the means to survey directly and later through more and more complex devices of his own design - the space - further away up to distant stars and galaxies; and the time - further back - down to the oldest light imprinted on the sky when our Universe was only 380 000 years old.

But how did the story of vision begin?

1.1 The beginning

Before searching for the beginning, one must first define vision as the answer is intimately related to definition. Does vision equals photoreception? If that would be the case, synthesizing photoreception (photosynthesis) would qualify as a form of vision, which is obviously not the case. As a sense, vision is indissolubly linked to information and therefore vision defines as a system that recognizes and extracts information from light.

The first witness of light among the living things on Earths is yet borrowed in the mist of time. Little we know about the first eon of our planet – *the hadean* (4600 - 3750 million years ago), but we believe that it was the chemical laboratory that allowed the emergence of prebiotic compounds (amino acids, reactive molecules, and finally the ribonucleic acid) and maybe even life (Schwab 2012). The next eon – *the archean* (3750 - 2500 million year ago) - was likely the one when photoreception appeared for the first time. It was an age of unicellular life forms - archea and bacteria (Schwab 2012). Some of these organisms evolved in photic marine environment and developed the first light receptors – chlorophylls (chlorine-derived pigment), rhodopsins (vitamin A-derived opsins) and photolyases (riboflavin derived enzymes, Willstutter 1906; Lucas-Lledó and Lynch 2009; Schwab 2012). In these organisms, chlorophylls act as photosynthetic machines converting carbon dioxide in organic compounds, rhodopsins, light-driven proton pumps produce energy and photolyases, light-activated enzymes, repair DNA damaged by the exposure to ultraviolet light. These functions cannot be qualified as vision, but bacterial and archeal rhodopsins and photolyases are ancestors of rhodopsin and chromophores, used for vision by metazoans (multicellular eukaryote organisms). However, before metazoan radiation, the protists, unicellular eukaryotes, which likely emerged in proterozoic (2500 - 543 million years ago), achieved a certain degree of visual information integration.

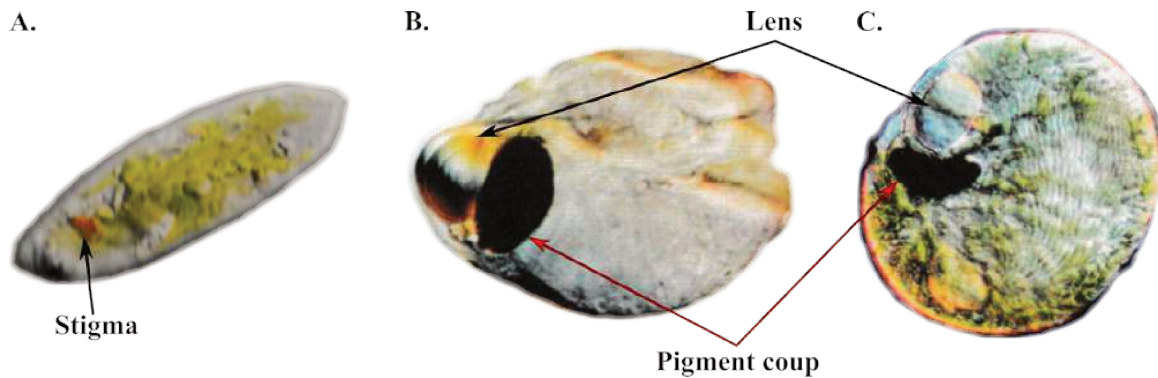


Figure 1 – Visual pigments in unicellular eukaryotes. A. *Euglena gracillis*. Note the “eyespot” or stigma that contains a rhodopsin and flavins for photoreception. **B.** *Erithropsidium* and **C.** *Warnowia* - two dinoflagellates, unicellular eukaryotes, that exhibit complicated camera-style eyespots composed of a lens and a pigment cup (modified from Schwab, 2012)

In these organisms, rhodopsine and flavine-based photopigments are closely related to the function of flagellum and allow them to travel toward or away from light (positive or negative phototaxy). The association between flagellum and photopigment in species like *euglena gracillis* suggests an analogy with a supposed extinct protist that deposited rhodopsin in a cilium and used the light to power it up. This protist might have been the ancestor of photoreceptors (Schwab 2012).

Most intriguing, some flagellated protists - dinoflagellates like *Erytropsidium* or *Warnowia* - actually have a complicated type of light receptors, which resembles to a camera-style eye, called ocelloid. This “eye” is composed of a lens and a cup filled with a folded membrane, which is studded with visual pigment (Schwab 2012, see Figure 1).

Overview

The unicellular organisms – archaea, bacteria and protists developed the biochemical background for vision and even a sketch of an eye.

1.2 The evolution

1.2.1 Photoreceptors

The emergence of photoreceptor cells in metazoans

With the rise of metazoans, which radiated in the *neoproterozoic* (1000 – 543 million years ago), the true story of vision began. It is in this eon and those that followed that eye and nervous system developed and further perfected to optimize the capture and integration of visual information.

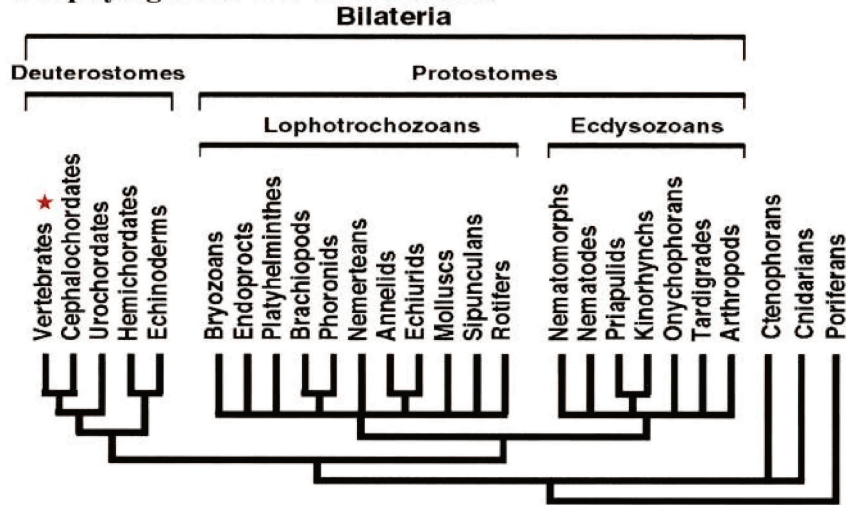
Metazoans developed an impressing array of eye designs, but certain pieces are common to all of them (see Figure 5). Each eye includes a photoreceptor cell structure, a lens and is connected to a neural network. To increase its capacity to gather light and to sample spatial characteristics, eye had two possible ways to develop: invagination (e.g. a pit) or evagination (e.g. a bulge). Invagination leads to a camera-style eye like our own eyes (also common to all vertebrates and certain invertebrates like cephalopods), while evagination constitutes the basic design of compound eye (common in invertebrates) and founds its most exquisite exponents in arthropods (insects, crustaceans; Schwab 2012; see Figure 5).

Lenses, made of various compounds (i.e. minerals, carbohydrates, proteins), are present in both designs and their role is to focus the image on the photoreceptor layer.

Another common structure for all eyes is the retina, the layer containing the photoreceptors. Beside photoreceptors, it also includes pigmentary cells and other neural cells. The pigmentary cells limit the direction of the incoming light and allow the spatial organization of information. They may also have metabolic or protection roles in regard to photoreceptors (Schwab 2012). The various neural cells in the retina allow a certain degree of local information processing. Converging axons of these neural cells form the optic nerve that transfer the visual information to higher processing centers (i.e. the brain).

Metazoans developed two major classes of photoreceptive cells – ciliary and rhabdomeric. Ciliary cells have a single long projection with many folds and stacked appearance called cilium, while rhabdomeric cells have multiple short projections called microvilli. Both photoreceptor types developed from an epidermal ciliated cell ancestor containing photopigment molecules embedded in the membrane and evolved to increase the membrane surface and to stock a maximal quantity of photopigment (Arendt and Wittbrodt 2001). Rhabdomeric and ciliary photoreceptors diverged from a common ancestor, likely before the split between protostomes (most of the invertebrates) and deuterostomes (tunicates and vertebrates). The differences between these photoreceptors are not limited to morphology but extend to opsins and their phototransduction pathway (see Figure 2) (Arendt 2003).

I. A phylogenetic tree of metazoans



II. Rhabdomeric and ciliary photoreceptor sister cell types

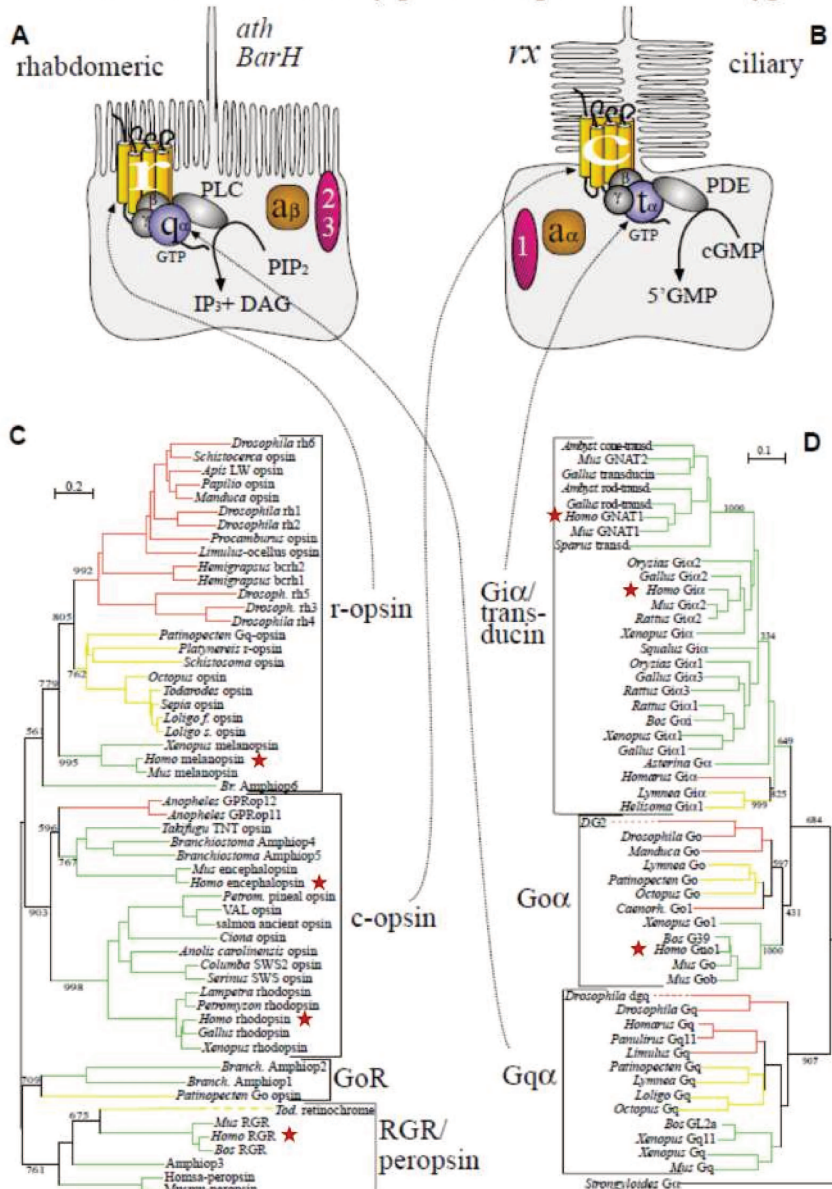


Figure 2 – The evolution of rhabdomeric and ciliary photoreceptor sister cells. **I.** A phylogenetic tree of metazoans. **II.** Rhabdomeric and ciliary photoreceptor cells with schematics of rhabdomeric (**A**) and ciliary (**B**) photoreceptors and their main phototransductions cascades. **C** and **D** – paralogy of the effector genes of rhabdomeric and ciliary photoreceptors. **C** – tree calculated on opsin protein sequences. **D** – tree calculated on G- DNA sequences. cGMP – cyclic guanosylmonophosphate; DAG – diacylglycerol; GTP – Guanosytriphosphate; IP3 – inositol-1, 3, 5 triphosphate; PDE – phosphodiesterase; PIP2 – phosphatidylinositol-4,5-biphosphate; PLC – phospholipase C. The tree brackets enclose orthologous genes that can be traced back to the same precursor gene in Urbilateria. On the phylogenetic tree colors code with green Deuterostomia, with yellow Lophotrochozoa and with red Ecdysozoa. The red star marks the human genes (modified from Balavoine and Adoutte 2003, and Arendt 2003)

Opsins are membrane proteins that combined to photopigments (retinal-derived) form all known light sensors in Neurelia (Cnidaria, Ctenophora and Bilateria; Feuda *et al.* 2012). The role of opsins and their photopigment is to absorb light in the visible spectrum and to trigger signal transduction through G-protein activation. Noteworthy, the chromophore retinal has maximum absorption in the ultraviolet spectrum but the opsins shift the absorption peak in the visible region (Terakita 2005). There are seven opsin subfamilies, of which not all are visual. The rhabdomeric cells, the photoreceptors of most invertebrates, have a rhabdomeric opsins (r-opsin), while ciliary cells the photoreceptors of vertebrates (and tunicates), ciliary opsins (c-opsin). Phototransduction for c-opsins employ transducin-cGMP cascade and its activation results in hyperpolarization whereas r-opsins employ Gq- α -phospholipase C cascade and its activation results in depolarization. Most interestingly, if vertebrates' photoreceptors are ciliary and evolved from a ciliate precursor, retinal neurons like the amacrine cells, horizontal cells and ganglion cells evolved from a rhabdomeric photoreceptor (see Figure 3, Arendt 2003; Graham *et al.* 2008; Nilsson and Arendt 2008). Moreover, various retinal ganglion cells express melatonin, a vertebrate ortholog of invertebrate r-opsins and are involved in pupillary light response and circadian rhythm (Hattar 2002).

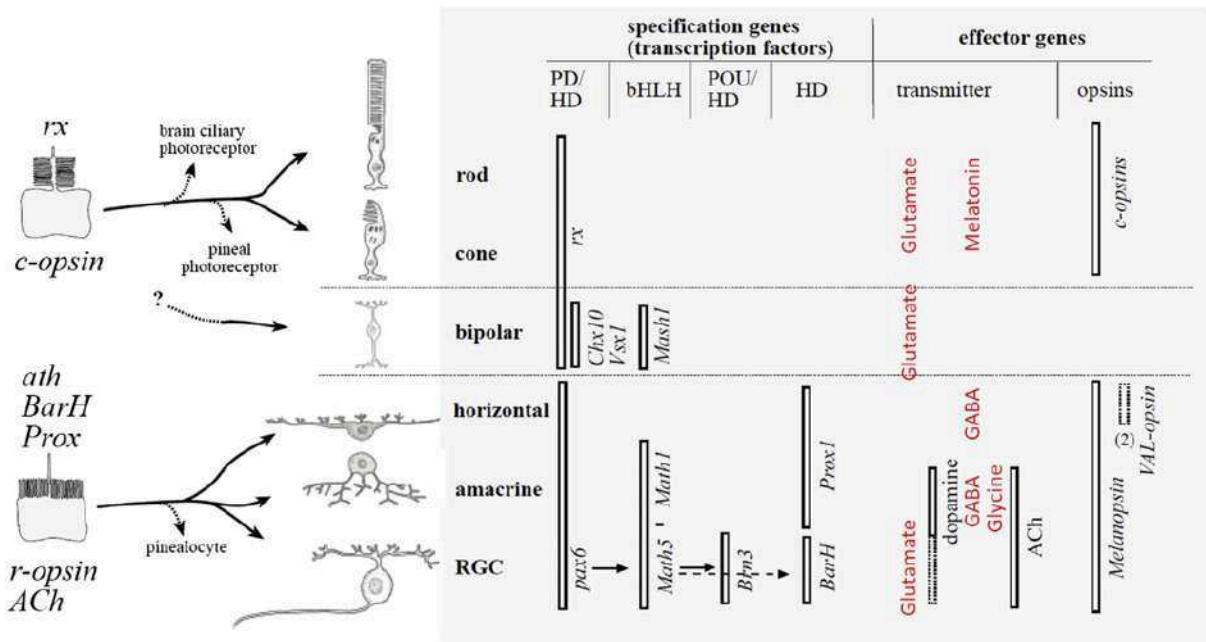


Figure 3 – The evolutionary origin of retinal neuronal cells in human retina. Data from molecular comparative cell biology points that photoreceptors (rods and cones) evolved from a common ciliary photoreceptor precursor while horizontal, amacrine and ganglion cells evolved from a common rhabdomeric photoreceptor precursor. The origin of bipolar cells is uncertain, but it might also be derived from a ciliary precursor (modified from Arendt 2003; Lamb 2013).

Overview

Metazoans developed two different types of photoreceptor cells derived from a presumed ciliated ancestor – *rhabdomeric* and *ciliary*. Ciliary photoreceptors became the visual photoreceptors in vertebrate lineage and possibly bipolar cells, while rhabdomeric photoreceptors evolved in amacrine, horizontal and ganglion cells. Some of the cells derived from rhabdomeric photoreceptors (i.e. melatonin containing ganglion cells) preserve intrinsic photosensitivity and their main role is probably non-visual. These aspects are essential in optogenetics and related attempts to restore vision in degenerative disorders affecting the photoreceptors.

Evolution of photoreceptors in vertebrates

Vertebrate photoreceptors (ciliate cells) are the cones and the rods. Cones were the first to appear in vertebrate ancestors, probably > 540 million years ago (Davies *et al.* 2012) and duplex retina containing both cones and rods likely developed for the first time in jawless vertebrates (agnatostoma, Yokoyama and Yokoyama 1996; Yokoyama 1997; Lamb 2013). Cones developed for vision in photopic conditions while rods evolved to ensure vision in low luminance (mesopic and scotopic conditions). The capacity to provide a rapid response, light sensitivity over a very broad range of intensities, which also prevents saturation in steady light, and the ability to recover almost instantaneously a substantial degree of responsiveness following the vanishing of an intense light stimulus, represent the critical traits of cones (Lamb 2013). The main feature distinguishing rods from a cones is rods ability to respond reliably to the absorption of individual photons, with a good signal-to-noise ratio and under dark-adapted conditions (Hecht 1942; Baylor *et al.* 1979; Lamb 2013).

Cone opsins evolved from genetic duplication of the ancestral cone opsin. The first duplication created a pair of retinal cone opsins – SWS (short wavelength sensitive) and LWS (long wavelength sensitive, Okano *et al.* 1992). Through further duplication of SWS gene, new opsins with pick sensitivities to different wavelengths appeared in jawed fish – SWS1, SWS2 (SWS-1 like), RH1 (rhode 1) and RG2 (Rh-1 like, middle wavelength sensitive; for details see Figure 4; Pisani *et al.* 2006; Lamb 2013; Kim *et al.* 2016). It is believed that rods evolved from a RH-1 cone through gradual changes. Almost their entire outer segment became sealed over, allowing for extensive longitudinal spread and shut-off reactions sufficiently slow that the response to a single photoisomeration exceeds the intracellular noise (Lamb 2013). Therefore, the rods became steadily slower but more sensitive and fit for scotopic vision (Lamb 2013). Noteworthy, cones remain major photoreceptor population in most vertebrates, excepting mammals and some nocturnal, non-mammal species (Davies *et al.* 2012).

Later in vertebrate evolution, the five initial opsines were preserved, multiplied (i.e. zebrafish), lost (i.e. mammals), or reinvented (i.e. primates) (see Figure 4; Davies *et al.* 2012). Mammals, whom extant representatives are divided into three branches – monotremes (*Protheria*), marsupials (*Metatheria*) and placentals (*Eutheria*) - radiated from the therapsid lineage of synapsids (reptile-like amniotes) between 267 and 310 million years ago with the first fossils records dating from 255 million years ago (Lucas and Luo 1993; Kemp 2006). Rods dominate mammals' retinae, nocturnal species exhibiting

only 3 % cones and diurnal species 5-30 % (Peichl 2005), with some rare exceptions where cones are preponderant (> 50 %, Müller and Peichl 1989; Kryger *et al.* 1998). Marsupials and placentals lost SWS2 and medium wavelength RH2 and preserved only SWS1, LWS and RH1 (rod opsin) opsins genes. This loss is explained by the “*twilight (mesopic) bottleneck hypothesis*” that states that adaptation to mesopic and scotopic lifestyle determined the loss of the redundant SWS2 and RH2 opsines (Davies *et al.* 2012). Consequently, the majority of mammals are dichromatic in bright light and might exhibit conditioned trichromacy in dim-light (mesopic condition) when both cones and rods are activated (Davies *et al.* 2012). Primates however, constitute a particular case that “*recovered*” trichromatic vision in bright light through duplication of the X-linked LWS gene, the copies of the gene coding pigments with peak spectral sensitivity around 560 nm (L) and 535 nm (M), respectively. This “*reinvention*” also puts closer L and M cones in terms of downstream circuitry (Lee and Grünert 2007).

In mammalian retina, S cones are considered the default fate of postmitotic generic photoreceptor precursors (i.e. without other influence will become a S cones, Swaroop *et al.* 2010; Hunt and Peichl 2014). Exposure to various factors (i.e. TR β 2 or NRL/NR2E3) will induce differentiation into L and M cones or into rods (Lamb *et al.* 2007; Swaroop *et al.* 2010). Moreover, the intense recruitment of S cones into the rod pathway during the embryological development may explain the rod-dominant retinas of the overwhelming majority of mammals (Kim *et al.* 2016). Persistence of rod-dominant retinas in most of the extant mammal species is attributed to their complex interactions with cones, which is not limited to the rod-cone coupling that mediates mesopic vision (i.e. rod-cone gap junctions, DeVries and Baylor 1995; Soucy *et al.* 1998; Pang *et al.* 2012; Asteriti *et al.* 2014) but also concerns the circadian photoentrainment (Altimus *et al.* 2010), horizontal cell mediated surround inhibition of cone signal (Szikra *et al.* 2014) and the trophic support of cones (Aït-Ali *et al.* 2015).

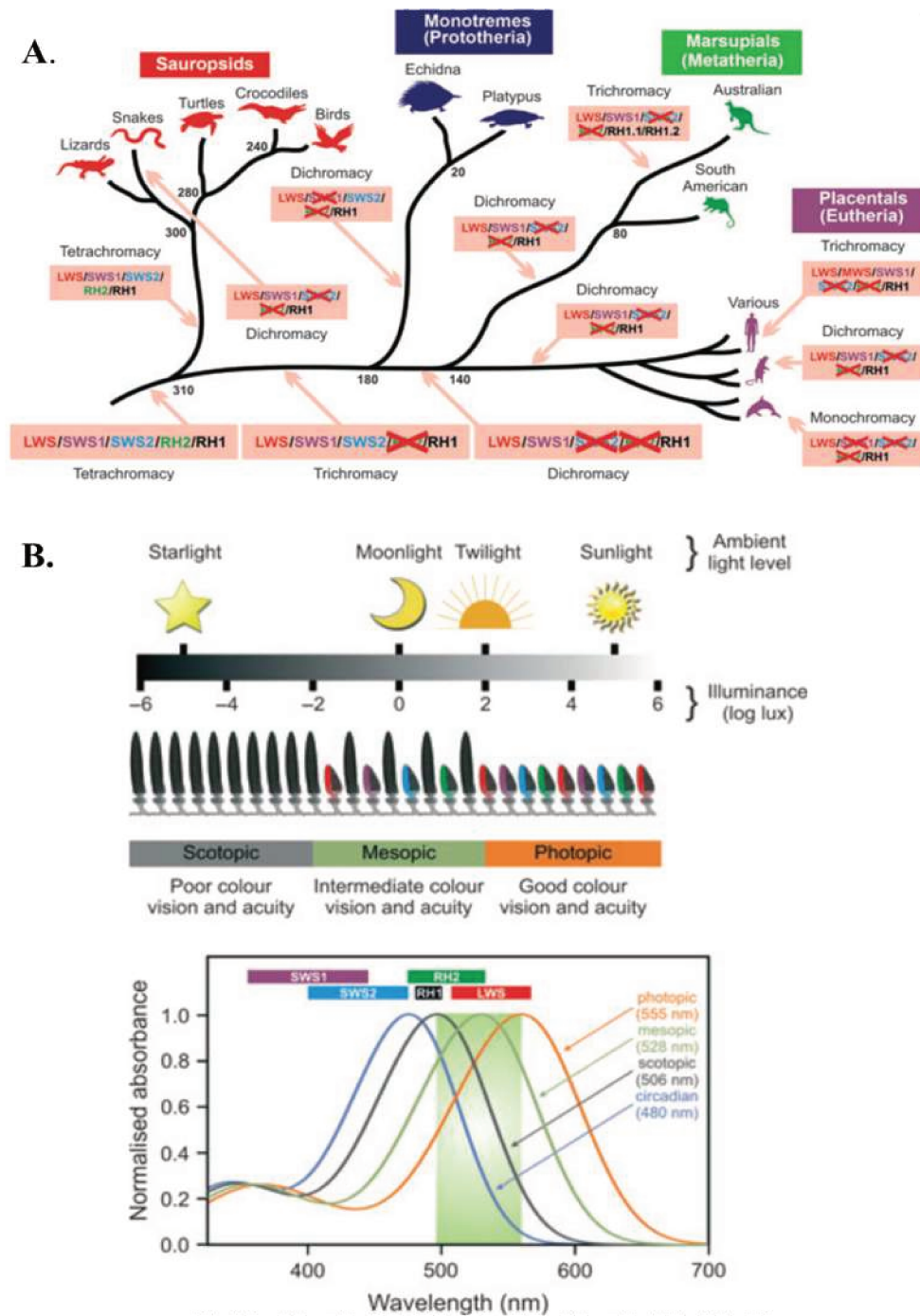


Figure 4 – The evolutionary fate of opsins in vertebrates. **A.** The five primordial opsines of the common ancestor in the extant branches of vertebrates. **B.** Illustration of the presumed mesopic trichromacy when both cones and rods are activated and when rods might feed colour information. The lower diagram depicts the spectral sensitivity of photopic, mesopic scotopic and circadian photoreception in humans compared with the range of maximal wavelength sensitivity for SWS1 (violet), SWS2 (blue), RH1 (black), RH2 (green), LWS (red) photopigments. The maximal wavelength sensitivity in mesopic conditions is estimated at 528 nm but the actual pick would lie within the green shading, between scotopic and photopic photoreception (480 – 506 nm, from Davies *et al.* 2012).

Overview

Early after their radiation, vertebrates developed cones photoreceptors and at least five types of opsins. The default mode differentiation of photoreceptor precursors in embryological development is the S cone; different factors induce their differentiation in L cone, M cone and rods. Mammals have preserved only SWS and LWS cone opsins and therefore are dichromatic. Primates “*reinvented*” photopic trichromacy by evolving a medium wavelength sensitivity opsin (MWS) through LWS gene duplication. Rods appeared later than cones in vertebrate lineage, as adaptation to scotopic and mesopic conditions and they rarely constitute the dominant photoreceptor class in vertebrate retina. At least in mammals, where they are the dominant, rods also assure other complex visual and non-visual functions.

1.2.2 Eyes

Emergence of the metazoan eyes and retinas - inverted and everted retinas

Metazoan retina evolved in two different models of photoreceptor disposition – towards the light or everted (the composed eye of insects, camera style eye of the cephalopodes) or away from the incident light or inverted (all vertebrates). If the everted type seems the most ergonomical because there is no cell interposed between the light and photoreceptor, the inverted retina has its own unique advantages. In camera-style eye, it allows a maximal density of photoreceptors (photoreceptors and pigmentary cells are not in the same layer) and provides the necessary space for the retinal neurons, which assures a local, low-order visual information processing (Kröger and Biehlmaier 2009). The contact between photoreceptors outer segments with pigmentary epithelium permits the later to assist the regeneration of isomerised visual pigment and to regulate the light flux to the photoreceptors (Lamb *et al.* 2007).

The “*capital sin*” of inverted retina - the interposition of intermediary cells between incident light and photoreceptors resulting in light scattering - is reduced through local modification of the retinal architecture over a limited area, called fovea in the most developed vertebrate eyes. This structure exhibits a pit-like configuration and an increased number of photoreceptors that are exposed directly to the incoming light due to the lateral displacement of inner retina cells (see Figure 4 - D, F). Moreover, the deep fovea of certain species (fishes, reptile birds) – called *convexiclivate fovea* - behaves as a third refractive element and provides a telescope-like magnification of the image (Kröger and Biehlmaier 2009; Schwab 2012). Significant telescope-like magnification is likely to be absent in humans but the concave form of the fovea behaves like a mirror and focalizes light into the vitreous; the presence of this reflected spot of light is used as a sign of retinal integrity (Safran *et al.* 1984).

For light scattering in the rest of the retina, Franze *et al.* proposed that Müller cells (radial retinal glial cells that span the entire retinal thickness) might act as optic fibers, transporting light with minimal distortion and loss through the entire retina down to photoreceptors (Franze *et al.* 2007).

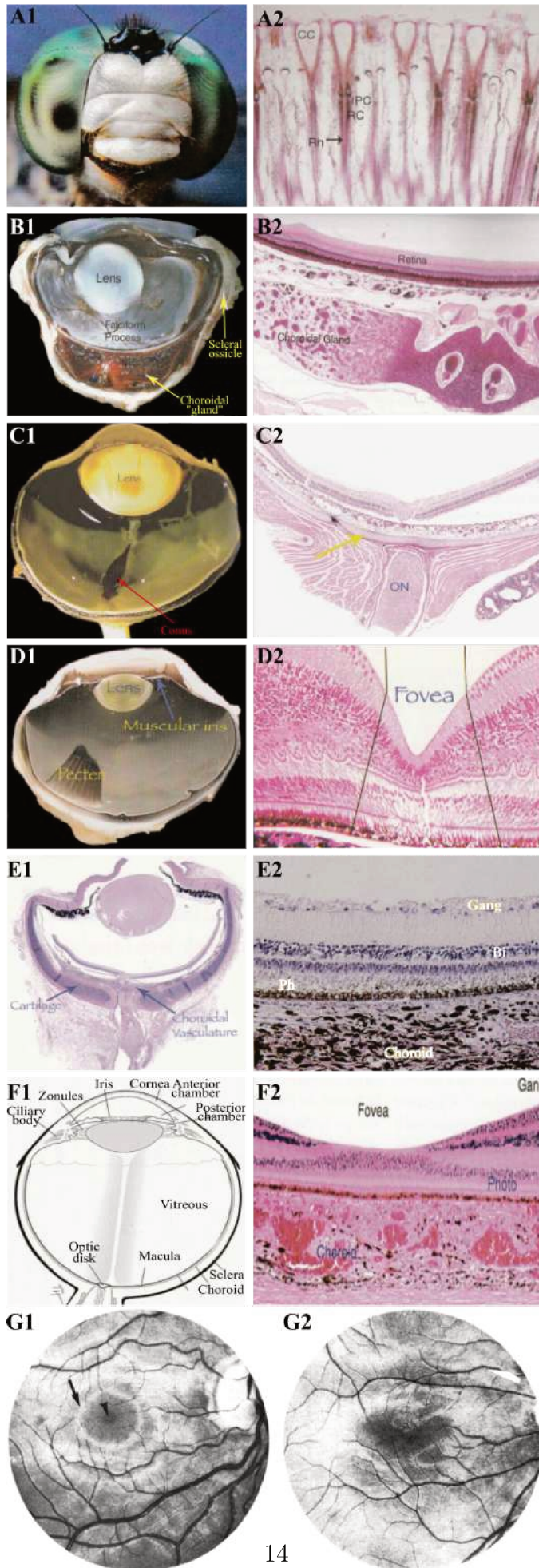


Figure 5 – Various eyes designs. **A. The compound eye of the dragonfly.** 1. *Macroscopic view* – note the smaller and more densely packed ommatidia (“little eyes”) placed frontally and offering a better spatial acuity. 2 *Microscopic view* – the corneal lens has been lost. Note the crystalline cone (CC) that focuses the light, the iris pigment (IPC) that prevent light from spilling across adjacent cells, the rhabdomeric photoreceptor cells (RC) and the rhabdom (Rh), formed by the microvilli of several adjacent receptor cells and acting like a fiber optic cable. **B. Bony fish eye.** 1. *Macroscopic view* – note the spheric lens, the falciform process providing nutrition to the inner retina, the choroidal gland providing nutrition to the outer retina and the scleral ossicles that evolved to strengthen the eye wall. 2. *Microscopic view* - note the thin retina and the choroid gland. **C. Reptilian eye.** 1. *Macroscopic view* – note the different shape of the lens and the conus (red arrow) a structure derived from the hyaloid artery that is responsible for the nutrition of the inner retina. 2. *Microscopic view* – note the cartilaginous cup (yellow arrow), the thicker retina and the optic nerve (ON). **D. Avian eye.** 1. *Macroscopic view* – note the flattened shape and the pecten a vascular structure similar to the reptilian conus and responsible for eye’s thermoregulation and the nutrition of the inner retina. 2. *Microscopic view* – note the thick steep fovea that allow for a supplementary “telescopic” magnification of the image. **E. Monotreme eye.** 1. *Macroscopic view* – note the presence of a cartilaginous cup in the sclera (like in the reptilian eye) and the thick choroid. The eye is spherical; the current flattened image is a preparation artifact. 2 *Microscopic view* – note the thick choroid; Ph – photoreceptors, Gang – ganglion cells. Interestingly, cones in monotremes are both simple and double with some double cones presenting, as in reptiles, eye droplets that contribute in discrimination and spatial tuning (not shown). **F. Human eye.** 1. *Macro schematics of the human eye.* 2. *Microscopic view of the fovea* – the depression and the lateral displacement of the neural cells allows a direct exposure of photoreceptors and the avoidance of light scattering. **G. Human eye fundus and macular reflexes.** 1. The exterior annular reflex demarcates the ridge of the pit; the central reflex - a reflected telescope-like image of the incident light, due to the concave shape of the fovea. 2. Loss of ganglion cells axons in optic nerve atrophy flattens the ridge of the macula inducing the disappearance of the central reflex and the distortion of the annular reflex. (modified from Safran *et al.* 1984; Schwab 2012)

Retinal vascularization in vertebrates

Development of more and more complex eyes and thicker retinas implied increased metabolic demand. To supply photoreceptors and inner neural structures, the eye of higher vertebrates relies on two blood sources - the choroid and intraocular vascular structures. Choroid is mainly responsible for the nutrition of outer retina (pigmentary epithelium and photoreceptors) and its rudimental ancestor (simple vascular sinuses containing lakes of blood but not capillaries networks like in higher vertebrates) is already present in lower vertebrates (lampreys; Schwab 2012). However, the extension of retinal neuronal configuration and the consequent thickening of the retina required new solutions for its nutrition. Two main sources of blood supply were available for the inner retina: choroid vessels and hyaloid artery (an artery that irrigate the crystalline and vitreous body during embryological development). Lower vertebrates (i.e. teleosts, amphibians) employ mostly the first design, while higher vertebrates the second (reptiles, birds, mammals; François and Neetens 1962; Wolburg *et al.* 1999; Schwab 2012). In humans, the irrigation of the inner retina, up to the bipolar cells layer depends on the central retinal artery (derived from the hyaloid artery) with the possible exception of some limited areas supplied by cillio-retinal arteries, derived from choroidal system (Hayreh 1963).

Visual stabilization in vertebrates – the extraocular muscles and the vestibular system

Vision evolved in closed relation with ocular motricity, assured in vertebrates by extraocular muscles and crucial for image stabilization (particularly in species with well-developed area centralis/fovea) and image refreshing through discrete movements, called micro-saccades (Schwab 2012; Straka *et al.* 2014). Extraocular muscles require integrative input from the vestibular system (graviception/ translational linear acceleration and angular acceleration) and proprioceptors for image stabilization during body movements and during relative movements of the head, (Szentágothai 1950; Straka *et al.* 2014). Without proper stabilization retinal image drifts and, for drifts beyond few degrees per second, visual acuity significantly deteriorates (Westheimer and McKee 1975).

Vestibulo-ocular stabilization of the image is assisted by secondary systems based on visual feedback - the optokinetic system and, in higher vertebrates, the pursuit system.

Optokinetic system responds to wide field motion across retina by generating movements that reduce the drift of the image and corrects residual slips non-corrected by vestibulo-ocular reflex, while pursuit system is particularly sensitive to small moving images in the foveal region and permits the tracking of these images even when they cross a featured background (Miles, F.A, Lisberger 1981).

Overview

Vision requires image refreshing and image stabilization both which are assured by the action of the extraocular muscles. Vestibulo-ocular reflex represents the main visual stabilization system, operates both in light and dark conditions and is assisted by the “*accessory*” optokinetic and pursuit systems that require light and the integrity of the entire visual field for adequate function (Miles, F.A, Lisberger 1981).

1.2.3 Brains

As seen before, an unexpected kind of intracellular “eye”, the *ocelloid*, appears in protists. Considering its complex structure, it is conceivable that light information it gathers requires complex processing. However, the structure of the “*intracellular brain*” that performs these operations remains obscure (Schwab 2012).

In metazoans, the presence of eyes necessitates at least a basic neural circuit, connecting them with the effector - the muscular cells (i.e. cnidarians), Schwab 2012). More complex metazoans have dedicated neural networks that process the visual information. Neural networks, through parallel hierarchical processing, decompose visual information into various attributes (i.e. position, wavelength and time) and transmit it to the subsequent stations that recombine it into new ones and so on until it is suited to regulate responses and to embed percepts (i.e. luminance, contrast, colour, contours, shape, texture, depth, movement; Wässle 2004; Bloomfield and Volgyi 2009; Nassi and Callaway 2009; see Figure 6).

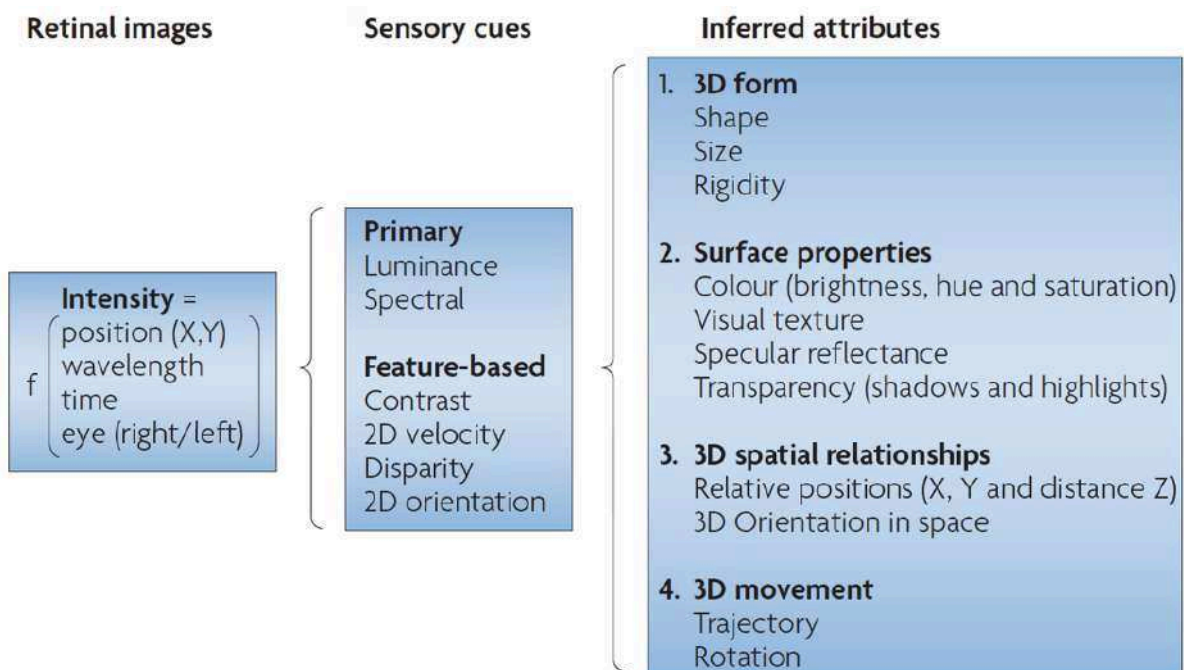
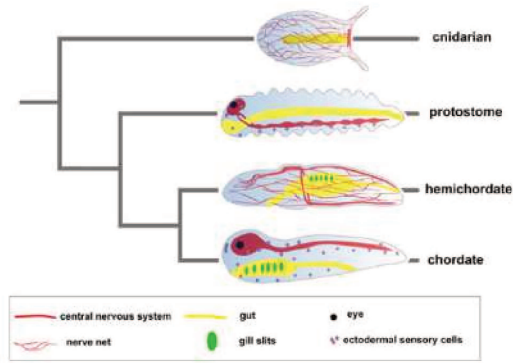


Figure 6 – Visual information from the visual input to the emergence of visual percepts(from Nassi and Callaway 2009)

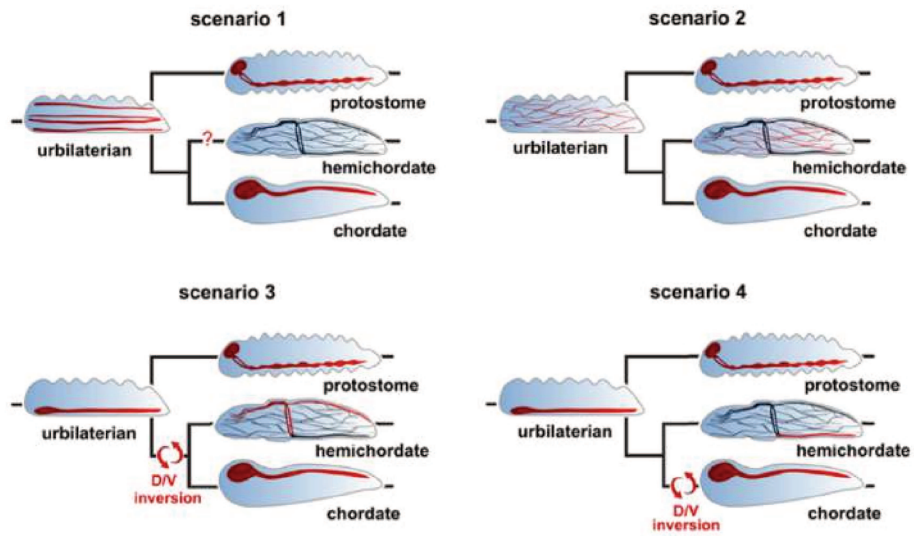
The emergence of central nervous system

If simple metazoans, like certain cnidarians, have a nervous system represented by a neural net, it is yet unclear if the bilaterian ancestor (clade that results in the vertebrate and invertebrate lineages) possessed a diffused nervous system or a centralized network, namely a central nervous system (Holland *et al.*, 2013). Central nervous system is roughly defined as a structure where neurons are concentrated and interpolated in a more complex way than elsewhere in the body (Holland *et al.*, 2013). It may be subdivided into separate parts (ganglia) and connects with the periphery through nerves. Physiologically, central nervous system integrates sensory information originating in the periphery and initiates body-wide responses through direct stimulation of the effector structures (i.e. musculature) or through neurosecretion into the body fluid (Arendt *et al.*, 2008). Most evidence advocates that bilaterian ancestor already had a central nervous system that later evolved into the dorsal central nervous system of chordates and the ventral central nervous system of protostomes (see Figure 7A, B, Holland *et al.*, 2013). Centralization of central nervous system allowed not only a local concentration of neurons, but also their functional and spatial segregation and interrelation, marking thus the beginnings of the “operational centralization” (Arendt *et al.*, 2008). Evolution of central nervous system also paralleled the one of sensory structures, including the development of photoreceptors and eyes (Arendt and Wittbrodt, 2001; Nilsson and Arendt, 2008). Thus, the visual processing starts in the periphery, in the eye and the neuronal networks of the retina, and continues in specific regions of the central nervous system.

A.



B.



C.

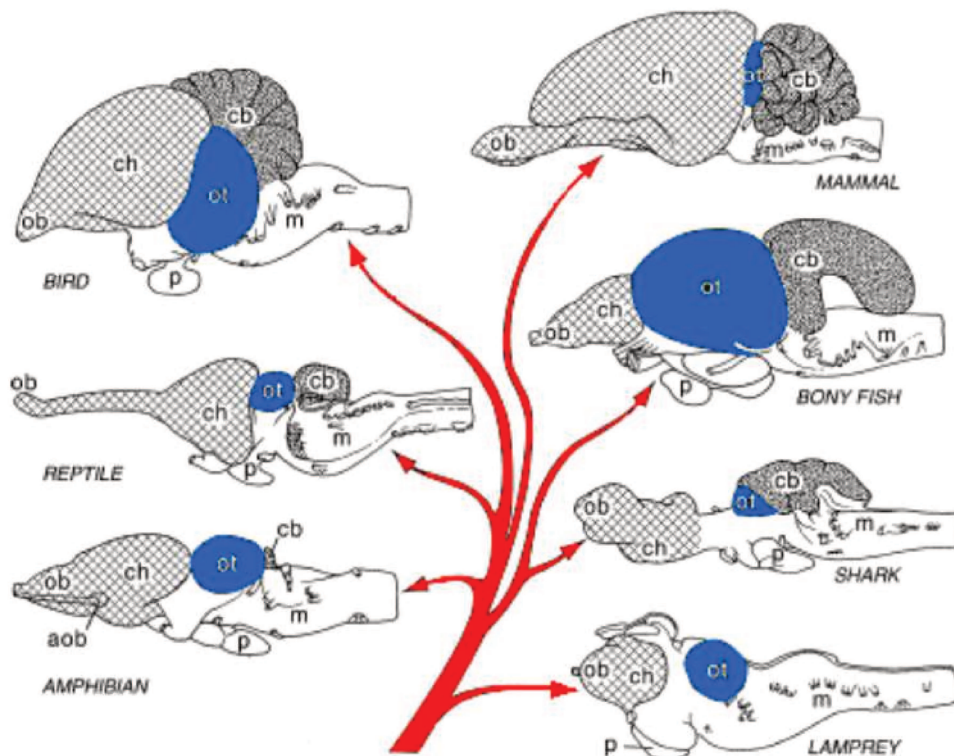


Figure 7 – Central nervous system evolution. **A.** Comparison between different metazoan nervous systems and body plans. **B.** Different scenarios for the evolution of nervous system in bilaterians. **C.** Conservation of brain divisions in vertebrates. aob - accessory olfactory bulb, cb - cerebellum, ch, cerebral hemispheres, m - medula oblongata, ob - olfactory bulb, ot - optic tectum, p - pituitary gland (modified from Holland *et al.* 2013 and Northcutt, 2002).

Overview

One of the most important “*inventions*” of bilaterians was the central nervous system, namely a condensed network of neurons that allowed the operational centralization of information.

The emergence and evolution of vertebrate brain

In vertebrates, the anterior part of the central nervous system evolves into a brain and finally, in *Homo sapiens*, into “*The Brain*”. Brain evolves as a modular structure, that initially presents three cranio-caudal divisions (e.g. forebrain, midbrain and hindbrain) that through further segmentation and compartmentalisation, increases in size, complexity and processing power (Puelles and Rubenstein, 2003; Schlosser and Wagner, 2004). All vertebrates have the same number of brain divisions with the exception of agnathans (e.g. jawless fishes) that lack cerebellum (see Figure 7 C, Northcutt, 2002). This high conservation of the major brain divisions across vertebrates suggest it appeared early in their evolution.

The evolution of main divisions of vertebrate brain was however unequal with certain structures changing little, like medulla or cerebellum, others changing more, like optic tectum, and some changing dramatically, like the forebrain, particularly the cerebral hemispheres (Northcutt, 2002). Increase in the number of neural centers induced an increase in brain size, more evolved vertebrates exhibiting bigger brains. Noteworthy, despite different macroarchitectures, the main types of cortical cells and neuronal circuits are likely present in all amniotes (Karten, 2013). The six layers neocortex for example, which is the newest part of the forebrain in mammals and the most developed part of the brain in primates (Kaas, 2013a), is homologous to specific cortical areas in non avian

reptiles and to the dorsal ventricular ridge nuclei in birds (Dugas-Ford, Rowell and Ragsdale, 2012).

Visual brain in birds and mammals exhibit both divergent and shared neural characters that likely reflect the requirements of their ecological niche (Butler, 2012). Visual processing in birds relays chiefly on collothamic pathway that presumably allows a more rapid, reflex processing of information, likely more fitted for flight (Butler, 2012; Schwab, 2012). Birds are nevertheless able to categorize a wide array of stimuli, to generalize the categories to novel stimuli, to perform complex tasks depending on working memory, episodic memory, transitive interference and multistability of ambiguous visual perceptions rising questions about the neural basis of these high-level mental abilities (Butler, 2012).

Overview

Vertebrate brains evolved in multiples designs to suit the requirements of specific ecological niches. Nevertheless, all vertebrate brains evolved on the modular brain structure present in early vertebrates and using similar neuronal cells types and circuits.

Mammal brain

Early mammals radiated from mammal-like synapsids over 200 million years ago and they likely had 15-20 anatomically and functionally distinct cortical areas, including V1, V2, visual area(s) in temporal cortex and a visual area medial to V1 - *area prostriata* (Kaas 2011). Interestingly, early mammals seem to have possessed no distinct motor or premotor cortex, the cortical motor function being mediated by the somatosensory cortex (Kaas, 2013a).

Early placental mammals radiated about 125 million years ago, and likely continued to have small brains, with relatively little neocortex and the addition of motor cortex (Kaas, 2013a). Placental radiation includes 4 superorders - *Xenartra* (i.e. armadillos, sloths), *Afrotheria* (i.e. tenrecs, elephants), *Laurasiatheria* (shrews, bats, cats, bovines, whales) and *Euarchontoglires* (i.e. rodents, rabbits, tree shrews, primates) - that evolved brains of different sizes and adapted to different ecological niches (Murphy, Pevzner and O'Brien, 2004; Kaas, 2013a). Certain representatives of these superorders, like whales,

elephants and primates considerably developed the stem brain design of early mammals (Kaas, 2013a).

The evolution of primate brain

Archaic primates radiated about 82 million years ago from *Euarchonta superorder* (includes also *scadentia* – i.e. tree shrews and *dermoptera* – i.e. flying lemurs) and formed *strepsirrhin* and *haplorhine* branches about 65 million years ago. *Haplorhine* further divided into *tarsiers* and *anthropoid primates* (simiformes) that emerged about 35 million years ago. From *catarrhin branch* (old world monkeys) of the *anthropoid primates*, 6 million years ago, radiated genus *Homo* of which the only extant species is *Homo sapiens* (Murphy, Pevzner and O'Brien, 2004; Steiper and Seiffert, 2012).

Extinct, stem primates had grasping hands and feet, convergent orbits and a large brain relative to body size with an expanded temporal lobe suggesting an evolved visual function (Kaas, 2013a). Extant primates have greatly expanded representations of central vision in V1 and other visual areas (Rosa *et al.*, 1997). Moreover, primate V1 has structural differences compared to other mammals, namely sublayers of the layer 4. In primates, the inner half of layer 4 receives input from the parvocellular layers of the lateral geniculate nucleus and is important in high spatial resolution processing, while the outer part receives input from the magnocellular layers of the lateral geniculate nucleus and is important in kinetic information processing (Casagrande and Kaas, 1994). Moreover, the superficial layers of V1 are organized in dot-like distributed functional modules, called blobs important in colour vision (Casagrande and Kaas, 1994). This line of evidence suggest these features evolved in the primate ancestors (Kaas, 2012).

In anthropoid primates, V2 exhibits a unique design of repeated subdivisions of three types of band-like modules, each having neurons with specific properties that receive input from specific regions of V1 and provides input to other cortical areas (Casagrande and Kaas, 1994; Kaas, 2012). As these characteristics are already present in a simpler form in prosimian primates (i.e. *Galago a strepsirrhine primate*), and absent in rodents and tree shrews (non-primate *Euarchontoglires*), it is likely that V2 bands evolved with the early primates and become more complex and individualized in higher primates (Kaas, 2012).

V3 and dorsal motor middle temporal area (MT) are other areas that are present only in primates (although very primitive in lower primates) and no other members of *Euarchontoglire clade* (Lyon and Kaas, 2002, Kaas and Preuss, 1993; Kaas, 2012). Noteworthy, in the light of the current available data, V3 area that was described in cats and other carnivores seem to have evolved independently (Kaas, 2012).

Together with V1, V2, V3 and MT, some additional areas with no described homologues in other mammals are part of the primate visual brain : dorsolateral visual area (V4), dorsomedial visual area (V3A), temporal areas related to MT such as the medial superior temporal area (MST), the fundus of superior temporal area (FST) and the middle temporal crescent (MTc; Kaas, 2012). To these regions should be added the limbic *area prostriata*, common to all mammals (Kaas, 2012). Moreover, in all primates, an extensive part of the posterior parietal cortex is involved in visual information processing, allowing to elaborate, initiate and guide the movements of eyes, forelimbs and other parts of the body (Kaas, Gharbawie and Stepniewska, 2011, Kaas, 2013b). Areas involved in grasping, reaching, defence of the face and eye movements were described in lower primates but not in *non-primate Euarchontoglires* like tree shrews and rodents, suggesting that these movement-specific parietal domains emerged with the early primates. Within *primates order*, the parietal cortex differs in organization and complexity, with more functional domains existing in humans, than in prosimians and monkeys (Orban *et al.*, 2006; Kaas, 2013b). It also seems that the developmental advantage of *Homo sapiens* over other *Homo* species was the extensive development of the parietal cortex, especially of the precuneus that allowed for complex computations related to body-tool and body-tool-environment interactions (Bruner and Iriki 2016).

Overview

- Compared to other mammals, primates expanded the neocortex and within neocortex, the visual areas. In primates, the visual brain has more numerous and complex areas including V3, MT and temporal visual areas. They also have a more developed parietal cortex, likely related to a more complex visuo-motor control.
- Compared to other primates, humans have more specialized visual areas and a more developed parietal lobe. Moreover, the expansion of the posterior parietal cortex possibly represented the evolutionary advantage of *Homo sapiens* over the other *Homo* species.

Visual processing

2.1 Retinal processing

2.1.1 General organization and photoreceptor distribution

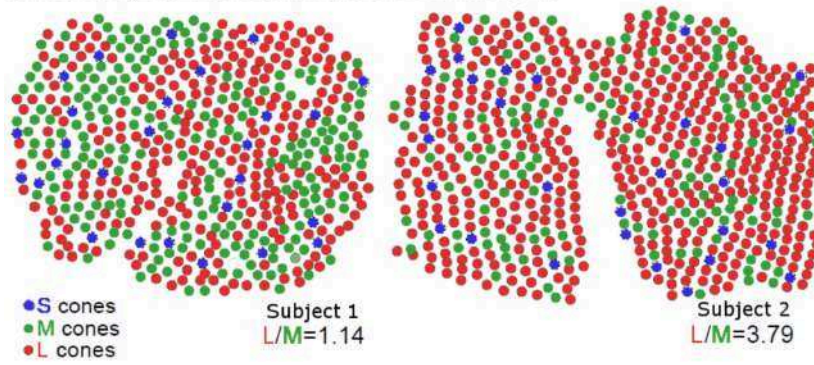
Retina is the first level where processing of the visual information occurs. It contains five classes of neuronal cells – photoreceptors (cones and rods), bipolar, horizontal, amacrine and ganglionar cells. Retinal cells are organized into three layers of neuron cell bodies called nuclear layers separated by two layers of synaptic connections, called plexiform layers (y Cajal 1893). Due to the anatomically limited capacity of information transfer through the optic nerve, the retinal output has to be properly compressed. Therefore, numerous computations are performed in the retina, between photoreceptors and ganglion cells (Bloomfield and Volgyi 2009). The processing starts at the level of photoreceptors, which encode light as a function of wavelength, position (2D), intensity and time (Bloomfield and Volgyi 2009). Further on, photoreceptors connect with bipolar and horizontal cells; bipolar cells transfer the signal to amacrine and ganglion cells; ganglion cells axons form the optic nerve that transfer visual information to the brain (Wässle 2004).

Photoreceptor type and distribution vary across retina in a pattern designed to optimize the sampling for parallel processing. Consequently, in vertebrates with good vision, retina presents an area with increased photoreceptor density allowing for maximal spatial sampling; eccentrically to this region, photoreceptor density decreases (Osterberg 1935). Cones populate this area in most species (Schwab 2012). Besides other properties mentioned above, cones exhibit peak sensitivities at various wavelengths and the comparison of their output opens a processing channel resulting in chromatic percepts that further enhance discrimination (Wässle 2004; Schwab 2012).

In mammals and therefore in humans, retina is dominated by rods with the exception of fovea, where cones are dominant. Actually, in the very center of the fovea, in an area of 350 μm (1.25°), rods are totally absent. Cones maximal density is in the central 500 μm of the fovea, in an area called foveola (98,200 - 324,100 cones/ mm^2 , the highest values being close to those measured in birds of prey, Reymond 1987; Curcio *et al.* 1990). Cone density is 40-45% higher in the nasal than temporal retina. It falls rapidly outside foveola,

faster along the vertical than horizontal meridian, reaching half of the maximal density at an eccentricity of 120 μm inferior and 150 μm temporal. Rods density increase rapidly outside the rod-free zone, reaching its highest value (157,900 - 188,600 rods/ mm^2) in a broad, horizontal elliptic ring at the same eccentricity as the optic disk and extending more into nasal retina. Rod density is higher in the superior retina, especially in its nasal part and is reduced by 15-25% in the region where the ring intersects the horizontal meridian, both nasally and temporally (Curcio *et al.* 1990). Beyond the ring, rod also present a progressive decrease in density, but much slower than cones to a minimum of 49,000 rods/ mm^2 at 20 mm from the center of the fovea (see Figure 8, Curcio *et al.* 1990).

I. Variable L, M and S cones distribution in human retina



II. Cones and rods distribution and density across retina

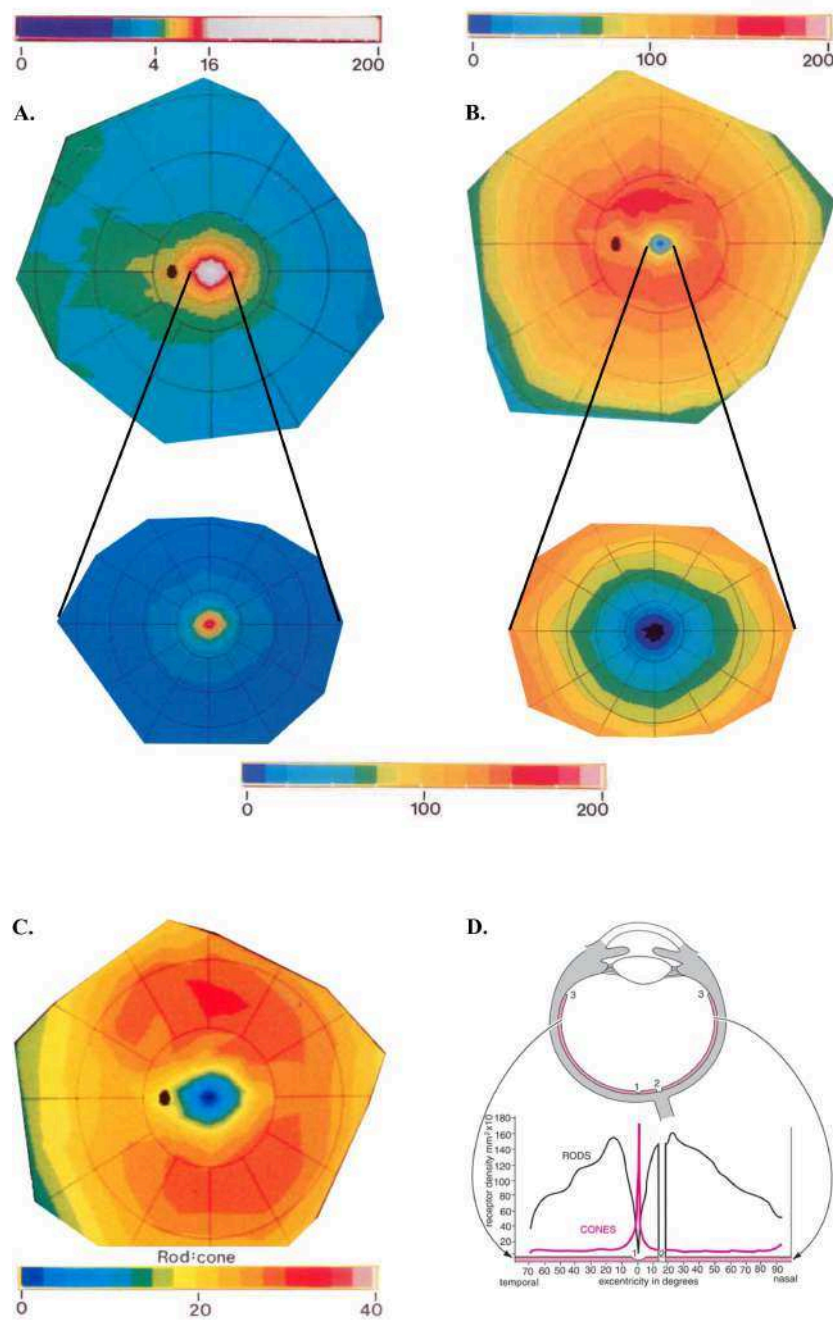


Figure 8 – Cones and rods retinal distribution in humans. I. Note the variable distribution in L, M and S cones in two different individuals. **II. A.** Cone densities over the entire retina. Detail – foveal cones densities. **B.** Rod densities over the entire retina. Detail – central slope of rod ring and the foveal rod-free zone. **C.** Rods : cones ratio in the retina (Curcio *et al.* 1990). **D.** The classical diagram of Osterberg with cone and rods distribution over the horizontal meridian (1 – fovea centralis, 2- optic disk, 3 – ora serrata) (modified from Dacey 2000, Curcio *et al.* 1990 and Nieuwenhuys *et al.* 2008).

Overview

Cones and rods have different local densities across retina. In humans, in the center of the fovea, cone have maximal density, whereas rods are absent. Outside fovea, cone density falls rapidly. Rods have maximal density on a horizontal ellipse at about the eccentricity of the optic disc.

2.1.2 Cones neural circuitry.

Cone circuitry is the backbone of the retinal processing toolkit (Masland 2012). Phylogenetically newer rods end-up “*pigging back*” the existing pathways. Both cones and rods transmit the light-evoked signals to bipolar and horizontal cells. In mammals, three types of horizontal cells provide lateral interactions in the outer plexiform layer. Horizontal cells are depolarized by the light, sum light responses from a broad area and subtract them from the local signal (their receptive fields are larger than their dendritic fields due to gap-junctions coupling). It is believed that through this mechanism, they diminish the response to areas with uniform brightness and enhance the response to edges of visual stimuli (Wässle 2004).

More than nine types of cone bipolar cells and one type of rod bipolar cell grouped in two functional classes - ON and OFF - transmit the light-evoked signals to amacrine and ganglion cells. Blue cone bipolar cell and rod bipolar cell are of ON type. In the inner plexiform layer, ON bipolar neurons connect with ON ganglion cells and OFF bipolar neurons with OFF ganglion cells through excitatory synapses. Consequently, ON ganglion cells are triggered by stimuli brighter than background while OFF ganglion cells by stimuli darker than background (Wässle 2004).

Like in cones, bipolar and ganglionic cells density is higher in central retina and lower

in peripheral retina. Moreover, the dendritic field of bipolar and ganglionic cells decreases towards the center of the retina with the anatomic limit reached when each cone is connected to a single bipolar and ganglionic cell (Wässle and Boycott 1991). This design establishes a direct link between cone and brain thus optimizing the spatial resolution (visual acuity). It also allowed the “*reinvention of trichromacy*” in old world monkeys and humans (Wässle 2004). It is believed that this one-to-one connection in the central retina was required before the subsequent mutation of LWS gene that resulted in the L-cone and M-cones pigments (Mollon and Jordan 1988; Nathans 1999) and suggests that trichromatic channels “*piggy-backs*” on the high acuity system. The impossibility of transgenic mouse expressing human L and M opsins to perform trichromatic colour discrimination (Jacobs *et al.* 1999; Wässle 1999; Smallwood *et al.* 2003; Wässle 2004) and the steep decline in red and green perception outside the foveal projection area in humans support this view (Franze *et al.* 2007; Hansen *et al.* 2009).

The outputs of the various types of bipolar cells are sampled by specific sets of amacrine and ganglion cells. The main structural characteristic defining a bipolar cell is the level of the inner plexiform layer where its axon terminates. It dictates the type of ganglion and amacrine cells it will connect with and the specific information channel to the brain it belongs to. Most of the retina connectivity is done within the layers, with only some interlayer connectivity assured by amacrine cells. The partially selective inputs transmitted by bipolar cells are refined by feedbacks from amacrine cells. Therefore, the bipolar cells output to ganglion cells results from the intrinsic response of bipolar cells and the tuning of amacrine cells (Euler and Masland 2000; Masland 2012; Saszik and DeVries 2012).

Amacrine cells are a numerous and yet poorly understood class of retinal interneurons (29 types in rabbit retina, MacNeil *et al.* 1999; Masland 2012). Most of them are axonless and the lack of obvious polarity makes difficult to recognize their sites of input and output. Moreover, amacrine cells have complex output synapses that make even more difficult their study: feedback synapses to the bipolar cells that drive them, synapses with other amacrine cells and with various types of ganglion cells (Lin *et al.* 2000; Jusuf *et al.* 2005; Hadzibeganovic *et al.* 2010; Eggers and Lukasiewicz 2011). Overall, it is considered that they create contextual effects for the responses of ganglion cells like center-surround antagonism and stimulus over background motion detection (Gollisch and Meister 2010), perform some variety of vertical integration between various layers of the inner plexiform layer (called crossover inhibition; Demb and Singer 2012; Buldyrev *et al.* 2012), participate in task-specific functions like motion direction discrimination (starburst amacrine cells; Fried *et al.* 2002; Lee and Zhou 2006), mediate of blue-OFF signals (Sher and DeVries 2012; Chen and Li 2012) and optimize of the information conveyed by the rod bipolar cells (Grimes *et al.* 2010).

The total number of ganglion cell functional types in mammals is unknown but it is estimated that there might be around 20 (Masland 2012). The classical textbook view

recalls only three types (midget, parasol and bi-stratified) representing about 90% of the primate retina and linked to parallel pathways that remain anatomically segregated through lateral geniculate nucleus and primary visual cortex (see Figure 9) attributed to each stream (i.e. P– high acuity, red-green opponency, M – achromatic, low acuity, K–blue-green opponency).

The “*three paths*” model is however contested by numerous anatomical, physiological and psychophysical findings, which show that these pathways do not fulfill the required characteristics, namely homogeneity, independence (structural and perceptual) and compatibility between the stream’s properties and its presumed function (Kaplan 2008; Kaplan 2014). The current knowledge is unfortunately insufficient and unable to produce a better, comprehensive model of visual channels. It is likely that the numerous types of ganglion cells encode visual information in more parallel channels than previously believed. It is now clear that ganglion cells response and receptive field are dynamic and modulated by various contextual influences such as object motion segmentation, direction selectivity, anticipatory responses to moving stimuli and saccadic suppression (Oliveczky *et al.* 2003; Roska and Werblin 2003; Hosoya *et al.* 2005; Münch *et al.* 2009; Masland 2012).

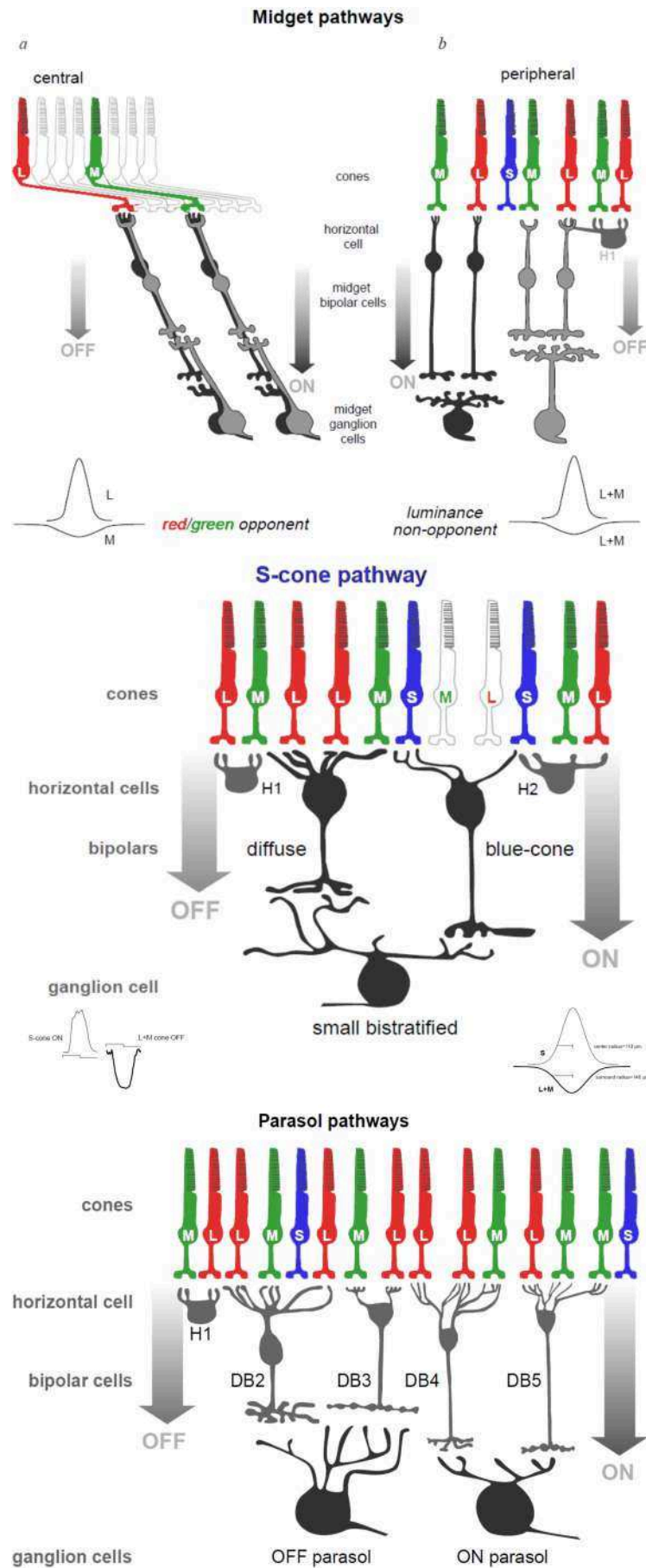


Figure 9 – Cone circuitry. Midget pathways for fovea and peripheral retina (parvocellular); S-cones pathways (koniocellular) and parasol pathway (magnocellular). H-horizontal cell; DB – diffuse bipolar cell (modified from Dacey 2000).

Overview

Parallel visual processing starts in the retina and *cone circuitry* represents its foundation. Visual information is decomposed and structured in various information channels by the retinal neurons and conveyed to central structures by the axons of ganglion cells. Noteworthy, the reinvented trichromatic vision in primates “*piggy-backs*” the high acuity system of the central vision. The “*three paths*” model (parvocellular, magnocellular, koniocellular) is obsolete, as likely more numerous output channels exist. Unfortunately, the insufficient current knowledge cannot provide a better, comprehensive model.

2.1.3 Rod neural circuitry

Rod photoreceptors are a later phylogenetic acquisition and in terms of information transmission, they “*piggy-back*” cone circuitry. As developed in previous chapters, rods are responsible for the scotopic vision, but their role is much complex including the relay of cone-driven, horizontal cell-mediated surround inhibition (photopic conditions, Szikra *et al.* 2014). Rod signal is transmitted through at least three different pathways, each tuned for a primarily non-overlapping range of intensities, the ganglion cells receiving either convergent or segregated inputs (Volgyi 2004). The “*classical*” rod transmission pathway is preeminent in scotopic conditions and likely conveys slow, low-threshold rod signals (Volgyi 2004). It relays the rod signal to the unique type of rod bipolar cell that conveys it radially into the inner plexiform layer to AII amacrine cells that form sign-inverting synapses with ON cone bipolar cells and sign-conserving synapses with OFF cone bipolar cells (See Figure 10). Two secondary pathways are active at higher light intensities, when the primary pathway is saturated and they convey the signal through gap-junctions located between photoreceptor axonal terminals (Volgyi 2004; Bloomfield and Volgyi 2009). The first one conveys fast, high-threshold rod signals through rod-cone coupling and is active in mesopic conditions; the signal is transmitted to cones and further to cone bipolar cells and then to ganglion cells (see Figure 10, Volgyi 2004). Interestingly, the rod-cone coupling is modulated by the circadian retinal clock through dopamine release during the day, which inhibits the conductance of rod-cone gap-junctions (Ribelayga *et al.* 2008). The second path (see Figure 10), less well understood, conveys relatively low-threshold signals through rod-rod coupling; the signal is transmitted to an OFF bipolar cell, which further relay it to a subset OFF ganglion cell. It was proposed that this pathway helps identifying dark objects moving through the visual field and that it evolved to improve predators detection during the dusk and dawn (Tsukamoto *et al.* 2001; Volgyi 2004).

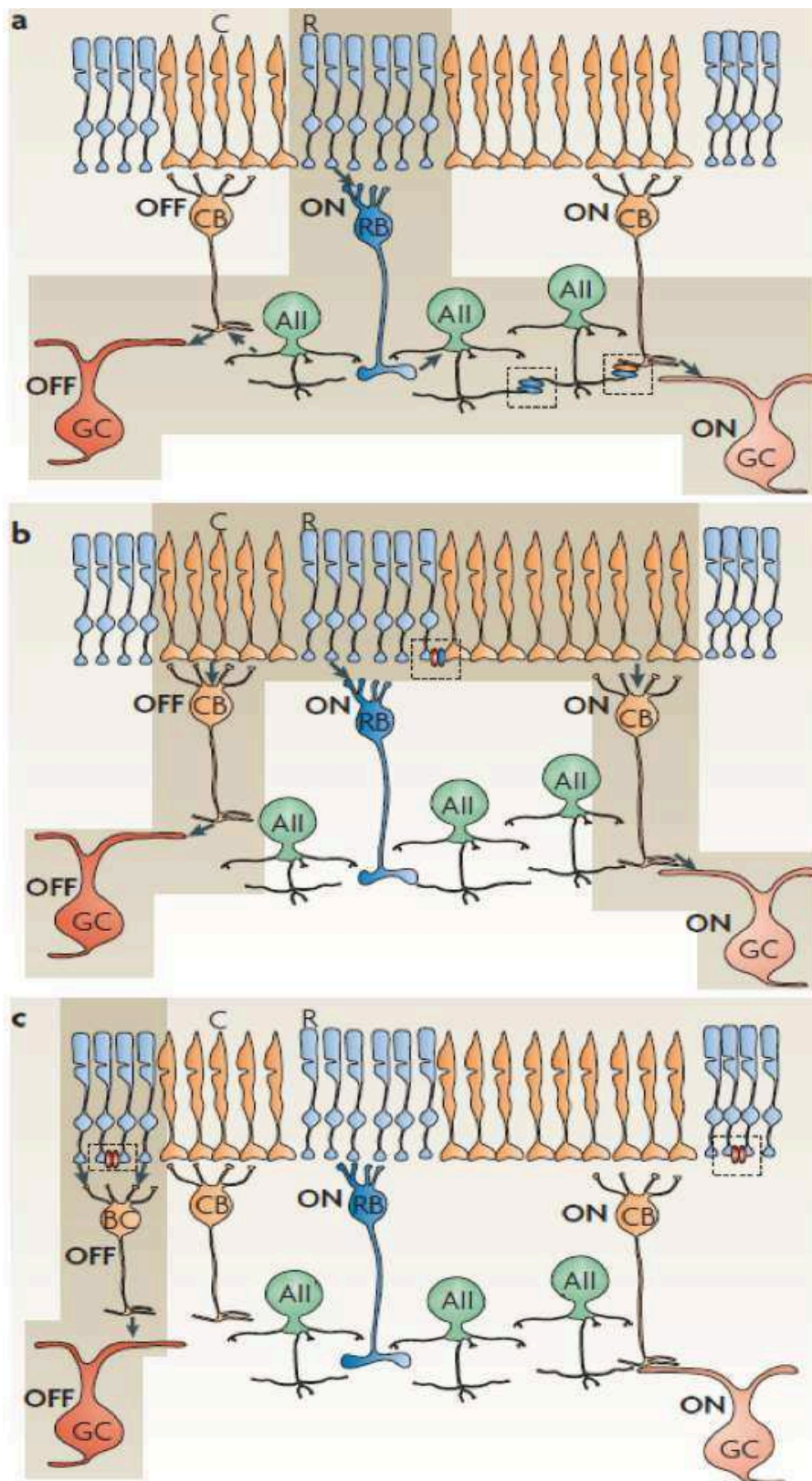


Figure 10 – Rod circuitry. A. The primary rod pathway comprises synapses between AII amacrine cells and between AII amacrine cells and cone bipolar cells. Rods transmit signals to rod bipolar cell that convey them to AII cells that relay through electrical synapses to cone bipolar cells (sign conserving with ON cone bipolar cells and sign-inverting synapses with OFF cone bipolar cells) that further transmit it to ganglion cells. **B.** The secondary rod pathway involving electric synapses between rods and cones. Rods convey the signal directly to cones that further relay it through their downstream circuitry. **C.** The tertiary rod pathway that involves only electric synapses between rods. Rods make direct chemical synapses with an OFF subtype of bipolar cell that relays the signal to specific OFF ganglion cells. No ON counterpart was identified for this pathway. Solid arrows represent excitatory and dotted arrows inhibitory chemical synapses. C – cone; R – rod; CB – cone bipolar; RB – rod bipolar; GC – ganglion cell (from Bloomfield and Volgyi 2009).

Overview

Rods have three currently known transmission pathways. All of them employ cones' neural circuitry. They demonstrate that rods intervene not only in scotopic conditions, but also have a visual role in mesopic conditions (dim-light).

2.2 Cerebral visual processing

2.2.1 General view on the central nervous system organization

Different groups of vertebrates exhibit a common general plan of central sensory and motor pathways. In the case of sensory system, incoming information is initially conveyed to intermediary stations in brainstem (body and trigeminal somatosensory and visceral senses, lateral line/ vestibulocochlear, gustatory senses), to the olfactory bulb (olfaction) or to various layers in the retina (vision). Further on, in amniotes, most of information follows two paths - it can be relayed through the midbrain roof structures and from there to dorsal thalamic nuclei (the collothalamic pathway, in reference to colliculi) or can reach directly the dorsal thalamus (the lemnothalamic pathway, meaning “*ribbon-like*”); from dorsal thalamus, information is conveyed to various parts of telecephalic pallium (cortex). Dorsal thalamus has two fundamental divisions across all jawed vertebrates: an embryologically more rostral part that receives direct sensory input (lemnothalamus) and a more caudal part that receives information relayed through midbrain roof nuclei (collothalamus; Butler 2007; Butler 2012). In what concerns vision, in mammals, geniculostriate pathways are lemnothalamic and relay directly into the lateral geniculate nuclei in dorsal thalamus, while retinotectothalamocortical pathways are collothalamic and relay in the superior colliculi before reaching the lateral posterior/pulvinar nuclei in dorsal thalamus. From their thalamic relay, lemnothalamic visual pathway projects into the lemnopallium, namely into the primary visual cortex and collothalamic visual pathway into association visual cortices (parietal and temporal) but also the basolateral division of the pallial amygdala, especially its lateral nucleus (Butler 2012). The exact role of collothalamic pathways is poorly understood but it is believed that it participates in visual attention mechanisms and blindsight, a form of vision that persists after the destruction of the primary visual cortex (V1), the destination region of lemnothalamic pathway (Zeki and Ffytche 1998; Tamietto and Morrone 2016; see Figure 11).

Besides lemnothalamic and collothalamic pathways, other less well understood visual projections have been described. Direct retino-pulvino-cortical pathways ending in middle temporal area (MT) area exist in primates, at least in early life, and are responsible for remarkably good residual vision they exhibited after postnatal removal of the primary visual cortex (Kaas 2015; Warner *et al.* 2015). Interestingly, MT structure is closer to a primary sensory area than to associative cortex (Bourne and Rosa 2006). The role of

this regressive, direct pulvino-MT connection is unknown. Warner *et al* speculated that it might be required for the dorsal expansion of the visual cortex in primates (Warner *et al.* 2015) while Kaas argued that it might prevent the significant wiring of the visual cortex by the collothalamal pathway as seen in close relatives of primates (i.e. three shrews, Kaas 2015).

Accessory optic system, represented by the dorsal, lateral and medial nuclei positioned in the periphery of rostral mesencephalon on a side branch of the optic tract of the optic tract, complements the vestibular system in detecting self motion. It registers the speed and direction of of the environment's global movements and relay them to cerebellum via the inferior olive. This information is also employed in the long-term adaptation of vestibulo-ocular reflex (Nieuwenhuys *et al.* 2008).

Motor pathways are also unidirectional relay systems, which are regulated and gated by recurrent circuits controlling the initiation and the guidance of movements (Butler 2012). Visuomotor system deserves a particular interest due to its complexity and similarity across the major taxa. In addition to the lemnothalamic and collothalamal pathways, retina also projects to multiple pretectal and accessory optic nuclei, involved in oculomotor control and pupillary light reflex. Moreover, in mammals, the tectum and reticular formation have important roles in eye movement regulation both as response to visual stimuli or vestibular input (Butler 2012).

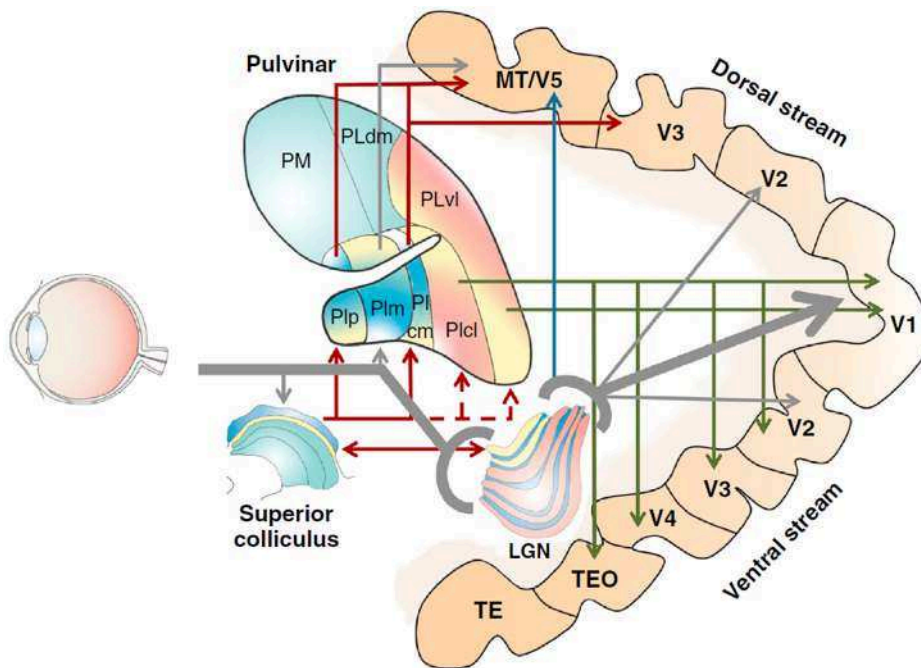


Figure 11 – Retinocortical connections potentially involved in blindsight. Thick, gray arrow depicts the lemnothalamic pathway that projects to V1. Red arrows mark projections originating in superior colliculus and reaching the dorsal cortical stream through a thalamic relay in the pulvinar. Green arrows indicate projection from specific pulvinar subnuclei to areas of the ventral cortical stream. Blue arrow marks the projections from koniocellular layers of lateral geniculate nucleus to middle temporal area. Color codes in lateral geniculate and superior colliculus: yellow – magnocellular, blue – koniocellular, pink – parvocellular channels. In pulvinar the segregation of the channels is unclear and depicted in blue-yellow and pink-yellow gradients. LGN – lateral geniculate nucleus; MT – middle temporal; Plcl – pulvinar inferior centro-lateral; Plcm – pulvinar inferior centro-medial; Plm – pulvinar inferior medial; Plp – pulvinar inferior posterior; PLdm – pulvinar lateral dorso-medial; PLvl – pulvinar lateral ventro-lateral; PM – pulvinar medial; TE – temporal inferior rostral; TEO – temporal inferior posterior (from Tamietto and Morrone 2016).

Overview

Cortical visual input follows two main afferent channels: lemnothalamic and collothalamic. Lemnothalamic pathway relays directly in the dorsal thalamus from where it projects to cerebral cortex. Collothalamic pathway, preeminent in many vertebrates has a first relay in the superior colliculus from where visual information is conveyed to the dorsal thalamus and further to the cerebral cortex.

2.2.2 Lemnothalamic pathway

Lemnothalamic projections constitute the chief visual projections in primates (Kaas 2015). The current view described bellow is based on the “*three paths model*”.

Retinothalamic projections

Axons of ganglion cells positioned in the temporal half of the retina project on the ipsilateral LGN, while axons of ganglion cells positioned in the nasal half of the nasal retina cross at the level of the optic chiasm and reach the contralateral LGN. Retinal ganglion cells terminate into a highly ordered manner into parvocellular (P), magnocellular (M) or koniocellular (K) layers of lateral geniculate nuclei (LGN) and from there, to different layers of the primary visual cortex (V1) (see Figure 12). Layers M1, P4 and P6 receive contralateral fibers, layers M2, P3 and P5 ipsilateral fibers, while K layers receive the same kind of fibers as the overlaying main layer (see Figure 12, Nieuwenhuys *et al.* 2008). Small bistratified blue/yellow opponent ganglion cells terminate in the layers K3 and K4 and the remaining K layers receive input from other retinal ganglion cells (Hendry and Reid 2000; Nieuwenhuys *et al.* 2008). Moreover, ventral K layers receive extraretinal input from superior colliculus and its satellite, the parabigeminal nucleus (see Figure 12, Harting *et al.* 1973; Harting *et al.* 1980; Hendry and Reid 2000).

Thalamocortical projections

Fibers from the LGN project to the ipsilateral area V1, in the calcarin sulcus, on the medial aspect of the occipital lobe. They cross through the retrolenticular part of the internal capsule, arch around the lateral ventricle and pass posteriorly toward the occipital cortex. Fibers from the lateral aspect of LGN and bearing the projections from the superior visual field will take a longer route, sweeping around the inferior horn of the lateral ventricle (*“the temporal knee”* of the optic radiations) before reaching the inferior bank of the calcarine sulcus (see Figure 12, Nieuwenhuys *et al.* 2008).

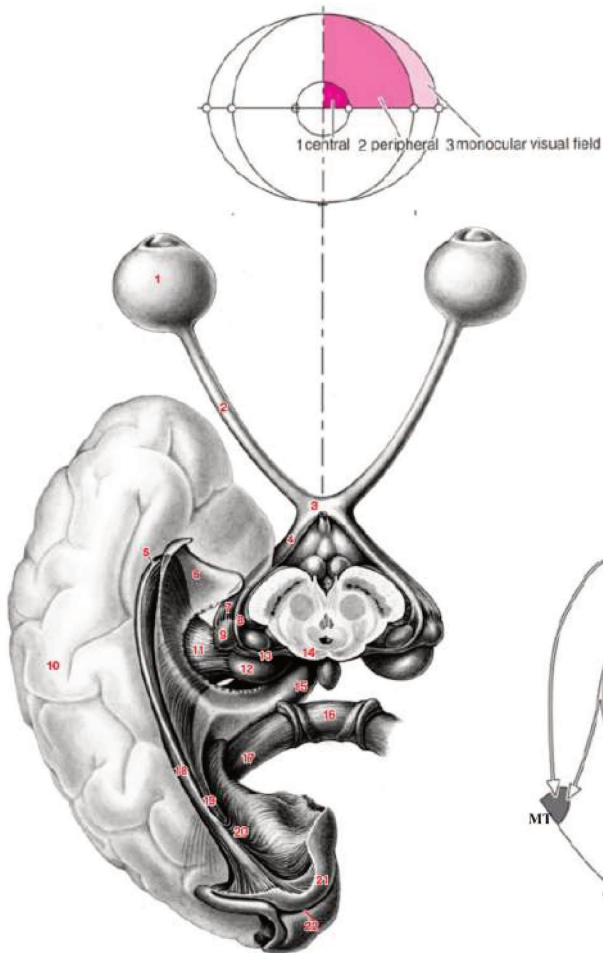
Primary visual cortex (V1) exhibits retinotopic organization. The foveal region over represented, thus reflecting differences in information processing. Foveal projection is located in the posterior part of V1, whereas the peripheral retina projection in the anterior part of V1 (Horton and Hoyt 1991). The nasal periphery of the retina, sampling the temporal, monocular part of the visual field project most anteriorly in the proximity of the splenius of corpus callosum (Nieuwenhuys *et al.* 2008). Will we refer to the posterior part of V1, where foveal region project, as *“central V1”* and to the anterior part of V1, where peripheral retina projects, as *“peripheral V1”*. The segregation between the projection of the left and right retina is persevered not only within LGN’s layers but also in V1 where the afferences of the ipsilateral eye terminate in columns separated by other columns receiving afferences from the contralateral eye (see Figure 12, Nieuwenhuys *et al.* 2008).

V1 is formed by 6 functional layers. Magnocellular and parvocellular LGN neurons project into the 4th V1 layer, namely into sublayers 4C and 4C, 4A respectively; the koniocellular neurons project into layers 2/3. Koniocellular LGN neurons also project into MT area, bypassing V1. The three paths intermix into the blobs and interblobs of V1’s layers 2/3 and are further transmitted via the thin and thick stripes of area V2 into the ventral and dorsal visual streams (see Figure 14, Nieuwenhuys *et al.* 2008). Likewise, V1 receives feedforward and feedback projections and send feedforward and feedback projections to various cortical and subcortical structures and suggesting a parallel multilevel processing of information (Schmolesky 2007). Direct feedforward projections to V1 from pulvinar, LGN, claustrum, nucleus paracentralis, the raphe system, Meynert’s basalis nucleus (Ogren and Hendrickson 1976; Rezak and Benevento 1979; Graham 1982; Blasdel and Lund 1983; Doty 1983; Perkel *et al.* 1986; Lachica and Casagrande 1992; Hendry and Yoshioka 1994; Adams *et al.* 2000; Schmolesky 2007), direct feedforward projections originating in V1 reaching V2, V3, V5, MT, medial superior temporal area (MST), frontal eye field (FEF) (Lund *et al.* 1975; Maunsell and van Essen 1983; Ungerleider and Desimone 1986; Livingstone and Hubel 1987; Shipp and Zeki 1989; Boussaoud *et al.* 1990; Fitzpatrick *et al.* 1994; Schmolesky 2007), direct feedback projection to V1 from V2, V3, V4, V5, MT, MST, frontal eye field (FEF), lateral intraparietal cortex (LIP) (Perkel *et al.* 1986; Ungerleider and Desimone 1986; Shipp and Zeki 1989, Rockland *et al.* 1994;

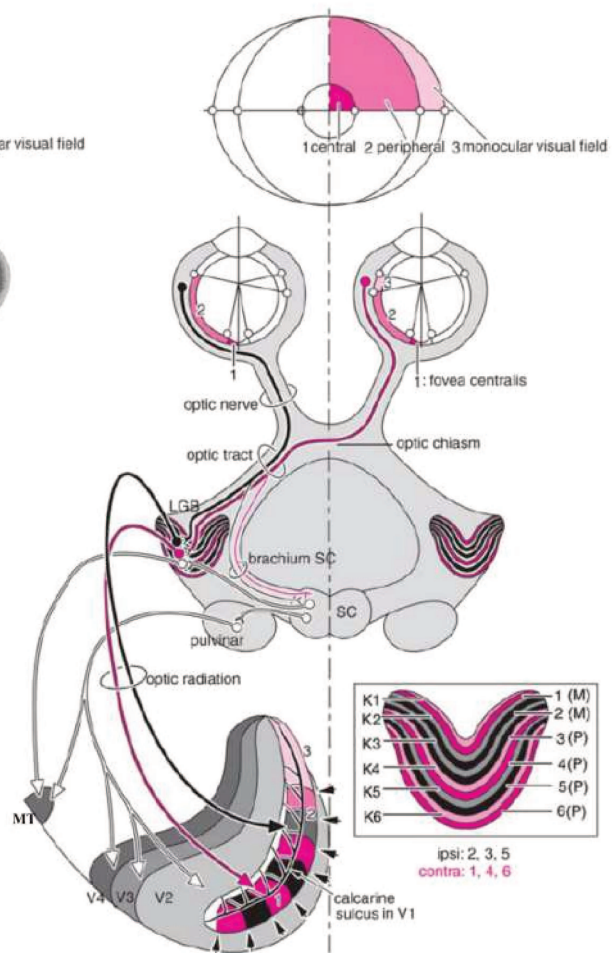
Barone *et al.* 2000; Suzuki *et al.* 2000; Schmolesky 2007) and direct feedback projection from V1 to superior colliculi, LGN, pulvinar, pons (Lund *et al.* 1975; Graham 1982; Fries, W., Distel 1983; Fries 1990; Gutierrez and Cusick 1997; Schmolesky 2007) sustain this concept.

Lemnothalamic pathway

I. 3D View



II. Retinogeniculocortical projections



1. Eye
2. Optic nerve
3. Optic chiasm
4. Optic radiation, temporal knee
5. Inferior horn of the lateral ventricle
7. Optic tract
8. Medial root of the optic tract joining the brachium of the superior colliculus
9. Lateral geniculate body (LGB)
10. Optic radiation
12. Pulvinar
13. Brachium of the superior colliculus
14. Superior colliculus (SC)
15. Central part of the lateral ventricle
16. Splenius of the corpus callosum
17. Radiation of the corpus callosum
18. Sagittal stratum
19. Posterior horn of the lateral ventricle
20. Optic radiation, occipital knee
21. Primary visual cortex (V1)
22. Calcarine sulcus

III. Projections of the right visual field

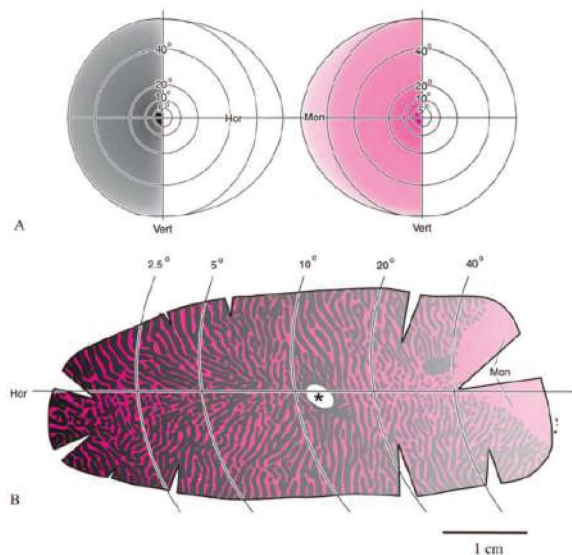


Figure 12 – Lemnothalamic pathway I. 3D ventral view of the retinogeniculocortical projections. **II.** Diagram of the retinogeniculocortical, extrageniculate and extrastriate visual pathways corresponding to A and depicting projections of the upper right visual field. In the cassette, detail from the lateral geniculate nucleus. **III.** Projections of the right visual field. **A.** On the left temporal and right nasal retina. **B.** V1 projections. Note the ocular dominance columns in the left primary visual cortex. Red codes contralateral projections, black codes ipsilateral projections; color intensity codes eccentricity: pale – far, monocular periphery (only contralateral projection); intermediate intensity - intermediate, binocular periphery; high intensity – central visual field (macular vision). Abbreviations: M – magnocellular, P – parvocellular, K – koniocellular., MT – medial temporal; Hor – horizontal meridian; Mon – monocular visual field, Vert – vertical meridian, * - blind spot projection (from Nieuwenhuys *et al.* 2008)

Overview

Lemnothalamic pathway represents the principal visual pathway responsible for conscious vision in primates. Its projections terminate in primary visual cortex with the exception of some koniocellular fibers that terminate in MT area. Lesion of the lemnothalamic pathway in adult primates results in cortical blindness and some degree of visual behavior can be regained through the reinforcement of the collothalamic pathways.

2.2.3 Collothalamic pathway

Collothalamic projections represents the chief visual projections in in most vertebrates and are particularly developed in birds. They also important in most mammals except for primates (Butler 2012).

Superior colliculi play an important role in orienting behavior by directing the line of sight toward the targets of interest through coordinated movements of the eyes, head and body as well as in other visuo-attentional processes and blindsight (Nieuwenhuys *et al.* 2008; Tamietto and Morrone 2016).

In primates, various type of retinal ganglion cells, accounting for up to 10% of the total retinal output, terminate in the superficial layers of the superior colliculi (Leventhal *et al.* 1981). Retinocollicular projections are bilateral, with a contralateral dominance: temporal fibers have both ipsilateral and contralateral projections, while the nasal fibers have only contralateral projections (Cynader and Berman 1972). Therefore, while the binocular visual field has bilateral collicular representation, the monocular eye field has only contralateral representation (see Figure 13). Moreover, the superior colliculus receives input from the ipsilateral cerebral cortex mainly from the visual and visuomotor areas (V1, V2, area 19, MT, frontal and parietal visual areas, Leichnetz *et al.* 1981; Fries, W., Distel 1983; Lynch *et al.* 1985; Abel *et al.* 1997; Nieuwenhuys *et al.* 2008) and subcortical structures (pretectum, parabigeminal nucleus, nucleus of the optic tract, nucleus intercalatus and substantia nigra, Voogdt *et al.* 1998; Nieuwenhuys *et al.* 2008, see Figure 13).

The superior colliculus sends efferences to thalamic and other subcortical structures. The collothalamic fibres originating in the superficial layers, terminate in the ventral lateral geniculate nucleus, the inferior and lateral pulvinar and lateral geniculate nucleus, koniocellular layers. From thalamus, they further project in various cortical locations - V1, V2, MT, MT MST, parietal visual area and FEF (Nieuwenhuys *et al.* 2008).

Overview

Compared with most vertebrates and even mammals, in primates and thus in humans, collothalamic pathway is less well represented. It is also less well understood. Collothalamic pathway is responsible for the residual vision following lesions that block the lemnothalamic input (i.e. primary visual cortex lesions) and represents an invaluable resource for the sensory rehabilitation.

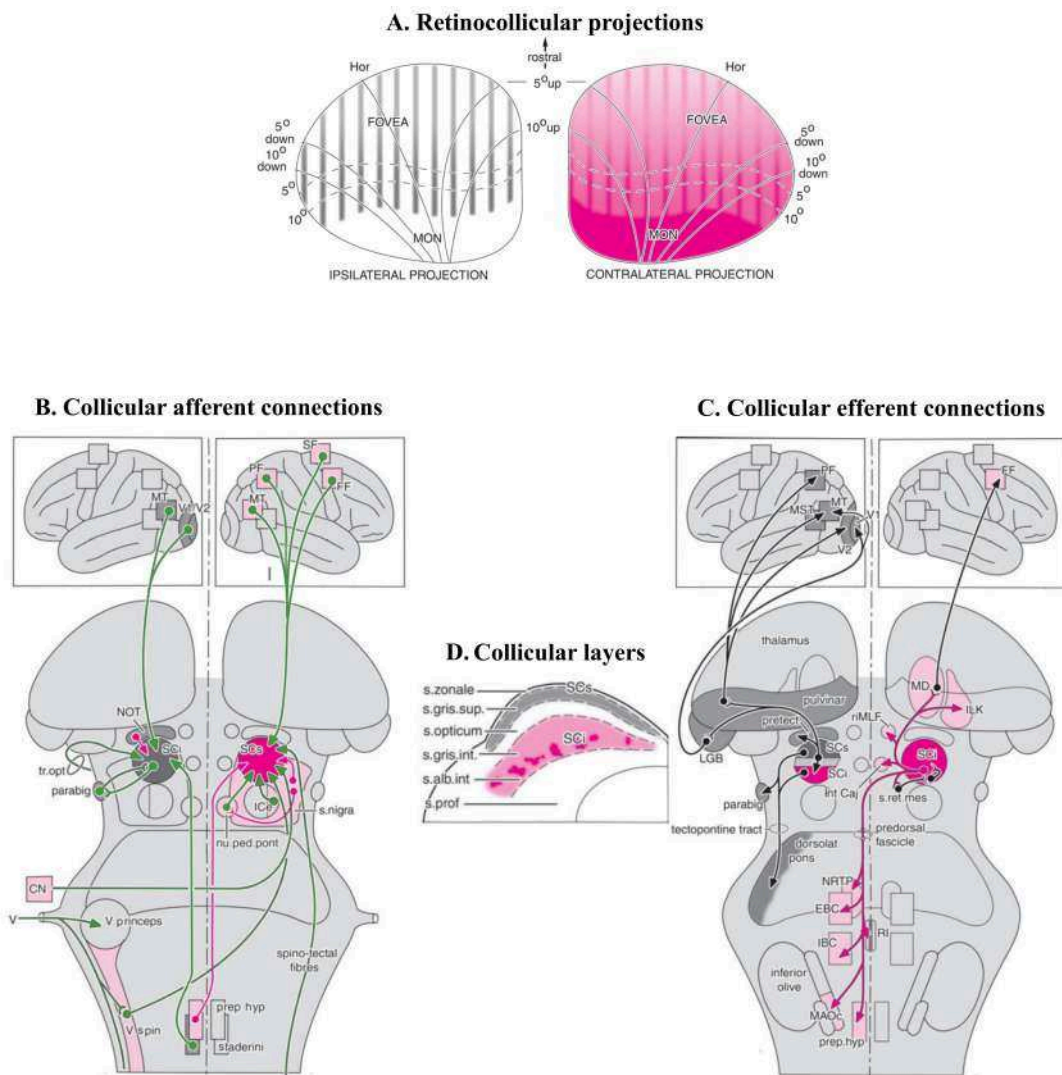


Figure 13 – Afferences and efferences of the superior colliculus. **A.** Collicular retinotopy of the left hemifield in macaque monkey. Color code: grey – ipsilateral connections; red contralateral connections. Note the bilateral projections of the hemifield with predominance of contralateral connections. **B.** The afferent connections of the superior colliculus. Afferences to the superficial layers are depicted on the left half of the brainstem diagram; afferences to intermediate layers are depicted in the intermediate layers. Red arrows mark inhibitory connections. **C.** The efferent connections of the superior colliculus. Color code: grey arrows – efferent connections from the superficial layers; red arrows - efferent connections from the intermediate layers. **D.** Detail with the superficial (grey), intermediate (red) and profound layers of the superior colliculus. CN – cerebellar nuclei; EBC – excitatory burst cells; FF – frontal eye field; Hor – horizontal meridian; IBC – inhibitory burst cells; Ice - external nucleus of the inferior colliculus; ILK – intralaminar thalamic nuclei; Int Cajal – interstitial nucleus of Cajal; LGB – lateral geniculate body; MAOc – caudal part of medial accessory olive; MD – mediodorsal thalamic nucleus; Mon – monocular periphery projection (only contralateral projections); MST – medial superior temporal visual area; MT middle temporal visual area; nu.ped.pont – nucleus pedunculopontinus; NOT – nucleus of the optic tract; parabis – parabisgeminal nucleus; NRTP – nucleus reticularis tegmenti pontis; parabis – parabisgeminal nucleus; PF – parietal eye field; prep. hyp. – prepositus hypoglossi; pretect – pretectum; RI – nucleus raphe interpositus; rMLF – rostral interstitial nucleus of the medial longitudinal fasciculus; s.alb.int, s.gris.int – intermediate gray layers; s.gris.sup – superficial gray layer; s. prof – deep layers; SCi – intermediate layers; SCs – superficial layers; SF – supplementary frontal eye field; s.ret.mes – reticular formation of the mesencephalon; staderini – nucleus intercalatus of Staderini; tr.opt – optic tract; V princeps – principal trigeminal sensory nucleus; V spin – trigeminal spinal nucleus; V – trigeminal nerve. V1/ V2 – early visual cortex (from Nieuwenhuys *et al.* 2008)

2.2.4 Associative visual cortex

Visual areas beyond V2, treat information issued from specific channels and are arranged into two streams: a dorsal stream directed toward the parietal lobe and a ventral stream directed to the temporal lobe. Ventral stream is identified with perceptual identification (the “*what*” pathway) while dorsal stream with action and visuo-motor control (the “*where*” pathway) (see Figure 14, Goodale and Milner 1992). Noteworthy, even though the two streams are separated processing channels, numerous interactions exist between them (Wang *et al.* 1999; McKyton and Zohary 2007; Roe *et al.* 2012). Like V1, associative visual cortex exhibit retinotopic organization, yet less definite, especially in higher-order visual areas (van Essen and Zeki 1978; Sereno *et al.* 1995; Malach *et al.* 2002; Wandell *et al.* 2007; Wandell and Winawer 2011). The main sensory input to these regions is from the primary visual cortex (lemnthalamic pathway) with a secondary sensory input from the collothamic pathway (Nieuwenhuys *et al.* 2008).

Ventral stream

It is canonically considered that ventral stream processes information related to form and color and that it represents the continuation of the parvocellular pathway (Troncoso *et al.* 2011). Within this stream, information processed in V1 and V2 is relayed to areas like V4, V8, lateral occipital complex (LOC), fusiform gyrus (FG) and parahippocamic gyrus (PH). V4 was considered the area for colour perception as suggested by animal studies, but in humans this view is contested and presumed that color information is processed in more anterior areas such as V8. (Bartolomeo *et al.* 2014). V4 is however central for the figure-ground segmentation. It integrates multiple stimulus properties like contour, shape, texture, motion, disparity through bottom-up salience-driven attentional mechanisms or top-down, proactive, spatial and feature selection (Reynolds and Desimone 2003; Qiu *et al.* 2007; Poort *et al.* 2012; Roe *et al.* 2012; Schmid *et al.* 2013). LOC participates both in object identification and the spatial information related to objects (Malach *et al.* 1995; Larsson and Heeger 2006; McKyton and Zohary 2007; Malikovic *et al.* 2016). FG contains several subdivisions involved in word, object, body and face recognition (Kanwisher 2001; Dehaene and Cohen 2011; Caspers *et al.* 2013a; Caspers *et al.* 2013b; Lazzarino De Lorenzo *et al.* 2014). A subdivision of PH, the “*parahippocampal place area*” (PPA) participates in place scene and large objects identification (Kanwisher 2001). The “*extra body area*” (EBA), located in the lateral temporal cortex processes information related to the different body parts (Taylor *et al.* 2007; Weiner and Grill-Spector 2011).

Dorsal stream

Canonically, dorsal stream continues the magnocellular pathway at cortical level and process information related to motion, spatial representation and visuo-motor coordination. Within this stream, information originating in V1 and V2 is conveyed to MT/V5, V3d, V3A and further into parietal regions. MT is an area central for movement processing and receives sensory input from V1/V2, koniocellular layers of LGN and the collothalamic pathway (Nieuwenhuys *et al.* 2008). Areas V3d and V3A are involved in various aspects of motion perception including the extraction of kinetic contours, chromatic motion perception and 3D form-from-motion (Vanduffel 2002; Zeki *et al.* 2003; McKeefry *et al.* 2010). V6 area responds to unidirectional motion, has strong preference for coherent motion and participates in the detection of object and self-motion (Pitzalis *et al.* 2010; Pitzalis *et al.* 2012).

Dorsal and ventral visual streams

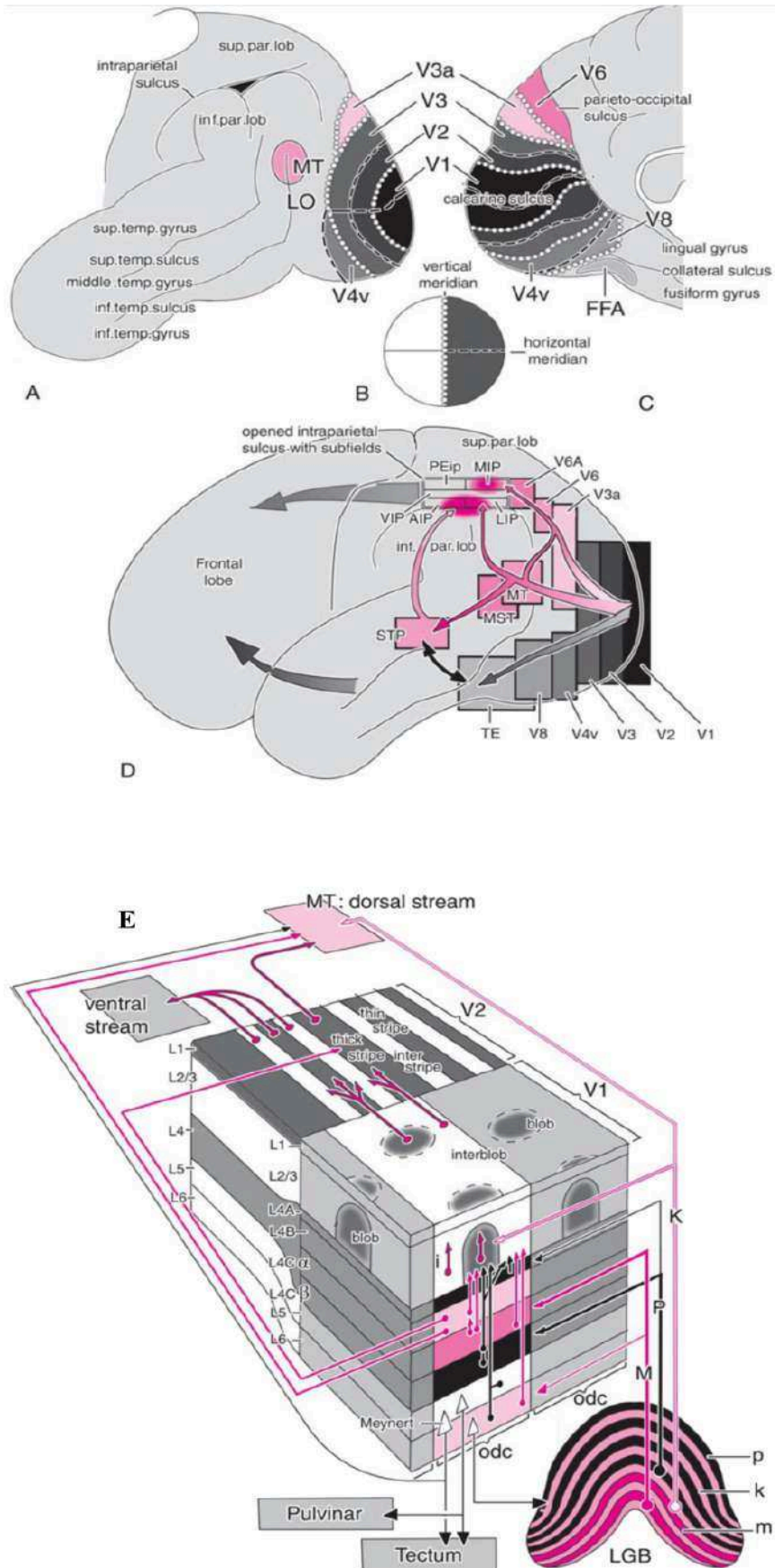


Figure 14 – Ventral and dorsal visual streams. A, B. Boundaries and retinotopical organization of visual areas. A – lateral view; B – medial view. **C** – Diagram of the visual field. Dotted line codes the vertical meridian and the dashed line the horizontal meridian. Note correspondent retinotopic representation of meridians in A. **D.** Diagram of the dorsal and ventral visual streams. Color code: red – dorsal stream; gray – ventral stream; black – V1; dark gray – V2. **E.** Diagram of the origin of dorsal and ventral streams. Both ventral and dorsal stream originate in V1 or V2. Magnocellular (black, M, m), parvocellular (red, P,p) and koniocellular (red contour, K, k) pathways originate in the correspondent layers of the lateral geniculate body (LGB). Main direct and indirect projections of M pathway end up in V1 layers 4C and 4B. From 4B M pathway projects onto the thick stripes of V2 and onto middle temporal area (MT) of the dorsal stream. M, P and K pathways combine in the and interblobs of V1’s layer 2/3. Thus, local projections (i) and remote projections of layer 2/3 via the thin and thick layers of V2 into dorsal and ventral stream carry mixed M, P and K signals. The intrinsic connections are shown for one ocular dominance column (odc). Meynert cells, involved in motion detection and located in small clusters in the V1’s L5/L6 layers boundary, in the region containing the representation of the far periphery projects both to superior colliculus and MT area. K pathway also send direct projections to MT area. AIP- anterior parietal area; FFA – fusiform face area; inf.par.lob – inferior parietal lobule; LIP – lateral intraparietal area; LO – lateral occipital area; MST – medial superior temporal visual area; MIP – medial intraparietal area; PEip intraparietal part of area PE; STP – superior temporal polysensory area; sup.par.lob- superior parietal lobule; TE – inferior temporal area; V1-V6A, V8 - visual areas; VIP – visual intraparietal area (from Nieuwenhuys *et al.* 2008).

Overview

Ventral and dorsal streams are canonical models based on the “*three paths*” model and therefore inherit its flows. Roughly, the ventral stream has identification attributes and the dorsal stream localization attributes.

2.2.5 Brain’s non-perceptual light processing

We proposed at the beginning of the first chapter (Chapter 1.1) a definition of vision, namely that it represents a system that recognizes and extracts information from light. Information extraction should by no means be reduced to spatial frequency, position and wavelength that following processing result in visual percepts. In all bilaterians, the “*perceptual*” facet of vision is coupled with at least another facet that synchronizes physiological functions to the environmental light periods. It is a more “*silent*” type of vision, one that does not emerge explicitly into conscience.

In vertebrates, regulatory, synchronizing photoreception even disposes of its own “*eye*” - the pineal complex - with most developed exponents in certain reptilians where they present a cornea, lens and retina (Ralph 1975). Interestingly, the most developed reptilian pineal complex is encountered in reptilians living at higher latitudes, while those with underdeveloped pineal complexes grouped mostly around the equator (Ralph 1975). It is currently believed that one of the roles of this complex is thermoregulation (Ralph 1975; Cipolla-Neto *et al.* 2014); even in mammals and humans, which have a rudimentary pineal gland, melatonin (the main pineal hormone) activates the highly metabolic brown adipose tissue that converts energy into heat (Tan *et al.* 2011). Noteworthy, the pineal complex is a part of the “*photosensitive vertebrate brain*” that also includes deep septal and hypothalamic photosensitive nuclei (Vigh *et al.* 2002). If strong evidence supports the deep-brain photoreception in non-mammal vertebrates (Peirson *et al.* 2009), in mammals evidence for true deep-brain photoreception remains largely circumstantial (Fernandes *et al.* 2013). This peculiarity in mammals was related to the presumed evolutionary “*twilight (mesopic) bottle-neck*” (see also Chapter 1.2.1, Davies *et al.* 2012), when deep-brains photoreceptors diminished or even lost light sensitivity, their physiological role being roughly taken over by retina presumably to maximize function in a poorly-lit environment (Heesy and Hall 2010; Fernandes *et al.* 2013). In humans, photoperiodicity was suggested by sleep disturbances in night shift work, seasonal depression and jet-lag (Vigh *et al.* 2002). Moreover, several studies on night-shift workers suggested an increased risk for cancer (Schernhammer *et al.* 2001; Schernhammer *et al.* 2003), vascular disorders (Kawachi *et al.* 1995; Chen *et al.* 2010), obesity (Chen *et al.* 2010) and decreased cognitive performance (Maltese *et al.* 2016).

Non-perceptual, regulatory and synchronizing photosensitive brain is a part of the periventricular cerebrospinal fluid (CSF) contacting neuronal system (Vigh *et al.* 2002) that belongs to the circumventricular organs (Vigh and Vigh-Teichmann 1998). Interestingly, CSF- contacting neurons form the major population in echinoderm starfishes and the cephalocordate *Branchiostoma lanceolatus* (Vigh and Vigh-Teichmann 1998) arguing for the ancient phylogenetic nature of this part of the visual brain.

2.2.6 Action and the evolution of visual processing

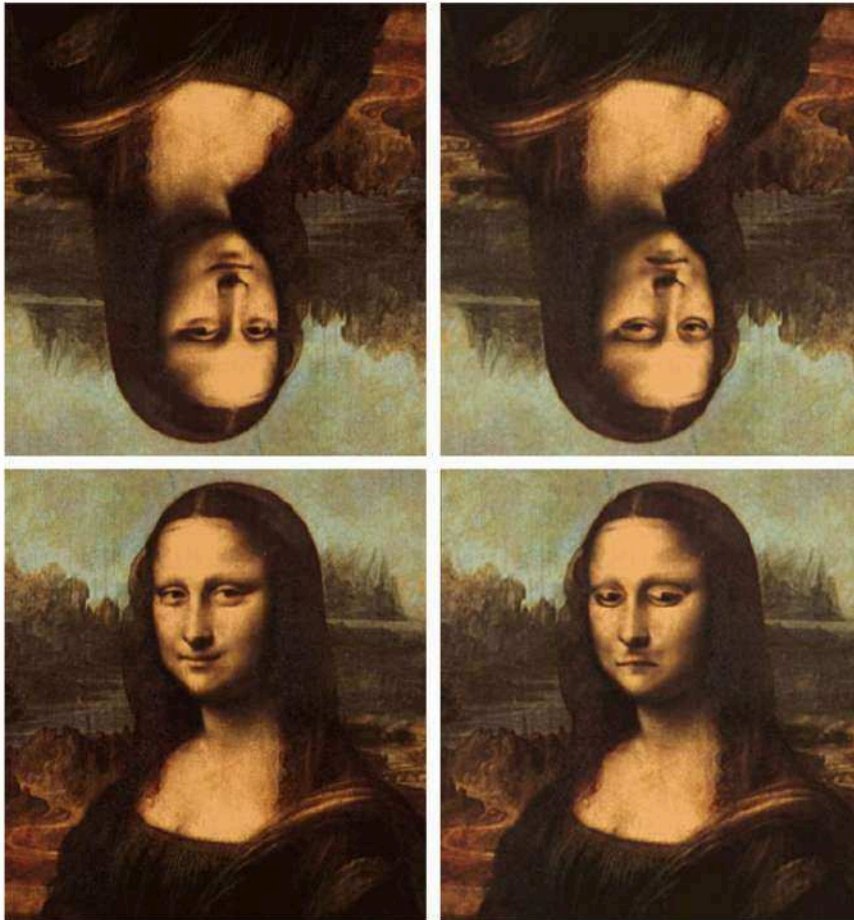
Brain continuously integrates information and unceasingly updates the ways it does it. Validated, constant patterns of information and the appropriate visuo-motor responses are imbedded in unconscious circuits. Therefore, most of the visual processing is unconscious and likely the main role of the “*perceptual*” vision (conscious) is to detect incongruences between the incoming signal and the expected pattern, to further orient processing (top-down control) and to orient action. However, important changes in the expected pattern may result in impaired performance as illustrated by difficult recognition of the grotesque version of da Vinci’s Mona Lisa when presented in an unnatural, “*upside-down*” position (see Figure 15A).

In mammals, more particularly in primates and hominids action also shaped the evolution of visual brain. As illustrated by Zhuangzi’s classical story of the skilled cook Ding, novel action requires sustained cognitive control, but once the optimal processing and response sequences are computed it became “*mindless*” (highly automatic) and precise (Cheng 1997). The use and design of complex tools, a defining particularity of *homo sapiens*, relays on visual integration and visuo-motor coordination. In contrast to some primates and birds that can display tool-assisted foraging, *homo sapiens* became a tool-dependent forager (Plummer 2004). Tools-handling requires complex computations crucial for the appropriate body-tool and body-tool-environment interactions. Within the conceptual framework offered by theory of extended mind (Clark 2013), Bruner and Iriki (Bruner and Iriki 2016) proposed that tools-handling “*embodied*” tools and tool-action extending thus the peripersonal space, the world and the mind. It is believed that mastering tools determined cerebral adaptive morphological changes affecting especially the parietal lobe, namely longitudinal and lateral bulging of the parietal lobes (Bruner and Iriki 2016). Theses changes affected especially the precuneus, area with an important role in visuo-spatial integration (Bruner *et al.* 2016; Pereira-Pedro and Bruner 2016).

Tool-design tool-handling and the development of language, with the later possibly emerging from the first (Hewes *et al.* 1973) further enlarged mind and the conscious domain. This expansion of mind affected also the range perceptual experience and most interesting, in the case of impairment in information processing, determined various types of altered perceptual experience (see Figure 15B, ffytche 2007).

Different aspects of visual perception

A. Perception accuracy in ecological and non_ecological, in unusual display



C. Neurophenomenological classification of perceptual visual experience

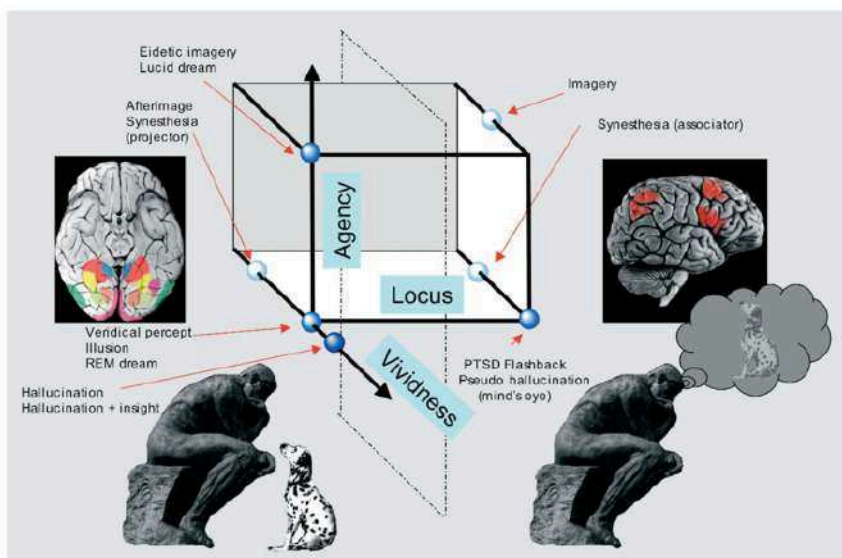


Figure 15 – Aspects of visual perception. A. Abnormal perceptive accuracy when visual input is presented in a non-ecological way (i.e. upside-down). **B.** Neurophenomenological classification of human perceptual experience presented in a 3D spaces: x axis – perceptual locus (external perception or in the “mind’s eye); y – vividness (color saturation, definition); z axis – agency (volitional control). To the left of the vertical, dotted plane are depicted visual experiences related to activity that predominates in specialized visual cortex, while to the right of the vertical plane are depicted visual experiences related to activity that predominates in parietal and frontal areas (from <https://www.exploratorium.edu/exhibits/mona/mona.html> and ffytche 2007)

Visual loss

3.1 Models of visual loss

The concept of visual loss subtends a large spectrum ranging from total blindness to the “*exotic*” loss of certain visual functions like prosopagnosia (incapacity to recognize faces), alexia (incapacity to read) or akinetopsia (incapacity to recognize certain types of movement). Disorders affecting lemnothalamic visual pathways up to V1 result in a specific configuration of visual field defects. Lesions to retina and optic nerve may result in the complete loss of the central or peripheral vision. Due to their different structure and function, the loss of central or peripheral vision determines different disabilities. Herein, we preferred to focus on two retinal disorders that specifically affect photoreceptors and therefore spare the inner retina – *Stargardt macular dystrophy* and *pigmentary retinopathy*. These disorders induce very structured visual field defects that allow the selection of clinically homogenous patients groups. Moreover, the selected forms of retinal dystrophies are restricted to retina and not associated with widespread cerebral neurodegenerative alterations, allowing for an unambiguous evaluation of the cerebral reorganization following central and peripheral visual loss.

3.1.1 Central visual field loss – Stargardt macular dystrophy

Stargardt macular dystrophy (SMD), initially described by Stargardt in 1909, is the most common juvenile-onset macular dystrophy with a prevalence of 1/10000 (Stargardt 1909; Meunier and Puech 2012); it induces slow, progressive, symmetrical visual loss. Eye fundus shows bilateral, beaten bronze-like pigmentary changes in the macula and pisciform shaped, yellow-white flecks at the level of the retinal pigment epithelium called “*fundus flavimaculatus*” (see Figure 16, Franceschetti 1963). The mutation of the ABCA4 gene (on the chromosome 1p13–p21) is the cause of SMD. It codes for an “*ATP binding cassette*”, a flippase that intermediates the clearance of all-trans-retinal after the photoexcitation of rhodopsin and prevents the accumulation of toxic by-products, namely bis-retinoid, N-retinylidene-N-retinylethanolamine (A2E) (Meunier and Puech 2012; Sahel *et al.* 2015). Retinal pigment epithelium fagocitates A2E that induces its degeneration, and consequently the death of photoreceptors. Degeneration is focused on the macular region due to the high concentration of cones and rods in the foveal and parafoveal region



Figure 16 – Eye fundus – Stargardt macular degeneration. Note the beaten bronze-like pigmentary changes in the macula and “fundus flavimaculatus” - the pisciform shaped, yellow-white flecks at the level of the retinal pigment epithelium.

(Meunier and Puech 2012). If the extent of the spared peripheral field allows sufficient sampling of the visual world and appropriate orientation and navigation, its low spatial resolution impairs drastically reading, object and face recognition (Safran *et al.* 1999b; Boucart *et al.* 2010; Calabrèse *et al.* 2014). Moreover, the loss of the central vision compels SMD patients to fixate in the peripheral retina, in the vicinity of the field defect (Duret *et al.* 1999).

3.1.2 Peripheral visual field loss – pigmentary retinopathy (retinitis pigmentosa)

Firstly described by Donders in 1857, pigmentary retinopathies are heterogeneous, blinding hereditary disorders with more than 22 genes involved in autosomal dominant, 34 in recessive and 2 in X-linked forms and a prevalence of 1/4000-5000 (Audo *et al.* 2012). They are characterized by progressive visual loss beginning in the periphery of the visual field (Donders 1857; Audo *et al.* 2012; Sahel *et al.* 2015; Rahman and Shah 2016); degeneration starts with and mainly affects rods (Audo *et al.* 2012). Early stages present nyctalopia and loss of the peripheral vision while advanced stages exhibit progressive decrease in central vision and ultimately, blindness. Eye funds shows vessel attenuation, bone spicule-like pigmentary deposits in the peripheral retina in early stages (see Figure 17) and waxy optic disc pallor, cystoid macular edema and pigmentary deposits involving the macula in advanced stages (Rahman and Shah 2016).

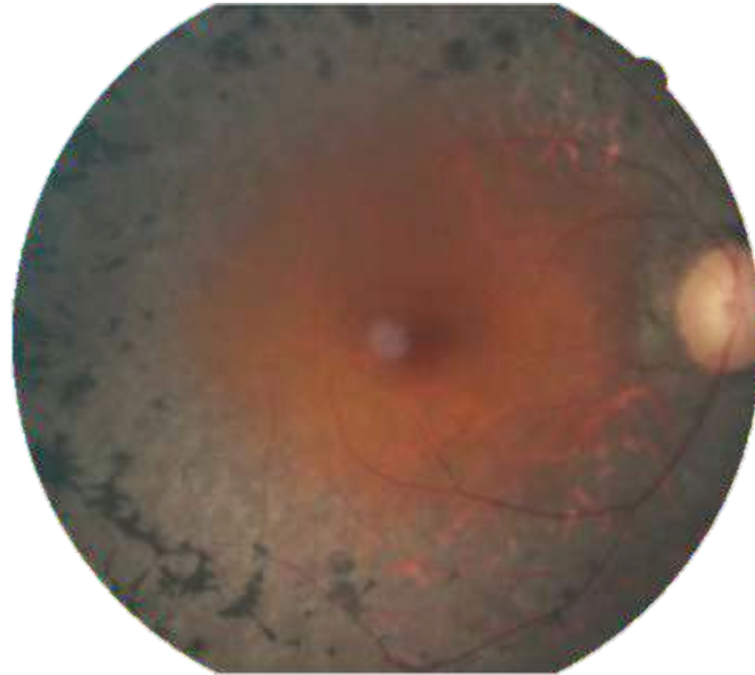


Figure 17 – Eye fundus – Pigmentary retinopathy (retinitis pigmentosa). Note vessel attenuation, bone spicule-like pigmentary deposits in the peripheral retina and waxy optic disc pallor.

In intermediate stages when the periphery is lost but the central vision is yet spared, patients experience a narrow visual field, a condition called “*tunnel vision*”. They preserve certain functions related to the high visual acuity in central vision like face and small object recognition. However, due to the severely restricted coverage of visual field exhibit difficulties in scene perception (Fortenbaugh *et al.* 2007), spatial orientation (Wittich *et al.* 2011), altered postural control (Berencsi 2005), increased object-collision risk during walking (Turano *et al.* 2002) and consequently reduce walking speed and independent navigation (Turano *et al.* 1999; Authié *et al.* 2016). Moreover, the restricted visual field excludes the use of covert visual attention and constrains the patients to increase their saccade rate and laboriously explore the environment (Authié *et al.* 2016).

Overview

Stargardt macular degeneration and pigmentary retinopathy constitute excellent models to study the cerebral plasticity induced by central and peripheral visual loss for several reasons: both are disorders affecting photoreceptors; visual field defects induced by one of these conditions can roughly be superposed on the spared visual field of the other and conversely; in non-syndromic forms, they are not known to associate widespread neurodegeneration.

3.2 Plasticity induced by visual loss

3.2.1 Retinal plasticity following photoreceptor loss

Like in other central nervous system degenerations, deafferentation also activates remodelling in retina. Therefore, neuronal remodelling is a common feature in all photoreceptor degenerations. Retinal degenerations often result in photoreceptors loss regardless of the site of the initiating dysfunction or the genetic defect. The ensuing deafferentation of the neural retina suppresses the intrinsic glutamatergic drive and eliminates the coordinated Ca^{2+} -coupled signalling to neural retina (Jones *et al.* 2003; Jones and Marc 2005).

In mammal models of rod-cone retinal degeneration, reorganisation can be divided into three phases (see Figure 18, Marc *et al.* 2003; Jones and Marc 2005). *Phase I* represents the initiating event that is responsible for rod insult, the loss of their outer segments and ultimately their death. During the initial stress and the loss of the outer segments, rods neurites sprout and enter the inner retina down to the ganglion layer. In *phase II*, cones start to degenerate by losing their outer segments, redistributing cone opsins into the inner segments and projecting transient extensions into the inner retina. Cones finally die due to multiple factors : metabolic, trophic and inflammatory. Following rods and cones death, deafferented bipolar and horizontal cells retract most of their dendrites. Dendrite truncation in rod bipolar cells induces changes in their macromolecular phenotype and transduction pathway, while horizontal cells develop anomalous axonal processes and dendritic stalks that enter the inner plexiform layer. Later, cones loss induces Müller cells to elaborate a dense fibrotic layer in the subretinal space, sealing the remnant outer retina from the choroid. If bipolar cell death starts in phase II, depletion of all neuronal classes is obvious in *phase III*. With time and the evolution of the retinal disorder (years), more and more neurones are lost and patches of ganglion cells can completely lose their afferent connection. This phase is also marked by the remodelling activity in the synaptic terminals of the surviving neuronal cells. Some can elaborate new neurites that travel long distances beneath the glial seal and form with other types of processes microneuromas in the inner nuclear layer and cryptic connections through the retina. Moreover, some bipolar and amacrine cells are displaced into the former ganglion cell layer while other amacrine cells are everted to the distal glial seal through the inner nuclear layer (Marc *et al.* 2003; Jones and Marc 2005). The new circuits engaged by bipolar, amacrine and ganglion cells are likely corruptive, manifesting as re-entrant, oscillatory, but visually fictive mechanisms (Jones *et al.* 2003; Marc *et al.* 2003; Marc and Jones 2003; Jones and Marc 2005).

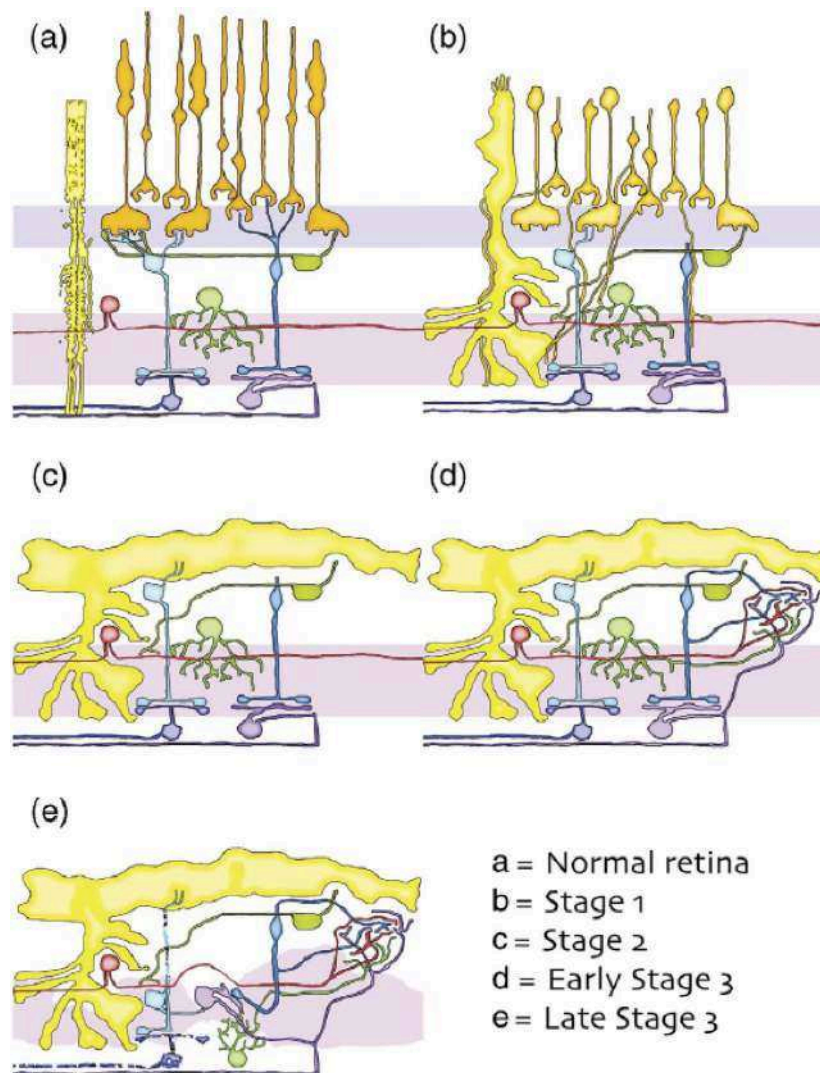


Figure 18 – Diagram depicting the three stages of retinal degeneration and consecutive retinal reorganization. (a) normal lamination and connectivity of retinal cells. (b) *Stage 1* - photoreceptor stress; outer segments shortening; rod, cone and horizontal cells neurite projections to the inner retina; dendrite retraction in rod and cone bipolar cells; early stage of Müller cells hypertrophy. (c) *Stage 2* - complete photoreceptor loss and elaboration of Müller cells seal between retina and choroid. (d) Early stage 3 - complex neurites extensions evolved in complex tangles called microneurinomas and formed by GABAergic and glycinergic amacrine cells, bipolar and ganglion cells. Microneurinomas exhibit active synapses corruptive of normal signalling. (e) *Late stage 3* - final stage exhibiting degeneration and death of various retinal cells; note the bidirectional cell migration from inner nuclear and ganglion cell layers. Color code: yellow - Müller cells; orange - normal photoreceptors; light orange - degenerated photoreceptors (b); light blue - cone bipolar cells; dark blue - rod bipolar cells; dark green - horizontal; light green glycinergic amacrine cells; red - GABAergic amacrine cells; violet ganglion cells (from Jones and Marc 2005)

Overview

Plastic changes in visual loss due to photoreceptor disorders begin at the very retinal level and include dramatic alterations in its neural circuitry.

3.2.2 Cerebral plasticity following visual loss

Canonically, cerebral plasticity canonically is viewed as an inherited dynamic capacity to undergo maturation, to organize and change functionally and structurally in response to experience and to adapt following injury (Ismail *et al.* 2016). Therefore, plasticity represents brain's response to change and it is balanced by homeostatic mechanisms that assure the stability of neural networks (Dennis *et al.* 2013). However, not all plasticity is beneficial and could lead to some maladaptive outcomes depending on factors like the extent and localization of the neuropathological process, the age of onset and the integrity of homeostatic mechanisms (Dennis *et al.* 2013; Tomaszczyk *et al.* 2014; Ismail *et al.* 2016). Conceivably, maladaptive changes, the "*dark side*" of plasticity, represent a non-intended side effect, similar to "*the spandrels of Saint Marco*" (Gould and Lewontin 1979; Nava and Röder 2011; Dennis *et al.* 2013).

Plastic capacity differs between the developing and the adult brain. Multiple clinical observations supporting children's enhanced learning and memory capacity (Klein *et al.* 2014; Li *et al.* 2014), easy acquisition of complex motor skills (Barrett *et al.* 2013) and the recovery after major brain injuries (Kastrup *et al.* 2000) indicate that developing brain has a better intrinsic capacity for plasticity than adult brain (Ismail *et al.* 2016). However, this increased plastic capacity in young age may also associate more debilitating and long-lasting maladaptive plastic effects (Dennis *et al.* 2013). Of particular interest for the young age plasticity are the critical periods - time points in development with high impact on neurogenesis, brain sculpting and learning (Hubel and Wiesel 1963). It is important to underline that there are multiple critical periods for different domains of the same sense (Dennis *et al.* 2013) In the case of human vision, the sensitive period for the development of global motion starts early after birth and ends around the first year of life, for visual acuity starts around 10 days after birth and ends around 10 years of age and for peripheral vision starts at birth and lasts until the early teenage years (Lewis and Maurer 2005). Developmental sensitive periods are followed by periods of vulnerability when the sensory system is adult-like but yet flexible and sensitive to sensory deprivation (Levi 2005; Lewis and Maurer 2005).

Overview

During development and the following “*flexible period*” brain tunes-up its networks and promote specialization. Plasticity, the intrinsic response capacity to change of the nervous system, is bridled by homeostatic mechanisms that ensure stability and is not restricted to early life but persists throughout the entire life span. Noteworthy, not plasticity alone, but the balance between plasticity and homeostatic mechanisms is responsible for positive or undesired outcomes of brain organization or reorganization. During the lifespan the functional duplex “*plasticity-homeostatic mechanisms*” exhibit different dynamics depending on the state of the neural networks and the degree of specialization.

3.2.3 Cerebral plasticity and MRI

Functional specialization and segregation in brain lays on an anatomical base that stretches from molecular level, up to complex neural systems. Cytoarchitectonic areas represent functionally relevant units in the cerebral cortex, their basic features being the specific regional and laminar distribution of diverse types of projection neurons and interneurons that characterize specific sensory, motor and associative brain regions. Fiber tracts connect different cytoarchitectonic areas and represent the foundation of the functional connectivity (Zilles and Amunts 2015). Available methods to asses in vivo, in humans, the morphology of gray matter are usually the voxel-based morphometry (VBM) and cortical thickness measurement (CoTks), while for the white matter - fiber tracts diffusion tensor imaging (DTI) or diffusion weighted images (DWI). These methods are currently used to explore neuroanatomical correlates both in normal brain and in neurological disorders. (Hutton *et al.* 2009).

The specific cellular mechanisms underlying the variations in cortical thickness as measured by MRI could be related to different factors like neuronal apoptosis, variations in cortical myelination, alterations in synaptic complexity or the summation of these events (Burge *et al.*, 2016; Zilles and Amunts, 2015). Thus, to understand the meaning of the cortical thickness variations, the assessment of these factors through complementary approaches is required. Magnetization transfer ratio imaging (MTR) reflects the presence of large lipid macromolecules and therefore of the myelin. It provides a reliable method to identify and quantify changes in cerebral tissue myelin content due to demyelination or

remyelination (Schmierer *et al.* 2004; Giacomini *et al.* 2009). The functional MRI entropy measured during resting-state (CoEn), a method derived from information theory, represents an indirect measure of the neural and synaptic complexity (Tononi *et al.*, 1998). In this approach increase in the cortical entropy relates to higher connective properties, while reduction in cortical entropy imply synaptic and dendritic degeneration (Sokunbi *et al.*, 2011; Thiebaut de Schotten *et al.*, 2016; Yao *et al.*, 2013).

DTI combined with tractography represents an exquisite approach allowing to visualise white tracts in vivo. However, this approach has several limitations: DTI spatial resolution and the histologic properties of the cortical ribbon with its small, low myelinated fibres prevent the accurate identification of tract origin; fibres intermingle in large tracts (i.e. corpus callosum) misleads the identification of both their origin and destination; “kissing” or “crossing” fibres can led to errors in fibres tracking that are still incompletely solved by the available algorithms (Zilles and Amunts 2015).

Several MRI approaches allow the assessment of functional plastic changes following sensory loss. The most employed is the task-based *fMRI* that quantifies the BOLD signal (blood oxygenation level dependent) in the cerebral cortex following the execution of a specific task (e.g. colour or word identification). Another approach is the resting-state *fMRI*, a very low-demanding method, also based on the BOLD signal that quantifies spontaneous fluctuations of regional brain activity at rest (without performing any task) (Biswal *et al.* 1995). Resting-state fluctuations are well-organized into networks, identified during a variety of cognitive tasks (Biswal *et al.* 1995; Greicius *et al.* 2003; Hampson *et al.* 2004; Damoiseaux *et al.* 2006; Fox *et al.* 2006; Dosenbach *et al.* 2007; Vincent *et al.* 2008; Smith *et al.* 2009; Spreng *et al.* 2010; Buckner *et al.* 2013). Theses fluctuations are sufficiently specific be be used for the extraction of retinotopic or mototopic maps both in health and disease (Butt *et al.* 2013; Bock *et al.* 2015; Butt *et al.* 2015; Striem-Amit *et al.* 2015; Zeharia *et al.* 2015).

Overview

MRI techniques, such as cortical morphometry, DTI, task-based *fMRI*, resting-state *fMRI* are available for in vivo evaluation of the plastic changes induced by visual loss.

3.2.4 Cerebral plasticity in early blindness

Numerous studies treat the cerebral reorganization following the early blindness and suggest that it induces complex plastic changes (Pascual-Leone *et al.* 2005). However, in the available literature “*early blindness*” is a fuzzy concept in what concerns the age of blindness. As developed in the previous chapter, the various sensitive periods have different dynamics and plastic potential. Therefore, a real congenitally blind subject may have significant differences in brain structure and functional connectivity, compared with a subject that loses vision when 6 months or 1-year-old. Therefore, the results of studies with inhomogeneous populations should be weighted with caution.

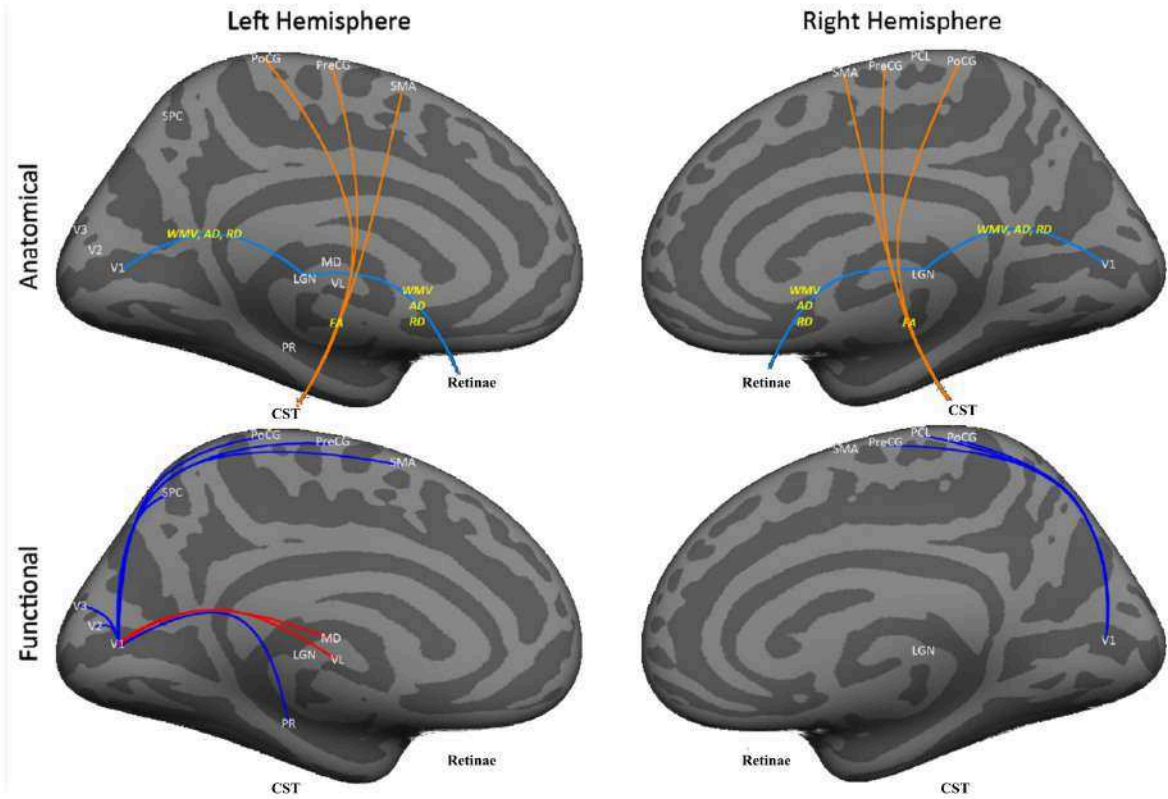
Subjects with early visual loss, compared to normally sighted, exhibit both enhancement of certain functions and deterioration of others (Bock and Fine 2014). They seem to have superior aptitudes in certain non-visual tasks like tactile acuity (Goldreich and Kanics 2003), pitch discrimination and sound localization (Gougoux *et al.* 2004; Gougoux *et al.* 2005) as well as higher-order tasks like speech discrimination (Niemeyer and Starlinger 1981), verbal memory (Amedi *et al.* 2003), tactile and auditory selective spatial attention (Collignon *et al.* 2006) and certain aspects concerning navigation (Fortin *et al.* 2008). Moreover, visual cortex in early blind presents enhanced functional connectivity with frontal areas involved in language (Liu *et al.* 2007; Butt *et al.* 2013) and attention (Burton *et al.* 2014; Wang *et al.* 2014; Striem-Amit *et al.* 2015; Qin *et al.* 2015). Increased non-visual aptitudes associate the activation of the visual cortex and suggest a reorganization allowing the intermodal reallocation of the processing capacity (Merabet and Pascual-Leone 2010; Ricciardi and Pietrini 2011). These peculiarities, together with a similar visual brain organization in early blind and normally sighted (Dormal and Collignon 2011; Dormal *et al.* 2012; Striem-Amit *et al.* 2012; Striem-Amit *et al.* 2015) point that brain is rather organized in a function-specific manner designed to treat a particular type of information (i.e. motion, object form, word form, body parts) regardless of the type of sensory input (Pascual-Leone and Hamilton 2001; Amedi *et al.* 2001; Renier *et al.* 2010; Reich *et al.* 2011; Striem-Amit and Amedi 2014; Abboud *et al.* 2015).

Vision is essential for the build-up of certain representations like form or space and early visual loss impairs their development in other sensory modalities (i.e. tactile, auditory, Pascual-Leone *et al.* 2005). Moreover, diminished functional connectivity between visual cortex and somatosensory (Qin *et al.* 2013; Burton *et al.* 2014), motor, auditory and multisensory areas in early blind (Liu *et al.* 2007; Yu *et al.* 2008) supports this view (see Figure 19).

In terms of structural changes, atrophy of the visual pathways from the retina to early visual cortex (Ptito *et al.* 2008; Bridge *et al.* 2009; Shu *et al.* 2009), reduced occipito-temporal connections, increased occipito-frontal connections (Noppeney *et al.* 2005; Ptito *et al.* 2008; Shu *et al.* 2009) and increased cortical thickness of the early visual cortex

(Jiang *et al.* 2009; Park *et al.* 2009; Voss and Zatorre 2012; Anurova *et al.* 2014; Bock and Fine 2014) represent the most consistent findings in early blindness (see Figure 19). If the atrophy of the visual pathways can easily be explained by the lack of sensory input, the altered connections of the occipital cortex are yet poorly understood. They may be related to the different function devoted to occipital cortex in early blindness (Bock and Fine 2014). The thicker occipital cortex of these subjects might reflect reduced pruning of the juvenile exuberant connections and their persistence in adult life as suggested by the fact that early visual input is a crucial factor in the selection of the relevant connections and the maturation of visual areas (Innocenti and Price 2005).

I. Long range projections



II. Intra-hemispheric corticocortical connections

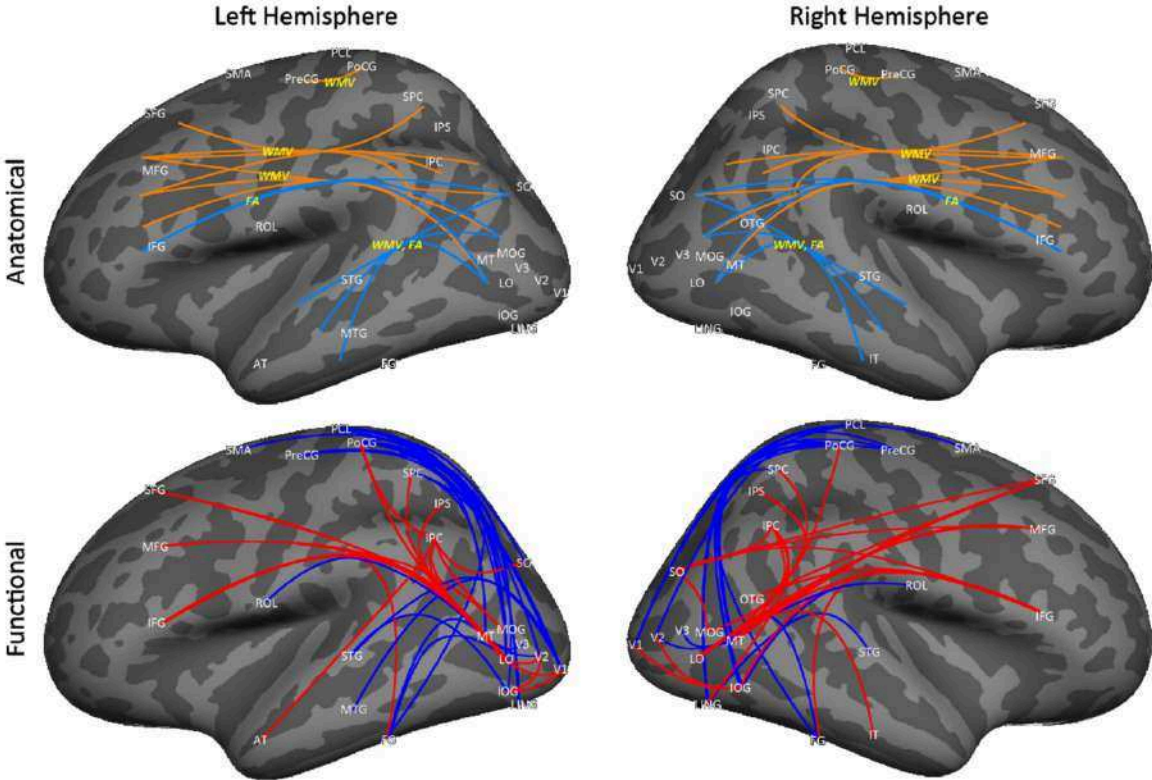


Figure 19 – Anatomical and functional plasticity in early blind. I. Long-range projections. **II.** Inter-hemispheric connections. Colour code: orange – increase in anatomical connectivity; teal – decrease in anatomical connectivity; red – increase in functional correlations; blue – decrease in functional correlations. Method abbreviations (yellow): AD - axial diffusivity; FA - fractional anisotropy; RD - radial diffusivity; WMV - white matter volume. Regions abbreviations (white): AT - anterior temporal cortex; CST - corticospinal tract; FG - fusiform gyrus; IFG - inferior frontal gyrus; IOG - inferior occipital gyrus; IPC - intraparietal cortex; IPS - intraparietal sulcus; LGN - lateral geniculate nucleus; LING - lingual gyrus; LO - lateral occipital area; MD - medial dorsal nucleus; MFG - middle frontal gyrus; MOG - middle occipital gyrus; MT - middle temporal area; MTG - middle temporal gyrus; PCL - paracentral lobule; PreCG - precentral gyrus; PoCG - postcentral gyrus; PR - perirhinal cortex; ROL - rolandic cortex; SFG - superior frontal gyrus; SMA - supplementary motor area; SO - superior occipital cortex; SPC - superior parietal cortex; STG - superior temporal gyrus; V1 - Brodmann area 17; V2 - Brodmann area 18; V3 - Brodmann area 19; VL – thalamic ventral lateral nucleus (Bock and Fine 2014).

Overview

Early visual loss induces complex plastic changes resulting in enhanced aptitudes in certain domains and altered abilities in other domains that require visual input for development and specialization. Plasticity in early blindness also suggests that brain is organized in a function-specific manner and that sensory deprived areas may treat information issued from other sensory modalities.

3.2.5 Cerebral plasticity in late blindness

After several days of sensory deprivation (blindfolding), normally sighted individuals exhibit activation of visual cortex during auditory and tactile tasks, activation that is absent in normal conditions (Pascual-Leone and Hamilton 2001; Merabet *et al.* 2008). Moreover, in normally sighted individuals trained in Braille character discrimination, the repetitive transcranial magnetic stimulation of the visual cortex impaired Braille lecture only in subjects trained while blindfolded. However, the effect disappeared after 24 hours of visual exposure (Merabet *et al.* 2008). This experiment demonstrated that sensory deprivation induced a rapid, dramatic and transitory change in brain activity likely representing the unmasking of preexistent multimodal connectivity (Merabet *et al.* 2008). This pattern of connectivity, inhibited by visual input, might represent the background for adaptive changes following visual loss in adulthood. Indeed, late blind activate occipital areas in auditory (Kujala *et al.* 1997; Voss *et al.* 2006; Voss *et al.* 2008; Collignon *et al.* 2013), tactile (Cohen *et al.* 1999; Sadato *et al.* 2002; Burton *et al.* 2002; Sadato *et al.* 2004) and linguistic tasks (Amedi *et al.* 2003; Burton *et al.* 2003; Bedny *et al.* 2011b; Bedny *et al.* 2011a). This activity however is different from the one observed in early blind (Cohen *et al.* 1999; Burton *et al.* 2003; Goyal *et al.* 2006; Voss *et al.* 2008; Bedny *et al.* 2012; Collignon *et al.* 2013). In a recent study we explored the resting-state functional connectivity between Broca area and early visual cortex in normally sighted, blind individuals from pigmentary retinopathy and individuals with an intermediate stage of pigmentary retinopathy exhibiting concentric peripheral visual loss and preserved central “*tunnel vision*” (see Figure 20). Interestingly, we found that functional connectivity starts in deafferented early visual cortex, namely the peripheral V1 and progresses to the entire early visual cortex and certain extrastriate areas after the complete visual loss (Sabbah *et al.* 2016). The gradual increase in functional connectivity between Broca and visual cortex suggests that residual visual input limits the multimodal interactions between language and visual areas.

The presence of plasticity and especially of multimodal plasticity should be considered carefully both in sensory restoration and sensory substitution attempts, as it could both enhance and hamper their success. One example is the case of blind patients from pigmentary retinopathy fitted with camera-connected retinal prosthesis. As the head-mounted camera requires head movements to scan the environment, the vestibulo-ocular reflex inherently induces a misalignment between head and eyes impairing the perceptual localization of the generated image and the visuomotor coordination (Sabbah *et al.* 2014). To attenuate the impact of these effects, the patients are constrained to employ different strategies of visually guided movements.

In terms of structural changes, late visual loss seems to induce only a thinning of visual areas, mostly the early visual cortex (Park *et al.* 2009; Voss and Zatorre 2012; Voss *et al.*

2014) even though there are some controversies (Schoth *et al.* 2006; Jiang *et al.* 2009). In acquired, late blindness, optic tracts and optic radiations present reductions in fractional anisotropy that are likely dependent on the etiology of blindness, optic neuropathies being more likely to affect the retinofugal pathways (i.e. glaucoma) (Wang *et al.* 2013; Dietrich *et al.* 2015; Rokem *et al.* 2016). Interestingly, in late blind the Voss *et al.* (Voss *et al.* 2014) find a reduction of the magnetization transfer ratio, a marker of myelination, in the occipital areas with decreased cortical thickness, but these differences didn't survived after correction for multiple comparisons. The effects of late blindness on cortico-cortical connections is unclear. Several studies explored these connectivity: Wang *et al.* (Wang *et al.* 2013) found widespread alterations in corpus callosum, anterior thalamic radiations, frontal and parietal white matter regions, Reisleiv *et al.* (Reisleiv *et al.* 2016) noted instead a reduction in fractioned anisotropy in inferior longitudinal fasciculus and inferior fronto-occipital fasciculus while others found no difference in cortio-cortical white matter tracts between late blind and sighted (Schoth *et al.* 2006).

Overview

Plastic changes in blindness occurring after the maturation of visual function likely employs and reinforces preexisting pathways that are inhibited by the visual input in normally sighted. The effects of this plasticity are less dramatic than in congenitally blind as it develops in a mature system with stronger homeostatic mechanisms. Moreover, in late blind there are multiple controversies about how plasticity occurs. Understanding plasticity in these patients is crucial for the design of effective rehabilitation strategies, as well as sensory restitution or sensory substitution.

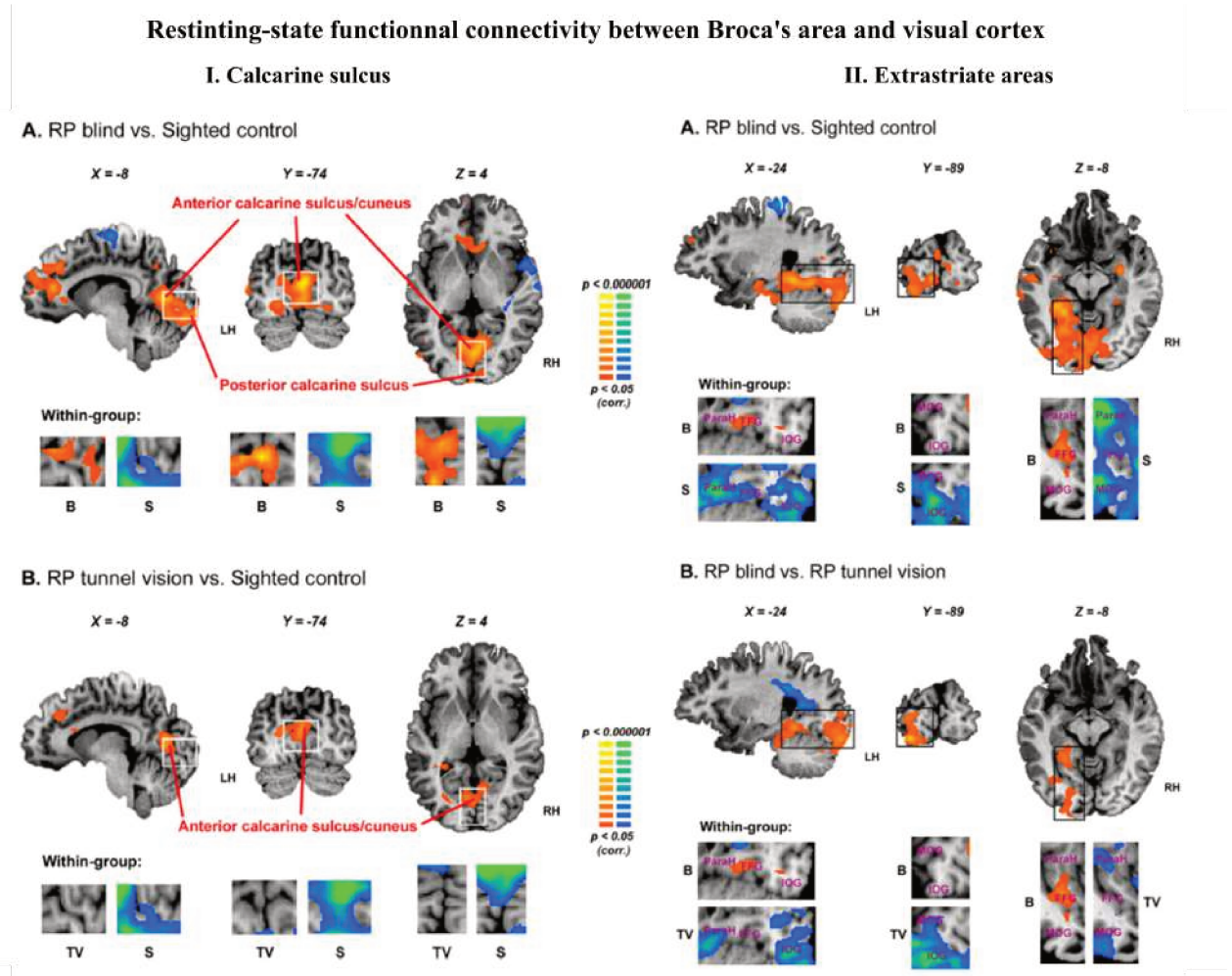


Figure 20 – Resting-state functional connectivity between Broca's area and visual cortex. I. Connectivity with primary visual cortex. **II.** Connectivity with extrastriate visual areas. B – blind; FFG – fusiform gyrus; IOG – inferior occipital gyrus; LH – left hemisphere; ParaH – parahippocampal gyrus; RH – right hemisphere; RP – retinitis pigmentosa; S – sighted (from Sabbah *et al.* 2016).

3.2.6 Plasticity in partial visual loss

In congenital defects limited to the central part of the visual field, namely in rod monochromats, Morland *et al* (Morland *et al.* 2001) and Baseler *et al* (Baseler *et al.* 2002) found evidence of cortical reorganization in the central V1 area. These populations however, due to congenital cone absence, present a visual system differently organized than normally sighted and an abnormal foveal structure (Fahim *et al.* 2013).

In acquired central visual defects a similar reorganization pattern in the visual cortex was claimed (Baker *et al.* 2005; Baker *et al.* 2008), but later challenged (Baseler *et al.* 2011). Other authors (Masuda *et al.* 2008; Dilks *et al.* 2009; Masuda *et al.* 2010) found that adults with either central or peripheral field defects exhibit only task-related activation of the deafferented regions of the visual cortex. Following these findings it was proposed that in partial visual loss, deafferented primary visual cortex contributes to higher-order mechanisms such as attention or mental imagery (Masuda *et al.* 2008; Dilks *et al.* 2009; Masuda *et al.* 2010). It was also suggested that deafferented primary visual cortex might intervene in multimodal sensory processing since in patients with acquired peripheral visual defects, crossmodal activation of V1 was proportional to the extent of the visual impairment (Cunningham *et al.* 2015).

Since partial visual loss generates sensory deprivation in a part of the visual cortex, structural alterations are also expected. Indeed, acquired central visual field defects associates gray matter thinning in the posterior part of the primary visual cortex (Boucard *et al.* 2009; Plank *et al.* 2011; Prins *et al.* 2016), while peripheral visual field loss apparently induces thinning of the anterior part of the primary visual cortex (Boucard *et al.* 2009; Yu *et al.* 2013; Hernowo *et al.* 2014). Moreover, in a study on patients with central visual loss, Burge *et al* found no overall cortical thickness reduction in V1, but noted decreased cortical thickness near the border of the scotoma projection zone, on deafferented side and increased cortical thickness on afferented side (Burge *et al.* 2016).

Overall, the literature on the reorganization of visual cortex following partial or total visual loss remains controversial and sometimes contradictory. In the available studies, factors such as the limited number of participants (Baker *et al.* 2005; Baker *et al.* 2008; Masuda *et al.* 2008; Dilks *et al.* 2009; Masuda *et al.* 2010; Baseler *et al.* 2011) and/ or heterogeneity in the extent of visual field defects in the samples (Baker *et al.* 2005; Baker *et al.* 2008; Masuda *et al.* 2008; Baseler *et al.* 2011) might have contributed to the divergent results and precluded comparisons between the functional reorganization induced by central and peripheral visual loss. To avoid these obstacles when assessing the way brain processes central and peripheral visual information in health and in disease - the lesional level, the etiology and the extent of visual defects should be comparable. Thus, in the studies described herein, we enrolled patients with central and peripheral visual field loss from retinal disorders affecting photoreceptors (Stargardt macular degeneration and

pigmentary retinopathy) and presenting comparable, converse visual field defects.

Overview

The literature on the reorganization of visual cortex following partial or total visual loss is controversial and sometimes contradictory. Better designs are required to assess the induced plastic changes.

3.2.7 Visual input and peculiar perceptive phenomena

As developed above, sensory input is crucial for the adequate cerebral wiring during development. Early, external fluctuations in sensory input or a particular genetic background modulating sensory input may result in different perceptive phenotypes, such as synesthesia (Safran and Sanda 2015). In synesthets, stimulation in a given sensory modality triggers additional experiences in one or multiple domains (Hochel *et al.* 2009). Concerned individuals have better performances in certain domains and worse in others. While visual synesthets have a better colour perception, they exhibit altered motion and speech perception (Banissy *et al.* 2013; McCarthy and Caplovitz 2014; Sinke *et al.* 2014). It is believed that brain wiring in synesthesia involves more short-range connections between sensory regions and less long-range connections with remote regions like the frontal cortex (van Leeuwen *et al.* 2011). This connectivity profile might be determined by the abnormal synaptic pruning due to anomalous sensory input (Safran and Sanda 2015).

In partial visual loss, a common form of illusion, namely the “*filling-in*”, occults the circumscribed visual field defects by completing them with a percept embodying visual attributes (i.e., luminance, contrast, texture, Safran and Landis 1996). However, the resulting percept is not accurate and the objects crossing the filled-in area may appear squeezed and distorted (Safran *et al.* 1999a; Mavrakanas *et al.* 2009).

An analogous visual completion phenomenon known as “*filling-out*” (Wittich *et al.* 2011) occurs with peripheral non-circumscribed field defects (e.g. those occurring in retinitis pigmentosa) and results in a stretching of perceived space and objects at the limit of the residual visual field (Temme *et al.* 1985; Dilks *et al.* 2007).

Acquired partial or total visual loss or even temporal visual sensory deprivation in normally sighted (blindfolding) may induce a particular type of visual hallucinatory phenomenon – the Charles Bonnet syndrome (Merabet *et al.* 2004; Singh and Sørensen 2012; O’Hare *et al.* 2015). Charles Bonnet syndrome has a particular perceptual pattern and the

restoration of the visual function, when possible, represents the best treatment (Santhouse *et al.* 2000; fytche 2005; fytche 2007) (see also Figure 15C).

Overview

Visual input has a major role in shaping visual pathways and normal visual perception. Disruption of visual input in early life or later in life may associate specific sensory phenomena like synesthesia, filling-in of visual field defects or hallucinations.

PART II

Experimental contributions

Morphological changes: “*Visual brain plasticity induced by central and peripheral visual field loss*”

Both central and peripheral visual loss generate sensory deprivation in the correspondent regions of the visual cortex. Therefore, it is expected that this deafferentation induces structural alteration. Several studies have explored the morphological changes developed following partial visual loss and found that disorders affecting the central visual field seem to induce thinning in the posterior, deafferented part of V1 (Boucard *et al.* 2009; Plank *et al.* 2011; Hernowo *et al.* 2014; Prins *et al.* 2016) and that disorders affecting peripheral visual field induce thinning in the anterior, deafferented part of V1 (Boucard *et al.* 2009; Yu *et al.* 2013; Yu *et al.* 2014). Interestingly, in a population with central visual defects of various etiologies, Burge *et al.* found no overall change in V1 cortical thickness, but noted cortical thickness alterations in areas adjacent to the border of scotoma projection zone, namely decreased cortical thickness on deafferented side and increased in cortical thickness on afferented side (Burge *et al.* 2016).

Herein, we studied the long-term effect of central and peripheral visual loss on the occipital lobe structure in two models of retinal degeneration described in the previous chapters – *Stargardt macular degeneration* and *pigmentary retinopathy* (retinitis pigmentosa). For this purpose, in a population composed of twelve subjects with Stargardt macular degeneration, twelve subjects with pigmentary retinopathy and fourteen normally sighted, we employed two complementary approaches – the measure of cortical thickness and of the cortical entropy. Cortical thickness can be influenced by various factors (e.g. neuronal apoptosis, variation in cortical myelination, the degree of synaptic complexity) therefore was interpreted in association with the cortical entropy a marker of neural and synaptic complexity. Increased entropy reflects higher connective properties and increased synaptic complexity (Sokunbi *et al.* 2013; Yao *et al.* 2013; Thiebaut de Schotten *et al.* 2016) while the reduction in entropy, synaptic and dendritic degeneration (Sokunbi *et al.* 2013). The occipital lobe was partitioned in the corresponding cytoarchitectonic regions, using cytoarchitectonic probability maps (Amunts *et al.* 2007; Zilles K 2010; Mohlberg *et al.* 2012).

Compared to normally sighted, we found that central visual field loss associates de-

creased cortical thickness in dorsal areas V3d and V3a while peripheral visual field loss determined more widespread alterations including thinning of the early visual cortex (V1 and V2), dorsal area V3d and ventral area V4. None of these areas had altered cortical entropy suggesting that the remaining networks exhibit preserved synaptic complexity.

The study of the occipital lobe cortical entropy revealed increased values in areas LO-2 and FG1 in central visual field loss compared with normally sighted and in FG1 compared with peripheral visual field loss. These areas are involved in object recognition and the observed differences may represent an adaptive increase in synaptic complexity to compensate the loss of the central vision and its high spatial resolution.

Résumé

- La perte de champs visuel central et périphérique produite par une atteinte rétinienne entraîne une déafférentation dans les régions correspondantes du cortex visuel. Par conséquent, on peut s'attendre à des anomalies structurelles dans ces régions. Plusieurs études ont exploré les altérations morphologiques induites par la déafférentation et ont démontré que la perte visuelle centrale s'accompagne d'un amincissement du cortex dans la partie postérieure, déafférentée du cortex visuel primaire (Boucard *et al.* 2009; Plank *et al.* 2011; Hernowo *et al.* 2014; Prins *et al.* 2016) et que la perte visuelle périphérique induit un amincissement dans la partie antérieure, déafférentée, du cortex visuel primaire (Boucard *et al.* 2009; Yu *et al.* 2013; Yu *et al.* 2014). Plus intéressant encore, en étudiant une population avec perte visuelle centrale causée par des étiologies variées, Burge *et al.*, retrouvent un amincissement du cortex visuel primaire seulement dans la vicinity de la limite du scotome, du côté déafférenté, et un épaissement cortical limité aux alentours des bords du scotome, du côté afférenté (Burge *et al.* 2016).
- Dans cette étude, nous avons étudié l'effet à long terme de la perte du champs visuel central ou périphérique sur la structure du lobe occipital, en employant deux modèles de dégénérescences rétinienne, que nous avons détaillés dans les chapitres antérieurs - *la maculopathie de Stargardt et la rétinopathie pigmentaire*. Dans un groupe de sujets composé de douze patients avec maculopathie de Stargardt, douze patients avec rétinopathie pigmentaire et quatorze contrôles avec une vision normale, nous avons évalué l'épaisseur corticale et l'entropie corticale. La mesure de l'épaisseur corticale peut être influencée par plusieurs facteurs (par ex. l'apoptose neuronale, des variations dans la myéline corticale, le degré de complexité synaptique), et par conséquent elle fut interprétée à l'aide de l'entropie corticale qui représente une mesure indirecte de la complexité neurale et synaptique. Une augmentation de l'entropie corticale traduit une amplification des capacités de connexion et de la complexité synaptique (Sokunbi *et al.* 2013; Yao *et al.* 2013; Thiebaut de Schotten *et al.* 2016), tandis qu'une diminution de l'entropie corticale, une dégénérescence synaptique et dendritique (Sokunbi *et al.* 2013).

Résumé

Pour réaliser ces mesures, en respectant l’anatomie et la cytoarchitecture du lobe occipital, nous avons conduit les analyses en utilisant des cartes cytoarchitectoniques de probabilité (Amunts *et al.* 2007; Zilles K 2010; Mohlberg *et al.* 2012).

- Par rapport aux sujets normovoyants, nous avons observé que la perte de la vision centrale induit une réduction de l’épaisseur corticale dans les régions V3d et V3a du flux dorsal, tandis que la perte de la vision périphérique induit des altérations plus complexes, en particulier un amincissement du cortex visuel primaire, du V2, de la région du flux dorsal V3d et la région du flux ventral V4. On note que l’entropie corticale ne présentait des modifications dans aucune de ces régions ce qui suggère que malgré une perte neuronale vraisemblable, la complexité synaptique des réseaux résiduels reste inchangée. L’étude de l’entropie corticale dans les mêmes régions cytoarchitectoniques a révélé que par rapport aux normo-voyants, les patients avec une perte du champs visuel central présentent une augmentation des valeurs de l’entropie dans les aires LO-2 et FG1, et que par rapport au sujets avec une perte de la vision périphérique, les sujets avec une perte de la vision centrale présentent une augmentation des valeurs de l’entropie dans l’aire FG1. Ces régions sont impliquées dans la reconnaissance des objets et les différences observées pourraient traduire une amplification de la complexité synaptique visant de compenser la perte de la vision centrale et sa haute résolution spatiale.

Visual brain plasticity induced by central and peripheral visual field loss

Nicolae Sanda¹⁻⁵, Leonardo Cerliani^{6,7}, Colas Niels Authié¹⁻⁴, Norman Sabbah¹⁻⁴, José Alain Sahel^{1-4,8-10}, Christophe Habas^{1-3,11}, Avinoam Bezael Safran^{1-4,12}, Michel Thibaut de Schotten^{6,7}

*For correspondence:

herrisanda@gmail.com (NS)

Present address: ¹Institut de la vision, 17 rue Moreau 75012, Paris, France

¹Sorbonne Universités, UPMC Université Paris 06, UMR S968, Institut de la Vision, Paris, F-75012, France; ²INSERM, U968, Institut de la Vision, Paris, F-75012, France; ³CNRS, UMR 7210, Institut de la Vision, Paris, F-75012, France; ⁴Centre d'investigation clinique, Centre Hospitalier National d'Ophtalmologie des Quinze-Vingts, INSERM-DHOS CIC 1423, Paris, F-75012, France; ⁵Service de neurologie, Hôpital Foch, Suresnes, France; ⁶Sorbonne Universités, UPMC Univ Paris 06, Inserm, CNRS, Institut du cerveau et la moelle (ICM) - Hôpital Pitié-Salpêtrière, Boulevard de l'hôpital, F-75013, Paris, France; ⁷Brain Connectivity and Behaviour group, Frontlab, Brain and Spine Institute, Paris, France; ⁸Institute of Ophthalmology, University College of London, United Kingdom; ⁹Fondation Ophtalmologique Adolphe de Rothschild, Paris, France; ¹⁰Department of Ophthalmology, The University of Pittsburgh School of Medicine, Pittsburgh, PA 15213, US; ¹¹Centre de neuroimagerie, Centre Hospitalier National d'Ophtalmologie des Quinze-Vingts, Paris, F-75012, France; ¹²Department of Clinical Neurosciences, Geneva University School of Medicine, Geneva, Switzerland

Abstract Disorders that specifically affect central and peripheral vision constitute invaluable models to study how human brain adapts to visual deafferentation. We explored cortical changes subsequent to the loss of central or peripheral vision. Cortical thickness (CoTks) and resting-state cortical entropy (*rs-CoEn*), as surrogate for neural and synaptic complexity, were extracted in twelve Stargardt macular dystrophy (SMD), twelve retinitis pigmentosa tunnel vision (RPTV) and fourteen normally sighted subjects. When compared to controls, both groups with visual loss exhibited decreased CoTks in dorsal area V3d. Peripheral visual field loss also showed a specific CoTks decrease in early visual cortex and ventral area area V4, while central visual field loss in dorsal area V3A. Only central visual field loss exhibited increased CoEn in LO-2 area and FG1. Current results revealed biomarkers of brain plasticity within the dorsal and the ventral visual streams following central and peripheral visual field defects.

Introduction

Vision is the most elaborated sensorial input in the human brain. Central vision is captured at retinal level by the macula, which samples about 20° of the central visual field and provides a high spatial resolution. The peripheral visual field is collected by the remaining of the retina and has a low spatial resolution. The distinction between central and peripheral vision is also maintained within the brain. Particularly, dorsal visual areas receive relatively more projections from areas

processing peripheral visual field representations, whereas ventral visual areas are more densely connected to those processing central representations (*Ungerleider and Desimone, 1986; Gattass et al., 2005*). Hence, the loss of central or peripheral visual field should impair in different ways the visual brain and its neuroanatomy. Yet, little is known on the anatomical consequences and compensation mechanisms occurring after central or peripheral visual deprivation.

Central visual field loss prevents the central fixation, compelling patients to employ strategies of fixation in the peripheral retina, near the limit of the field defect (*Duret et al., 1999*). Whilst the remaining of visual field allows for an appropriate spatial orientation and navigation, its low spatial resolution impairs drastically object, face recognition and reading (*Safran et al., 1999; Boucart et al., 2010*). Reversely, peripheral visual field loss excludes the use of covert visual attention, constraining the affected individuals to increase their saccade rate in order to laboriously explore their environment (*Authié et al., 2016*). Affected individuals preserve functions related to the high spatial resolution of the residual central vision like face and small objects recognition but exhibit impaired spatial orientation (*Wittich et al., 2011*) and scene perception (*Fortenbaugh et al., 2007*), altered postural control (*Berencsi et al., 2005*) and increased risk of object-collision during locomotion (*Turano et al., 1999, 2002*) due to the limited coverage of the residual visual field. However, little is known on the brain reorganization consequent to the adjustment of these behaviors.

Preliminary evidence suggests that following a visual defect, the deafferented primary visual cortex alters its connections and the residual afferented primary visual cortex reinforces preexistent functional connections (*Sabbah et al., 2017*). The latter is presumably an attempt to compensate for the loss of the former, to sustain higher order visual mechanisms. As central or peripheral visual loss generates sensory deprivation in a part of the visual cortex, structural alterations are also expected. This has been previously reported for central visual field defects associated gray matter thinning in the posterior part of the primary visual cortex (*Boucard et al., 2009; Plank et al., 2011; Hernowo et al., 2014; Prins et al., 2016*), while peripheral visual field loss induced thinning of the anterior part of the primary visual cortex (*Boucard et al., 2009; Yu et al., 2013*). However, above-mentioned studies evaluate disorders like glaucoma and age-related macular degeneration that are not limited to the eye but imply widespread neurodegenerative cerebral alterations (*McKinnon, 2003; Pham et al., 2006; Woo et al., 2012; Chen et al., 2013; Cheung and Wong, 2014*). Such approaches may have hampered the identification of differences strictly related to early visual deafferentation and further research on disorders restricted to the retina may clarify the brain modification occurring after a pure early visual deprivation.

In the current study, we investigated long-term brain changes associated to two well-described pure and progressive retinal disorders that induce bilateral, converse visual field defects – Stargardt macular degeneration, for central visual loss, and non-syndromic retinitis pigmentosa, for peripheral visual field loss. Stargardt macular degeneration is an hereditary cone-rod dystrophy that, in advanced stages, destroys the macular region, constraining affected individuals to rely only on the peripheral vision (*Stargardt, 1909*). Reversely, retinitis pigmentosa – a rod-cone dystrophy – primarily affects peripheral retina and results in a progressive constriction of the visual field. It leads to a “tunnel vision” stage, with retained central vision, and later, in the most advanced stage, to blindness (*Donders, 1857; Sahel et al., 2015*).

To evaluate the effects of the remote loss of central or peripheral vision, we estimated the cortical morphology derived from measures of cortical thickness (*Das et al., 2009*). However, the specific cellular mechanisms underlying the variations in cortical thickness remain obscure. They may be related to neuronal apoptosis, variations in cortical myelination, alterations of the synaptic complexity or a summation of these events (*Wagstyl et al., 2015; Zilles and Amunts, 2015; Burge et al., 2016*). To explain the eventual differences in cortical thickness we measured the functional MRI entropy during resting state session (*rs-CoEn*). *rs-CoEn* is a method derived from information theory, and linked to neural and synaptic complexity (*Tononi, 1998*). According to this approach, increased entropy corresponds to higher connective properties (*Sokunbi et al., 2011; Yao et al., 2013; Thiebaut de Schotten et al., 2016*), while the reduction in entropy may imply synaptic and

Table 1. Cytoarchitectonic areas showing significant differences in cortical thickness. NS – normally sighted; cVfL – central visual field loss (SMD); pVfL – peripheral visual field loss (RPTV). The significant differences are in BOLD.

Region	Mean CoTks ratio $\pm \sigma$			ANOVA			Multiples comparisons (Bonferroni corrected)		
	Groups			df	F	p	NS > cVfL NS > pVfL cVfL > pVfL		
	NS	cVfL	pVfL				p	p	p
Occipital RH	0.938 \pm 0.054	0.899 \pm 0.484	0.887 \pm 0.07	2, 35	2.716	0.08	-	-	-
Occipital LH	0.916 \pm 0.074	0.891 \pm 0.072	0.85 \pm 0.062	2, 35	2.873	0.07	-	-	-
hOc1	0.749\pm0.113	0.652\pm0.104	0.619\pm0.152	2, 35	3.882	0.03	-	0.036	-
hOc2	0.847\pm0.132	0.773\pm0.162	0.68\pm0.155	2, 35	4.051	0.026	-	0.022	-
hOc3d	0.835\pm0.093	0.707\pm0.084	0.722\pm0.109	2, 35	7.09	0.003	0.005	0.015	-
hOc3v	0.766 \pm 0.118	0.704 \pm 0.147	0.646 \pm 0.125	2, 35	2.794	0.075	-	-	-
hOc4d	0.817\pm0.122	0.715\pm0.094	0.736\pm0.083	2, 35	3.633	0.037	0.05	-	-
hOc4v	1.072\pm0.075	0.959\pm0.124	0.934\pm0.153	2, 35	5.013	0.012	-	0.017	-
hOc4la	1.155 \pm 0.105	1.184 \pm 0.12	1.106 \pm 0.1	2, 35	1.612	0.214	-	-	-
hOc4lp	1.181 \pm 0.19	1.083 \pm 0.145	1.134 \pm 0.146	2, 35	1.172	0.322	-	-	-
hOc5	0.976 \pm 0.198	1.039 \pm 0.128	0.876 \pm 0.156	2, 35	2.975	0.064	-	-	-
FG1	1.253 \pm 0.223	1.179 \pm 0.185	1.198 \pm 0.225	2, 35	0.43	0.654	-	-	-
FG2	1.278 \pm 0.182	1.282 \pm 0.087	1.233 \pm 0.19	2, 35	0.336	0.717	-	-	-
FG3	1.362 \pm 0.195	1.483 \pm 0.203	1.409 \pm 0.266	2, 35	0.971	0.389	-	-	-
FG4	1.597 \pm 0.192	1.591 \pm 0.107	1.52 \pm 0.17	2, 35	0.852	0.435	-	-	-

dendritic degeneration (Sokunbi et al., 2013).

To intimately respect its anatomy, the occipital lobe was partitioned in its corresponding cytoarchitectonic regions using cytoarchitectonic probability maps (Amunts et al., 2000; Malikovic et al., 2007; Rottschy et al., 2007; Mohlberg et al., 2012; Kujovic et al., 2013; Caspers et al., 2013; Lorenz et al., 2015; Rosenke et al., 2017). CoTks and rs-CoEn extracted from each of these regions were used to perform group comparisons.

Results

Cortical thickness analysis

The measured CoTks of occipital lobe cytoarchitectonic areas was normalized with the average CoTks of the occipital lobe. The ratio between each cytoarchitectonic area CoTks and the average CoTks of the occipital lobe was further employed in the subsequent analysis (Ferreira et al., 2016). ANOVA revealed a significant group effect for the cytoarchitectonic areas hOc1 [$F_{(2, 35)} = 3.882$, $p = 0.03$], hOc2 [$F_{(2, 35)} = 4.05$, $p = 0.026$], hOc3d [$F_{(2, 35)} = 7.09$; $p = 0.003$], hOc4d [$F_{(2, 35)} = 3.633$; $p = 0.037$], hOc4v [$F_{(2, 35)} = 5.013$; $p = 0.012$]. Left hemispheric regions did not differ significantly from right hemisphere regions [occipital LH, $F_{(2, 35)} = 2.873$, $p = 0.07$; occipital RH, $F_{(2, 35)} = 2.716$; $p = 0.08$]. Post-hoc independent-sample t-tests (Bonferroni corrected for multiple comparisons) are summarized in Table 1 and in the following paragraphs.

Visual brain CoTks in visual field loss compared to normally sighted

All the following post hoc comparisons were Bonferroni corrected for multiple comparisons.

Compared to normally sighted we found a significant reduction of CoTks in the dorsal region hOc3d for both central ($p = 0.005$) and peripheral ($p = 0.015$) visual field defects (see Table 1). In central visual field loss/ SMD we also noted significant reduction in dorsal area hOc4d ($p = 0.05$) (see Figure 1A.1, and Table 1) and in peripheral visual field loss/ RPTV in early visual cortex [hOc 1 ($p = 0.036$), hOc2 ($p = 0.022$)] and the ventral region hOc4v ($p = 0.017$) (see Figure 1A2 and Table 1).

Visual brain CoTks differences in central and peripheral visual field loss

There was no CoTks difference between central and peripheral visual loss (see Table 1).

Table 2. Cytoarchitectonic areas showing significant differences in resting-state cortical entropy. NS – normally sighted; cVfL – central visual field loss (SMD); pVfL – peripheral visual field loss (RPTV). The significant differences are in BOLD.

Region	Mean CoEn ratio $\pm \sigma$			ANOVA			Multiples comparisons (Bonferroni corrected)		
	Groups			df	F	p	NS < cVfL	NS / pVfL	cVfL > pVfL
	NS	cVfL	pVfL				p	p	p
Occipital RH	1.126 \pm 0.022	1.129 \pm 0.017	1.128 \pm 0.026	2, 35	0.082	0.922	-	-	-
Occipital LH	1.122 \pm 0.021	1.129 \pm 0.019	1.122 \pm 0.024	2, 35	0.43	0.654	-	-	-
hOc1	1.071 \pm 0.034	1.079 \pm 0.019	1.071 \pm 0.031	2, 35	0.367	0.696	-	-	-
hOc2	0.964 \pm 0.045	0.913 \pm 0.27	0.991 \pm 0.043	2, 35	0.771	0.47	-	-	-
hOc3d	0.946 \pm 0.079	0.944 \pm 0.078	0.903 \pm 0.073	2, 35	1.239	0.302	-	-	-
hOc3v	1.042 \pm 0.028	1.052 \pm 0.051	1.06 \pm 0.037	2, 35	0.693	0.507	-	-	-
hOc4d	0.911 \pm 0.048	0.91 \pm 0.106	0.839 \pm 0.104	2, 35	2.664	0.084	-	-	-
hOc4v	1.1 \pm 0.045	1.123 \pm 0.046	1.093 \pm 0.052	2, 35	1.356	0.271	-	-	-
hOc4la	1.117\pm0.029	1.144\pm0.02	1.136\pm0.025	2, 35	3.856	0.031	0.033	-	-
hOc4lp	1.08 \pm 0.029	1.096 \pm 0.03	1.095 \pm 0.035	2, 35	1.242	0.301	-	-	-
hOc5	0.096 \pm 0.066	1.016 \pm 0.036	0.974 \pm 0.064	2, 35	2.835	0.072	-	-	-
FG1	1.128\pm0.025	1.158\pm0.022	1.12\pm0.033	2, 35	6.566	0.004	0.025	-	0.005
FG2	1.091 \pm 0.06	1.1 \pm 0.052	1.087 \pm 0.062	2, 35	0.177	0.839	-	-	-
FG3	1.159 \pm 0.027	1.166 \pm 0.026	1.15 \pm 0.032	2, 35	0.935	0.402	-	-	-
FG4	1.127 \pm 0.008	1.136 \pm 0.009	1.12 \pm 0.009	2, 35	0.849	0.437	-	-	-

Resting-state cortical entropy analysis

The measured *rs*-CoEn of occipital lobe cytoarchitectonic areas was normalized with the average *rs*-CoEn of the occipital lobe. The ratio between each cytoarchitectonic area *rs*-CoEn and the average *rs*-CoEn of the occipital lobe was further employed in the subsequent analysis. ANOVA revealed a significant group effect for the cytoarchitectonic areas hOc4la ($F_{(2, 35)} = 3.856$; $p = 0.031$) and FG1 ($F_{(2, 35)} = 6.566$; $p = 0.004$). There was no significant effect for the factor hemisphere [occipital LH, $F_{(2, 35)} = 0.43$, $p = 0.654$; occipital RH, $F_{(2, 35)} = 0.082$; $p = 0.922$]. Note that none of the areas with altered CoTks compared to normally sighted exhibited significant *rs*-CoEn alterations. Post-hoc independent-sample t-tests (Bonferroni corrected for multiple comparisons) are summarized in Table 2 and in the following paragraphs.

Visual brain *rs*-CoEn in visual field loss compared to normally sighted

Compared to normally sighted we found in central visual field defect/ SMD group a significant increase of *rs*-CoEn in areas hOc4la ($p = 0.031$) and FG1 ($p = 0.025$) (see Figure 1B.1 and Table 2). There was no *rs*-CoEn difference between peripheral visual loss / RPTV and the normally sighted.

Visual brain *rs*-CoEn differences in central and peripheral visual field loss

Compared to the peripheral visual field loss/RPTV group, central visual field loss/SMD exhibited significantly higher *rs*-CoEn in the area FG1 ($p = 0.005$) (see Figure 1B.2 and Table 2).

Impact of age and duration deficit on CoTks and *rs*-CoEn

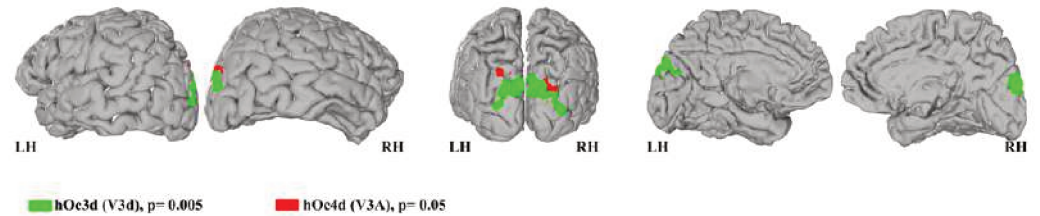
There was no impact of age and deficit duration on the CoTks and *rs*-CoEn in areas exhibiting differences between groups (for regression differences in other areas see Supplementary Table 1).

Discussion

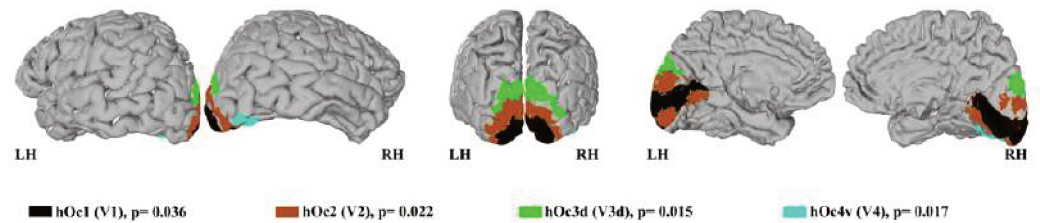
We assessed the impact of central and peripheral vision loss on the cortical morphology (i.e. cortical thickness, CoTks) and neural and synaptic complexity (i.e. *rs*-fMRI entropy, *rs*-CoEn). Three findings emerge from our work. First, compared to normally-sighted both groups with visual field defects exhibited reduced CoTks in the dorsal region hOc3d; peripheral visual field defect group also presented reduced CoTks in early visual cortex (hOc1 and hOc2) and the ventral region hOc4V, while central visual field defect group in the dorsal region hOc4d. Second, compared both to normally sighted and peripheral visual field defect groups, central visual field defect group showed

A. Between-groups cortical thickness analysis

1. Cytoarchitectonic areas with reduced cortical thickness in central visual loss compared to normally sighted

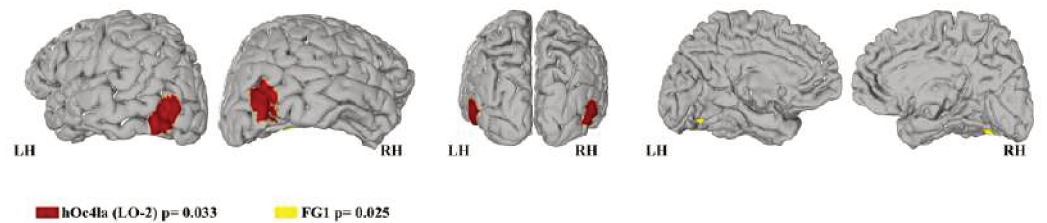


2. Cytoarchitectonic areas with reduced cortical thickness in peripheral visual loss compared to normally sighted



B. Between-groups cortical entropy analysis

1. Cytoarchitectonic areas with increased cortical entropy in central visual loss (SMD) compared to normally sighted



2. Cytoarchitectonic areas with increased cortical entropy in central visual loss compared (SMD) to peripheral visual loss (RPTV)

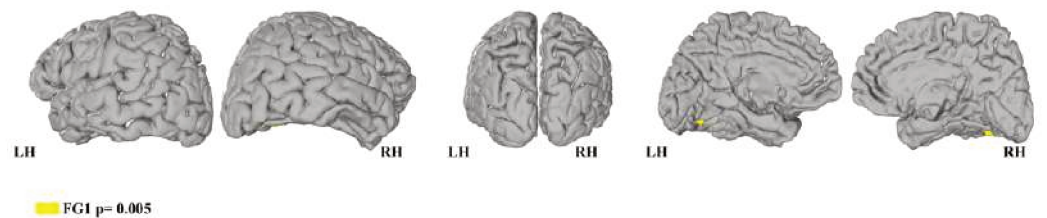


Figure 1. A. Between-groups analysis of cortical thickness. B. Between-groups analysis of cortical entropy. Cytoarchitectonic areas are shown on neutral brains extracted from JuBrain CytoViewer Atlas (<https://www.jubrain.fz-juelich.de>).

increased *rs*-CoEn in FG1 area; also, compared with normally sighted, central visual field defect group exhibited increased *rs*-CoEn in hOc4la area. Finally, areas with altered CoTks had normal *rs*-CoEn and conversely.

Differences in cortical thickness

Compared to normally sighted only the subjects with peripheral visual loss showed decreased CoTks in hOc1 and hOc2, which correspond to the functional regions V1 and V2 of the early visual cortex (*Amunts et al., 2000*). Previous studies noted decreased CoTks in the early visual cortex both in central and visual loss, but the anomalies were mainly concentrated in their deafferented regions (*Boucard et al., 2009; Plank et al., 2011; Yu et al., 2013; Hernowo et al., 2014; Prins et al., 2016*). The fact that in our study only peripheral visual loss was associated with a thinning of the early visual cortex suggests that peripheral input has a greater trophic impact on this area, despite its lesser cortical representation. The loss of the peripheral vision represents the loss of an extensive visual field area and affects the output of numerous wide-field retinal informational channels (*Ölveczky et al., 2003; Roska and Werblin, 2003; Hosoya et al., 2005; Münch et al., 2009; Masland, 2012*). Yet poorly understood, these channels might play an important role in the functioning of the early visual cortex. Moreover, retinitis pigmentosa, which affects primarily rods and secondary cones, also concerns central visual field despite the visual preservation. Photoreceptor degeneration induces local retinal plasticity and likely impairs certain channels and functions (*Jones and Marc, 2005; Jones et al., 2003*).

The reduced hOc3d CoTks in both visual field defects when compared to normally sighted, suggests a comparable contribution of central and peripheral visual field to the dorsal portion of V3 (V3d), which is canonically included in the dorsal stream (*Kujovic et al., 2013*). Anatomical and functional data indicate that the primarily role of V3d area is the processing kinetic information (*Gegenfurtner et al., 1997; Felleman et al., 1997; Rosa and Manger, 2005*), the extraction of kinetic contours (*Zeki, 2003*), and 3D form (*Vanduffel, 2002*). Moreover, V3d has the particularity that its retinotopical map represents only the lower quadrant of the visual field, while the upper quadrant is being represented in the ventral part of V3, area V3v (hOc3v) (*Rottschy et al., 2007; Kujovic et al., 2013*). It is possible that the spatial nature of information processing in hOc3d/ V3d is responsible for the decreased CoTks observed with both central and peripheral visual field loss. Indeed, the build-up of an accurate referential system, essential for functions like stereopsis (i.e. 3D perception), requires both central vision, which provides high spatial resolution and fixation, and peripheral vision, which provides wide-field sampling (*Goldstein and Clahane, 1966; Luria, 1971; Causer et al., 2011; Dessing et al., 2012*).

In central visual loss, the physiological foveal fixation lacks and compels to fixation in the vicinity of the visual field defect, in the residual functional periphery. These eccentric fixation loci (usually multiple) are used both for detection (*Duret et al., 1999*) and visuomotor coordination (*Timberlake et al., 2012*) and occur in different retinal positions for each eye. These peculiarities lead to an inadequate extraction of fixation disparities (*Wheatstone, 1962*) impairing the very mechanism of the stereopsis.

In peripheral visual field loss, foveal vision, physiologic fixation and visual acuity are preserved, but stereopsis is nevertheless impaired through mechanisms like a non-uniform drifting of the two eyes in the absence of the peripheral visual field superposition, the loss of fusion due to brief occlusions (i.e. eye-blinks) (*Fender and Julesz, 1967*) or "empty-field myopia" (i.e. accommodation impairment due to increased amplitude oscillation of accommodation in the absence of peripheral clues resulting in increased difficulty for detection) (*Whiteside, 1957; Campbell et al., 1959*).

Interestingly, compared to normally sighted, central visual field loss also exhibited decreased CoTks in the dorsal area hOc4d, corresponding to the functional region V3A. This area seems to be involved in the processing of kinetic and static 3D shapes (*Georgieva et al., 2009*), especially contour curvature (*Caplovitz and Tse, 2006*), stereoscopic and chromatic motion (*McKeefry et al., 2010; Anzai et al., 2011*), perceptual stability during eye movements (*Braddick et al., 2001; Fischer*

et al., 2012), the prediction of the visual motion (*Maus et al., 2010*), its structural damage commonly resulting in simultanagnosia, namely the inability to interpret complex visual displays despite the preserved capacity to recognize single objects (*Coslett and Saffran, 1991*). Impaired fixation and stereoscopic vision in patients with central visual loss may account for the CoTks loss in this area.

Another intriguing result was the decreased CoTks in area hOc4v in peripheral field loss, when compared to normally sighted. Area hOc4, to the best of our knowledge, probably corresponds to human V4 (hV4) or at least to its ventral subdivision V4v (hV4v). The role of hV4 in color perception is still debated (*Bartolomeo et al., 2014*), but its central participation in the figure-ground segmentation through the integration of multiple stimulus properties (i.e. contour, shape, texture, motion, color, disparity) by bottom-up salience driven attentional mechanism or top-down proactive spatial or feature selection makes consensus (*Reynolds and Desimone, 2003; Qiu et al., 2007; Poort et al., 2012; Roe et al., 2012*). Peripheral visual field loss and the resulting severely constricted visual field, may limit covert visual attention, reduces the sensory input in area hOc4 and consequently its CoTks.

Differences in cortical entropy

Compared to normally sighted, central visual field loss group exhibited increased *rs*-CoEn in area hOc4la that likely corresponds to functionally defined LO-2 region (*Larsson and Heeger, 2006*) involved in shape processing, object and face recognition, visual attention, action observation, visual tracking, spatial location discrimination, mental imagery and subjective emotional picture discrimination (*Malikovic et al., 2016*). The increased *rs*-CoEn in area hOc4la/ LO-2 suggests an adaptive increase in synaptic complexity points in this area, which is crucial for shape perception, figure-ground segregation and visuomotor coordination (*Malikovic et al., 2016*). Moreover, in a previous study exploring the resting state functional connectivity of central and peripheral V1 in the exact populations explored here, we found that in central visual field loss, isolated afferented peripheral early visual cortex exhibited increased functional connectivity with LOC compared to corresponding region in normally sighted (*Sabbah et al., 2017*). Therefore, in central visual loss the increased *rs*-CoEn in LO-2 might be linked to the increased functional connectivity of this area with the residually afferented peripheral early visual cortex.

Subjects with central visual field loss presented increased *rs*-CoEn in area FG1 when compared to normally sighted and peripheral visual field loss participants. This area, located in the posterior part of the fusiform gyrus, medial to the middle fusiform sulcus (*Caspers et al., 2013; Lorenz et al., 2015*) exhibits a bias for the peripheral visual field representations. More precisely, FG1 and the anteriorly situated FG3 overlap with places, inanimate large objects and peripheral biased representations (*Lorenz et al., 2015*). This line of evidences suggests that the observed difference in *rs*-CoEn may relate to an enhanced peripheral visual field treatment in FG1 area in order to compensate for the central visual field loss. In the above mentioned resting-state study, we also noted that compared to afferented peripheral early visual cortex in normally sighted, isolated afferented peripheral early visual cortex in central visual field group showed increased resting-state functional connectivity with fusiform gyrus.

Combined cortical thickness and cortical entropy data

Interestingly, the regions with altered CoTks had normal *rs*-CoEn and conversely. The decreased CoTks in the early visual cortex (HoC1/ V1 and hOc2/V2), hOc3d (V3d), hOc4v in peripheral visual field loss, and the decreased CoTks in hOc3d (V3d) and hOc4d (V3A) in central visual loss compared with normally sighted, corroborated with the normality of the CoEn indicate a possible mixture of apoptotic neuronal loss and variation in myelination but with preserved synaptic complexity in the remaining networks.

The increased *rs*-CoEn in FG1 in central visual field loss compared with both normally sighted and peripheral visual loss, in hOc4la (LO-2) in central visual field loss compared with normally

sighted, suggest an increase in synaptic complexity possibly to compensate for the impairment of certain functions associated with the central visual field loss. Therefore, the normal cortical thickness in these regions may obscure an eventual neuronal loss induced by deafferentation, compensated by the increase in synaptic complexity.

Limitations

Cytoarchitectonic areas are highly variable across subjects (*Amunts et al., 1999*). Herein, we extracted occipital cytoarchitectonic areas from an atlas based on observer-independent probabilistic mapping of 10 post mortem brains (*Zilles and Amunts, 2015; Mohlberg et al., 2012*). To reduce the effect of inter-individual variability, CoTks and *rs-CoEn* were sampled only in voxels where the same cytoarchitectonic area overlaps in more than 5 out of 10 of the post-mortem brains investigated.

Myelin density in the cortex and various technical parameters (field strength, tissue segmentation methods, smoothing, etc) may influence the MRI measure of cortical thickness and lead to incorrect estimations (*Glasser et al., 2014*). These effects can be particularly deceptive in disorders that impact myelination (i.e. multiple sclerosis) or in physiological states exhibiting different degrees of cortical myelination (i.e. development or aging) (*Westlye et al., 2010; Zilles and Amunts, 2015*). Both models of visual loss we employed in this study have no known association with developmental myelination anomalies or active demyelination. Therefore, we can consider that the above-mentioned biases of cortical thickness by MRI had little, if no impact on the results.

Resting-state *fMRI* signal is notoriously affected by motion (*Van Dijk et al., 2012*). Increased movements would virtually increase measures of entropy. To reduce this effect, we regressed out the motion related signal from the *fMRI* data prior to the calculation of entropy. In this way we maximized the likelihood that the entropy measures reflect the spontaneous hemodynamic fluctuations related to brain activity.

Overall, central and peripheral visual loss induced complex structural changes unpredicted by the canonical segregation central vision – ventral visual field, peripheral vision – dorsal visual field. We found that central visual field loss induces a thinning in dorsal stream areas hOc3d (V3d) and hOc4d (V3A) and peripheral visual field loss in early visual cortex (hOc1/V1 and hOc2/V2), dorsal stream area hOc3d (V3d) and ventral stream area hOc4v (V4). Central visual field loss also induces an increase in synaptic complexity in areas hOc4la (LO-2) and FG-1 reflecting possible alternative, compensatory processing. These results offer a new and interesting insight on the effect of central and peripheral visual field deafferentation and also invite to revisit the canonical concepts of “ventral” and “dorsal” stream. Moreover, this data suggests complex adaptive changes that should be considered in the development of new visually rehabilitation strategies, sensory substitution devices or visual restitution attempts.

Methods and Materials

Participants : The Ethics Committee (Comité de protection des personnes, Ile de France V, and Agence Nationale de Sécurité du Médicament et des Produits de Santé) approved the study protocol (number 12873). 38 subjects gave their written informed consent prior to inclusion. Twelve subjects suffered from Stargardt macular dystrophy (SMD) (six women; all right-handed, age range from 18 to 58 year-old, mean 38.4 ± 12 , median 39). This group presented a central scotoma, 10-20 degrees in diameter (as evaluated by Goldmann III/4 kinetic perimetry), without foveal sparing, with a best-corrected visual acuity equal or superior to 20/400 (measured by EDTRS charts). Twelve subjects suffered from retinitis pigmentosa, tunnel vision stage (RPTV) (six women; nine right-handed, age-range from 18 to 62 year-old, mean 41.7 ± 16.7 , median 40), and presented a central residual visual field limited to a 10-20 degree diameter (as evaluated by Goldmann III/4 kinetic perimetry) with a best-corrected visual acuity equal or superior to 20/40 (measured by EDTRS charts). Additionally, fourteen normally sighted controls (seven women; all right-handed, age-range from 18 to 59 year-old, 41.6 ± 14.6 , median 41), with normal routine ophthalmological examinations were

also recruited for this study. Groups were matched for age and no significant difference between groups was observed (Kruskal-Wallis, $c2(2)=.445$, $p=.801$, mean rank age 19.83 in SMD group, 20.79 in RPTV group and 19.82 in normally sighted group) (see for details Table 3).

Table 3. Clinical data about vision loss onset and evolution. Note that determining the real onset of retinitis pigmentosa is very challenging. Individuals become aware about the visual field defect relatively late in the disease due to fading and filling-in processes. Therefore, the recorded onset age should be regarded with caution for certain subjects.

Visual field	Subject	Sex	Age	Disorder	Age of onset	Duration (years)
Normal visual field	1	M	18	-	-	-
	2	F	24	-	-	-
	3	M	26	-	-	-
	4	F	28	-	-	-
	5	M	31	-	-	-
	6	F	36	-	-	-
	7	F	40	-	-	-
	8	F	42	-	-	-
	9	F	54	-	-	-
	10	F	54	-	-	-
	11	M	56	-	-	-
	12	M	57	-	-	-
	13	M	58	-	-	-
	14	M	59	-	-	-
Central visual field defect	1	M	18	Stargardt macular degeneration	12	6
	2	F	25	Stargardt macular degeneration	13	12
	3	M	27	Stargardt macular degeneration	23	4
	4	M	32	Stargardt macular degeneration	15	17
	5	M	39	Stargardt macular degeneration	7	32
	6	M	39	Stargardt macular degeneration	10	29
	7	F	39	Stargardt macular degeneration	17	22
	8	F	40	Stargardt macular degeneration	16	24
	9	M	41	Stargardt macular degeneration	23	18
	10	F	47	Stargardt macular degeneration	18	29
	11	F	56	Stargardt macular degeneration	24	32
	12	F	58	Stargardt macular degeneration	17	41
Peripheral visual field defect	1	F	18	Retinitis pigmentosa	1	17
	2	F	23	Retinitis pigmentosa	3	20
	3	M	27	Retinitis pigmentosa	4	23
	4	F	28	Retinitis pigmentosa	16	12
	5	M	29	Retinitis pigmentosa	10	19
	6	F	37	Retinitis pigmentosa	20	17
	7	F	43	Retinitis pigmentosa	28	15
	8	M	54	Retinitis pigmentosa	21	33
	9	M	59	Retinitis pigmentosa	6	53
	10	M	60	Retinitis pigmentosa	4	56
	11	F	61	Retinitis pigmentosa	15	46
	12	M	62	Retinitis pigmentosa	39	23

Neuroimaging: MRI was performed with a whole-body 3T clinical imager (Sigma Horizon) using an 8-channel head coil.

T1-weighted gradient-echo images were acquired with the following parameters TE/TR/flip angle, 3.9 ms/9.5 ms/20°; FOV, 25.6 x 25.6 mm; matrix, 512 x 512; source voxel size, 1.2 x 0.5 x 0.5 mm; thickness, 1.2 mm, no gap.

Additionally, 32 contiguous axial T2*- weighted gradient-echo echo-planar images (TE/TR, 93 ms/3000 ms; FOV, 240 x 240 mm; matrix, 64 x 64; voxel size, 4 x 3.75 x 3.75 mm converted to 3 x 3 x 3 mm; thickness, 4 mm; no gap; NEX, 1) were recorded to encompass the entire brain. 184 volumes were acquired including 4 “dummy” volumes obtained at the start of the session. Scan duration was 9.25 minutes for the whole sequence. No explicit task was required, and subjects were instructed to keep their eyes closed.

Cortical thickness analysis (CoTks): A registration-based method (Diffeomorphic Registration based Cortical Thickness, DiReCT) was employed to estimate the cortical thickness (*Das et al., 2009*) from the T1-weighted imaging dataset. The first step of this method consists in creating a two voxel thick sheet, one that lies just between the grey matter and the white matter and a second lying between the grey matter and the cerebrospinal fluid. Then, the grey/white interface is expanded to the grey/cerebrospinal fluid interface using diffeomorphic deformation estimated with ANTs (*Avants et al., 2007; Klein et al., 2009; Tustison and Avants, 2013*). The registration produces a correspondence field that allows an estimate the distance between the grey/white and the grey/cerebrospinal fluid interfaces, and thus cortical thickness. This approach has good scan-rescan repeatability and good neurobiological validity as it can predict, with high statistical power the age and gender of the participants (*Tustison et al., 2014*). All these steps were carried on automatically using BCBtoolkit (<http://toolkit.biclab.com>). Average cortical thickness of the occipital lobes of each subject was also measured to account for the inter-individual variability (*Ferreira et al., 2017*).

Entropy analysis (rs-CoEn): First, T1-weighted gradient-echo images were skull stripped using Brain Extraction Tool (BET) as part of the FMRIB software package (FSL, <http://fsl.fmrib.ox.ac.uk>). T2*-weighted images were subsequently registered to the anatomical (T1-weighted) image using affine deformations. Skull stripped T1-weighted gradient-echo images were registered to the MNI152 template (<http://nist.mni.mcgill.ca/?p=904>) using affine and diffeomorphic deformations (<http://stnava.github.io/ANTs>) (*Klein et al., 2009; Avants et al., 2011*). The latter deformations were applied to the T1 registered T2*-weighted images. Since the resting-state fMRI signal can be heavily affected by motion, even following motion correction between temporally-adjacent volumes (*Van Dijk et al., 2012*), we estimated the signal fluctuation associated with motion and regressed it out from the fMRI data prior to the calculation of entropy. To this aim, we employed a recently developed and validated procedure based on data-driven Independent Component Analysis (ICA), termed ICA-Aroma (*Pruim et al., 2015*). This method performs an ICA decomposition of the data and estimates which components reflect motion-related artifacts in the fMRI signal on the basis of a robust set of spatial and temporal features. This is made possible due the distinctiveness of the motion-related components isolated by ICA on the fMRI signal (*Salimi-Khorshidi et al., 2014*). This approach outperforms other methods like the regression of the motion parameter estimates, while limiting in the same time the loss in degrees of freedom (*Pruim et al., 2015*). Compared to spike-removal methods such as scrubbing (*Power et al., 2012*), ICA-Aroma has the advantage of preserving the temporal structure of the fMRI signal. Finally, the resting-state cortical entropy (rs-CoEn) was estimated using FSL fslstats by first binning - using a fixed amount of 1,000 bins - the preprocessed fMRI signal within each region of interest (ROI), and subsequently estimating the mean Shannon entropy over the entire ROI. Like in the case of CoTks, to account for inter-individual variability, we extracted the average cortical entropy for each subject. These values were estimated on a grey matter mask from the MNI single subject template, in turn obtained from FAST segmentation, and subsequent thresholding at 0.4 the partial volume estimate map of the grey matter. In addition, we removed deep-brain structures and the cerebellum (which remain after segmentation) using the group-level template of subcortical structures provided by the Harvard-Oxford subcortical

atlas contained in FSL.

Regions of interest: To intimately respect the anatomy and cytoarchitecture of the cerebral cortex, we used probabilistic cytoarchitectonic maps of the occipital lobe (*Amunts et al., 2007; Zilles and Amunts, 2010; Mohlberg et al., 2012*) to extract region specific measures of cortical thickness and entropy. These regions included hOc1 (V1), hOc2 (V2), hOc3d (V3d), hOc4d (V3A), hOc3v (VP/V3v), hOc4v (V4/V4v), hOc5 (V5/ hMT+), hOc4la (LO-2), hOc4lp (LO-1), FG1, FG2 and FG4 (http://www.fz-juelich.de/inm/inm-1/EN/Forschung/_docs/SPMAnatomyToolbox/SPMAnatomyToolbox_node.html).

Statistical analysis: We confirmed the Gaussian distribution of the data for the three groups using the Shapiro-Wilk test (*Shapiro and Wilk, 1965*), as well as the homogeneity of variance with the Levene test (*Levene, 1960*).

Statistical analysis was performed with SPSS 20 (SPSS, Chicago, IL). Two consecutive repeated measures ANOVA were employed to assess differences in CoTks and *rs*-CoEn between the three groups. Cytoarchitectonic areas were considered as between subject factors and hemisphere as within subject factor. Post-hoc analyses Bonferroni corrected for multiple comparisons were performed when statistically appropriate.

The relation between age, visual deficit duration and the cortical thickness and cortical entropy of each cytoarchitectonic ROI was analyzed through linear regression in SPSS 20 (SPSS, Chicago, IL).

Acknowledgments

We would like to thank the team of the “Centre d’investigation clinique” of the “Centre Hospitalier National d’Ophtalmologie des Quinze-Vingts”, particularly Saddek Mohand-Saïd MD and Céline Devisme PhD for their invaluable help in patients’ recruitment and the members of “Forschungszentrum Jülich GmbH” for providing us with the cytoarchitectonic maps of the occipital lobe.

Additional information

Funding: The research leading to these results received funding from the programs: “Jeune Chercheuses et Jeunes Chercheurs” ANR-13-JSV4-0001-01, “Investissements d’avenir” ANR-10-IAIHU-06, “LABEX” and “Humanis”.

Competing financial interests: There is no conflict of interest to declare for any author excepting José-Alain Sahel, consultant for Pixium Vision, GenSight Biologics, Sanofi-Fovea, and Genesignal. However, this had no influence on the results or discussion reported in this paper.

References

- Amunts K, Schleicher A, Zilles K.** Cytoarchitecture of the cerebral cortex—More than localization. *Neuroimage*. 2007; 37(4):1061–1065. doi: [10.1016/j.neuroimage.2007.02.037](https://doi.org/10.1016/j.neuroimage.2007.02.037).
- Amunts K, Malikovic A, Mohlberg H, Schormann T, Zilles K.** Brodmann’s Areas 17 and 18 Brought into Stereotaxic Space—Where and How Variable? *Neuroimage*. 2000; 11(1):66–84. doi: [10.1006/nimg.1999.0516](https://doi.org/10.1006/nimg.1999.0516).
- Amunts K, Schleicher A, Bürgel U, Mohlberg H, Uylings HBM, Zilles K.** Broca’s region revisited: cytoarchitecture and intersubject variability. *J Comp Neurol*. 1999; 412(2):319–341. doi: [10.1002/\(SICI\)1096-9861\(19990920\)412:2<319::AID-CNE10>3.0.CO;2-7](https://doi.org/10.1002/(SICI)1096-9861(19990920)412:2<319::AID-CNE10>3.0.CO;2-7).
- Anzai A, Chowdhury SA, DeAngelis GC.** Coding of Stereoscopic Depth Information in Visual Areas V3 and V3A. *J Neurosci*. 2011; 31(28):10270–10282. doi: [10.1523/JNEUROSCI.5956-10.2011](https://doi.org/10.1523/JNEUROSCI.5956-10.2011).
- Authié CN, Berthoz A, Sahel JA, Safran AB.** Adaptive gaze strategies for locomotion with constricted visual field. *Front Hum Neurosci*. 2016; *submitted*.
- Avants B, Duda JT, Zhang H, Gee JC.** Multivariate Normalization with Symmetric Diffeomorphisms for Multivariate Studies. In: *Med. Image Comput. Comput. Interv. – MICCAI 2007*, vol. 10 Berlin, Heidelberg: Springer Berlin Heidelberg; 2007.p. 359–366.

- Avants BB**, Tustison NJ, Song G, Cook PA, Klein A, Gee JC. A reproducible evaluation of ANTs similarity metric performance in brain image registration. *Neuroimage*. 2011; 54(3):2033–2044. doi: [10.1016/j.neuroimage.2010.09.025](https://doi.org/10.1016/j.neuroimage.2010.09.025).
- Bartolomeo P**, Bachoud-Lévi AC, Thiebaut de Schotten M. The anatomy of cerebral achromatopsia: a reappraisal and comparison of two case reports. *Cortex*. 2014 Jul; 56:138–144. doi: [10.1016/j.cortex.2013.01.013](https://doi.org/10.1016/j.cortex.2013.01.013).
- Berencsi A**, Ishihara M, Imanaka K. The functional role of central and peripheral vision in the control of posture. *Hum Mov Sci*. 2005; 24(5-6):689–709. doi: [10.1016/j.humov.2005.10.014](https://doi.org/10.1016/j.humov.2005.10.014).
- Boucard CC**, Hernowo AT, Maguire RP, Jansonius NM, Roerdink JBTM, Hooymans JMM, Cornelissen FW. Changes in cortical grey matter density associated with long-standing retinal visual field defects. *Brain*. 2009; 132(7):1898–1906. doi: [10.1093/brain/awp119](https://doi.org/10.1093/brain/awp119).
- Boucart M**, Naili F, Despretz P, Defoort-Dhellemmes S, Fabre-Thorpe M. Implicit and explicit object recognition at very large visual eccentricities: No improvement after loss of central vision. *Vis cogn*. 2010; 18(6):839–858. doi: [10.1080/13506280903287845](https://doi.org/10.1080/13506280903287845).
- Braddick OJ**, O'Brien JMD, Wattam-Bell J, Atkinson J, Hartley T, Turner R. Brain Areas Sensitive to Coherent Visual Motion. *Perception*. 2001; 30(1):61–72. doi: [10.1068/p3048](https://doi.org/10.1068/p3048).
- Burge WK**, Griffis JC, Nenert R, Elkhatali A, DeCarlo DK, ver Hoef LW, Ross LA, Visscher KM. Cortical thickness in human V1 associated with central vision loss. *Sci Rep*. 2016; 6(23268). doi: [10.1038/srep23268](https://doi.org/10.1038/srep23268).
- Campbell FW**, Robson JG, Westheimer G. Fluctuations of accommodation under steady viewing conditions. *J Physiol*. 1959; 145:579–594.
- Caplovitz GP**, Tse PU. V3A Processes Contour Curvature as a Trackable Feature for the Perception of Rotational Motion. *Cereb Cortex*. 2006; 17(5):1179–1189. doi: [10.1093/cercor/bhl029](https://doi.org/10.1093/cercor/bhl029).
- Caspers J**, Zilles K, Eickhoff SB, Schleicher A, Mohlberg H, Amunts K. Cytoarchitectonical analysis and probabilistic mapping of two extrastriate areas of the human posterior fusiform gyrus. *Brain Struct Funct*. 2013; 218(2):511–526. doi: [10.1007/s00429-012-0411-8](https://doi.org/10.1007/s00429-012-0411-8).
- Causser J**, Holmes PS, Williams AM. Quiet eye training in a visuomotor control task. *Med Sci Sports Exerc*. 2011; 43(6):1042–1049. doi: [10.1249/MSS.0b013e3182035de6](https://doi.org/10.1249/MSS.0b013e3182035de6).
- Chen WW**, Wang N, Cai S, Fang Z, Yu M, Wu Q, Tang L, Guo B, Feng Y, Jonas JB, Chen X, Liu X, Gong Q. Structural brain abnormalities in patients with primary open-angle glaucoma: a study with 3T MR imaging. *Invest Ophthalmol Vis Sci*. 2013; 54(1):545–554. doi: [10.1167/iovs.12-9893](https://doi.org/10.1167/iovs.12-9893).
- Cheung CMG**, Wong TY. Is age-related macular degeneration a manifestation of systemic disease? New prospects for early intervention and treatment. *J Intern Med*. 2014; 276(2):140–153. doi: [10.1111/joim.12227](https://doi.org/10.1111/joim.12227).
- Coslett HB**, Saffran E. Simultanagnosia. To see but not two see. *Brain*. 1991; 114(4):1523–1545. doi: [10.1093/brain/114.4.1523](https://doi.org/10.1093/brain/114.4.1523).
- Das SR**, Avants BB, Grossman M, Gee JC. Registration based cortical thickness measurement. *Neuroimage*. 2009; 45(3):867–879. doi: [10.1016/j.neuroimage.2008.12.016](https://doi.org/10.1016/j.neuroimage.2008.12.016).
- Dessing JC**, Rey FP, Beek PJ. Gaze fixation improves the stability of expert juggling. *Exp Brain Res*. 2012; 216(4):635–644. doi: [10.1007/s00221-011-2967-6](https://doi.org/10.1007/s00221-011-2967-6).
- Donders FC**. Beiträge zur pathologischen Anatomie des Auges. *Albr von Graefes Arch für Ophthalmol*. 1857; 3(1):139–165. doi: [10.1007/BF02720685](https://doi.org/10.1007/BF02720685).
- Duret F**, Issenhuth M, Safran AB. Combined use of several preferred retinal loci in patients with macular disorders when reading single words. *Vision Res*. 1999; 39(4):873–879. doi: [10.1016/S0042-6989\(98\)00179-5](https://doi.org/10.1016/S0042-6989(98)00179-5).
- Felleman DJ**, Burkhalter A, Van Essen DC. Cortical connections of areas V3 and VP of macaque monkey extrastriate visual cortex. *J Comp Neurol*. 1997; 379(1):21–47. doi: [10.1002/\(SICI\)1096-9861\(19970303\)379:1<21::AID-CNE3>3.0.CO;2-K](https://doi.org/10.1002/(SICI)1096-9861(19970303)379:1<21::AID-CNE3>3.0.CO;2-K).
- Fender D**, Julesz B. Extension of Panum's fusional area in binocularly stabilized vision. *J Opt Soc Am*. 1967; 57(6):819–830. doi: [10.1364/JOSA.57.000819](https://doi.org/10.1364/JOSA.57.000819).

- Ferreira S**, Pereira AC, Quendera B, Reis A, Silva ED, Castelo-Branco M. Primary visual cortical remapping in patients with inherited peripheral retinal degeneration. *NeuroImage Clin.* 2017; 13:428–438. doi: [10.1016/j.nicl.2016.12.013](https://doi.org/10.1016/j.nicl.2016.12.013).
- Fischer E**, Bühlhoff HH, Logothetis NK, Bartels A. Human Areas V3A and V6 Compensate for Self-Induced Planar Visual Motion. *Neuron.* 2012; 73(6):1228–1240. doi: [10.1016/j.neuron.2012.01.022](https://doi.org/10.1016/j.neuron.2012.01.022).
- Fortenbaugh FC**, Hicks JC, Hao L, Turano KA. Losing sight of the bigger picture: Peripheral field loss compresses representations of space. *Vision Res.* 2007; 47(19):2506–2520. doi: [10.1016/j.visres.2007.06.012](https://doi.org/10.1016/j.visres.2007.06.012).
- Gattass R**, Nascimento-Silva S, Soares JGM, Lima B, Jansen AK, Diogo ACM, Farias MF, Botelho, M M EP, Mariani OS, Azzi J, Fiorani M. Cortical visual areas in monkeys: location, topography, connections, columns, plasticity and cortical dynamics. *Philos Trans R Soc B Biol Sci.* 2005; 360(1456):709–731. doi: [10.1098/rstb.2005.1629](https://doi.org/10.1098/rstb.2005.1629).
- Gegenfurtner KR**, Kiper DC, Levitt JB. Functional properties of neurons in macaque area V3. *J Neurophysiol.* 1997; 77(4):1906–1923.
- Georgieva S**, Peeters R, Kolster H, Todd JT, Orban GA. The Processing of Three-Dimensional Shape from Disparity in the Human Brain. *J Neurosci.* 2009; 29(3):727–742. doi: [10.1523/JNEUROSCI.4753-08.2009](https://doi.org/10.1523/JNEUROSCI.4753-08.2009).
- Glasser MF**, Goyal MS, Preuss TM, Raichle ME, Van Essen DC. Trends and properties of human cerebral cortex: Correlations with cortical myelin content. *Neuroimage.* 2014; 93:165–175. doi: [10.1016/j.neuroimage.2013.03.060](https://doi.org/10.1016/j.neuroimage.2013.03.060).
- Goldstein JH**, Clahane AC. The role of the periphery in binocular vision. *Am J Ophthalmol.* 1966; 62(4):702–706. doi: [10.1016/0002-9394\(66\)92198-2](https://doi.org/10.1016/0002-9394(66)92198-2).
- Hernowo AT**, Prins D, Baseler Ha, Plank T, Gouws AD, Hooymans JMM, Morland AB, Greenlee MW, Cornelissen FW. Morphometric analyses of the visual pathways in macular degeneration. *Cortex.* 2014; 56:99–110. doi: [10.1016/j.cortex.2013.01.003](https://doi.org/10.1016/j.cortex.2013.01.003).
- Hosoya T**, Baccus Sa, Meister M. Dynamic predictive coding by the retina. *Nature.* 2005; 436(7047):71–77. doi: [10.1038/nature03689](https://doi.org/10.1038/nature03689).
- Jones BW**, Marc RE. Retinal remodeling during retinal degeneration. *Exp Eye Res.* 2005; 81(2):123–137. doi: [10.1016/j.exer.2005.03.006](https://doi.org/10.1016/j.exer.2005.03.006).
- Jones BW**, Watt CB, Frederick JM, Baehr W, Chen CK, Levine EM, Milam AH, Lavail MM, Marc RE. Retinal remodeling triggered by photoreceptor degenerations. *J Comp Neurol.* 2003; 464(1):1–16. doi: [10.1002/cne.10703](https://doi.org/10.1002/cne.10703).
- Klein A**, Andersson J, Ardekani BA, Ashburner J, Avants B, Chiang MC, Christensen GE, Collins DL, Gee J, Hellier P, Song JH, Jenkinson M, Lepage C, Rueckert D, Thompson P, Vercauteren T, Woods RP, Mann JJ, Parsey RV. Evaluation of 14 nonlinear deformation algorithms applied to human brain MRI registration. *Neuroimage.* 2009; 46(3):786–802. doi: [10.1016/j.neuroimage.2008.12.037](https://doi.org/10.1016/j.neuroimage.2008.12.037).
- Kujovic M**, Zilles K, Malikovic A, Schleicher A, Mohlberg H, Rottschy C, Eickhoff SB, Amunts K. Cytoarchitectonic mapping of the human dorsal extrastriate cortex. *Brain Struct Funct.* 2013; 218(1):157–172. doi: [10.1007/s00429-012-0390-9](https://doi.org/10.1007/s00429-012-0390-9).
- Larsson J**, Heeger DJ. Two Retinotopic Visual Areas in Human Lateral Occipital Cortex. *J Neurosci.* 2006; 26(51):13128–13142. doi: [10.1523/JNEUROSCI.1657-06.2006](https://doi.org/10.1523/JNEUROSCI.1657-06.2006).
- Levene H**. Robust tests for equality of variances. In: Olkin I, Ghurye SG, Hoeffding W, Madow W, Mann HB, editors. *Contrib. to Probab. Stat. Essays Honor Harold Hotell.* Stanford: Stanford University Press; 1960.p. 278–292.
- Lorenz S**, Weiner KS, Caspers J, Mohlberg H, Schleicher A, Bludau S, Eickhoff SB, Grill-Spector K, Zilles K, Amunts K. Two New Cytoarchitectonic Areas on the Human Mid-Fusiform Gyrus. *Cereb Cortex.* 2015; bhv225:1–13. doi: [10.1093/cercor/bhv225](https://doi.org/10.1093/cercor/bhv225).
- Luria SM**. Duction, stereoacuity and field of view. *Am J Optom Arch Am Acad Optom.* 1971; 48(9):728–735.
- Malikovic A**, Amunts K, Schleicher A, Mohlberg H, Eickhoff SB, Wilms M, Palomero-Gallagher N, Armstrong E, Zilles K. Cytoarchitectonic analysis of the human extrastriate cortex in the region of V5/MT+: A probabilistic, stereotaxic map of area hOc5. *Cereb Cortex.* 2007; 17(3):562–574. doi: [10.1093/cercor/bhj181](https://doi.org/10.1093/cercor/bhj181).

- Malikovic A**, Amunts K, Schleicher A, Mohlberg H, Kujovic M, Palomero-Gallagher N, Eickhoff SB, Zilles K. Cytoarchitecture of the human lateral occipital cortex: mapping of two extrastriate areas hOc4la and hOc4lp. *Brain Struct Funct*. 2016; 221(4):1877–1897. doi: 10.1007/s00429-015-1009-8.
- Marc RE**, Jones BW. Retinal Remodeling in Inherited Photoreceptor Degenerations. *Mol Neurobiol*. 2003; 28(2):139–148. doi: 10.1385/MN:28:2:139.
- Masland RH**. The Neuronal Organization of the Retina. *Neuron*. 2012; 76(2):266–280. doi: 10.1016/j.neuron.2012.10.002.
- Maus GW**, Weigelt S, Nijhawan R, Muckli L. Does Area V3A Predict Positions of Moving Objects? *Front Psychol*. 2010; 1(168):1–11. doi: 10.3389/fpsyg.2010.00186.
- McKeefry DJ**, Burton MP, Morland AB. The contribution of human cortical area V3A to the perception of chromatic motion: a transcranial magnetic stimulation study. *Eur J Neurosci*. 2010; 31(3):575–584. doi: 10.1111/j.1460-9568.2010.07095.x.
- McKinnon SJ**. Glaucoma: ocular Alzheimer's disease? *Front Biosci*. 2003; 8(12):s1140–s1156.
- McKinnon SJ**. The cell and molecular biology of glaucoma: common neurodegenerative pathways and relevance to glaucoma. *Invest Ophthalmol Vis Sci*. 2012; 53(5):2485–2487. doi: 10.1167/iovs.12-9483j.
- Mohlberg H**, Eickhoff SB, Schleicher A, Zilles K, Amunts K. A new processing pipeline and release of cytoarchitectonic probabilistic maps – JuBrain. In: *OHBM Peking*; 2012. .
- Münch Ta**, da Silveira RA, Siegert S, Viney TJ, Awatramani GB, Roska B. Approach sensitivity in the retina processed by a multifunctional neural circuit. *Nat Neurosci*. 2009; 12(10):1308–1316. doi: 10.1038/nn.2389.
- Ölveczky BP**, Baccus SA, Meister M. Segregation of object and background motion in the retina. *Nature*. 2003; 423(6938):401–408. doi: 10.1038/nature01652.
- Pham TQ**, Kifley A, Mitchell P, Wang JJ. Relation of Age-Related Macular Degeneration and Cognitive Impairment in an Older Population. *Gerontology*. 2006; 52(6):353–358. doi: 10.1159/000094984.
- Plank T**, Frolo J, Brandl-Rühle S, Renner AB, Hufendiek K, Helbig H, Greenlee MW. Gray matter alterations in visual cortex of patients with loss of central vision due to hereditary retinal dystrophies. *Neuroimage*. 2011; 56(3):1556–1565. doi: 10.1016/j.neuroimage.2011.02.055.
- Poort J**, Raudies F, Wannig A, Lamme VAF, Neumann H, Roelfsema PR. The Role of Attention in Figure-Ground Segregation in Areas V1 and V4 of the Visual Cortex. *Neuron*. 2012; 75(1):143–156. doi: 10.1016/j.neuron.2012.04.032.
- Power JD**, Barnes KA, Snyder AZ, Schlaggar BL, Petersen SE. Spurious but systematic correlations in functional connectivity MRI networks arise from subject motion. *Neuroimage*. 2012; 59(3):2142–2154. doi: 10.1016/j.neuroimage.2011.10.018.
- Prins D**, Plank T, Baseler HA, Gouws AD, Beer A, Morland AB, Greenlee MW, Cornelissen FW. Surface-Based Analyses of Anatomical Properties of the Visual Cortex in Macular Degeneration. *PLoS One*. 2016; 11(1):e0146684. doi: 10.1371/journal.pone.0146684.
- Pruim RHR**, Mennes M, Buitelaar JK, Beckmann CF. Evaluation of ICA-AROMA and alternative strategies for motion artifact removal in resting state fMRI. *Neuroimage*. 2015; 112:278–287. doi: 10.1016/j.neuroimage.2015.02.063.
- Qiu FT**, Sugihara T, von der Heydt R. Figure-ground mechanisms provide structure for selective attention. *Nat Neurosci*. 2007; 10(11):1492–1499. doi: 10.1038/nn1989.
- Reynolds JH**, Desimone R. Interacting Roles of Attention and Visual Saliency in V4. *Neuron*. 2003; 37(5):853–863. doi: 10.1016/S0896-6273(03)00097-7.
- Roe AW**, Chelazzi L, Connor CE, Conway BR, Fujita I, Gallant JL, Lu H, Vanduffel W. Toward a Unified Theory of Visual Area V4. *Neuron*. 2012; 74(1):12–29. doi: 10.1016/j.neuron.2012.03.011.
- Rosa MGP**, Manger PR. Clarifying homologies in the mammalian cerebral cortex: the case of the third visual area (V3). *Clin Exp Pharmacol Physiol*. 2005; 32(5-6):327–339. doi: 10.1111/j.1440-1681.2005.04192.x.
- Rosenke M**, Weiner KS, Barnett MA, Zilles K, Amunts K, Goebel R, Grill-Spector K. A cross-validated cytoarchitectonic atlas of the human ventral visual stream. *Neuroimage*. 2017; doi: 10.1016/j.neuroimage.2017.02.040.

- Roska B**, Werblin F. Rapid global shifts in natural scenes block spiking in specific ganglion cell types. *Nat Neurosci*. 2003; 6(6):600–608. doi: 10.1038/nn1061.
- Rottschy C**, Eickhoff SB, Schleicher A, Mohlberg H, Kujovic M, Zilles K, Amunts K. Ventral visual cortex in humans: Cytoarchitectonic mapping of two extrastriate areas. *Hum Brain Mapp*. 2007; 28(10):1045–1059. doi: 10.1002/hbm.20348.
- Sabbah N**, Sanda N, Authié CN, Mohand-Saïd S, Sahel JA, Habas C, Amedi A, Safran AB. Reorganization of early visual cortex functional connectivity following selective peripheral and central visual loss. *Sci Rep*. 2017; 7(43223):1–19. doi: 10.1038/srep43223.
- Safran AB**, Duret F, Issenhuth M, Mermoud C. Full text reading with a central scotoma: pseudo regressions and pseudo line losses. *Br J Ophthalmol*. 1999; 83(12):1341–1347. doi: 10.1136/bjo.83.12.1341.
- Sahel JA**, Marazova K, Audo I. Clinical Characteristics and Current Therapies for Inherited Retinal Degenerations. *Cold Spring Harb Perspect Med*. 2015; 5(2):a017111. doi: 10.1101/cshperspect.a017111.
- Salimi-Khorshidi G**, Douaud G, Beckmann CF, Glasser MF, Griffanti L, Smith SM. Automatic denoising of functional MRI data: Combining independent component analysis and hierarchical fusion of classifiers. *Neuroimage*. 2014; 90:449–468. doi: 10.1016/j.neuroimage.2013.11.046.
- Shapiro SS**, Wilk MB. An analysis of variance test for normality. *Biometrika*. 1965; 52(3-4):591–611. doi: 10.1093/biomet/52.3-4.591.
- Sokunbi MO**, Fung W, Sawlani V, Choppin S, Linden DEJ, Thome J. Resting state fMRI entropy probes complexity of brain activity in adults with ADHD. *Psychiatry Res Neuroimaging*. 2013; 214(3):341–348. doi: 10.1016/j.psychres.2013.10.001.
- Sokunbi MO**, Staff RT, Waiter GD, Ahearn TS, Fox HC, Deary IJ, Starr JM, Whalley LJ, Murray AD. Inter-individual Differences in fMRI Entropy Measurements in Old Age. *IEEE Trans Biomed Eng*. 2011; 58(11):3206–3214. doi: 10.1109/TBME.2011.2164793.
- Stargardt K**. Über familiäre, progressive Degeneration in der Maculagegend des Auges. *Albr von Graefes Arch für Ophthalmol*. 1909; 71(3):534–550. doi: 10.1007/BF01961301.
- Thiebaut de Schotten M**, Urbanski M, Batrancourt B, Levy R, Dubois B, Cerliani L, Volle E. Rostro-caudal Architecture of the Frontal Lobes in Humans. *Cereb cortex*. 2016; doi: 10.1093/cercor/bhw215.
- Timberlake GT**, Omoscharka E, Grose SA, Bothwell R. Preferred retinal locus–hand coordination in a maze-tracing task. *Invest Ophthalmol Vis Sci*. 2012; 53(4):1810–1820. doi: 10.1167/iovs.11-9282.
- Tononi G**. Complexity and coherency: integrating information in the brain. *Trends Cogn Sci*. 1998; 2(12):474–484. doi: 10.1016/S1364-6613(98)01259-5.
- Turano Ka**, Geruschat DR, Stahl JW, Massof RW. Perceived visual ability for independent mobility in persons with retinitis pigmentosa. *Invest Ophthalmol Vis Sci*. 1999; 40(5):865–877.
- Turano KA**, Massof RW, Quigley HA. A self-assessment instrument designed for measuring independent mobility in RP patients: generalizability to glaucoma patients. *Invest Ophthalmol Vis Sci*. 2002; 43(9):2874–2881.
- Tustison NJ**, Avants BB. Explicit B-spline regularization in diffeomorphic image registration. *Front Neuroinform*. 2013; 7(39). doi: 10.3389/fninf.2013.00039.
- Tustison NJ**, Cook PA, Klein A, Song G, Das SR, Duda JT, Kandel BM, van Strien N, Stone JR, Gee JC, Avants BB. Large-scale evaluation of ANTs and FreeSurfer cortical thickness measurements. *Neuroimage*. 2014; 99:166–179. doi: 10.1016/j.neuroimage.2014.05.044.
- Ungerleider LG**, Desimone R. Projections to the superior temporal sulcus from the central and peripheral field representations of V1 and V2. *J Comp Neurol*. 1986; 248(2):147–163. doi: 10.1002/cne.902480202.
- Van Dijk KRA**, Sabuncu MR, Buckner RL. The influence of head motion on intrinsic functional connectivity MRI. *Neuroimage*. 2012; 59(1):431–438. doi: 10.1016/j.neuroimage.2011.07.044.
- Vanduffel W**. Extracting 3D from Motion: Differences in Human and Monkey Intraparietal Cortex. *Science (80-)*. 2002 oct; 298(5592):413–415. doi: 10.1126/science.1073574.
- Wagstyl K**, Ronan L, Goodyer IM, Fletcher PC. Cortical thickness gradients in structural hierarchies. *Neuroimage*. 2015; 111:241–250. doi: 10.1016/j.neuroimage.2015.02.036.

- Westlye LT**, Walhovd KB, Dale AM, Bjørnerud A, Due-Tønnessen P, Engvig A, Grydeland H, Tamnes CK, Østby Y, Fjell AM. Differentiating maturational and aging-related changes of the cerebral cortex by use of thickness and signal intensity. *Neuroimage*. 2010; 52(1):172–185. doi: [10.1016/j.neuroimage.2010.03.056](https://doi.org/10.1016/j.neuroimage.2010.03.056).
- Wheatstone C**. On some remarkable and hitherto unobserved phenomena of binocular vision. *Optom Wkly*. 1962; 53(1838):2311–2315.
- Whiteside TCD**. Effect of empty-field myopia upon the minimum visual angle for a distant target. In: *Probl. Vis. flight high Alt*. London: Butterworths Scientific publications; 1957.p. 105–112.
- Wittich W**, Faubert J, Watanabe DH, Kapusta MA, Overbury O. Spatial judgments in patients with retinitis pigmentosa. *Vision Res*. 2011; 51(1):165–173. doi: [10.1016/j.visres.2010.11.003](https://doi.org/10.1016/j.visres.2010.11.003).
- Woo SJ**, Park KH, Ahn J, Choe JY, Jeong H, Han JW, Kim TH, Kim KW. Cognitive Impairment in Age-related Macular Degeneration and Geographic Atrophy. *Ophthalmology*. 2012; 119(10):2094–2101. doi: [10.1016/j.ophtha.2012.04.026](https://doi.org/10.1016/j.ophtha.2012.04.026).
- Yao Y**, Lu WL, Xu B, Li CB, Lin CP, Waxman D, Feng JF. The increase of the functional entropy of the human brain with age. *Sci Rep*. 2013; 3(2853):1–8. doi: [10.1038/srep02853](https://doi.org/10.1038/srep02853).
- Yu L**, Xie B, Yin X, Liang M, Evans AC, Wang J, Dai C. Reduced Cortical Thickness in Primary Open-Angle Glaucoma and Its Relationship to the Retinal Nerve Fiber Layer Thickness. *PLoS One*. 2013; 8(9):e73208. doi: [10.1371/journal.pone.0073208](https://doi.org/10.1371/journal.pone.0073208).
- Zeki S**. The Processing of Kinetic Contours in the Brain. *Cereb Cortex*. 2003; 13(2):189–202. doi: [10.1093/cercor/13.2.189](https://doi.org/10.1093/cercor/13.2.189).
- Zilles K**, Amunts K. Centenary of Brodmann's map — conception and fate. *Nat Rev Neurosci*. 2010; 11(2):139–145. doi: [10.1038/nrn2776](https://doi.org/10.1038/nrn2776).
- Zilles K**, Amunts K. Anatomical Basis for Functional Specialisation. In: Uludag K, Ugurbil K, Berliner L, editors. *fMRI From Nucl. Spins to Brain Funct*. New York: Springer; 2015.p. 27–66.

Appendix 1

Supplementary table

Table 1. Regression analysis showing the significant effects of age and visual defect duration on CoTks and CoEn.

Area	ANOVA p	r ²	Beta	Regression equations
CoTks_{predicted} = b₀ + age (b₁)				
Occipital RH	0.949	-	-	-
Occipital LH	0.525	-	-	-
hOe1	0.867	-	-	-
hOe2	0.389	-	-	-
hOe3d	0.886	-	-	-
hOe3v	0.448	-	-	-
hOe4d	0.144	-	-	-
hOe4v	0.969	-	-	-
hOe4la	0.371	-	-	-
hOe4lp	0.016	0.15	0.39	CoTks = 0.952 + age (0.004)
hOe5	0.898	-	-	-
FG1	0.312	-	-	-
FG2	0.248	-	-	-
FG3	0.02	0.14	-0.38	CoTks = 1.653 + age (-0.006)
FG4	0.524	-	-	-
CoTks_{predicted} = b₀ + deficit duration (b₁)				
Occipital RH	0.644	-	-	-
Occipital LH	0.726	-	-	-
hOe1	0.927	-	-	-
hOe2	0.196	-	-	-
hOe3d	0.745	-	-	-
hOe3v	0.496	-	-	-
hOe4d	0.489	-	-	-
hOe4v	0.393	-	-	-
hOe4la	0.049	0.17	0.41	CoTks = 1.058 + deficit duration (0.003)
hOe4lp	0.003	0.34	0.58	CoTks = 0.953 + deficit duration (0.006)
hOe5	0.564	-	-	-
FG1	0.165	-	-	-
FG2	0.461	-	-	-
FG3	0.001	0.38	-0.62	CoTks = 1.714 + deficit duration (-0.011)
FG4	0.107	-	-	-
CoEn_{predicted} = b₀ + age (b₁)				
Occipital RH	0.279	-	-	-
Occipital LH	0.868	-	-	-
hOe1	0.97	-	-	-
hOe2	0.972	-	-	-
hOe3d	0.064	-	-	-
hOe3v	0.88	-	-	-
hOe4d	0.158	-	-	-
hOe4v	0.33	-	-	-
hOe4la	0.429	-	-	-
hOe4lp	0.027	0.13	-0.36	CoEn = 1.121 + age (-0.001)
hOe5	0.001	0.26	-0.51	CoEn = 1.072 + age (-0.002)
FG1	0.129	-	-	-
FG2	0.844	-	-	-
FG3	0.002	0.25	-0.5	CoEn = 1.199 + age (-0.001)
FG4	0.043	0.11	-0.33	CoEn = 1.156 + age (-0.001)
CoEn_{predicted} = b₀ + deficit duration (b₁)				
Occipital RH	0.947	-	-	-
Occipital LH	0.417	-	-	-
hOe1	0.672	-	-	-
hOe2	0.367	-	-	-
hOe3d	0.208	-	-	-
hOe3v	0.508	-	-	-
hOe4d	0.088	-	-	-
hOe4v	0.333	-	-	-
hOe4la	0.124	-	-	-
hOe4lp	0.046	0.17	-0.41	CoEn = 1.12 + deficit duration (-0.001)
hOe5	0.06	-	-	-
FG1	0.458	-	-	-
FG2	0.707	-	-	-
FG3	0.005	0.31	-0.56	CoEn = 1.188 + deficit duration (-0.001)
FG4	0.033	0.19	-0.44	CoEn = 1.155 + deficit duration (-0.001)

Functional changes: “*Reorganization of early visual cortex functional connectivity following selective peripheral and central visual loss*”*

Besides the morphological impact of the sensory deafferentation, another important question concerns the way the residually afferented early visual cortex and deafferented early visual cortex reorganize their networks following central or peripheral visual loss. To explore these changes, we analyzed the resting-state functional connectivity of central and peripheral early visual cortex (V1 and V2)¹. This functional analysis was conducted on same subjects as the first study, which investigated the morphological changes induced by visual loss (e.g. twelve subjects with Stargardt macular degeneration, twelve subjects with pigmentary retinopathy and fourteen normally sighted subjects). As developed in Chapter 3.2.3, resting-state *fMRI*, is a very low demanding technique, easily accepted by patients (Wang *et al.* 2008; Butt *et al.* 2013; Striem-Amit *et al.* 2015). Herein, to selectively explore the resting-state functional connectivity of the central and peripheral early visual cortex, we employed a partial correlation method (Striem-Amit *et al.* 2015; Zeharia *et al.* 2015). Unlike simple correlation, partial correlation holds a greater ability to identify false positives when looking for direct connections. This method applies linear regression to remove fluctuations induced by a specific brain area in the functional connectivity network of the seed region, thus rendering a predicted functional connectivity that reflects more precisely a direct link between seed region and other brain areas. Partial correlation is of particular interest for the exploration of the functional connectivity of the central and peripheral early visual cortex since the strong interconnectivity between these two regions could mask some of their specific connections (Falchier *et al.* 2002).

We found that compared to normally sighted, afferented central and peripheral early visual cortex in patients with visual field loss enhance their functional connectivity in

1. *An early version of this research was presented in “Réorganisation cérébrale consécutive à la perte tardive d’une partie ou de la totalité du champ visuel et à la restitution sensorielle : approche comportementale et par IRM fonctionnelle.”, Norman Sabbah, Neurosciences [q-bio.NC]. Université Pierre et Marie Curie - Paris VI, 2015. Français. <NNT : 2015PA066532>. <tel-01318951>

occipital lobe, whereas deafferented central and peripheral early visual cortex increase their functional connectivity with more remote regions. The functional connectivity pattern of the part of the early visual cortex receiving the remaining visual input suggests that the isolated afferented early visual cortex strengthens local connections, presumably to *tune-up* visual information processing. In deafferented early visual cortex, remodeling affects more remote connections, suggesting that deafferented early visual cortex likely diverts its processing capacity to higher-order functions (*top-down*) that could optimize the residual visual function. The absence of increased local connectivity in the deafferented compared to the normally afferented early visual cortex or its decreased local connectivity when compared to the isolated afferented early visual cortex imply that deafferented early visual cortex rewires different type of information than the afferented early visual cortex. It is unlikely that increased functional connectivity of the sensory deprived visual cortex represents noise generated by aberrant autonomous activity, because this would imply strengthened connections between the deafferented early visual cortex and regions to which they are strongly linked in normal vision, effect not confirmed by our data. Rather, the enhanced connectivity of the deafferented primary visual cortex concerned long-range connections involved in higher-order processing. Therefore, the connectivity pattern of afferented early visual cortex suggests adaptive changes that might enhance the visual processing capacity whereas the connectivity pattern of deafferented early visual cortex may reflect the involvement of these regions in high-order mechanisms.

The current study also brings some light into the current debate on the plasticity of deafferented early visual cortex following a partial visual loss (Backer *et al.* 2005, Backer *et al.* 2008, Baseler *et al.* 2011, Masuda *et al.* 2008, Dilks *et al.* 2009, Masuda *et al.* 2010) by showing that both afferented and deafferented regions of early visual cortex reorganize, that their reorganization is different and that it likely backs different functions.

Résumé

- Outre que les changements structurels induits par la déafférentation sensorielle, le mode dont les régions du cortex visuel primaire qui reçoivent les afférences visuelles résiduelles et respectivement le mode dont les régions déafférentées réagissent réorganisent leurs connexions fonctionnelles, exigent également des réponses. Afin d'étudier ce type de plasticité nous avons analysé la connectivité fonctionnelle de région centrale et périphérique du cortex visuel primaire (V1 et V2) en IRM fonctionnel de repos. Cette étude fonctionnelle fut menée sur la même population que la première étude, c'est à dire douze sujets avec maculopathie de Stargardt, douze sujets avec rétinopathie pigmentaire et quatorze sujets avec une vision normale. L'IRM fonctionnelle de repos est une technique facilement acceptée par les patients car elle présume une participation passive, le sujet étant allongé dans la machine d'IRM, avec les yeux fermés pendant toute la durée de l'acquisition (voire Chapitre 3.2.3, Wang *et al.* 2008; Butt *et al.* 2013; Striem-Amit *et al.* 2015). Afin d'explorer de manière spécifique la connectivité fonctionnelle des régions déafférentées et recevant les afférences visuelles résiduelles, nous avons employé une méthode de corrélation partielle qui présente une fiabilité supérieure par rapport à la corrélation simple, notamment puisqu'elle permet l'indentification des faux positives (Striem-Amit *et al.* 2015; Zeharia *et al.* 2015). Pour soustraire les fluctuations induites dans le réseau neuronal de la région d'intérêt par une autre région corticale, la méthode de corrélation partielle utilise une régression linéaire. Par conséquent, le signal obtenu reflète mieux la connectivité fonctionnelle de la région d'intérêt. Cette méthode est particulièrement intéressante dans l'étude de la connectivité fonctionnelle de la partie centrale et périphérique du cortex visuel primaire, car la forte interconnexion physiologique de ces régions pourrait masquer certaines connexions qui leur sont propres (Falchier *et al.* 2002).
- Nous avons trouvé que par rapport régions correspondantes des sujets normovoyants, les régions centrale et périphérique du cortex visuel primaire qui reçoivent les afférences résiduelles, augmentent leur connectivité fonctionnelle locale, au niveau du lobe occipital, tandis que les régions déafférentées renforcent des connexions à distance. Le pattern de connexion du cortex afférenté avec des régions

Résumé

voisines suggère une réorganisation qui pourrait avoir comme finalité l’augmentation de la capacité de traitement de l’information visuelle. De l’autre côté, le pattern de connexion du cortex déafférenté avec des régions lointaines suggère une potentielle réorientation de la capacité de traitement de l’information vers des fonctions supérieures et donc pourraient optimiser indirectement la fonction visuelle résiduelle. L’absence de renforcement de la connectivité fonctionnelle locale du cortex déafférenté par rapport au cortex recevant des afférences normales et la diminution de sa connectivité fonctionnelle par rapport au cortex recevant les afférences résiduelles, indique que le cortex déafférenté traite un type différent d’information que le cortex afférenté. Il est fort improbable que la connectivité du cortex déafférenté soit du bruit généré par une activité autonome aberrante, puisque cette supposition demande un renforcement des connexions de proximité que nous n’avons pas retrouvé. Il est donc plus vraisemblable que l’activité du cortex déafférenté reflète des connexions à distance qui participent aux fonctions supérieures.

- Au total, le pattern de connectivité du cortex qui reçoit les afférences résiduelles suggère une réorganisation qui pourrait améliorer le traitement de l’information visuelle et le pattern de connectivité du cortex déafférenté suggère une possible rôle dans des fonctions supérieures.
- Cette étude apporte également un éclairage dans la dispute sur la réorganisation du cortex visuel primaire après la perte d’une partie du champ visuel (Backer *et al.* 2005, Backer *et al.* 2008, Baseler *et al.* 2011, Masuda *et al.* 2008, Dilks *et al.* 2009, Masuda *et al.* 2010), puisqu’elle démontre que la réorganisation concerne également le cortex afférenté et le cortex déafférenté, que leur réorganisation est différente, et qu’elle accompagne vraisemblablement des fonctions différentes.

SCIENTIFIC REPORTS

OPEN

Reorganization of early visual cortex functional connectivity following selective peripheral and central visual loss

Received: 08 August 2016
Accepted: 20 January 2017
Published: 24 February 2017

Norman Sabbah^{1,2,3,4,*}, Nicolae Sanda^{1,2,3,4,5,*}, Colas N. Authié^{1,2,3,4}, Saddek Mohand-Saïd^{1,2,3,4}, José-Alain Sahel^{1,2,3,4,6,7,8}, Christophe Habas^{1,2,3,9}, Amir Amedi^{1,2,3,10,11,12} & Avinoam B. Safran^{1,2,3,4,13}

Behavioral alterations emerging after central or peripheral vision loss suggest that cerebral reorganization occurs for both the afferented and deafferented early visual cortex (EVC). We explored the functional reorganization of the central and peripheral EVC following visual field defects specifically affecting central or peripheral vision. Compared to normally sighted, afferented central and peripheral EVC enhance their functional connectivity with areas involved in visual processing, whereas deafferented central and peripheral EVC increase their functional connectivity with more remote regions. The connectivity pattern of afferented EVC suggests adaptive changes that might enhance the visual processing capacity whereas the connectivity pattern of deafferented EVC may reflect the involvement of these regions in high-order mechanisms. Characterizing and understanding the plastic changes induced by these visual defects is essential for any attempt to develop efficient rehabilitation strategies.

The macular and peripheral parts of the retina constitute an intricate functional unit. Their combined input is responsible for the impression of a homogenous image over the entire visual field. This functional unity is not present from birth since ontogenically, the central and peripheral parts of the retina mature sequentially. Unlike the periphery, the central retina is immature at birth and only develops completely years later^{1–3}. After the visual function matures, damage to the central or peripheral retina impairs not only its specific functions related to the affected region, but also lessens the performance of the other retina⁴. How the brain behaves and potentially adapts to this challenge remains unclear. Nevertheless, a number of potential response mechanisms have been suggested: (1) the remaining afferented visual cortex tunes-up its processing capacity and compensates to a certain extent for the limited retinal input, whereas the deafferented visual cortex might (2) rewire and receive sensory input from the spared retina and end up treating roughly the same type of information as the afferented visual cortex; (3) divert its processing capacity to specific higher-order functions or multisensory processing; (4) supply the rest of the brain with meaningless input generated from aberrant intrinsic activity.

¹Sorbonne Universités, UPMC Université Paris 06, UMR S968, Institut de la Vision, Paris, F-75012, France. ²INSERM, U968, Institut de la Vision, Paris, F-75012, France. ³CNRS, UMR 7210, Institut de la Vision, Paris, F-75012, France. ⁴Centre d'investigation clinique, Centre Hospitalier National d'Ophthalmologie des Quinze-Vingts, INSERM-DGOS CIC 1423, Paris, F-75012, France. ⁵Service de neurologie, Hôpital Foch, Suresnes, France. ⁶Institute of Ophthalmology, University College of London, United Kingdom. ⁷Fondation Ophtalmologique Adolphe de Rothschild, Paris, France. ⁸Department of Ophthalmology, The University of Pittsburgh School of Medicine, Pittsburgh, PA 15213, US. ⁹Centre de neuroimagerie, Centre Hospitalier National d'Ophthalmologie des Quinze-Vingts, Paris, F-75012, France. ¹⁰Department of Medical Neurobiology, The Institute for Medical Research Israel-Canada, Faculty of Medicine, The Hebrew University of Jerusalem, Jerusalem 91220, Israel. ¹¹The Edmond and Lily Safra Center for Brain Sciences (ELSC), The Hebrew University of Jerusalem, Jerusalem 91220, Israel. ¹²The Cognitive Science Program, The Hebrew University of Jerusalem, Jerusalem 91220, Israel. ¹³Department of Clinical Neurosciences, Geneva University School of Medicine, Geneva, Switzerland. *These authors contributed equally to this work. Correspondence and requests for materials should be addressed to N.Sabbah (email: norman.sabbah@gmail.com) or N.Sanda (email: herrsanda@gmail.com)

Adaptive strategies such as the eccentric fixation employed in the case of central visual field defects induce proportional functional changes in the peripheral early visual cortex (EVC)^{5,6}, thus providing some support for the first hypothesis that the residual afferent visual cortex reorganizes to compensate for the loss in sensory input. In support of the second, rewiring hypothesis, Morland⁷ and Baseler⁸ found that in rod monochromats, deafferented regions of the visual cortex respond to visual stimulation of the functional retina, but that these populations present a differently organized visual system and an abnormal foveal structure⁹ due to the congenital absence of cones. In acquired visual field defects a similar reorganization was reported^{10,11}, but later challenged¹². Other authors^{13–15} reported that adults with conditions inducing either central or peripheral field defects only exhibited task-related activation of the deafferented regions of the visual cortex. This led to the third hypothesis of another type of reorganization in which the sensory-deprived visual regions contribute to higher-order mechanisms such as attention or mental imagery^{13–15} or intervene in multisensory processing¹⁶. The occurrence of visual hallucinations (i.e. the Charles Bonnet syndrome) following both central and peripheral visual loss and their induction through blindfolding in the normally-sighted advocate for the presence of aberrant intrinsic activity in sensory deprivation (the fourth hypothesis)^{17–19}. Thus overall, the literature on the reorganization of visual cortex subsequent to partial or total visual loss remains fraught with controversy. In previous studies, factors such as the limited number of participants^{10–15} and/or heterogeneity in the extent of visual field defects in the samples^{10–13} may have contributed to these divergent results and preclude comparisons between the functional reorganization induced by central and peripheral visual loss. To avoid these obstacles, samples must consist of subjects with comparable, converse visual field defects. In this study, we selected participants suffering from a condition that induces progressive visual loss in either the central retina; i.e., Stargardt macular dystrophy, or the peripheral retina; i.e. retinitis pigmentosa and whose visual field defects met the selection criteria for our experiments.

Stargardt macular dystrophy (SMD) is a well-documented bilateral, inherited retinal disorder that induces well-circumscribed, central visual defects^{20,21}. In its advanced stages, patients affected by this hereditary cone-rod dystrophy end up losing macular vision and in daily life can only rely on their residual peripheral vision. They are able to orient and navigate, but are markedly impaired for object or face identification and reading^{22,23}. In contrast, retinitis pigmentosa - a rod-cone dystrophy - is a disorder that primarily affects the peripheral retina, causes progressive bilateral constriction of the visual field and eventually, in its most advanced stages, leads to complete blindness²⁰. In the “tunnel vision stage” (RPTV), when the macular function is still preserved, these patients are able to correctly analyze relatively small images but experience difficulties in spatial orientation and scene perception^{24–26}.

We explored the changes induced by partial visual loss by analyzing resting-state functional connectivity (rs-FC), a method that places few demands on patients since they perform no task during scan acquisition. Resting-state fluctuations are well-organized into networks previously identified in a range of cognitive tasks^{27–36}, and are of particular interest when attempting to detect interactions between early visual areas, higher order visual areas, and non-visual brain regions both in normal and altered visual function^{37–39}. To selectively explore the resting-state FC of central and peripheral early visual cortex, we employed a partial correlation method^{39,40}. This method is used extensively as a research tool because it is sufficiently sensitive to recover retinotopic or mototopic maps from the resting-state both in the sighted^{39–42} and the blind^{38,39,43}. It constitutes a highly useful technique when aiming for a global view of these interactions and a detailed map of the background brain FC, a crucial first step in exploring the brain's response to visual loss. However, to the best of our knowledge, only a few studies have explored the rs-FC of EVC in the visually impaired^{44,45}, but none have differentiated between its central and peripheral regions^{44,45}. Given the nature of these patients' deprivation, it is clearly worth inquiring whether these FC changes are unique to the visual system. Therefore, as a control, we also investigated the possible FC changes in another topographic system, the somatosensory system.

Materials and Methods

Subjects and ethics. Subjects were recruited and assigned to the three groups as follows:

- Twelve Stargardt macular dystrophy (SMD) subjects (six women and six men; all subjects were right-handed), presenting a central scotoma, 10–20 degrees in diameter (as evaluated by Goldmann III/4 kinetic perimetry), without foveal sparing, and best-corrected visual acuity equal or superior to 20/400 (measured by EDTRS charts). Ages ranged from 18 to 58 years (average: 38.4, median: 39).
- Twelve retinitis pigmentosa tunnel vision (RPTV) subjects (six women and six men; nine subjects were right-handed), presenting a central residual visual field limited to a 10–20 degree diameter (as evaluated by Goldmann III/4 kinetic perimetry), and best-corrected visual acuity equal or superior to 20/40 (measured by EDTRS charts). Ages ranged from 18 to 62 years (average: 41.8, median: 40.0).
- Fourteen normally sighted controls (seven women and seven men; 14 subjects were right-handed), with normal routine ophthalmological examinations. Ages ranged from 18 to 59 years (average: 41.6, median: 41.0).

Subjects were matched for age, and no subject had any reported neurological or psychiatric diseases (see Table 1). The Ethics Committee (Comité de protection des personnes, Ile de France V, and Agence Nationale de Sécurité du Médicament et des Produits de Santé) approved the experimental protocol (number 12873), and all subjects gave their written informed consent before participating. All methods were performed in accordance with the relevant guidelines and regulations.

Functional imaging. fMRI was conducted with a whole-body 3T clinical imager (Sigma Horizon) using an eight-channel head coil. In each scanning sequence, 32 contiguous axial T2*-weighted gradient-echo echo-planar images (TE/TR, 93 ms/3000 ms; FOV, 240 × 240 mm; matrix, 64 × 64; voxel size, 3.75 × 3.75 × 4 mm; thickness, 4 mm; interslice spacing, 0 mm; NEX, 1) were recorded to encompass the entire brain. 180 volumes were

Subject	Sex	Age	Cause of disease	Age disease onset (first symptoms)	Visual deficit duration
SMD1	F	39	Stargardt macular dystrophy	17	22
SMD2	M	27	Stargardt macular dystrophy	23	4
SMD3	F	47	Stargardt macular dystrophy	18	29
SMD4	M	32	Stargardt macular dystrophy	15	17
SMD5	M	18	Stargardt macular dystrophy	12	6
SMD6	F	56	Stargardt macular dystrophy	24	32
SMD7	F	25	Stargardt macular dystrophy	13	12
SMD8	M	39	Stargardt macular dystrophy	10	29
SMD9	F	40	Stargardt macular dystrophy	16	24
SMD10	M	41	Stargardt macular dystrophy	23	18
SMD11	M	39	Stargardt macular dystrophy	7	32
SMD12	F	58	Stargardt macular dystrophy	17	41
RPTV1	F	43	Retinitis pigmentosa	28	15
RPTV2	H	54	Retinitis pigmentosa	21	33
RPTV3	H	62	Retinitis pigmentosa	39	23
RPTV4	F	37	Retinitis pigmentosa	20	17
RPTV5	F	28	Retinitis pigmentosa	16	12
RPTV6	H	60	Retinitis pigmentosa	4	56
RPTV7	F	61	Retinitis pigmentosa	15	46
RPTV8	H	59	Retinitis pigmentosa	6	53
RPTV9	H	27	Retinitis pigmentosa	4	23
RPTV10	H	29	Retinitis pigmentosa	10	19
RPTV11	F	23	Retinitis pigmentosa	3	20
RPTV12	F	18	Retinitis pigmentosa	1	17
S1	H	31	—	—	—
S2	F	28	—	—	—
S3	F	40	—	—	—
S4	H	59	—	—	—
S5	H	58	—	—	—
S6	F	42	—	—	—
S7	F	54	—	—	—
S8	F	36	—	—	—
S9	H	56	—	—	—
S10	F	54	—	—	—
S11	H	57	—	—	—
S12	H	18	—	—	—
S13	F	24	—	—	—
S14	H	26	—	—	—

Table 1. Subjects' clinical data. SMD: subjects with Stargardt macular dystrophy, RPTV: subjects with retinitis pigmentosa tunnel vision. S: sighted control subjects. Age disease onset: subjects' age when they experienced the first symptoms of the disease. Visual deficit duration: age minus age at disease onset.

acquired including 4 “dummy” volumes obtained at the start of the session. Scan duration was 9.25 minutes for the EPI sequence. Off-line, T2*-weighted images were co-registered and overlaid on the corresponding anatomic T1-weighted gradient-echo images (TE/TR/flip angle, 3.9 ms/9.5 ms/20°; FOV, 25.6 × 25.6 mm; matrix, 512 × 512; source voxel size, 1.2 × 0.5 × 0.5 mm converted to 1 × 1 × 1 mm; thickness, 1.2 mm; interslice spacing, 1.2 mm). During the scan, subjects were supine in the MRI scanner and wore earplugs to compensate for the noisy environment. Subjects were instructed to keep their eyes closed. No explicit task was required.

fMRI preprocessing. fMRI data were preprocessed using the BrainVoyager QX 2.8 software package (Brain Innovation, Maastricht, Netherlands) and complementary software written in MATLAB R2009a (The MathWorks, USA). Preprocessing of functional scans successively included: 3D motion correction (no head motion exceeded 2 mm/2 degrees in any of the six movement directions i.e. X, Y, Z translations, X, Y, Z rotations), slice-time correction, band-pass filtering between 0.01 and 0.1 Hz, voxel-to-voxel linear regression⁴⁶ of spurious signals from the white matter and ventricle regions anatomically defined for each subject, normalization in the Talairach coordinate system in the volume⁴⁷, and spatial smoothing with a 6 mm Gaussian filter kernel full-width-at-half-maximum. We did not include global signal removing to avoid the possible introduction of false negative correlations⁴⁸. For the between-group comparison, we tested and found no significant difference

in the maximum head movement⁴⁹ between the three groups (SMD: 0.29 ± 0.27 mm; RPTV: 0.16 ± 0.08 mm; sighted controls: 0.19 ± 0.18 mm; ANOVA $F(2, 35) = 1.5$; $p = 0.23$). We also performed a GLM analysis including the head movement predictors (control analysis; see Supplementary Figures S1, S2, S3 and S4). Including movement predictors in the GLM did not change the main results.

External functional localizers. External functional localizers were used to define the seed region-of-interest (ROI) from visual localizers (central EVC, peripheral EVC) in the volume. Each of these localizers was extracted from a group of normally sighted controls and analyzed in normalized Talairach space using a random effect GLM which enabled generalization of the findings to the population (see below; Friston *et al.* 1999).

To define the primary visual cortex seeds, a separate population of thirteen control subjects (seven women; six male; aged 22–35) was scanned in a standard phase-encoded retinotopic mapping experiment, using ring (eccentricity mapping) and wedge (polar mapping) stimuli^{39,50} delivered during two separate sessions. The stimuli were projected via an LCD screen positioned over the subject's forehead and watched through a tilted mirror. In the first session an annulus was projected, expanding in 30 seconds from 0° to 34° of the subject's visual field; the procedure was repeated ten times. The second session included a wedge stimulus with a 22.5° polar angle that rotated around the fixation point; each cycle was completed in 30 seconds, and repeated 20 times. Both the annulus in the first session and the wedge in the second session contained a flickering (6 Hz) radial checkerboard pattern with respect to standard retinotopic procedures⁵⁰ for the delineation of field maps. In both cases, there was a 30 second mute period before and after the visual stream for baseline. Group phase analysis was conducted on the two sessions⁵¹ resulting in group maps of eccentricity and angle mapping. Angle mapping was then used to define the borders of EVC, and the two maps were used to segregate it according to eccentricity (center or periphery of the visual field). The central EVC was considered under an eccentricity of 5 degrees and the peripheral EVC higher than 15 degrees.

For supplementary ROI analyses, we also used external functional localizers from previous studies by our team^{40,42,52} i.e. left hemisphere S1 lip and foot areas.

To validate the localizer definitions, we also ran a control analysis (see supplementary Figure S7) at the individual subject level to test for the time course correlations between seed regions defined based on external functional localizers and seed regions defined based on anatomical localizers (as defined by 7 mm spheres on the posterior and anterior portions of the calcarine sulcus of each subject).

Seed ROI definition and analysis.

- (1) A partial correlation analysis^{39,53} was conducted as follows. For each subject, a seed region of interest (ROI) based on external functional localizers (*e.g.*, the central EVC) served to extract and z-transform the blood-oxygen-level dependent time course of this region in volume⁵⁴ while regressing out the time course of the complementary part of the visual field component (*e.g.*, the peripheral EVC) to suppress the shared variance and conserve only the unique variance corresponding to the ROI predictor.
- (2) A random-effect analysis based on the general linear model (GLM)⁵⁵ was conducted for each group. This pair-wise correlation analysis led to four maps for each group: (a) the central EVC (regressed peripheral EVC), (b) the peripheral EVC (regressed central EVC), (c) the left S1 – lip area (regressed S1 – foot area) and (d) the left S1 – foot area (regressed S1 – lip area) with a significance level of $p < 0.05$, corrected for multiple comparisons using cluster-size thresholding^{39,56}, implemented in BrainVoyager using the Monte Carlo simulation approach (1000 iterations). This method directly takes into account the data contiguity of neighboring voxels and corrects for the false-positive rate of continuous clusters (a set-level statistical inference correction; corrected to $p < 0.05$).
- (3) For each patient group, we also tested the correlations between the following variables (*i*) the age at disease onset and, (*ii*) the duration of the visual deficit (Pearson Product-Moment Correlation, corrected for false discovery rate (FDR) for multiple comparisons) and the FC patterns found in the between-group maps (pairs of regions significantly connected; *e.g.* peripheral EVC and lingual gyrus).
- (4) To test for the main effect, a random-effect ANOVA was run on all the subjects with a between-subject factor enabling separation between groups with a significance level of $p < 0.05$, corrected for multiple comparisons using cluster-size thresholding.
- (5) To establish contrasts between groups, second-level analyses (post-hoc) were performed.

To summarize, an ROI-based functional connectivity analysis applied to the brain resting-state fMRI data was conducted on all groups. We used data from the seeded regions to establish resting-state functional connectivity maps intra-group. We then ran an ANOVA on all the subjects and post-hoc analysis to determine differences between groups in volume. The maps were then converted and displayed on the surface (data integrated in depth along vertex normals from -1 mm to 3 mm), enabling a complete view of the brain.

Results

All the results presented below were statistically significant ($p < 0.05$; corrected for multiple comparisons).

Intra-group analysis - Functional connectivity seeded from the central EVC. *Afferented central EVC* in the normally sighted exhibited a positive FC with the bilateral inferior and middle occipital and bilateral posterior part of the lingual gyri, bilateral orbitofrontal cortex but a negative FC with the bilateral inferior frontal gyrus, insula, cuneus, parieto-occipital sulcus, precuneus, cingulate sulcus, superior temporal and frontal gyrus, left intraparietal sulcus, inferior parietal lobule, precentral gyrus and right superior frontal sulcus (see Fig. 1A).

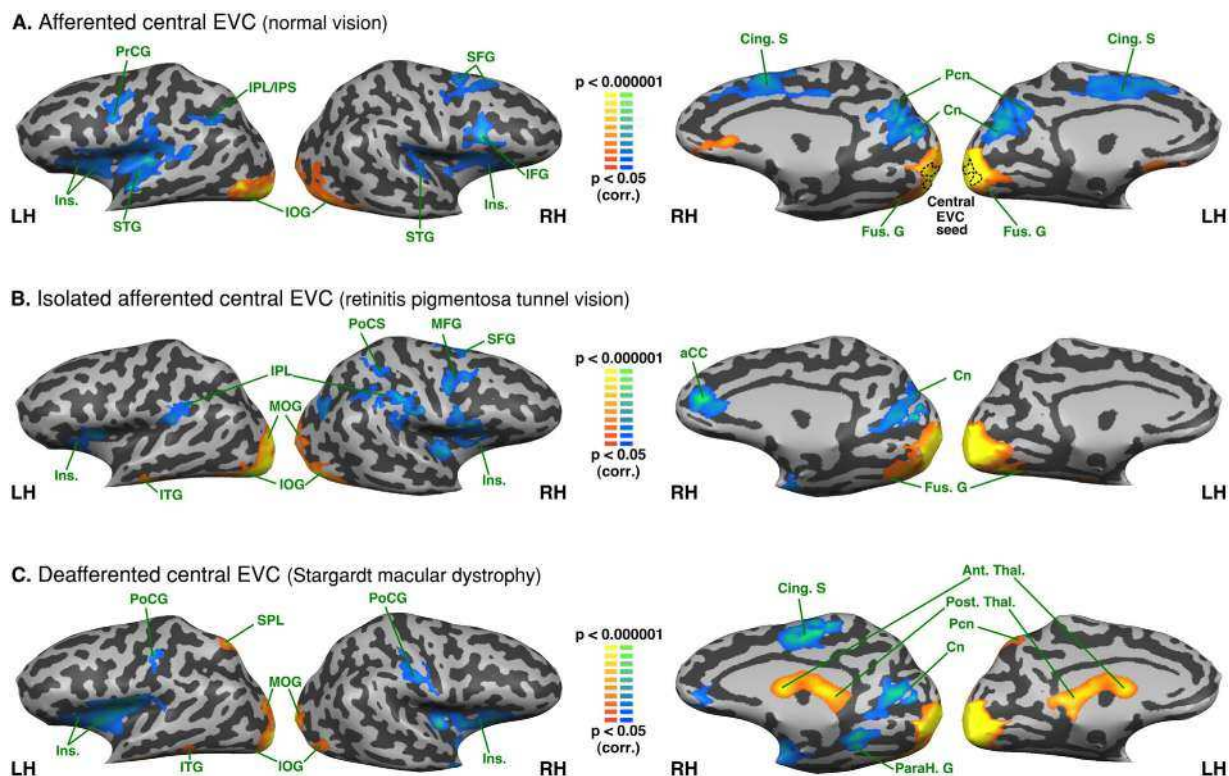


Figure 1. Intra-group analysis of functional connectivity seeded from the central EVC (peripheral EVC regressed). The maps are shown in mesh for the (A) afferented central EVC (normal vision); * the dotted line on the medial aspect of the brain represents the seed region (central EVC) (B) isolately afferented central EVC (retinitis pigmentosa tunnel vision) (C) deafferented central EVC (Stargardt macular dystrophy). Yellow-orange depicts areas of higher positive functional connectivity for each group, and green-blue higher negative functional connectivity. LH: left hemisphere, RH: right hemisphere. Ant. Thal.: anterior thalamus; Cing. S: cingulate sulcus; Cn: cuneus; Fus. G: fusiform gyrus; IFG: inferior frontal gyrus; Ins.: insula; IOG: inferior occipital gyrus; IPL: inferior parietal lobule; IPS: intraparietal sulcus; ITG: inferior temporal gyrus; Ling. G: lingual gyrus; MFG: middle frontal gyrus; MOG: middle occipital gyrus; ParaH. G: parahippocampal gyrus; Pcn: precuneus; Post. Thal.: posterior thalamus; PrCG: precentral gyrus; PoCS: postcentral sulcus; SFG: superior frontal gyrus; SPL: superior parietal lobule.

Isolated afferented central EVC in the RPTV exhibited a positive FC with the bilateral posterior part of the lingual gyrus, bilateral inferior and middle occipital and posterior fusiform gyri. It exhibited a negative FC with the bilateral inferior parietal lobule (supramarginal gyrus), insula, right anterior cingulate gyrus and right cuneus, right intraparietal sulcus, precentral sulcus and the posterior part of superior, middle and inferior frontal gyri (see Fig. 1B).

Deafferented central EVC in the SMD exhibited a positive FC with the bilateral posterior part of the lingual gyrus, bilateral inferior occipital gyrus, middle occipital gyrus, left superior parietal lobule, precuneus, bilateral anterior and posterior thalami. It exhibited a negative FC with the bilateral insula and postcentral gyrus, right posterior part of cingulate sulcus and the medial part of the precentral gyrus, right cuneus, anterior part of the lingual and parahippocampal gyri (see Fig. 1C).

There were no significant correlations for any group between either the age at disease onset or the duration of the visual deficit, and the FC of the central EVC with any other significant regions in the intra-group maps (Pearson correlations, FDR corrected; all p s > 0.05).

Intra-group analysis - Functional connectivity seeded from the peripheral EVC. *Afferented peripheral EVC* in the normally sighted exhibited positive FC with the bilateral cuneus, precuneus, posterior cingulate, lingual, parahippocampal, fusiform, superior and middle occipital gyri, posterior middle temporal gyrus and superior temporal sulcus, anterior superior temporal gyrus and right orbitofrontal and anterior cingulate cortex. It exhibited a negative FC with the bilateral inferior and middle frontal gyri, precentral sulcus, inferior frontal sulcus, inferior parietal lobule (supramarginal gyrus) and left superior frontal gyrus (see Fig. 2A).

Isolated afferented peripheral EVC in SMD exhibited a positive FC with the bilateral cuneus, lingual gyrus, parahippocampal gyrus, fusiform gyrus, precuneus, posterior cingulate, superior occipital gyrus, right middle occipital gyrus, bilateral inferior parietal lobule, right posterior superior parietal lobule and intraparietal sulcus, bilateral posterior middle temporal gyrus and superior temporal sulcus, bilateral lateral occipital complex, right superior, middle and temporal gyri and right superior and inferior temporal sulci, right pre and post central gyri, right central sulcus and bilateral orbitofrontal cortex. It exhibited a negative FC with the bilateral insula, inferior

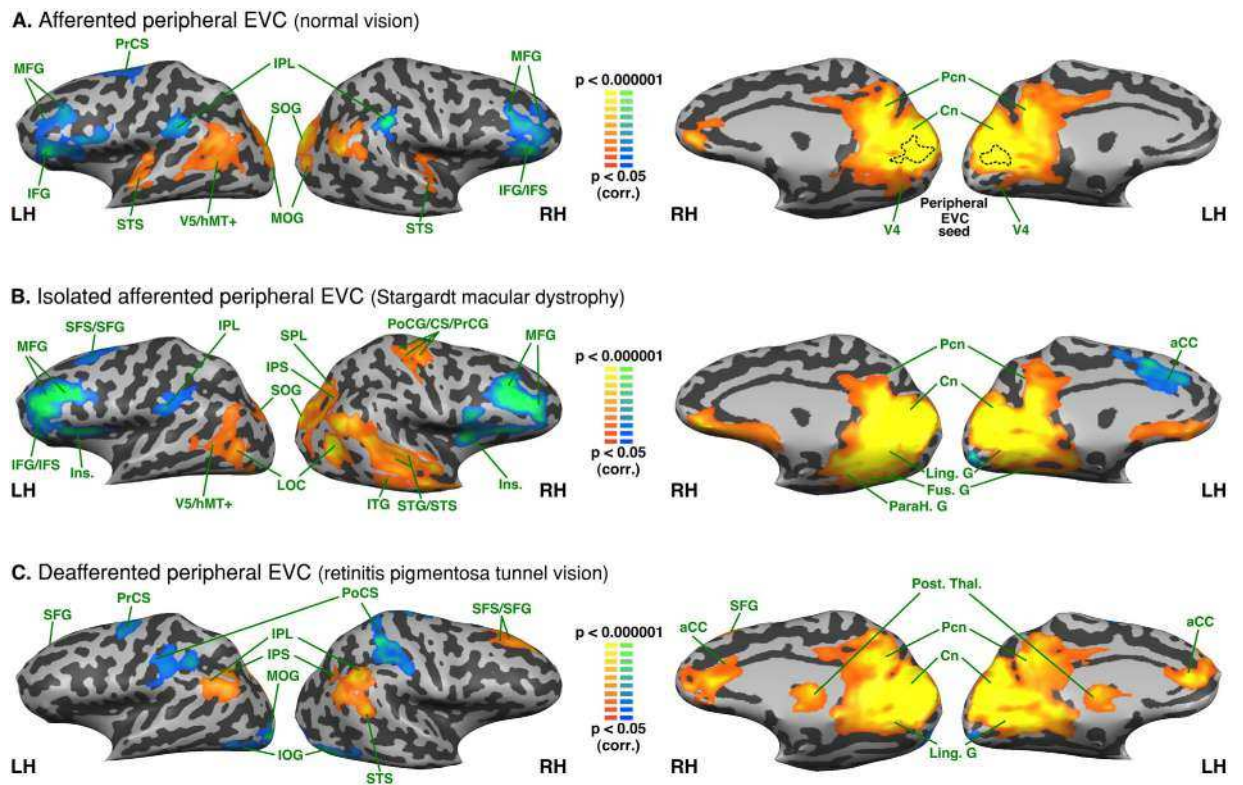


Figure 2. Intra-group analysis of functional connectivity seeded from the peripheral EVC (central EVC regressed). The maps are shown in mesh for the (A) afferented peripheral EVC (normal vision); * the dotted line on the median aspect of the brain represents the seed region (peripheral EVC) (B) isolated afferented peripheral EVC (Stargardt macular dystrophy) (C) deafferented peripheral EVC (retinitis pigmentosa tunnel vision). Yellow-orange depicts areas of higher positive functional connectivity for each group, and green-blue higher negative functional connectivity. LH: left hemisphere, RH: right hemisphere. aCC: anterior cingulate cortex; CS: central sulcus; Cn: cuneus; Fus. G: fusiform gyrus; IFG: inferior frontal gyrus; IFS: inferior frontal sulcus; Ins.: insula; IOG: inferior occipital gyrus; IPL: inferior parietal lobule; IPS: intraparietal sulcus; ITG: inferior temporal gyrus; ITS: inferior temporal sulcus; Ling. G: lingual gyrus; LOC: lateral occipital complex; MFG: middle frontal gyrus; MOG: middle occipital gyrus; Pcn: precuneus; PrCS: precentral sulcus; Post. Thal.: posterior thalamus; PrCG: precentral gyrus; PoCS: postcentral sulcus; SFG: superior frontal gyrus; SFS: superior frontal sulcus; SOG: superior occipital gyrus; SPL: superior parietal lobule; STG: superior temporal gyrus; STS: superior temporal sulcus; V5/hMT+: V5/human MT+.

and middle frontal gyri, inferior and superior frontal sulci, right superior frontal gyrus and left anterior cingulate cortex (see Fig. 2B).

Deafferented peripheral EVC in RPTV exhibited a positive FC with the bilateral cuneus, lingual and parahippocampal gyri, precuneus, posterior cingulate, anterior cingulate, inferior parietal lobule, posterior thalamus, right posterior superior temporal sulcus and superior frontal gyrus and sulcus. It exhibited a negative FC with the bilateral inferior occipital gyri, precentral gyri, postcentral sulci, the anterior part of intraparietal sulci and the left middle occipital gyrus (see Fig. 2C).

There were no significant correlations for any group between either the age at disease onset or the duration of the visual deficit, and the FC of peripheral EVC with any other significant regions in the intra-group maps (Pearson correlations, FDR corrected; all p s > 0.05).

Between group analysis - Functional connectivity differences seeded from the central EVC. As compared to normally sighted, the RPTV subjects showed increased FC of the afferented central EVC with the left middle occipital and left superior temporal gyri. There was also reduced central EVC FC with the anterior part of the right middle temporal gyrus, as well as the bilateral ventral anterior cingulate cortex (see Fig. 3A and Table 2). SMD subjects presented increased FC of the deafferented central EVC with the left inferior parietal lobule, bilateral cuneus, intraparietal sulcus, regions of the dorsal pathway, as well as the right precuneus (see Fig. 3B and Table 2). They also exhibited decreased central EVC FC with the ventral anterior cingulate cortex, the right superior and the middle temporal gyri.

A comparison of the two groups of visually deprived subjects indicated that the SMD subjects presented increased FC between the deafferented central EVC and the right cuneus and precuneus, the right inferior parietal lobule and the left superior parietal lobule (see Fig. 3C and Table 2). RPTV subjects showed increased FC

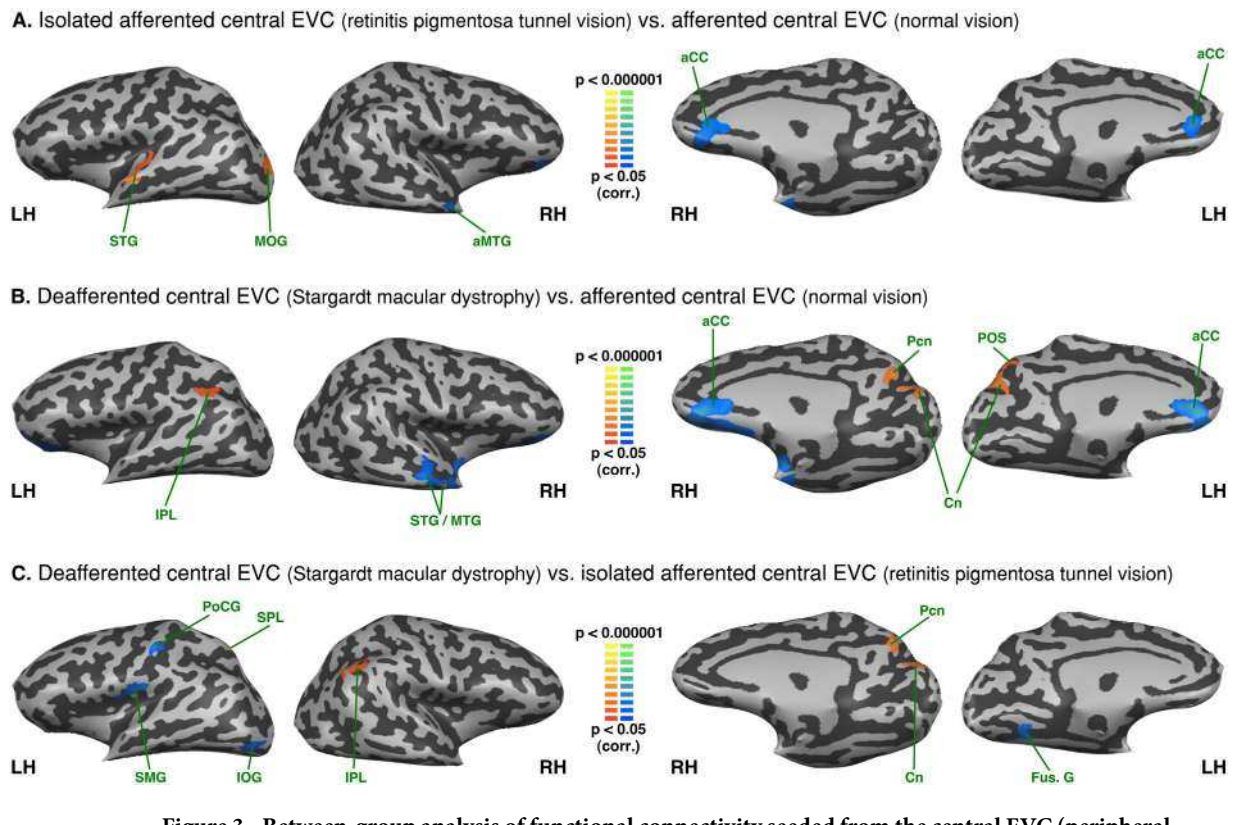


Figure 3. Between-group analysis of functional connectivity seeded from the central EVC (peripheral EVC regressed). The maps are shown in mesh for (A) retinitis pigmentosa tunnel vision vs. normal vision (B) Stargardt macular dystrophy vs. normal vision (C) Stargardt macular dystrophy vs. retinitis pigmentosa tunnel vision (yellow-orange depicts areas of higher positive/lower negative functional connectivity with the central EVC for the first group compared to the second, and green-blue the opposite comparison; LH: left hemisphere, RH: right hemisphere). aCC: anterior cingulate cortex; aMTG: anterior middle temporal gyrus; Cn: cuneus; Fus. G: fusiform gyrus; SPL: superior parietal lobule; IPL: inferior parietal lobule; IOG: inferior occipital gyrus; MOG: middle occipital gyrus; MTG: middle temporal gyrus; Pcn: precuneus; PoCG: postcentral gyrus POS: parieto-occipital sulcus; STG: superior temporal gyrus; SMG: supramarginal gyrus.

with the left posterior fusiform, the inferior occipital gyri as well as with the left supramarginal gyrus and the postcentral gyrus.

Between group analysis - Functional connectivity differences seeded from the peripheral EVC. As compared to normally sighted, the RPTV group exhibited increased FC with the right inferior parietal lobule, as well as with the posterior and anterior regions of the medial frontal gyrus (see Fig. 4A and Table 2). In contrast to the central EVC FC, the peripheral sensory deprived EVC of RPTV subjects showed decreased FC with the central sulcus left anterior middle temporal gyrus and the middle occipital gyrus as well as with the bilateral superior occipital gyrus, the right middle and the inferior occipital gyrus. The SMD group showed increased FC of their peripheral afferented EVC with regions of the ventral and dorsal pathway such as the right lateral occipital cortex, the bilateral lingual gyri, the right inferior occipital, fusiform, parahippocampal gyri as well as the right inferior temporal gyrus (see Fig. 4B and Table 2). There was decreased FC with the bilateral superior part of the cuneus, the right precuneus and the left dorsal anterior cingulate.

Comparing both groups of visually-deprived subjects showed increased FC of the SMD subjects' still afferented, peripheral EVC with both ventral and dorsal stream regions – the bilateral middle occipital, inferior occipital gyri, the right superior occipital gyrus, the right lateral occipital cortex, the bilateral lingual and fusiform gyri as well as the right parahippocampal gyrus (see Fig. 4C and Table 2). FC was also increased with the right sensorimotor cortex. By contrast, RPTV subjects had increased FC of their sensory deprived peripheral EVC with the bilateral cuneus on the dorsal pathway, the bilateral middle frontal and the right superior frontal gyri well as with the entire left anterior cingulate cortex.

Intra-group analysis - Functional connectivity seeded from the left S1 lip area and the left S1 foot area. Both S1 respective lip and foot areas were perfectly connected between hemispheres in the three groups (see Figs 5 and 6). The lip area was functionally connected to the bilateral post central gyrus, precentral gyrus, premotor cortex, insula, superior temporal gyrus and the left LOC/V5/hMT+ in all three groups. There was negative FC between the lip area and IPL, anterior cingulate cortex (aCC), anterior MTG, and fronto-orbital cortex, precuneus and cuneus.

ROI: Central EVC (regressed peripheral EVC) Contrast Peaks		Brodman area	Peak X	Peak Y	Peak Z	t value	p value
Retinitis pigmentosa tunnel vision > Normal vision							
	LH Middle/Superior occipital gyrus	BA 17/18	-23	-92	0	3,40	0,002
	LH Superior temporal gyrus	BA 22	-55	-11	-3	3,31	0,002
	LH Superior temporal gyrus	BA 41	-37	-29	3	4,36	0,000
Normal vision > retinitis pigmentosa tunnel vision							
	LH Anterior cingulate gyrus	BA 32	-7	34	9	3,34	0,002
	RH Anterior cingulate gyrus	BA 32	8	34	9	2,97	0,005
	RH Anterior middle temporal gyrus	BA 38	41	-2	-21	3,19	0,003
	RH Anterior inferior temporal gyrus	BA 38	35	3	-30	3,53	0,001
	RH Orbital gyrus	BA 11	23	40	6	3,24	0,003
Stargardt macular dystrophy > Normal vision							
	LH Inferior parietal lobule	BA 39	-40	-49	30	3,43	0,002
	LH Parieto-occipital sulcus/Cuneus	BA 19	-7	-71	24	3,19	0,003
	RH Cuneus	BA 19	8	-69	27	3,68	0,001
	RH Parieto-occipital sulcus/ Precuneus	BA 7/BA 19	8	-65	28	3,62	0,001
Normal vision > Stargardt macular dystrophy							
	LH Orbital gyri	BA 47	-25	39	1	2,79	0,008
	RH Superior temporal sulcus	BA 21	50	-17	-9	3,86	0,000
	RH Middle temporal gyrus	BA 38	50	-8	-15	3,27	0,002
	RH Orbital gyri	BA 47	20	40	0	4,57	0,000
Stargardt macular dystrophy > retinitis pigmentosa tunnel vision							
	LH Superior occipital gyrus	BA 18	-22	-89	27	3,68	0,001
	LH Parieto-occipital sulcus	BA 19	-7	-68	30	2,51	0,017
	RH Inferior parietal lobule	BA 19	47	-56	30	3,00	0,005
	RH Parieto-occipital sulcus/Cuneus	BA 19	5	-77	30	3,19	0,003
	RH Precuneus	BA 7	8	-70	34	2,85	0,007
retinitis pigmentosa tunnel vision > Stargardt macular dystrophy							
	LH Fusiform gyrus/Collateral sulcus	BA 37	-28	-56	-12	3,25	0,003
	LH Inferior occipital gyrus	BA 18	-40	-80	-12	3,39	0,002
	LH Supramarginal gyrus	BA 40	-49	-20	18	3,85	0,000
ROI: Peripheral EVC (regressed central EVC)							
retinitis pigmentosa tunnel vision > Normal vision							
	RH Inferior parietal lobule	BA 39	56	-50	36	3,61	0,001
	RH Posterior middle frontal gyrus	BA 6	44	1	42	4,48	0,000
	RH Anterior middle frontal gyrus	BA 44	35	28	33	3,01	0,005
	RH Superior frontal gyrus (BA 9)	BA 9	11	31	48	3,48	0,001
Normal vision > retinitis pigmentosa tunnel vision							
	LH Middle occipital gyrus	BA 18	-28	-89	-6	3,75	0,001
	LH Superior occipital gyrus	BA 18	-25	-89	3	3,05	0,004
	LH Middle temporal gyrus	BA 21	-55	-17	0	3,91	0,000
	LH Post central gyrus	BA 2	-13	-38	51	4,20	0,000
	RH Inferior occipital gyrus	BA 18	33	-86	-18	3,04	0,004
	RH Middle occipital gyrus	BA 18	26	-80	3	4,24	0,000
	RH Superior occipital gyrus	BA 18/19	20	-80	21	3,19	0,003
	RH medial central sulcus/medial post and precentral gyri	—	8	-41	59	3,26	0,002
Stargardt macular dystrophy > Normal vision							
	LH Lingual gyrus	BA 19	-22	-65	-9	2,91	0,006
	RH Lingual gyrus	BA 19	17	-50	-6	3,26	0,002
	RH Fusiform gyrus	BA 20	47	-38	-15	4,54	0,000
	RH parahippocampal gyrus	BA 35	35	-31	-21	3,10	0,004
	RH Inferior temporal gyrus	BA 20	55	-42	-11	2,53	0,016
	RH Inferior occipital gyrus	BA 18	44	-68	-12	3,04	0,004
	RH Inferior temporal gyrus	BA 20	53	-47	-9	3,57	0,001
	RH Inferior temporal sulcus	BA 19	35	-68	6	3,42	0,002
	RH Orbital gyrus	BA 11	14	40	-3	3,49	0,001
Continued							

ROI: Peripheral EVC (regressed central EVC) Contrast peaks	Brodman area	Peak X	Peak Y	Peak Z	t value	p value
Normal vision > Stargardt macular dystrophy						
LH Anterior cingulate gyrus	BA 24	-10	22	30	3,03	0,005
LH Cuneus	BA 18	-7	-71	27	3,26	0,002
RH Cuneus/Parieto-occipital sulcus	BA 18	8	-65	27	4,05	0,000
RH Pre-cuneus	BA 7	8	-65	27	4,05	0,000
Stargardt macular dystrophy > retinitis pigmentosa tunnel vision						
LH Lingual gyrus/Collateral sulcus	BA 19	-25	-62	-15	4,34	0,000
LH Fusiform gyrus	BA 19	-33	-68	-15	3,79	0,001
LH Inferior occipital gyrus	BA 18	-43	-80	-18	5,34	0,000
LH Middle occipital gyrus	BA 19/19	-35	-86	-3	3,50	0,001
LH Central sulcus (dorsal)	BA 1/BA 4	-10	-35	57	3,21	0,003
LH Medial precentral gyrus	BA 4	0	-32	59	3,47	0,001
RH Lingual gyrus/Collateral sulcus	BA 19	23	-53	-6	3,81	0,001
RH Inferior occipital gyrus	BA 19	33	-65	-17	3,19	0,003
RH Fusiform gyrus	BA 37	38	-47	-18	4,25	0,000
RH Parahippocampal gyrus	BA 35	26	-29	-21	3,76	0,001
RH Inferior temporal gyrus (posterior)	BA 20	46	-50	-15	2,86	0,007
RH Inferior occipital gyrus	BA 18/19	38	-68	-15	4,59	0,000
RH Middle occipital gyrus	BA 18	32	-71	6	4,59	0,000
RH Superior occipital gyrus	BA 18	26	-80	16	4,07	0,000
RH Middle occipital gyrus/Middle temporal gyrus	BA 19	41	-63	6	4,04	0,000
RH Superior temporal gyrus/Superior temporal sulcus	BA 21/22	50	-14	-6	3,80	0,001
RH Superior parietal lobule/Post central sulcus	BA 5	26	-38	45	3,61	0,001
RH Post central gyrus/Central sulcus	BA 2	29	-30	54	3,03	0,005
RH Precentral gyrus	BA 4	20	-17	54	3,09	0,004
retinitis pigmentosa tunnel vision > Stargardt macular dystrophy						
LH Cuneus	BA 19	-7	-71	27	-3,77	0,001
LH Anterior cingulate	BA 32	-4	22	24	-3,42	0,002
LH Middle frontal gyrus	BA 46	-28	40	21	-3,76	0,001
RH Inferior parietal lobule	BA 39	50	-59	30	-2,78	0,009
RH Middle frontal gyrus	BA 9	35	25	36	-4,46	0,000
RH Superior frontal gyrus	BA 9	14	31	45	-2,67	0,011
RH Cuneus	BA 19	11	-71	27	-3,63	0,001

Table 2. Peaks of functional connectivity differences between groups. ROI: region-of-interest. Peaks x, y, z: Talairach coordinates. P values corrected for multiple comparisons. LH: Left hemisphere. RH: Right hemisphere. BA: Brodmann areas.

The left foot area was functionally connected with bilateral post central gyrus, precentral gyrus, premotor cortex, and precuneus in all three groups. In all groups the left foot area also exhibited negative FC with bilateral IFG and in peripheral visual field defect (RPTV) and in normal vision also with the anterior insula as well. Moreover, the central visual field group (SMD) exhibited increased FC between the left foot area and the left SOG and the right inferior occipital gyrus whereas the peripheral visual field defect group (RPTV) exhibited increased FC with the right peripheral EVC, LOC, superior temporal gyrus and bilateral SPL (see Fig. 6B and C).

Between group analysis - Functional connectivity seeded from the left S1 lip area and the left S1 foot area. In patients with a peripheral visual field defect compared to normal vision, the left S1 lip area showed increased FC with STG and decreased FC with an area that overlaps V5/hMT+ and EBA as well as SPL (see Fig. 7A). In patients with central visual loss compared to normal vision, there was an increased FC of the lip area with MTG and anterior EVC (see Fig. 7B). In patients with central visual loss compared to patients with peripheral visual loss there is an increased FC of the left lip area with the posterior part of inferior and middle frontal gyri (posterior part of Broca area) and IPS (see Fig. 7C).

We found no FC difference for the left foot area between normally sighted and patients with peripheral visual field loss (RPTV) (see Fig. 8A). In patients with central visual field loss (SMD) compared to the normally sighted, there was increased FC with the right posterior superior temporal gyrus, SPL, postcentral gyrus, fusiform and lingual gyri (see Fig. 8B). Compared to central visual field loss (SMD), in peripheral visual field loss, the left foot area exhibited increased FC with the right anterior EVC, cuneus and left lingual and fusiform gyri and decreased FC with left MOG (see Fig. 8C).

The main results were summarized in Fig. 9.

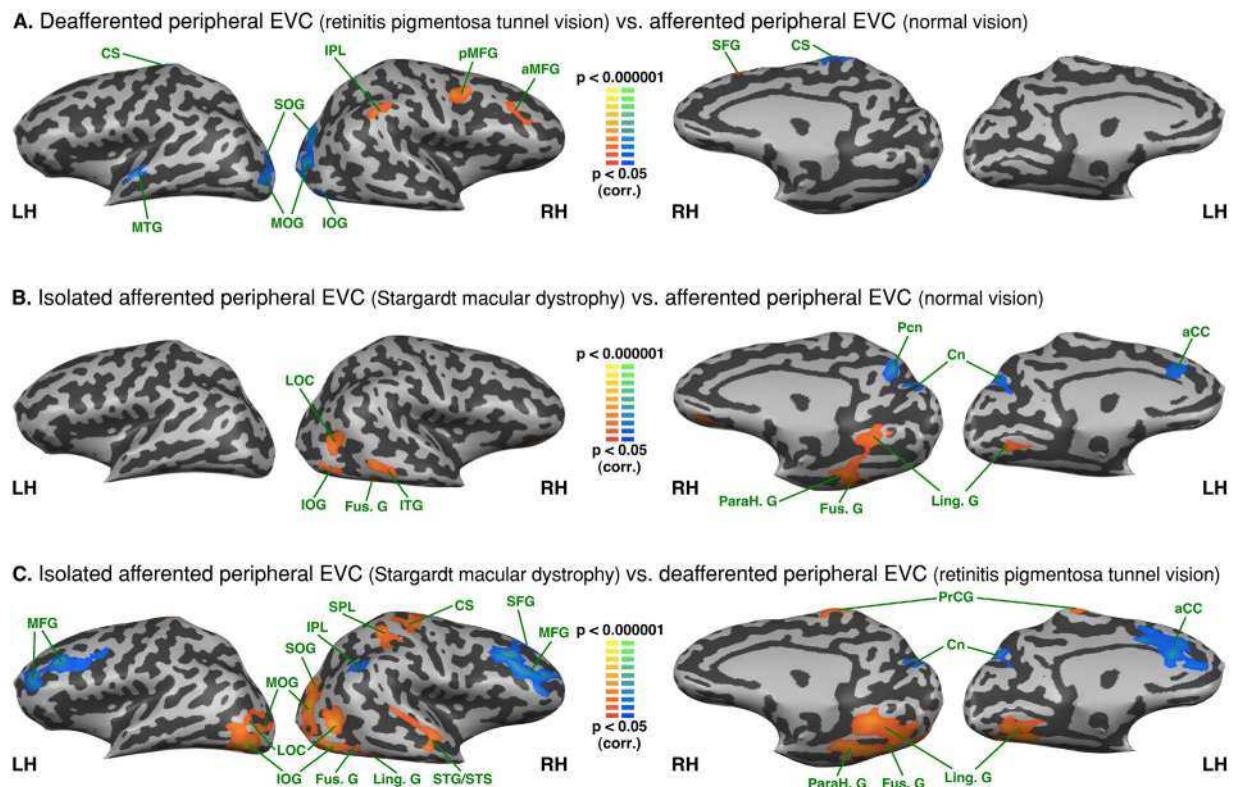


Figure 4. Between-group analysis of functional connectivity seeded from the peripheral EVC (central EVC regressed). The maps are shown in mesh for (A) retinitis pigmentosa tunnel vision vs. normal vision (B) Stargardt macular dystrophy vs. normal vision (C) Stargardt macular dystrophy vs. retinitis pigmentosa tunnel vision (yellow-orange depicts areas of higher positive/lower negative functional connectivity with central EVC for the first group compared to the second, and green-blue the opposite comparison; x, y, z are Talairach coordinates; LH: left hemisphere, RH: right hemisphere). aCC: anterior cingulate cortex; aMFG: anterior middle frontal gyrus; aMTG: anterior middle temporal gyrus; Cn: cuneus; CS: central sulcus; Fus. G: fusiform gyrus; Ling. G: lingual gyrus; LOC: lateral occipital complex; IOG: inferior occipital gyrus; ITG: inferior temporal gyrus; IPL: inferior parietal lobule; MFG: middle frontal gyrus; MOG: middle occipital gyrus; MTG: middle temporal gyrus; ParaH. G: parahippocampal gyrus; Pcn: precuneus; pMFG: posterior middle frontal gyrus; PoCG: postcentral gyrus; POS: parieto-occipital sulcus; SFG: superior frontal gyrus; SMG: supramarginal gyrus; SOG: superior occipital gyrus; SPL: superior parietal lobule; STG: superior temporal gyrus; STS: superior temporal sulcus.

Discussion

SMD and RPTV models were implemented to evaluate the effects of central and visual loss on the FC of the EVC. The five main findings can be summarized as follows: (1) in both patient groups, deafferented EVC exhibited a different FC pattern than the corresponding regions in normally sighted, suggesting that either the central or peripheral EVC could reorganize after deafferentation but more interestingly (2) we also found a different FC pattern in the patients' EVC that still received the residual visual input, implying that such reorganization also impacts afferented visual areas; (3) we found more changes in FC to peripheral than to central EVC (in both afferented and deafferented states); (4) compared to normal vision, the patients' afferented central or peripheral EVC demonstrated increased FC with many areas involved in visual processing whereas the deafferented central or peripheral EVC showed increased FC with remote regions; (5) The contrast between deafferented and isolated afferented early visual cortex revealed patterns of FC differences that were similar, but more complex compared to those observed in comparison to normally afferented visual cortex.

The functional connectivity of the normally afferented central and peripheral early visual cortex. In the normally sighted, the central and peripheral early visual cortex exhibited a positive FC with areas of the dorsal and ventral stream. The positive FC of the central and peripheral EVC was roughly similar to previous descriptions of the entire EVC connectivity with the exception of the primary sensorimotor cortex³⁷. However, we found a weak positive FC between the early visual cortex (central and peripheral) and the primary sensorimotor cortex (mostly in the right hemisphere) that did not survive the correction for multiple comparisons (data not shown).

FC differences between isolated afferented and normally afferented EVC. Compared to the subjects with normal vision, the afferented central EVC in RPTV exhibited increased FC with the left MOG and STG,

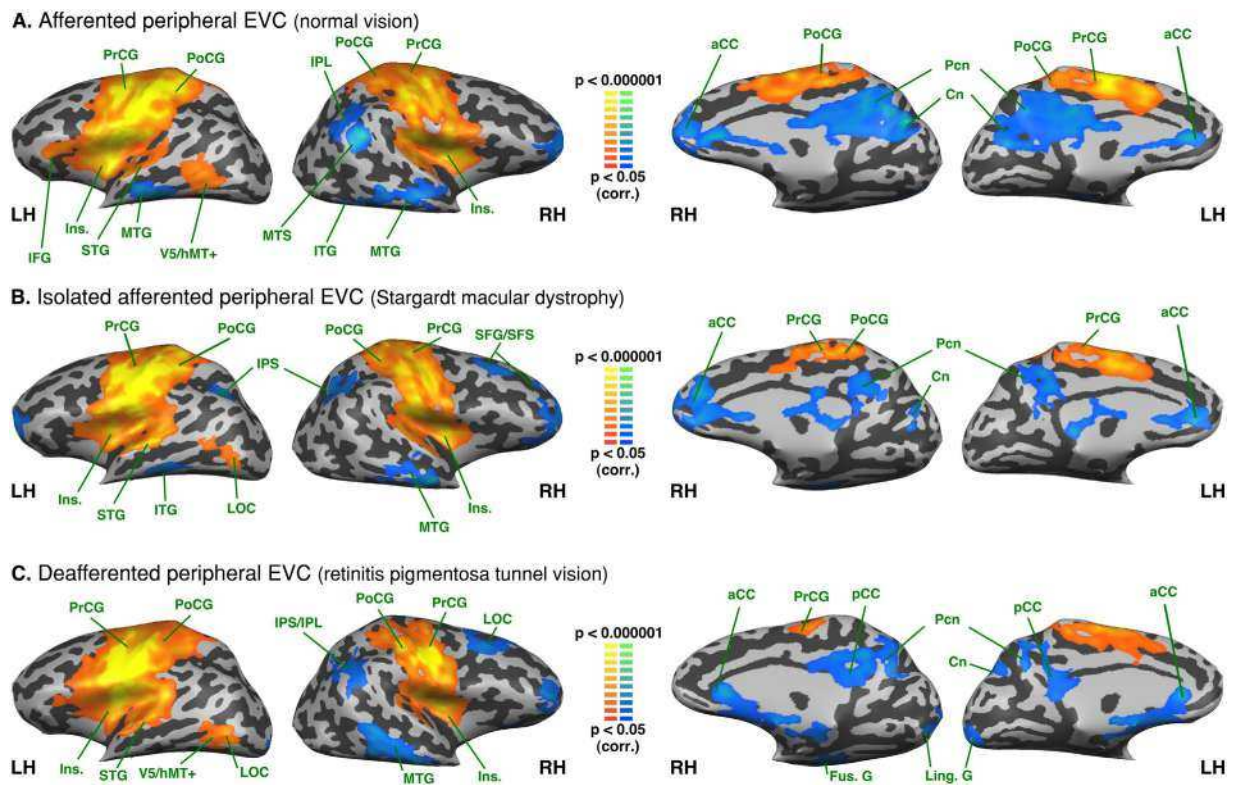


Figure 5. Intra-group analysis of functional connectivity seeded from the left hemisphere S1 lip area (S1 foot area regressed). The maps are shown in mesh for the (A) afferented peripheral EVC (normal vision) (B) isolated afferented peripheral EVC (Stargardt macular dystrophy) (C) deafferented peripheral EVC (retinitis pigmentosa tunnel vision). Yellow-orange depicts areas of higher positive connectivity for each group, and green-blue higher negative connectivity. LH: left hemisphere, RH: right hemisphere. Cn: cuneus; Fus. G: fusiform gyrus; IFG: inferior frontal gyrus; Ins.: Insula; IOG: inferior occipital gyrus; IPL: inferior parietal lobe; IPS: intraparietal sulcus; STG: superior temporal gyrus; ITG: inferior temporal gyrus; Ling. G: lingual gyrus; IFG: inferior frontal gyrus; MOG: middle occipital gyrus; Pcn: precuneus; PrCG: precentral gyrus; PoCG: postcentral gyrus; MTG: middle temporal gyrus; LOC: lateral occipital complex; aCC: anterior cingulate cortex; pCC: posterior cingulate cortex; SFG/SFS: superior frontal gyrus/sulcus.

whereas their deafferented EVC periphery showed decreased FC with these same regions. Interestingly, in normal vision these regions had stronger canonical connections with the peripheral EVC as found in previous studies (see Fig. 2)^{57–59}. It is conceivable that the increased FC of the central EVC with the left MOG and STS/STG, which are involved in space, scene processing and multisensory integration, reflects an adaptive process to partially compensate for the loss of peripheral vision^{60–63}.

Compared to the subjects with normal vision, the afferented peripheral EVC in SMD subjects showed an increased FC with areas of the ventral stream (i.e., the left lingual and inferior occipital gyri, the bilateral fusiform gyrus, the right parahippocampal gyrus) and associated functional areas (i.e., the right lateral occipital complex). Most of these regions are involved in the face perception network^{64,65} and even predict performance in multiple face-processing tasks⁶⁶. It is worth noting that in normal vision, face perception is associated with center-biased rather than peripheral-biased representations^{64,67}. Hence, the increased FC between isolated afferented peripheral EVC and the ventral stream areas in SMD subjects (as compared to the other groups) may be indicative of a compensatory mechanism for the loss of central vision. Similar results were obtained in an fMRI study exploring the effects of simulated central scotoma on face recognition⁶⁸. Moreover, developmental data on the early ability of neonates to process faces⁶⁹ although they have an immature fovea and low visual acuity¹ lend additional support to this hypothesis.

FC differences between afferented and deafferented EVC. Compared to the normally sighted, the deafferented peripheral EVC in RPTV group exhibited increased FC with the IPL/IPS and MFG. Interestingly, the isolated afferented central EVC showed decreased FC with the same region. IPS/IPL plays a role in top-down control, attention, multisensory integration, visuomotor coordinate transformation and task-demand in normal subjects^{58,70–72}. Therefore, the increased FC between the RPTV deafferented peripheral EVC with IPS and other areas involved in eye movements (FEF, SEF), multisensory integration, visuomotor coordinate transformation (IPL) and pre-motor control and planning (middle frontal gyrus) presumably reflects adaptive mechanisms to peripheral vision loss.

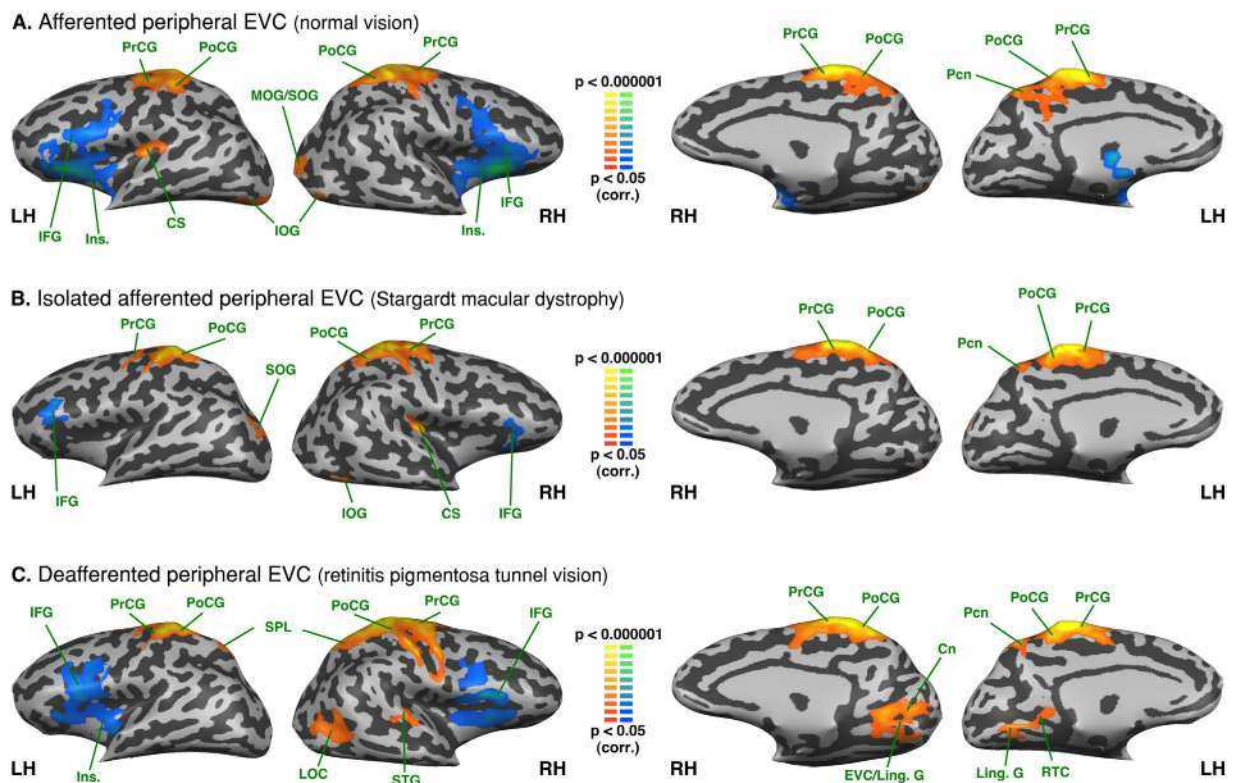


Figure 6. Intra-group analysis of functional connectivity seeded from the left hemisphere S1 foot area (S1 lip area regressed). The maps are shown in mesh for the (A) afferented peripheral EVC (normal vision) (B) isolated afferented peripheral EVC (Stargardt macular dystrophy) (C) deafferented peripheral EVC (retinitis pigmentosa tunnel vision). Yellow-orange depicts areas of higher positive connectivity for each group, and green-blue higher negative connectivity. LH: left hemisphere, RH: right hemisphere. EVC: early visual cortex; Cn: cuneus; RTC: retrosplenial cortex; Fus. G: fusiform gyrus; IFG: inferior frontal gyrus; Ins.: Insula; IOG: inferior occipital gyrus; SPL: superior parietal lobule; IPS: intraparietal sulcus; Ling. G: lingual gyrus; IFG: inferior frontal gyrus; MOG: middle occipital gyrus; SOG: superior occipital gyrus; LS: lateral sulcus; STG: superior temporal gyrus; Pcn: precuneus; PrCG: precentral gyrus; PoCG: postcentral gyrus; MTG: middle temporal gyrus; LOC: lateral occipital complex; aCC: anterior cingulate cortex; pCC: posterior cingulate cortex. CS: central sulcus.

Compared to the normally afferented (sighted) and isolated afferented central EVC (RPTV), the deafferented central EVC of the SMD exhibited increased FC with the cuneus, the parieto-occipital sulcus (POS) and the precuneus. The participation of these regions in switching attention, orientation selectivity and visuomotor processing⁷³ raises questions about their possible role in the development of a surrogate overt attention network in subjects lacking central vision. This remains true as well at the intragroup level given the positive FC of the deafferented central EVC not only with the precuneus but also with the MOG (see Fig. 1C), which is involved in space and scene processing⁶³. In the normally sighted EVC, the precuneus and MOG exhibit strong coactivation in visual imagery tasks⁷⁴ suggesting that the FC changes we observed in the deafferented central EVC might share common mechanisms with mental imagery⁷⁴. Interestingly, in contrast to the deafferented central EVC, the isolated afferented peripheral EVC of SMD patients exhibited decreased FC with the cuneus, the POS and the precuneus (see Fig. 4B) possibly reflecting a buffering mechanism to prevent noise and errors⁷⁵.

At the intra-group level, both the deafferented central (SMD) and peripheral (RPTV) EVC showed a positive FC with the posterior thalamus/pulvinar (non-significant difference when compared to normally sighted). The pulvinar is involved in attentional processes and is thought to play a fundamental role in cortico-cortical communication⁷⁶. Sensory deprivation imbalances the geniculate and cortical input^{13,15} and therefore, the positive FC between the visually deafferented early visual cortex and the pulvinar might unmask preexisting cortico-thalamo-cortical signals for top-down control. Activation found by previous studies in the V1 lesion projection zone (LPZ) during visual stimulus-related judgments but not during passive viewing suggests the participation of attentional mechanisms and supports this hypothesis^{13,15}.

Differences between isolated afferented EVC and deafferented EVC. The contrast between isolated afferented EVC and deafferented EVC is difficult to interpret as it compares two groups with a modified FC. It was primarily intended to be a control for the comparison to the normally afferented visual cortex. In fact, the differences in FC between the isolated afferented central EVC in the RPTV and the deafferented central EVC in the SMD group were roughly similar to the differences observed when compared to the normally afferented

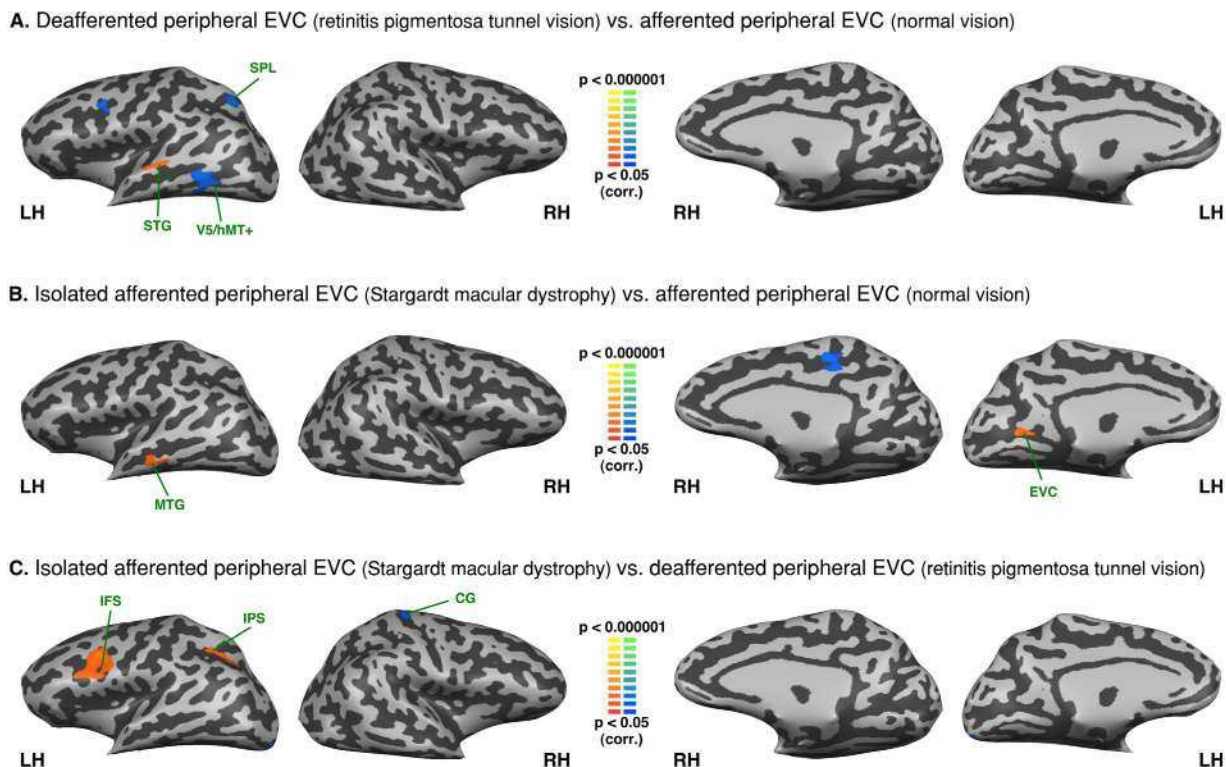


Figure 7. Between-group analysis of functional connectivity seeded from the left hemisphere S1 lip area (S1 foot area regressed). The maps are shown in mesh for (A) retinitis pigmentosa tunnel vision vs. normal vision (B) Stargardt macular dystrophy vs. normal vision (C) Stargardt macular dystrophy vs. retinitis pigmentosa tunnel vision (yellow-orange depicts areas of higher positive/lower negative functional connectivity with S1 lip area for the first group compared to the second, and green-blue the opposite comparison; LH: left hemisphere, RH: right hemisphere). SPL: superior parietal lobule; STG: superior temporal gyrus; MTG: middle temporal gyrus; EVC: early visual cortex; IFS: inferior frontal sulcus; IPS: intraparietal sulcus; CG: central gyrus.

central EVC, with the exception of the MOG. The lack of a FC difference in MOG, consistent with the results mentioned above, might reflect the increased adaptive connectivity of both the deafferented and isolated afferented central EVC with this region. The isolated afferented central EVC of RPTV also exhibited a relative increase in FC with the IOG and fusiform gyrus, which are areas of the ventral processing stream.

Compared to the deafferented peripheral EVC in the RPTV patients, the isolated afferented peripheral EVC in the SMD patients exhibited an increased FC with the right sensorimotor cortex, superior temporal gyrus and bilateral LOC. Thus, this unique contrast between afferented and deafferented peripheral EVC also exposes the multisensory connections of the afferented peripheral EVC with sensorimotor and auditory areas^{37,57,58}. Moreover, when seeding from the foot area in SMD patients we found a similar FC pattern, which confirms the multisensory connectivity between afferented peripheral EVC, LOC auditory and somatosensory areas (see Fig. 8).

The maps seeded from the S1 areas. The intra-group ROI analyses based on somatosensory seeds validate our resting-state partial correlation approach by showing that the somatosensory topographic system could be mapped in our sighted population as well as in both groups of visually-impaired patients (see Figs 5 and 6). The S1 respective lip and foot areas were perfectly connected between hemispheres in the three groups, see Figs 5 and 6). These results are in line with previous studies showing such a similar organization system in the sighted^{40,42}. Moreover, the lip area was functionally connected to bilateral inferior frontal gyrus, insula and the right LOC, which is consistent with the literature⁵². We found very minor between-group differences, (see Fig. 7). These results support the claim that observed differences in the visual cortex (Figs 1 to 4) are related to the plastic changes induced by visual field loss.

The analysis seeding the foot sensory projection area also yielded consistent results. The regression of the lip projection area resulted in a negative FC between the foot area and the inferior frontal gyrus and insula. In central visual field loss, the foot area is functionally connected to the isolated afferented peripheral EVC (see Fig. 6c). This coincides with what we found with EVC seeds (see Figs 2b and 8). However, there was no significant difference with the normally sighted (see Fig. 8b).

Comparison of the FC between congenital, late complete blindness and partial blindness. To the best of our knowledge, few studies^{39,41} have compared the rs-FC to retinotopic areas of the blind. Bock *et al.* found that resting-state correlations between V1 and V2/V3 were retinotopically organized in normally sighted, early blind

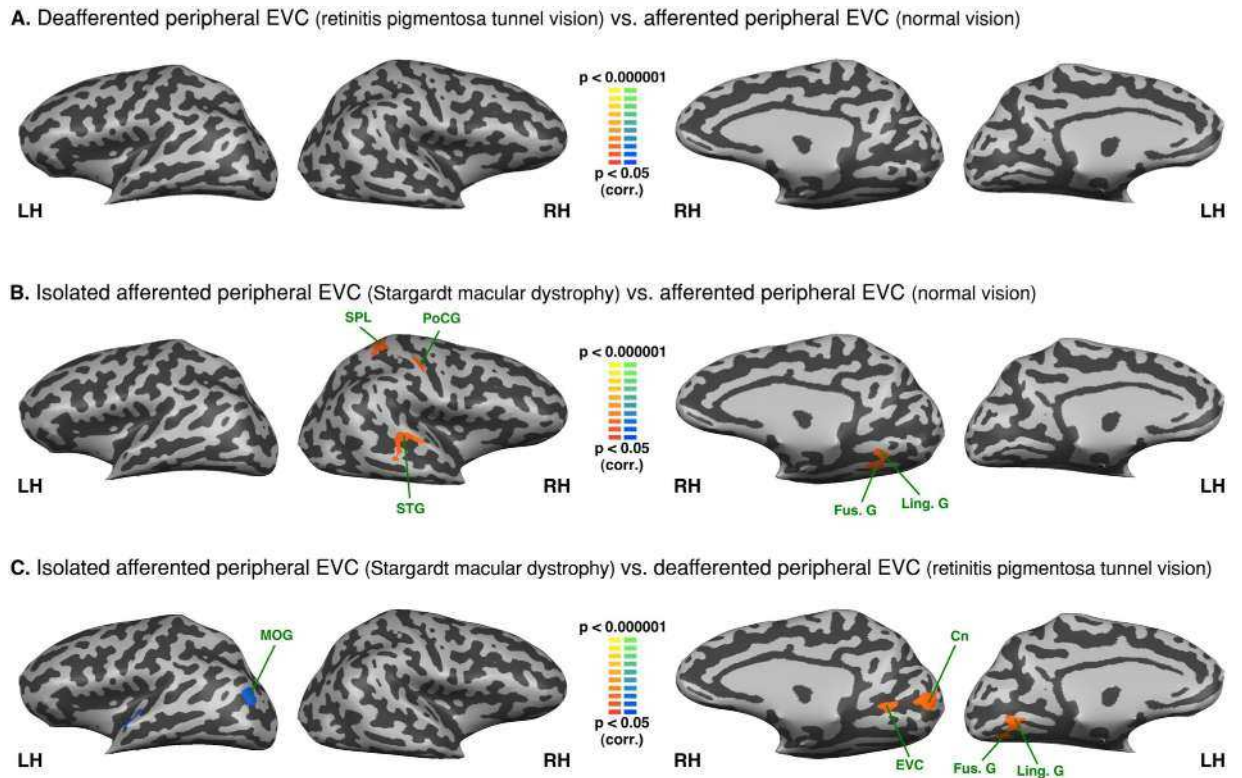


Figure 8. Between-group analysis of functional connectivity seeded from the left hemisphere S1 foot area (S1 lip area regressed). The maps are shown in mesh for (A) retinitis pigmentosa tunnel vision vs. normal vision (B) Stargardt macular dystrophy vs. normal vision (C) Stargardt macular dystrophy vs. retinitis pigmentosa tunnel vision (yellow-orange depicts areas of higher positive/lower negative functional connectivity with S1 foot area for the first group compared to the second, and green-blue the opposite comparison; LH: left hemisphere, RH: right hemisphere). SPL: superior parietal lobule; PoCG: post central gyrus; STG: superior temporal gyrus; Fus. G: fusiform gyrus; Ling. G: lingual gyrus; MOG: middle occipital gyrus; EVC: early visual cortex; Cn: Cuneus.

as well as anophthalmic subjects suggesting that retinal waves or visual experience are not necessary to develop a resting-state retinotopic pattern⁴¹. The team of Striem-Amit seeded both the central and peripheral EVC in congenitally blind subjects and also identified different FC patterns according to the seeds³⁹. Interestingly, as compared to sighted controls, they found an increased FC of the peripheral EVC in the congenitally blind group with the same areas that we found in the RP (i.e. IPL/IPS, MFG; see Fig. 4B) and SMD patients (LOC, IOG, ITG, fusiform gyrus; see Fig. 4A). They attributed their results to cross-modal attention plasticity which is consistent with the hypotheses we put forward for our populations. However, these authors found a FC increase of the central EVC with the left inferior frontal gyrus and a FC decrease of both retinotopic areas with the somatosensory and auditory regions. We did not find such results here (see Figs 3, 7 and 8). This might be explained by the extent of visual loss since in a previous study our team showed that the FC pattern of retinotopic regions with Broca's area differs between RP completely blind and tunnel vision patients⁷⁷. As also shown by the analyses seeding S1 areas (see Figs 5, 6, 7 and 8), certain robust systems (language, auditory, somatosensory) might need profound loss of vision to start developing plasticity^{78–81}.

Overall, the FC pattern of the part of the EVC receiving the remaining visual input supports the first hypothesis that the isolated afferented EVC strengthens the local connections, presumably to tune-up visual information processing. In the deafferented EVC, remodeling concerns more remote connections, and this pattern lends support to the third hypothesis that deafferented EVC likely diverts its processing capacity to higher-order functions that can optimize the residual visual function. The absence of increased local connectivity in the deafferented compared to the normally afferented EVC or its decreased local connectivity when compared to the isolated afferented EVC do not support the view that deafferented EVC rewires the same type of information as the afferented EVC (2nd hypothesis). An alternative explanation for the increased FC of the sensory deprived visual cortex is that it represents noise generated by aberrant autonomous activity⁸² (4th hypothesis). This scenario is unlikely because it would imply strengthened connections between the deafferented EVC and regions to which they are strongly linked in normal vision, an effect that was not confirmed by our data. Rather, the enhanced connectivity of the deafferented primary visual cortex concerned long-range connections involved in higher-order processing. However, as suggested by the thinning of the gray matter in the deafferented EVC in conditions inducing similar visual field defects^{83–88}, these long-range connections are not enough to preserve the processing function and structure of the visual areas that lost their sensory input.

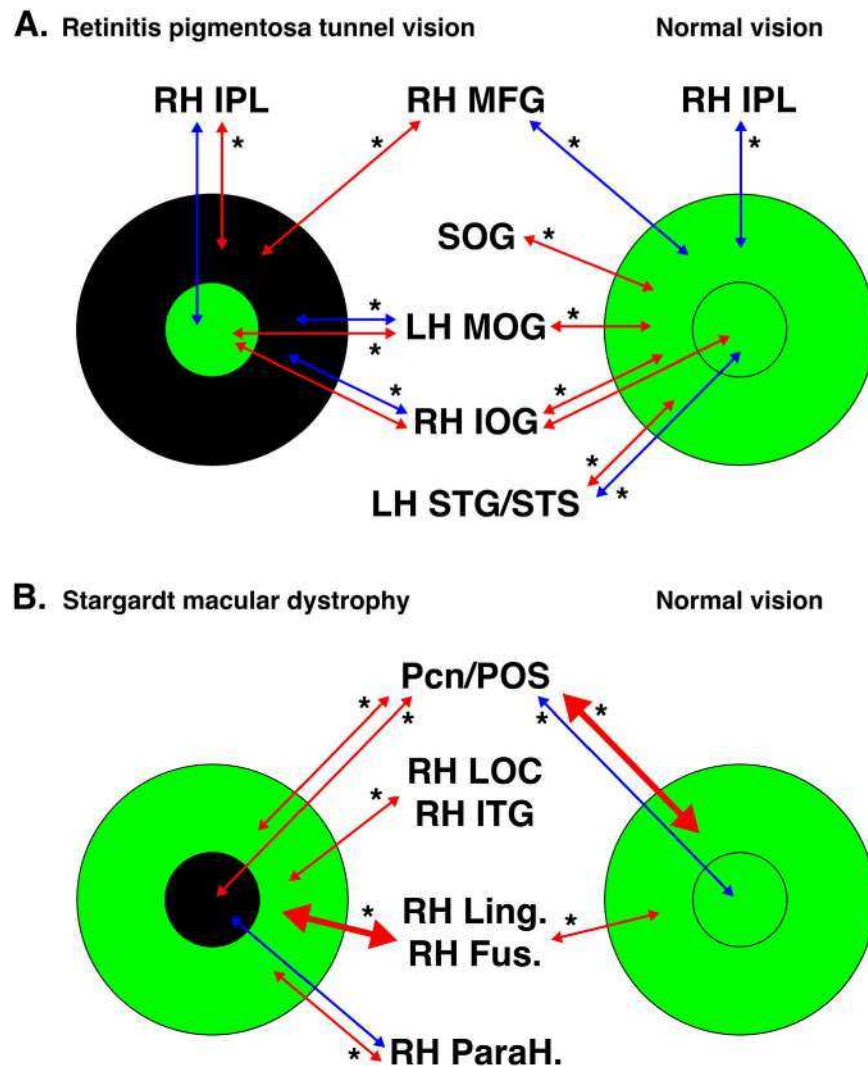


Figure 9. Summary of the main results of the FC analysis seeding peripheral and central EVC. The main FC results are shown for the comparison between (A). retinitis pigmentosa tunnel vision or (B). Stargardt macular dystrophy and normal vision. Small circles indicate regions of the EVC coding for the central projection of the retina, large circles indicate regions of the EVC coding for the peripheral projection of the retina. Green depicts afferented areas of the EVC. Black depicts deafferented areas of the EVC. Red arrows indicate positive FC between areas at the intra-group level and blue arrows negative FC between areas at the intra-group level. The arrow thickness indicates the level of FC at the intra-group level. Stars indicate statistical significance at $p < 0.05$ for the FC between groups. LH: left hemisphere, RH: right hemisphere. MFG: middle frontal gyrus; STG/STS: Superior temporal gyrus/sulcus; Cn: cuneus; Fus. G: fusiform gyrus; Ling. G: lingual gyrus; LOC: lateral occipital complex; IOG: inferior occipital gyrus; ITG: inferior temporal gyrus; IPL: inferior parietal lobule; MFG: middle frontal gyrus; MOG: middle occipital gyrus; ParaH G: parahippocampal gyrus; Pcn: precuneus; POS: parieto-occipital sulcus; SOG: superior occipital gyrus.

Limitations

Direct implications from the present data on patients' everyday life and hypotheses about precise cerebral mechanisms cannot be inferred from *rs*-FC data alone. Therefore, the present results and the hypothesis we advanced require further exploration with behavioral and task-based *f*MRI studies.

The best way of designing the ROI for central and peripheral EVC is retinotopy. Unfortunately in central visual loss, the fixation is eccentric and unsteady and as a result, retinotopy would have been particularly challenging and subject to errors. To bypass this limitation, we estimated the central and peripheral EVC by extrapolating the ROI from a retinotopy experiment conducted in a second group of normally sighted subjects. In addition, this method avoids the problem of differences in accuracy when defining EVC across patients and control subjects (see also supplementary Figure S7 for control analysis of localizer definitions). However, since the deafferented primary visual cortex suffers from structural alterations, primarily in the form of gray matter thinning, both in central^{83–86} and peripheral^{83,87} visual field loss, the central and peripheral ROI we employed may not be limited to V1, and overlapped to a certain extent with V2. For this reason we employed the term of “early visual cortex”.

Rs-fMRI is subject to reliability problems induced by movement^{49,89,90}. Therefore, we instigated extra measures to control for head movement and to verify that there was no significant difference in head movement across groups (see *pre-processing* section in *Materials and methods* and Supplementary Figures S1 to S4).

It is a convention in the field that increases in functional correlations may reflect increased functional connectivity. However, increases in the BOLD signal can be unrelated to plasticity as demonstrated by higher resting-state firing in blind animals⁹¹, or enhanced retinotopic rs-signals in anophthalmic individuals possibly due to metabolism alteration⁴¹. Furthermore, glucose utilization in the human visual cortex is abnormally elevated in early but decreases in late blindness⁹². We have a degree of certainty that the resting-state firing state was equivalent in our three populations since the control analyses seeding S1 areas (see Figs 5, 6, 7 and 8) revealed similar symmetric patterns between hemispheres in all the three groups. Moreover, the selection criteria were stringent to avoid the patients with associated disorders that could account for the metabolic disorders.

Despite numerous claims to the contrary in the literature^{28,34,93}, we cannot exclude that rs-fMRI reflects non neural signals such as blood flow^{46,94}. It has been shown that the vascular flow from the back to the front of the head is highly similar to the neural eccentric retinotopy⁹⁵. In an attempt to reduce the effect of the vascular component, we used the partial correlation method.

Unlike simple correlation, the partial correlation method has the advantage of identifying false positives when looking for direct connections^{53,96–101}, but can introduce false negative correlations⁴⁸. Compared to simple correlation analyses (see Supplementary Figures S5 and S6), we found similar negative FC patterns across groups and identified the false positives. Furthermore, we validated the coherence and specificity of the resting-state partial correlation approach through somatosensory seeds (see Figs 5, 6, 7 and 8) and showed that: (1) S1 respective lip and foot areas were perfectly connected between hemispheres as predicted (topographical homologies in the location based on topography) and (2) the somatosensory topographic system in our sighted population was similar to the one described in the literature^{40,42} and more importantly, to our visually-impaired subjects (3) analyses seeding EVC and S1 areas were coherent since the FC of S1 to EVC was found after both analyses.

Conclusion

The current study documented the functional reorganization induced in the primary visual cortex by visual loss specifically affecting either central or peripheral vision. The observed changes suggest two types of adaptive processes. The first involves the afferented parts of the primary visual cortex and engages certain preexisting pathways by enforcing their connections and presumably increasing their processing power to compensate for the loss of the deafferented EVC functions. The second concerns sensory-deprived parts of the primary visual cortex, which strengthens long-range connections, presumably to support high-order mechanisms. These results provide insights into the behavior of EVC functional regions in disease. A greater understanding of these processes is crucial for any attempt to develop efficient rehabilitation strategies or vision restoration.

References

- Hendrickson, A. E. Primate foveal development: A microcosm of current questions in neurobiology. *Investigative Ophthalmology and Visual Science* **35**, 3129–3133 (1994).
- Hendrickson, A., Possin, D., Vajzovic, L. & Toth, C. a. Histologic Development of the Human Fovea From Midgestation to Maturity. *American Journal of Ophthalmology* **154**, 767–778.e2 (2012).
- Vajzovic, L. *et al.* Maturation of the Human Fovea: Correlation of Spectral-Domain Optical Coherence Tomography Findings With Histology. *American Journal of Ophthalmology* **154**, 779–789.e2 (2012).
- Tadin, D., Nyquist, J. B., Lusk, K. E., Corn, A. L. & Lappin, J. S. Peripheral vision of youths with low vision: Motion perception, crowding, and visual search. *Investigative Ophthalmology and Visual Science* **53**, 5860–5868 (2012).
- Liu, T. *et al.* Incomplete cortical reorganization in macular degeneration. *Investigative Ophthalmology and Visual Science* **51**, 6826–6834 (2010).
- Plank, T. *et al.* Neural correlates of visual search in patients with hereditary retinal dystrophies. *Human Brain Mapping* **34**, 2607–2623 (2013).
- Morland, A. B., Baseler, H. A., Hoffmann, M. B., Sharpe, L. T. & Wandell, B. A. Abnormal retinotopic representations in human visual cortex revealed by fMRI. *Acta Psychologica* **107**, 229–247 (2001).
- Baseler, H. A. *et al.* Reorganization of human cortical maps caused by inherited photoreceptor abnormalities. *Nature neuroscience* **5**, 364–70 (2002).
- Fahim, A. T. *et al.* Diagnostic fundus autofluorescence patterns in achromatopsia. *American journal of ophthalmology* **156**, 1211–1219.e2 (2013).
- Baker, C. I., Peli, E., Knouf, N. & Kanwisher, N. G. Reorganization of visual processing in macular degeneration. *The Journal of neuroscience: the official journal of the Society for Neuroscience* **25**, 614–618 (2005).
- Baker, C. I., Dilks, D. D., Peli, E. & Kanwisher, N. Reorganization of visual processing in macular degeneration: Replication and clues about the role of foveal loss. *Vision Research* **48**, 1910–1919 (2008).
- Baseler, H. A. *et al.* Large-scale remapping of visual cortex is absent in adult humans with macular degeneration. *Nature neuroscience* **14**, 649–55 (2011).
- Masuda, Y., Dumoulin, S. O., Nakadomari, S. & Wandell, B. A. V1 projection zone signals in human macular degeneration depend on task, not stimulus. *Cerebral cortex (New York, N.Y.: 1991)* **18**, 2483–93 (2008).
- Dilks, D. D., Baker, C. I., Peli, E. & Kanwisher, N. Reorganization of visual processing in macular degeneration is not specific to the 'preferred retinal locus'. *The Journal of neuroscience: the official journal of the Society for Neuroscience* **29**, 2768–2773 (2009).
- Masuda, Y. *et al.* Task-dependent V1 responses in human retinitis pigmentosa. *Investigative ophthalmology & visual science* **51**, 5356–64 (2010).
- Cunningham, S. I., Weiland, J. D., Bao, P., Lopez-Jaime, G. R. & Tjan, B. S. Correlation of vision loss with tactile-evoked V1 responses in retinitis pigmentosa. *Vision research* **111**, 197–207 (2015).
- Singh, A. & Sorensen, T. L. The prevalence and clinical characteristics of Charles Bonnet Syndrome in Danish patients with neovascular age-related macular degeneration. *Acta Ophthalmologica* **90**, 476–480 (2012).
- O'Hare, F. *et al.* Charles Bonnet Syndrome in Advanced Retinitis Pigmentosa. *Ophthalmology* **122**, 1951–1953 (2015).
- Merabet, L. B. *et al.* Visual hallucinations during prolonged blindfolding in sighted subjects. *Journal of neuro-ophthalmology: the official journal of the North American Neuro-Ophthalmology Society* **24**, 109–113 (2004).

20. Sahel, J.-A., Marazova, K. & Audo, I. Clinical Characteristics and Current Therapies for Inherited Retinal Degenerations. *Cold Spring Harbor Perspectives in Medicine* **5**, a017111–a017111 (2015).
21. Stargardt, K. Über familiäre, progressive Degeneration in der Maculagegend des Auges. *Albrecht von Graefes Archiv für Ophthalmologie* **71**, 534–550 (1909).
22. Boucart, M., Naili, F., Despretz, P., Defoort-Dhellemmes, S. & Fabre-Thorpe, M. Implicit and explicit object recognition at very large visual eccentricities: No improvement after loss of central vision. *Visual Cognition* **18**, 839–858 (2010).
23. Safran, A. B., Duret, F., Issenhueth, M. & Mermoud, C. Full text reading with a central scotoma : pseudo regressions and pseudo line losses. *British Journal of Ophthalmology* **83**, 1341–1347 (1999).
24. Luo, G. & Peli, E. Use of an augmented-vision device for visual search by patients with tunnel vision. *Investigative Ophthalmology and Visual Science* **47**, 4152–4159 (2006).
25. Wittich, W., Faubert, J., Watanabe, D. H., Kapusta, M. A. & Overbury, O. Spatial judgments in patients with retinitis pigmentosa. *Vision Research* **51**, 165–173 (2011).
26. Fortenbaugh, F. C., Hicks, J. C., Hao, L. & Turano, K. a. Losing sight of the bigger picture: Peripheral field loss compresses representations of space. *Vision Research* **47**, 2506–2520 (2007).
27. Biswal, B., Yetkin, F. Z., Haughton, V. M. & Hyde, J. S. Functional connectivity in the motor cortex of resting human brain using echo-planar MRI. *Magnetic resonance in medicine: official journal of the Society of Magnetic Resonance in Medicine/Society of Magnetic Resonance in Medicine* **34**, 537–41 (1995).
28. Greicius, M. D., Krasnow, B., Reiss, A. L. & Menon, V. Functional connectivity in the resting brain: a network analysis of the default mode hypothesis. *Proceedings of the National Academy of Sciences of the United States of America* **100**, 253–8 (2003).
29. Hampson, M., Olson, I. R., Leung, H., Skudlarski, P. & Gore, J. C. Changes in functional connectivity of human MT/V5 with visual motion input. *Neuroreport* **15**, 1315–1319 (2004).
30. Damoiseaux, J. S. *et al.* Consistent resting-state networks across healthy subjects. *Proceedings of the National Academy of Sciences of the United States of America* **103**, 13848–53 (2006).
31. Fox, M. D., Corbetta, M., Snyder, A. Z., Vincent, J. L. & Raichle, M. E. Spontaneous neuronal activity distinguishes human dorsal and ventral attention systems. *Proceedings of the National Academy of Sciences of the United States of America* **103**, 10046–51 (2006).
32. Dosenbach, N. U. F. *et al.* Distinct brain networks for adaptive and stable task control in humans. *Proceedings of the National Academy of Sciences of the United States of America* **104**, 11073–8 (2007).
33. Vincent, J. L., Kahn, I., Snyder, A. Z., Raichle, M. E. & Buckner, R. L. Evidence for a frontoparietal control system revealed by intrinsic functional connectivity. *Journal of neurophysiology* **100**, 3328–42 (2008).
34. Smith, S. M. *et al.* Correspondence of the brain's functional architecture during activation and rest. *Proceedings of the National Academy of Sciences of the United States of America* **106**, 13040–5 (2009).
35. Spreng, R. N., Stevens, W. D., Chamberlain, J. P., Gilmore, A. W. & Schacter, D. L. Default network activity, coupled with the frontoparietal control network, supports goal-directed cognition. *NeuroImage* **53**, 303–17 (2010).
36. Buckner, R. L., Krienen, F. M. & Yeo, B. T. T. Opportunities and limitations of intrinsic functional connectivity MRI. *Nature neuroscience* **16**, 832–7 (2013).
37. Wang, K. *et al.* Spontaneous activity associated with primary visual cortex: a resting-state FMRI study. *Cerebral cortex (New York, N.Y.: 1991)* **18**, 697–704 (2008).
38. Butt, O. H., Benson, N. C., Datta, R. & Aguirre, G. K. The fine-scale functional correlation of striate cortex in sighted and blind people. *The Journal of neuroscience: the official journal of the Society for Neuroscience* **33**, 16209–19 (2013).
39. Striemi-Amit, E. *et al.* Functional connectivity of visual cortex in the blind follows retinotopic organization principles. *Brain: a journal of neurology* **138**, 1679–1695 (2015).
40. Zeharia, N., Hertz, U., Flash, T. & Amedi, A. New Whole-Body Sensory-Motor Gradients Revealed Using Phase-Locked Analysis and Verified Using Multivoxel Pattern Analysis and Functional Connectivity. *Journal of Neuroscience* **35**, 2845–2859 (2015).
41. Bock, A. S. *et al.* Resting-State Retinotopic Organization in the Absence of Retinal Input and Visual Experience. *Journal of Neuroscience* **35**, 12366–12382 (2015).
42. Zeharia, N., Hertz, U., Flash, T. & Amedi, A. Negative blood oxygenation level dependent homunculus and somatotopic information in primary motor cortex and supplementary motor area. *Proceedings of the National Academy of Sciences* **109**, 18565–18570 (2012).
43. Butt, O. H., Benson, N. C., Datta, R. & Aguirre, G. K. Hierarchical and homotopic correlations of spontaneous neural activity within the visual cortex of the sighted and blind. *Frontiers in Human Neuroscience* **9**, 25 (2015).
44. Dai, H. *et al.* Resting-state functional MRI: functional connectivity analysis of the visual cortex in primary open-angle glaucoma patients. *Human brain mapping* **34**, 2455–63 (2013).
45. Frezzotti, P. *et al.* Structural and functional brain changes beyond visual system in patients with advanced glaucoma. *PLoS ONE* **9** (2014).
46. Cole, D. M., Smith, S. M. & Beckmann, C. F. Advances and pitfalls in the analysis and interpretation of resting-state FMRI data. *Frontiers in systems neuroscience* **4**, 8 (2010).
47. Talairach, J. & Tournoux, P. Co-planar stereotaxic atlas of the human brain. *3-Dimensional proportional system: an approach to cerebral imaging.* (Thieme, New York 1988).
48. Murphy, K., Birn, R. M., Handwerker, D. A., Jones, T. B. & Bandettini, P. A. The impact of global signal regression on resting state correlations: Are anti-correlated networks introduced? *NeuroImage* **44**, 893–905 (2009).
49. van Dijk, K. R. A., Sabuncu, M. R. & Buckner, R. L. The influence of head motion on intrinsic functional connectivity MRI. *NeuroImage* **59**, 431–438 (2012).
50. Engel, S. A. *et al.* fMRI of human visual cortex. *Nature* **369**, 525 (1994).
51. Hertz, U. & Amedi, A. Disentangling unisensory and multisensory components in audiovisual integration using a novel multifrequency fMRI spectral analysis. *NeuroImage* **52**, 617–32 (2010).
52. Tal, Z., Geva, R. & Amedi, A. The origins of metamodality in visual object area LO: Bodily topographical biases and increased functional connectivity to S1. *NeuroImage* **127**, 363–375 (2016).
53. Zhang, D. *et al.* Intrinsic functional relations between human cerebral cortex and thalamus. *Journal of neurophysiology* **100**, 1740–1748 (2008).
54. Burton, H. Visual cortex activity in early and late blind people. *The Journal of neuroscience: the official journal of the Society for Neuroscience* **23**, 4005–11 (2003).
55. Friston, K. J., Holmes, A. & Worsley, K. J. How many subjects constitute a study? *NeuroImage* **10**, 1–5 (1999).
56. Forman, S. D. *et al.* Improved assessment of significant activation in functional magnetic resonance imaging (fMRI): use of a cluster-size threshold. *Magnetic resonance in medicine: official journal of the Society of Magnetic Resonance in Medicine/Society of Magnetic Resonance in Medicine* **33**, 636–47 (1995).
57. Falchier, A., Clavagnier, S., Barone, P. & Kennedy, H. Anatomical evidence of multimodal integration in primate striate cortex. *The Journal of neuroscience: the official journal of the Society for Neuroscience* **22**, 5749–59 (2002).
58. Eckert, M. A. *et al.* A cross-modal system linking primary auditory and visual cortices: Evidence from intrinsic fMRI connectivity analysis. *Human Brain Mapping* **29**, 848–857 (2008).
59. James, T. W. *et al.* Haptic study of three-dimensional objects activates extrastriate visual areas. *Neuropsychologia* **40**, 1706–1714 (2002).

60. Calvo, M. G., Beltrán, D. & Fernández-Martín, A. Processing of facial expressions in peripheral vision: Neurophysiological evidence. *Biological Psychology* **100**, 60–70 (2014).
61. Driver, J. & Noesselt, T. Multisensory interplay reveals crossmodal influences on 'sensory-specific' brain regions, neural responses, and judgments. *Neuron* **57**, 11–23 (2008).
62. Peyrin, C., Baciú, M., Segebarth, C. & Marendaz, C. Cerebral regions and hemispheric specialization for processing spatial frequencies during natural scene recognition. An event-related fMRI study. *NeuroImage* **23**, 698–707 (2004).
63. Stevens, W. D., Tessler, M. H., Peng, C. S. & Martin, A. Functional connectivity constrains the category-related organization of human ventral occipitotemporal cortex. *Human Brain Mapping* **0**, n/a–n/a (2015).
64. Levy, I., Hasson, U., Avidan, G., Hendler, T. & Malach, R. Center-periphery organization of human object areas. *Nature neuroscience* **4**, 533–539 (2001).
65. Zhang, H., Tian, J., Liu, J., Li, J. & Lee, K. Intrinsically organized network for face perception during the resting state. *Neuroscience letters* **454**, 1–5 (2009).
66. Zhu, Q., Zhang, J., Luo, Y. L. L., Dilks, D. D. & Liu, J. Resting-State Neural Activity across Face-Selective Cortical Regions Is Behaviorally Relevant. *Journal of Neuroscience* **31**, 10323–10330 (2011).
67. Kanwisher, N. Faces and places: of central (and peripheral) interest. *Nature neuroscience* **4**, 455–6 (2001).
68. Goesaert, E., Van Baelen, M., Spileers, W., Wagemans, J. & Op de Beeck, H. P. Visual space and object space in the cerebral cortex of retinal disease patients. *PLoS one* **9**, e88248 (2014).
69. Farroni, T. *et al.* Infant cortex responds to other humans from shortly after birth. *Scientific reports* **3**, 2851 (2013).
70. Grefkes, C., Ritzl, A., Zilles, K. & Fink, G. R. Human medial intraparietal cortex subserves visuomotor coordinate transformation. *NeuroImage* **23**, 1494–1506 (2004).
71. Jack, A. I., Shulman, G. L., Snyder, A. Z., McAvoy, M. & Corbetta, M. Separate Modulations of Human V1 Associated with Spatial Attention and Task Structure. *Neuron* **51**, 135–147 (2006).
72. Santangelo, V. & Macaluso, E. The contribution of working memory to divided attention. *Human Brain Mapping* **34**, 158–175 (2013).
73. Culham, J. C., Cavina-Pratesi, C. & Singhal, A. The role of parietal cortex in visuomotor control: What have we learned from neuroimaging? *Neuropsychologia* **44**, 2668–2684 (2006).
74. Whittingstall, K., Bernier, M., Houde, J.-C., Fortin, D. & Descoteaux, M. Structural network underlying visuospatial imagery in humans. *Cortex; a journal devoted to the study of the nervous system and behavior* **56**, 85–98 (2014).
75. Tipper, S. P. The negative priming effect: inhibitory priming by ignored objects. *The Quarterly journal of experimental psychology. A, Human experimental psychology* **37**, 571–590 (1985).
76. Arcaro, M. J., Pinsk, M. a. & Kastner, S. The Anatomical and Functional Organization of the Human Visual Pulvinar. *Journal of Neuroscience* **35**, 9848–9871 (2015).
77. Sabbah, N. *et al.* Increased functional connectivity between language and visually deprived areas in late and partial blindness. *NeuroImage* **136**, 162–173 (2016).
78. Bedny, M., Pascual-Leone, A., Dodell-Feder, D., Fedorenko, E. & Saxe, R. Language processing in the occipital cortex of congenitally blind adults. *Proceedings of the National Academy of Sciences of the United States of America* **108**, 4429–34 (2011).
79. Cohen, L. G. *et al.* Functional relevance of cross-modal plasticity in blind humans. *Nature* **389**, 180–183 (1997).
80. Collignon, O., Voss, P., Lassonde, M. & Lepore, F. Cross-modal plasticity for the spatial processing of sounds in visually deprived subjects. *Experimental Brain Research* **192**, 343–358 (2009).
81. Hamilton, R. H. & Pascual-Leone, A. Cortical plasticity associated with Braille learning. *Trends in Cognitive Sciences* **2**, 168–174 (1998).
82. Chen, Y.-C. *et al.* Aberrant spontaneous brain activity in chronic tinnitus patients revealed by resting-state functional MRI. *NeuroImage: Clinical* **6**, 222–228 (2014).
83. Boucard, C. C. *et al.* Changes in cortical grey matter density associated with long-standing retinal visual field defects. *Brain: a journal of neurology* **132**, 1898–1906 (2009).
84. Hernowo, A. T. *et al.* Morphometric analyses of the visual pathways in macular degeneration. *Cortex; a journal devoted to the study of the nervous system and behavior* **56**, 99–110 (2014).
85. Plank, T. *et al.* Gray matter alterations in visual cortex of patients with loss of central vision due to hereditary retinal dystrophies. *NeuroImage* **56**, 1556–1565 (2011).
86. Prins, D. *et al.* Surface-Based Analyses of Anatomical Properties of the Visual Cortex in Macular Degeneration. *Plos One* **11**, e0146684 (2016).
87. Yu, L. *et al.* Reduced Cortical Thickness in Primary Open-Angle Glaucoma and Its Relationship to the Retinal Nerve Fiber Layer Thickness. *PLoS ONE* **8**, 1–7 (2013).
88. Burge, W. K. *et al.* Cortical thickness in human V1 associated with central vision loss. *Scientific Reports* **6**, 23268 (2016).
89. Tagliazucchi, E. *et al.* Dynamic BOLD functional connectivity in humans and its electrophysiological correlates. *Frontiers in human neuroscience* **6**, 339 (2012).
90. Caceres, A., Hall, D. L., Zelaya, F. O., Williams, S. C. R. & Mehta, M. A. Measuring fMRI reliability with the intra-class correlation coefficient. *NeuroImage* **45**, 758–768 (2009).
91. Movshon, J. A. & Van Sluyters, R. C. Visual neural development. *Annual review of psychology* **32**, 477–522 (1981).
92. Veraart, C. *et al.* Glucose utilization in human visual cortex is abnormally elevated in blindness of early onset but decreased in blindness of late onset. *Brain research* **510**, 115–21 (1990).
93. Fox, M. D. *et al.* The human brain is intrinsically organized into dynamic, anticorrelated functional networks. *Proceedings of the National Academy of Sciences of the United States of America* **102**, 9673–8 (2005).
94. Tong, Y., Hocke, L. M., Fan, X., Janes, A. C. & Frederick, B. deB. Can apparent resting state connectivity arise from systemic fluctuations? *Frontiers in human neuroscience* **9**, 285 (2015).
95. Bock, A. S. & Fine, I. Anatomical and functional plasticity in early blind individuals and the mixture of experts architecture. *Frontiers in Human Neuroscience* **8**, 1–13 (2014).
96. Margulies, D. S. *et al.* Resting developments: A review of fMRI post-processing methodologies for spontaneous brain activity. *Magnetic Resonance Materials in Physics, Biology and Medicine* **23**, 289–307 (2010).
97. Smith, S. M. *et al.* Network modelling methods for FMRI. *NeuroImage* **54**, 875–891 (2011).
98. Calabro, F. J. & Vaina, L. M. Interaction of cortical networks mediating object motion detection by moving observers. *Experimental Brain Research* **221**, 177–189 (2012).
99. Pandit, A. S. *et al.* Traumatic brain injury impairs small-world topology.pdf. (2013).
100. Dawson, D. A., Cha, K., Lewis, L. B., Mendola, J. D. & Shmuel, A. Evaluation and calibration of functional network modeling methods based on known anatomical connections. *NeuroImage* **67**, 331–343 (2013).
101. Dawson, D. A. *et al.* Partial-correlation based retinotopically organized resting-state functional connectivity within and between areas of the visual cortex reflects more than cortical distance. *Brain connectivity* doi: 10.1089/brain.2014.0331 (2015).

Acknowledgements

We thank Zohar Tal and Noa Zeharia for providing the external functional localizers as well as Sami Abboud, Ella Striem-Amit, Céline Devisme, and Anne-Fleur Barfuss who provided valuable input and assistance on this work. This work was supported by the French State program “Investissements d’Avenir” managed by the Agence Nationale de la Recherche [LABEX LIFESENSES: ANR-10-LABX-65] and Groupe Optic 2000.

Author Contributions

No.S. and Ni.S. contributed equally to this work. A.B.S., S.M.S. and Ni.S. selected the subjects. No.S., Ni.S., C.N.A., C.A. ran the experiment. No.S., Ni.S., C.N.A. contributed to the data analysis. No.S., Ni.S. and C.N.A. designed the figures. No.S., Ni.S., A.A. and A.B.S. wrote the manuscript. J.A.S., A.A. and A.B.S. provided funding. All authors reviewed the manuscript.

Additional Information

Supplementary information accompanies this paper at <http://www.nature.com/srep>

Competing financial interests: There is no conflict of interest to declare for any author except Pr. José-Alain Sahel, consultant for Pixium Vision, GenSight Biologics, Sanofi-Fovea, and Genesignal. However, it has no influence on the results or discussion reported in this paper.

How to cite this article: Sabbah, N. *et al.* Reorganization of early visual cortex functional connectivity following selective peripheral and central visual loss. *Sci. Rep.* 7, 43223; doi: 10.1038/srep43223 (2017).

Publisher's note: Springer Nature remains neutral with regard to jurisdictional claims in published maps and institutional affiliations.



This work is licensed under a Creative Commons Attribution 4.0 International License. The images or other third party material in this article are included in the article’s Creative Commons license, unless indicated otherwise in the credit line; if the material is not included under the Creative Commons license, users will need to obtain permission from the license holder to reproduce the material. To view a copy of this license, visit <http://creativecommons.org/licenses/by/4.0/>

© The Author(s) 2017

Supplementary material

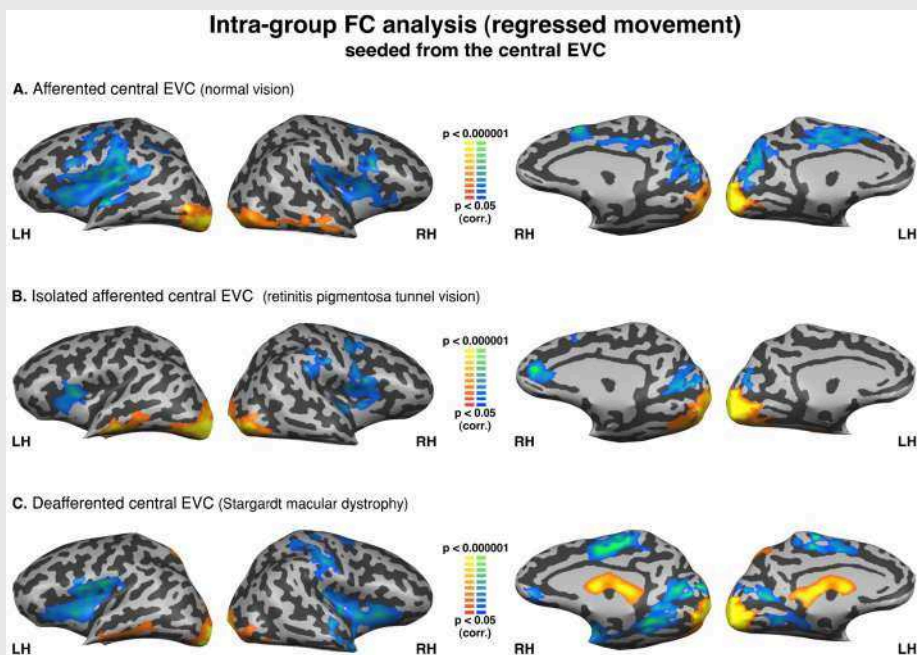


Figure S1. Intra-group analysis of functional connectivity seeded from the central EVC (peripheral EVC regressed and movement regressed). The maps are shown in mesh for the (A) afferented central EVC (normally sighted) (B) isolated afferented central EVC (retinitis pigmentosa tunnel vision) (C) deafferented central EVC (Stargardt macular dystrophy). Yellow-orange depicts areas of higher positive connectivity for each group, and green-blue higher negative connectivity. LH: left hemisphere, RH: right hemisphere.

Supplementary material

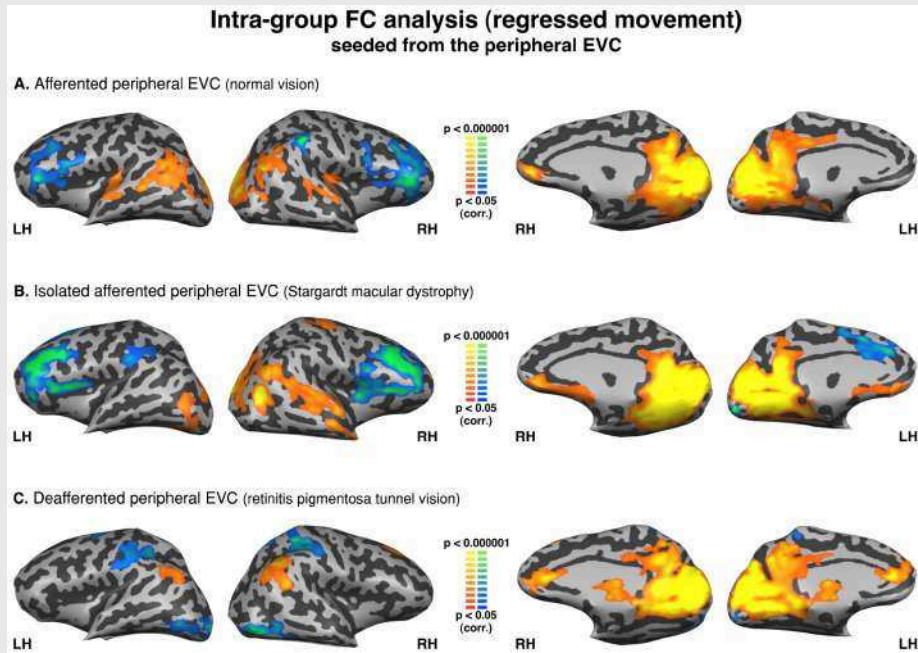


Figure S2. Intra-group analysis of functional connectivity seeded from the peripheral EVC (central EVC and movement regressed). The maps are shown in mesh for the (A) afferented peripheral EVC (normally sighted); * the dotted line on the median aspect of the brain represents the seed region (peripheral EVC) (B) isolated afferented peripheral EVC (Stargardt macular dystrophy) (C) deafferented peripheral EVC (retinitis pigmentosa tunnel vision). Yellow-orange depicts areas of higher positive connectivity for each group, and green-blue higher negative connectivity. LH: left hemisphere, RH: right hemisphere.

Supplementary material

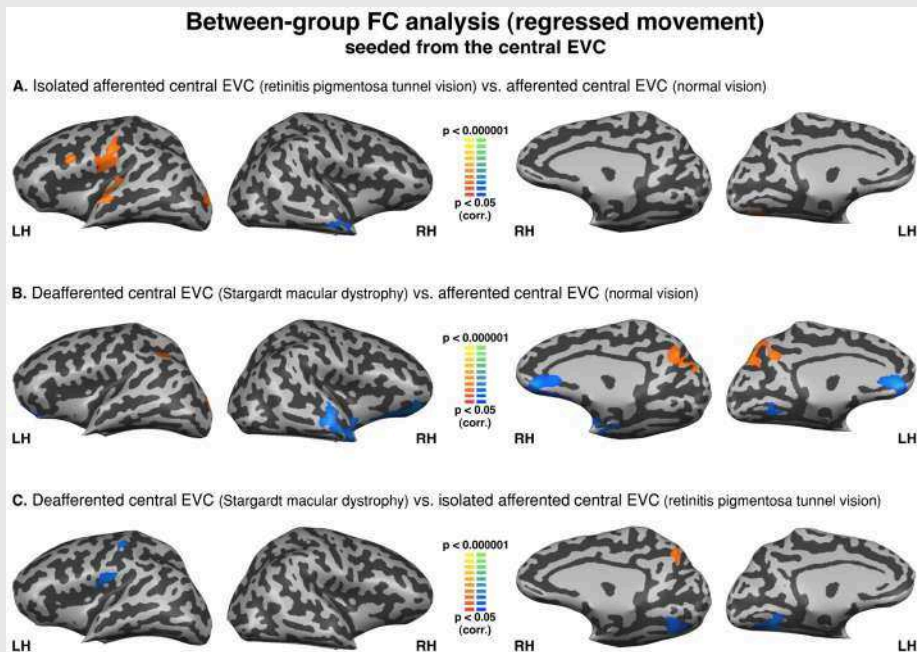


Figure S3. Between-group analysis of functional connectivity seeded from the central EVC (peripheral EVC and movement regressed). The maps are shown in mesh for (A) retinitis pigmentosa tunnel vision vs. normal vision (B) Stargardt macular dystrophy vs. normal vision (C) Stargardt macular dystrophy vs. retinitis pigmentosa tunnel vision (yellow-orange depicts areas of higher positive/lower negative functional connectivity with the central EVC for the first group compared to the second, and green-blue the opposite comparison; LH: left hemisphere, RH: right hemisphere).

Supplementary material

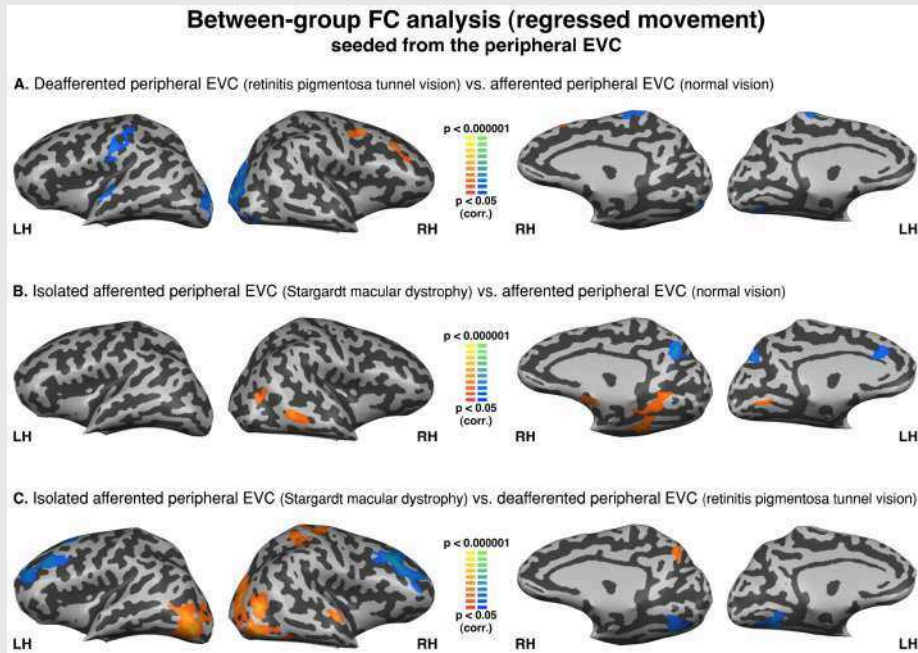


Figure S4. Between-group analysis of functional connectivity seeded from the peripheral EVC (central EVC and movement regressed). The maps are shown in mesh for (A) retinitis pigmentosa tunnel vision vs. normal vision (B) Stargardt macular dystrophy vs. normal vision (C) Stargardt macular dystrophy vs. retinitis pigmentosa tunnel vision (yellow-orange depicts areas of higher positive/lower negative functional connectivity with central EVC for the first group compared to the second, and green-blue the opposite comparison; LH: left hemisphere, RH: right hemisphere).

Comment to supplementary Figures S1, S2, S3, S4:

The maps are quite similar to the ones presented in main Figures 1 to 4 using the motion correction implemented during the pre-processing stages.

Supplementary material

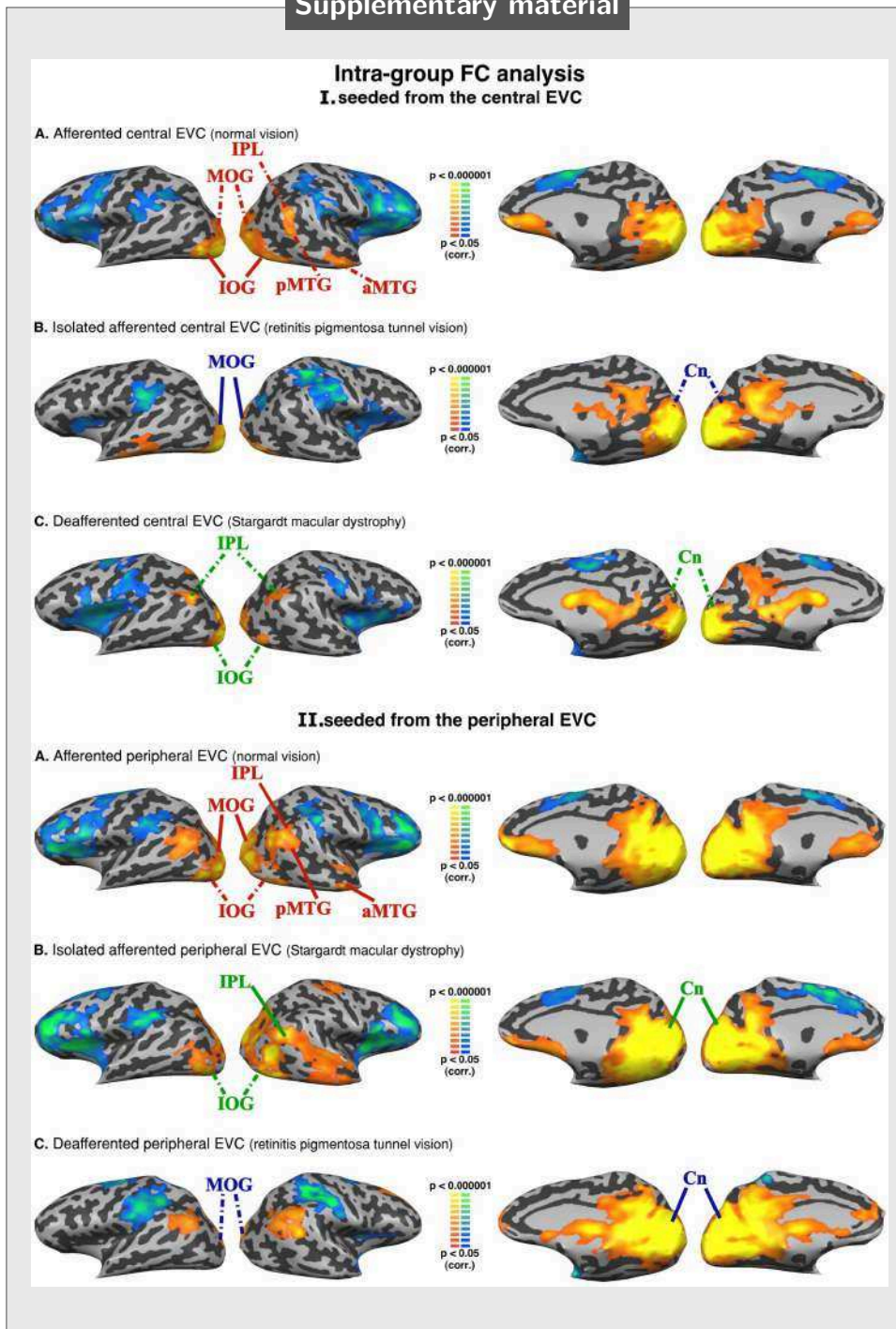


Figure S5. Intra-group analysis of functional connectivity seeded from I. The central and **II.** The peripheral EVC (without regression). The maps are shown in mesh. Yellow-orange depicts areas of higher positive functional connectivity for each group, and green-blue higher negative functional connectivity. **I.** The rs-FC seeded from the central EVC: (A) the afferented central EVC (normal vision) (B) the isolated afferented central EVC (retinitis pigmentosa tunnel vision) (C) the deafferented central EVC (Stargardt macular dystrophy) **II.** The rs-FC seeded from the peripheral EVC: (A) the afferented central EVC (normal vision) (B) the isolated afferented central EVC (retinitis pigmentosa tunnel vision) (C) deafferented central EVC (Stargardt macular dystrophy). Yellow-orange depicts areas of higher positive functional connectivity for each group, and green-blue higher negative functional connectivity. Dashed lines: probable false positive correlations; solid lines: the likely origin of the positive correlations. Red lines: areas that differ with vs. without the partial correlation method in normal vision. Green lines: areas that differ with vs. without the partial correlation method in Stargardt macular dystrophy. Blue lines: areas that differ with vs. without the partial correlation method in retinitis pigmentosa tunnel vision (see also **Figure 1**). Cn: cuneus; IOG: inferior occipital gyrus; IPL: inferior parietal lobule; MTS: middle temporal sulcus; MOG: middle occipital gyrus. pMTG: posterior middle temporal gyrus. aMTG: anterior middle temporal gyrus.

Supplementary material

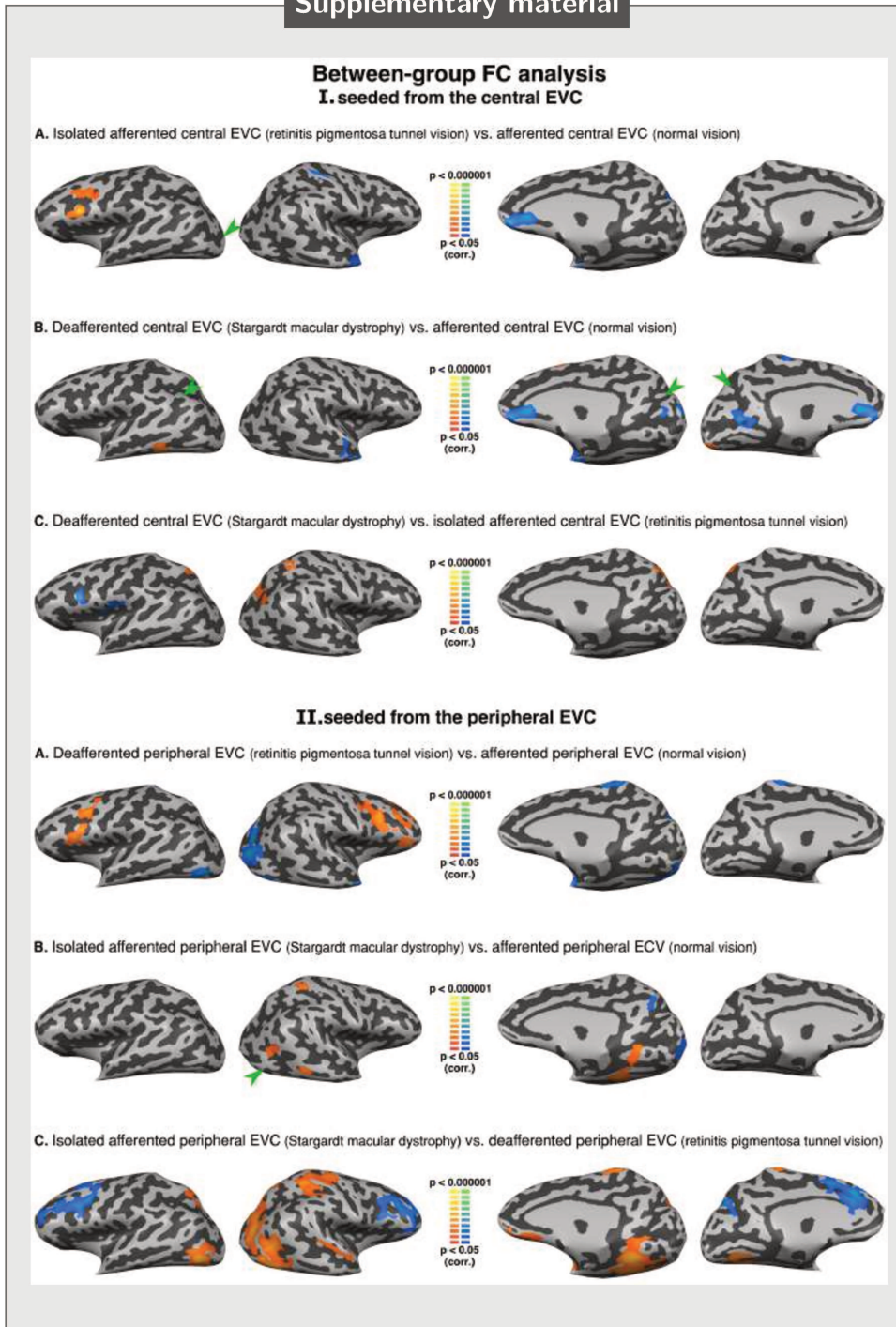


Figure S6. Between-group analysis of functional connectivity seeded from I. The central and II. The peripheral EVC (without regression). The maps are shown in mesh. Yellow-orange depicts areas of higher positive/lower negative functional connectivity with I. The central EVC or II. The peripheral EVC for the first group compared to the second, and green-blue the opposite comparison. I. Seeded from the central EVC: (A) retinitis pigmentosa tunnel vision vs. normal vision (B) Stargardt macular dystrophy vs. normal vision (C) Stargardt macular dystrophy vs. retinitis pigmentosa tunnel vision. II. seeded from the peripheral EVC: (A) retinitis pigmentosa tunnel vision vs. normal vision (B) Stargardt macular dystrophy vs. normal vision (C) Stargardt macular dystrophy vs. retinitis pigmentosa tunnel vision. Green arrowheads show lack of differences in rs-FC compared to the partial correlation analysis.

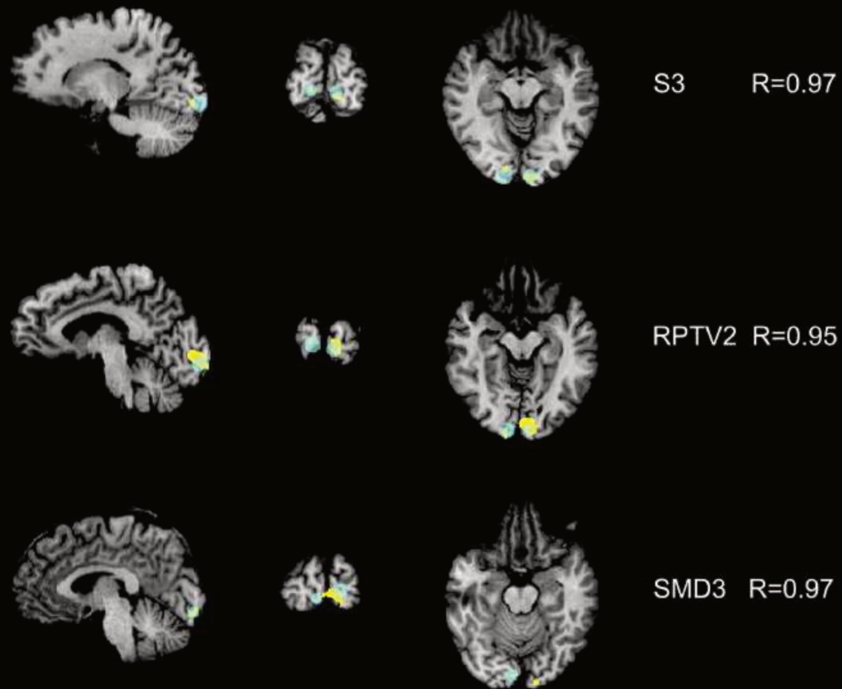
Comment to Supplementary Figures S5, S6:

The partial correlation method has the advantage of being able to exclude false positives, which was why it was chosen in the current study. Supplementary **Figures S5** and **S6** present the intra-group analysis for central and peripheral EVC as well as the intragroup comparisons without partial correlation. **Figure S5** depicts certain regions that are likely false positive correlations and we point to their probable origin. These false positive rs-FC may be the cause of the differences in FC between groups as illustrated by the green arrowheads in **Figure S6**. In addition, at the intra-group level, the negative FC to both central and peripheral EVC is fairly similar with (see **Figure 1** and **2**) or without (**Figure S5**) calculating by the partial correlation method.

Supplementary material

Functional versus anatomical localizers

A. Central EVC



B. Peripheral EVC

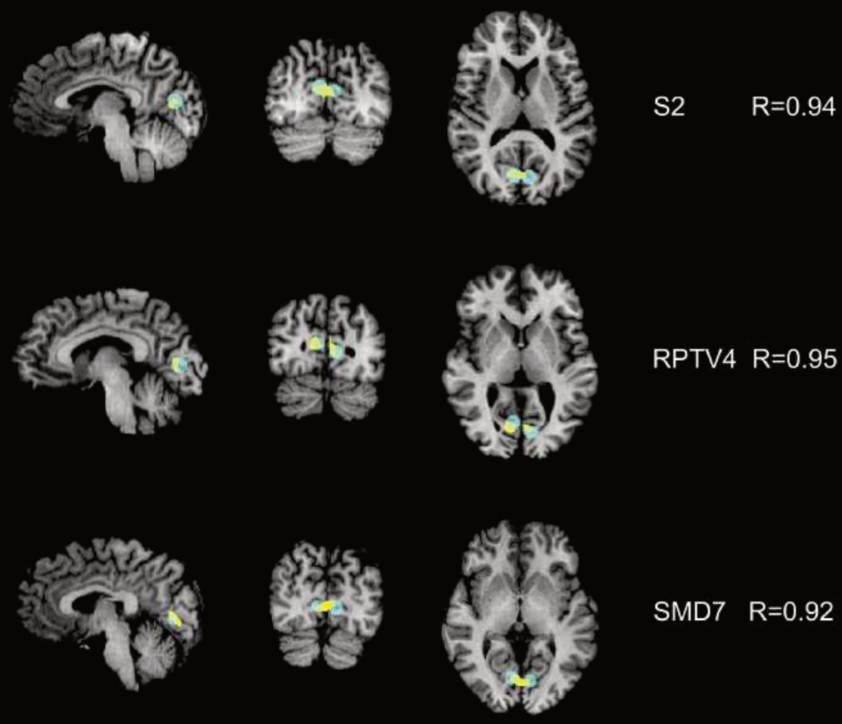


Figure S7. Correlation between functional and anatomical localizers at the individual level. Two individual subjects were randomly selected from each group. For each individual subject, Pearson correlation tests (R) were run to test for time courses correlation between seed regions defined based on external functional localizers and seed regions defined based on anatomical localizers (as defined by 7-mm spheres on A. posterior or B. anterior portions of the calcarine sulcus). Yellow depicts areas defined by the functional localizers whereas blue depicts areas defined by the anatomical localizers on the *fMRI* slices from each individual. S: sighted control subjects, RPTV: subjects with retinitis pigmentosa tunnel vision, SMD: subjects with Stargardt macular dystrophy.

The control analysis of the localizer definitions revealed a strong correlation between the time courses of seed regions defined based on external functional localizers and seed regions defined based on anatomical localizers for each individual, regardless of group.

PART III

General discussion

Synthesis of the principal results

In the current work we explored the structural and functional plasticity induced by the loss of the central and peripheral visual fields in retinal disorders that affect primarily the photoreceptor layer and induce opposite visual field defects: *Stargardt macular degeneration* for loss of central visual field and *non-syndromic pigmentary retinopathy* (retinitis pigmentosa) for the loss of peripheral visual field. With visual loss occurring at retinal level, structural and functional changes are likely the direct consequence of deafferentation. To properly compare the different effects of central and peripheral visual field loss, we recruited in each group subjects with a similar extent of visual field defect. Moreover, the area with visual field defect in one group (e.g. central visual field loss in Stargardt macular degeneration) matched the spared visual field of the other group (e.g. residual “*tunnel vision*” in pigmentary retinopathy).

As a first approach we explored the long-term impact of central and peripheral visual field loss on the structure of the occipital lobe. We measured the cortical thickness and complementary, the cortical entropy, marker of synaptic complexity. Three central findings emerged. First, compared to normally-sighted, central visual field loss exhibited decreased cortical thickness in dorsal areas V3d and V3A, while peripheral visual field loss in early visual cortex (V1 and V2), dorsal area V3d and ventral area V4. Secondly, compared to normally sighted only the central visual loss presented differences in cortical entropy, namely an increase in area FG1 compared both with normally sighted and peripheral visual loss and with LO-2 compared with normally sighted. It is conceivable that increased cortical entropy in these regions represents adaptive, compensatory, enhanced processing following the loss of central vision and its high spatial resolution. Third, no region with cortical thinning exhibited alterations in cortical entropy and conversely. The normality of cortical entropy in areas with cortical thinning indicate that synaptic complexity in the remaining networks is likely preserved. On the other hand, increased synaptic complexity in areas with normal cortical thickness could actually mask neuronal loss due to sensory deafferentation.

From the available literature on the structural changes induced by central and peripheral deafferentation (Boucard *et al.* 2009; Plank *et al.* 2011; Chen *et al.* 2013; Yu *et al.* 2013; Hernowo *et al.* 2014; Olivo *et al.* 2015; Burge *et al.* 2016; Ferreira *et al.* 2016; Prins *et al.* 2016) some studies emphasized on the cortical thinning in deafferented regions of the early visual cortex (Boucard *et al.* 2009; Plank *et al.* 2011; Yu *et al.* 2013; Prins *et*

al. 2016) suggesting a retinotopically-related pattern neuronal degeneration (Prins *et al.* 2015), other found widespread alterations (Chen *et al.* 2013; Hernowo *et al.* 2014; Olivo *et al.* 2015) and some failed to find any differences (Ferreira *et al.* 2016). Interestingly, Burge *et al.* found no overall change in V1's cortical thickness but noted alterations near the border of the scotoma projection area, namely a decrease on deafferented side and increase on afferented side. The different results recorded by the literature may be related to the heterogeneity of the studied visual field defects or to the peculiarities of the employed models. For example, glaucoma and age-related macular degeneration that were widely explored may represent the visual expression of more wide-spread degenerative disorders (Prins *et al.* 2015). By using models of visual loss that affect essentially the external retina and by including highly homogenous clinical populations (with very similar extent of the visual field defects) we avoid these issues. Moreover, by matching the visual defect in one visually impaired group with the spared visual field in the other visually impaired group we were able to isolate and evaluate the plastic changes induced by the loss of central and peripheral vision.

In a second time we explored the long-term impact of central and peripheral visual loss on the functional connectivity between central and peripheral early visual cortex and the rest of the brain. The functional connectivity pattern of the early visual cortex that receives the residual visual input shows a strengthening of its connections with neighboring areas, presumably to tune-up the processing of the visual information. By contrast, remodeling of deafferented early visual cortex imply a strengthening of its connections with more remote areas, possibly reflecting a redeployment of its processing capacity to assist high-order function that may in turn support and optimize the residual vision.

The absence of increased connectivity between deafferented early visual cortex with neighboring areas compared to normally afferented early visual cortex and the decreased functional connectivity of deafferented early visual cortex with the same regions when compared to the isolated afferented early visual cortex argument against a rewiring of deafferented cortex with information directly diverted from the afferented cortex. Another potential explanation for the increased functional connectivity of deafferented early visual cortex is that it represents noise generated by aberrant autonomous activity. This implies strengthened connections between deafferented cortex and regions to which they are strongly linked in normal vision. However, the increased functional connectivity of deafferented early visual cortex with remote and not with neighboring regions (strongly connected with normally afferented early visual cortex) advocates against this hypothesis.

Interestingly, in a resting-state functional connectivity study seeding from central and peripheral early visual cortex in congenitally blind and sighted controls, Striem-Amit *et al.* (Striem-Amit *et al.* 2015) found increased functional connectivity of the peripheral early visual cortex in congenitally blind with the same areas we found in peripheral (retinitis pigmentosa) and central visual loss (Stargardt macular dystrophy), namely in the inferior

parietal lobule/ intra-parietal sulcus, middle frontal gyrus and LOC, inferior occipital gyrus, inferior temporal gyrus and fusiform gyrus, respectively (see Figure 4A, Chapter B2). For the central early visual cortex, in congenitally blind, these authors found an increase in functional connectivity with the left inferior frontal gyrus (including Broca's area) and a functional connectivity decrease of both retinotopic areas with somatosensory and auditory regions, results that have without correspondence in our study. Both their results on congenitally blind and our study of functional connectivity in central or peripheral visual loss likely reflect cross-modal attention plasticity. The differences between their results and our data may be due to the extent of visual loss in studied populations and to developmental peculiarities due to congenital lack of visual sensory input (Pascual-Leone *et al.* 2005; Liu *et al.* 2007; Yu *et al.* 2008; Qin *et al.* 2013; Burton *et al.* 2014). Indeed, in retinitis pigmentosa, the extent of visual loss impacts the functional connectivity between retinotopic regions and Broca's area, as we showed in a previous study (Sabbah *et al.* 2016, see also Chapter 3.2.5 and 3.2.6).

Overview

Overall, the central visual loss induces cortical thinning in dorsal stream areas, whereas the peripheral visual loss in early visual cortex and both dorsal and ventral stream areas, suggesting a higher negative impact of the peripheral visual loss. Moreover, the study of the cortical entropy, marker of synaptic complexity, shows an increase only in the central visual loss and concerns areas LO-2 and FG-1 involved in shape recognition. This suggests that only the central visual loss induces a compensatory increase in synaptic complexity. Functional connectivity study revealed two types of adaptive processes. The first concerns the afferented parts of the early visual cortex, involves preexisting pathways and presumably enforces their processing power to compensate for the loss of the deafferented early visual cortex functions. The second concerns the sensory deprived early visual cortex that strengthens long-range connections, presumably to support high-order mechanisms.

Insight on visual brain plasticity from combined structural and functional data

An important aspect is the corroboration between structural and functional data. Due to the fact that structural data is limited to the occipital lobe, the discussion can only concern this structure.

Combined structural and functional data suggest that some of the thinner regions of the occipital cortex in patients with visual loss correspond to areas that exhibit reduced functional connectivity with peripheral EVC when compared to normally sighted. More precisely, in central visual field loss, thinner dorsal area V3d superpose with the superior part of cuneus that exhibits reduced functional connectivity with the isolated afferented peripheral V1, while in peripheral visual field loss, thinner V2, dorsal V3d and ventral V4 partially superpose with areas in superior, middle and inferior occipital gyrus that exhibit reduced functional connectivity with deafferented peripheral V1 (see Figure 20 A, B and Figure 21B, C). In peripheral visual field loss, thinner dorsal area V3d also partially superposes on a middle occipital gyrus area that has increased functional connectivity with isolated afferented central V1 (see Figure 21 A, B).

The increased cortical entropy in LO-2 and FG1 area in central visual loss (Stargardt macular dystrophy) compared with normally sighted, seems to correspond to lateral occipital complex and the fusiform gyrus that exhibit increased functional connectivity with the isolated afferented peripheral V1 (see Figure 20 B, C).

Overall, combined structural and functional data indicate two connections. First, a possible correspondence between the cortical thinning in several dorsal and ventral stream areas and the decrease in functional connectivity between these areas and peripheral early visual cortex in both types of visual loss, regardless of their afferentation status. Second, compared with normally sighted, the increased cortical entropy, marker of increased synaptic complexity in areas related to object identification in peripheral visual loss, possibly corresponds to the increase of functional connectivity between these areas and the isolated afferented peripheral early visual cortex. Both connections indicate that peripheral visual input and the functional connectivity of peripheral early visual cortex have a higher plastic impact on the occipital lobe. It is possible that this effect relates to the

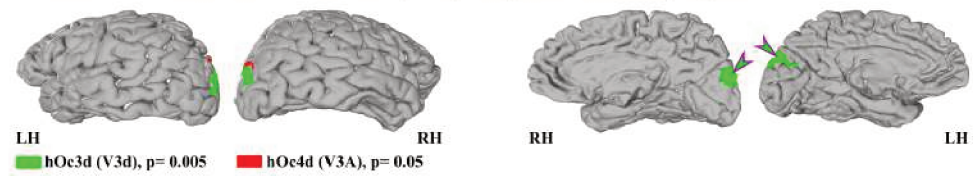
complex cross-modal connectivity of peripheral V1 (Falchier *et al.* 2002; Rockland and Ojima 2003; Zhang and Chen 2006). Of course, consequent specially designed studies are required to evaluate the validity of these possible connections between structural and functional data.

Overview

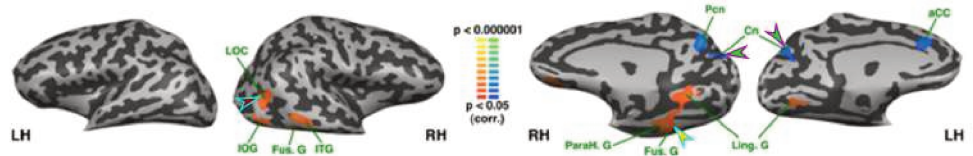
Combined structural and functional data indicate that following partial visual loss peripheral visual input and the functional connectivity of peripheral early visual cortex have a higher plastic impact on the occipital lobe.

Combined data from the rs-FC analysis , CoTks and CoEN analysis
in central visual field loss (Stargardt macular dystrophy) compared to normally sighted

A. Reduced CoTks in central visual loss (SMD) compared to normally sighted.



B. rs-FC - isolated afferented peripheral EVC (SMD) vs. afferented peripheral EVC (normal vision)



C. Increased cortical entropy in central visual loss (SMD) compared to normally sighted

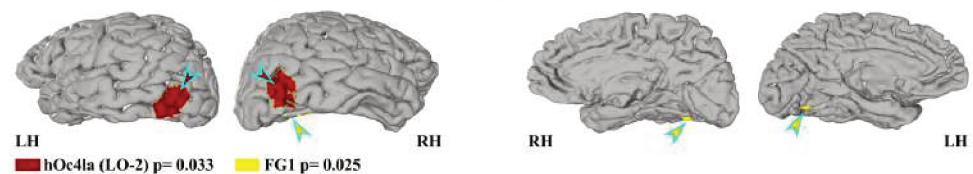
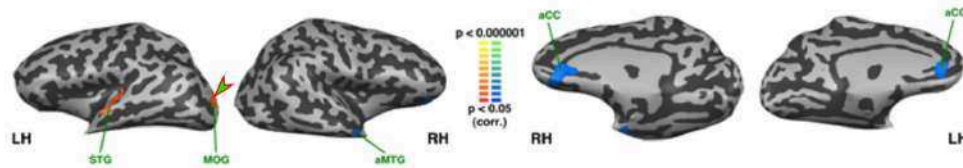


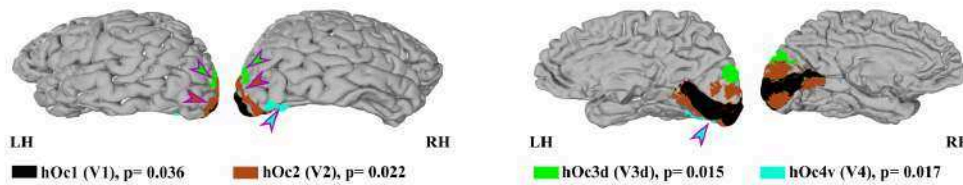
Figure 21 – Comparative display of structural and functional connectivity data in peripheral visual loss (retinitis pigmentosa) vs normally sighted. Regions are indicated through arrowheads filled with colors that correspond to the associated cytoarchytectonic area. Arrow border is colored magenta for the correspondence decreased CoTks – decreased functional connectivity and light blue for the correspondence CoEn – increased functional connectivity.

**Combined data from the rs-FC analysis and CoTks analysis
in peripheral visual field loss (retinitis pigmentosa tunnel vision) compared to normally sighted**

A. rs-FC - isolated afferented central EVC (RPTV) vs. afferented central EVC (normal vision)



B. Reduced CoTks in peripheral visual loss (RPTV) compared to normally sighted (excluding EVC)



C. rs-FC - deafferented peripheral EVC (RPTV) vs. afferented central EVC (normal vision)

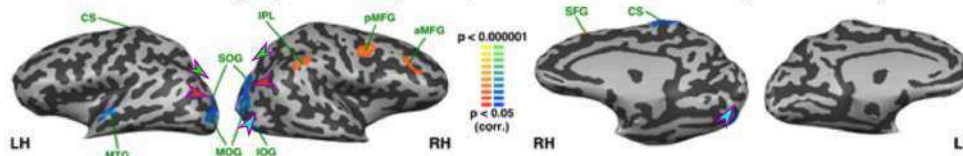


Figure 22 – Comparative display of structural and functional connectivity data in central visual loss (Stargardt macular dystrophy) vs normally sighted. Regions are indicated through arrowheads filled with colors that correspond to the associated cytoarchytectonic area. Arrow border is colored magenta for the correspondence decreased CoTks – decreased functional connectivity and red for the correspondence decreased CoTks – decreased functional connectivity

Limitations

3.1 Study design

Both studies presented in the current work are case-control, cross-sectional observational approaches allowing the detection of morphological and functional connectivity differences between subjects with visual field defects and normally sighted (Grimes and Schulz 2005). This type of study can be confounded by other factors and shows false relationships between the studied variables (i.e. central and peripheral visual loss) and the observed differences (i.e. differences in CoTks, CoEn rs-FC, Lawlor *et al.* 2004; Ioannidis 2005). To minimize this risk, we included age-matched subjects with highly homogenous clinical presentation and we also explored the impact of potential confounding factors, like age and deficit duration.

Other limitations of the employed study designs are that they fail to identify in which sequence changes occur and to provide the functional meaning of the observed differences. This investigation is however an essential step that allows consequent experimental studies that could explain how and why these changes occur and what are their perceptual and behavioral consequences.

3.2 MRI protocol

As cytoarchitectonic areas are highly variable across subjects, we extracted cytoarchitectonic areas of the occipital lobe from an atlas based on observer-independent probabilistic mapping of 10 postmortem brains, only in voxels where the same cytoarchitectonic area overlapped in more than half of the post-mortem investigated brains (Amunts *et al.* 1999; Zilles K 2010; Mohlberg *et al.* 2012). Through this approach, we aimed to reduce the effect of inter-individual variability. Moreover, for the same purpose, we normalized the cortical thickness of each cytoarchitectonic area with the average cortical thickness of the occipital lobes (Ferreira *et al.* 2016). This ratio was further employed in subsequent analysis.

Important factors in the MRI measurement of cortical thickness are the cortical myelin density and various technical parameters (i.e. field strength, tissue segmentation methods,

smoothing, etc). They can influence the measurement of the cortical thickness and lead to incorrect estimation, especially in disorders or particular physiological states (i.e. development or aging, Westlye *et al.* 2010; Zilles and Amunts 2015). The employed models of central and peripheral visual loss have no known association with developmental or acquired myelination anomalies. Therefore, the above-mentioned biases in the measure of cortical thickness have little or no impact in our study. However, it is unknown if sensory deafferentation per se translates into a certain degree of cortical myelin loss.

The structural study on the plasticity induced by central and peripheral visual was limited to the occipital lobe due to the absence of available cytoarchitectonic maps for the entire brain. Therefore, we ignore the structural effects of partial visual loss on remote brain areas and cannot present a global view of the induced plastic changes.

Resting-state *fMRI* signal, employed in the current work both in the study of the functional connectivity and in the study of the cortical entropy is particularly sensitive to motion (Caceres *et al.* 2009; Tagliazucchi *et al.* 2012; van Dijk *et al.* 2012). For the measure of the cortical entropy, where increased movement virtually increase the measured values, we regressed out the motion-related signal, thus maximizing the likelihood that measurement reflect the spontaneous hemodynamic fluctuations related to brain activity. For the study of the functional connectivity, we instigated extra measures to control for the head movements and to validate the absence of significant differences in head movements across groups.

The most accurate way of designing the ROIs for central and peripheral primary visual cortex is retinotopy, but in the study of the functional connectivity this approach was impossible due to the fixation peculiarities of the patients with central visual field loss. Therefore, we by-passed this limitation by extrapolating the ROIs from a retinotopy experiment conducted in a group of normally sighted. This approach also eludes the problem of differences in accuracy when defining the primary visual cortex across patients and control subjects. Nevertheless, as deafferented primary visual cortex in visual loss suffers from structural alterations, mainly in the form of gray matter thinning, both in central and peripheral visual loss (Boucard *et al.* 2009; Plank *et al.* 2011; Hernowo *et al.* 2014; Prins *et al.* 2016), the ROIs we employed in the functional connectivity study may not be limited to V1, and overlap to a certain extent with V2. Thus, to define accurately the ROI we employed the term of “*early visual cortex*”.

Increase in functional correlations is usually interpreted as an increase in functional connectivity, but increased BOLD signal can be produced by other mechanisms (i.e. metabolic alterations), as demonstrated by higher resting-state firing in blind animals, enhanced retinotopic resting-state signals in anophthalmic individuals (Bock *et al.* 2015) or abnormally elevated glucose utilization in early but not late blindness (Fox *et al.* 2005). We proved that the resting-state firing was equivalent in our three populations since control analysis seeding S1 areas revealed similar symmetric patterns between hemispheres in

all three groups.

Despite plentiful claims to the contrary in the literature, it cannot be excluded that resting-state *fMRI* reflects non-neural signals such as the blood flow, as the cerebral blood flow show similitudes with the neural eccentric retinotopy (Bock and Fine 2014). Therefore, to reduce the vascular component, we employed a partial correlation method. Unlike simple correlation, partial correlation identify false positives when looks for direct connections (Zhang *et al.* 2008; Margulies *et al.* 2010; Smith *et al.* 2011; Calabro and Vaina 2012; Dawson *et al.* 2013; Pandit *et al.* 2013; Dawson *et al.* 2015) but can induce false negative correlations (Murphy *et al.* 2009). Nevertheless, we found across the studied groups similar negative FC patterns compared to simple correlation analysis and identified the false positives. Moreover, we validated the coherence and specificity of the resting-state partial correlation approach through somatosensory seeds.

3.3 Visual loss models

To study central and visual loss we employed as models retinal disorders - Stargardt macular dystrophy for central visual loss and retinitis pigmentosa for peripheral visual loss. Both are disorders that results in photoreceptor loss. However, there are some clinical differences that should be discussed.

In Stargardt macular dystrophy, photoreceptor death (both cones and rods) follows the degeneration of the pigmentary epithelium and occurs mainly in areas with high photoreceptor concentration and metabolic activity, namely in the central retina (Meunier and Puech 2012, see also Chapter 3.2). In contrast, in retinitis pigmentosa, photoreceptor death starts with rods that further induce cone degeneration and ultimately blindness; it primarily affects peripheral retina, but also involves central retina, especially its rods (Audo *et al.* 2012, see also Chapter 3.3). This diffuse photoreceptor damage may also induce complex retinal plastic changes in the functional central retina (Jones and Marc 2005, see also Chapter 4.1.). Moreover, the loss of peripheral vision represents the loss of the largest part of the visual field. Therefore, in retinitis pigmentosa, the more diffuse photoreceptor damage and the massive visual field loss likely damage numerous parallel information channels originating in wide-field retinal cells (Masland 2012) (see also Chapter 2). Also, peripheral visual field and the correspondent cortical areas that subserve it seem to be more involved in cross-modal interactions (Falchier *et al.* 2002; Burton 2003; Zhang and Chen 2006). These peculiarities may account for the more complex structural effects observed in the peripheral visual field loss, especially in the case of the early visual cortex.

PART IV

Conclusion and perspectives

The results of the two studies exposed herein shed light on several aspects of the visual plasticity induced by the visual loss. The distinctive design opposing two models of visual loss affecting central or peripheral vision allowed a unique perspective on these processes. In the first study exploring the structural changes induced in the occipital lobe we observed changes in dissonance with the canonic segregation “*central vision – ventral stream*”, “*peripheral vision – dorsal stream*” as central visual loss induced cortical thinning in areas of dorsal stream, while the peripheral visual loss, in early visual cortex and in both dorsal and ventral stream areas. Only central visual field loss associated changes in cortical entropy, namely an increase in areas involved in object recognition. The increase in cortical entropy, marker of synaptic complexity, suggest adaptive, plastic changes in response to the loss of the central vision and its high spatial resolution. The second study, exploring the functional connectivity of afferented and deafferented parts of early visual cortex in both types of visual field defects shows different patterns of reorganization. Regions of early visual cortex receiving the residual visual input reinforce local connections presumably to enhance the processing of the incoming visual information, while deafferented regions of early visual cortex reinforce long-range connections presumably to assist high-order functions. Corroborating the structural and functional data it seems that the reduced cortical thickness in associative visual cortex superpose with areas presenting reduced functional connectivity with the peripheral part of early visual cortex in both types of visual field defects, while the increased cortical entropy areas in central field loss superpose with areas presenting increased functional connectivity with isolated afferented peripheral early visual cortex. Therefore, it is possible that alterations in the peripheral field input are more susceptible to induce plastic changes.

The current approaches provided a global picture of the structural and functional changes induced by the central and peripheral visual loss. This mapping represents a crucial point in the study of this type of plasticity. However, the design of the present investigations does not provide the proper tools to intimately explain the observed changes and their actual physiological role. They could be completed by structural approaches measuring the changes outside the occipital lobe, the changes in subcortical structures like the cerebellum, colliculi, thalamus as well as the white matter; global functional approaches like the assessment of the functionality between canonical resting-state networks; other seed-based resting-state approaches testing the functional connectivity between certain nodes involved in specific functions or task-based *fMRI*.

Overview

Overall, the current work shows a most interesting perspective of the plasticity induced by the loss of central and peripheral vision, demonstrating that it is far more complex than the canonical and probably simplistic view (the “*two channels*” dichotomy central vision – ventral stream/ central vision - parvocellular pathway or peripheral vision - dorsal stream/ peripheral vision – magnocellular pathway) would have led to presume. It paves the road for other approaches that might explain the exact functional role of the plastic changes we mapped and maybe help revising the current, insufficient model of visual information processing (see also Chapter 2).

PART V

References

Bibliography

- Abboud, S., Maidenbaum, S., Dehaene, S., & Amedi, A., (2015), A number-form area in the blind., *Nat. Commun.* *6*, 6026, doi:10.1038/ncomms7026
- Abel, P. L., O'Brien, B. J., Lia, B., & Olavarria, J. F., (1997), Distribution of neurons projecting to the superior colliculus correlates with thick cytochrome oxidase stripes in macaque visual area V2, *J. Comp. Neurol.* *377*3, 313–323, doi:10.1002/(SICI)1096-9861(19970120)377:3<313::AID-CNE1>3.0.CO;2-5
- Adams, M. M., Hof, P. R., Gattass, R., Webster, M. J., & Ungerleider, L. G., (2000), Visual cortical projections and chemoarchitecture of macaque monkey pulvinar, *J. Comp. Neurol.* *419*3, 377–393, doi:10.1002/(SICI)1096-9861(20000410)419:3<377::AID-CNE9>3.0.CO;2-E
- Aït-Ali, N., Fridlich, R., Millet-Puel, G., Clérin, E., Delalande, F., Jaillard, C., ... Léveillard, T., (2015), Rod-Derived Cone Viability Factor Promotes Cone Survival by Stimulating Aerobic Glycolysis, *Cell*, *161*4, 817–832, doi:10.1016/j.cell.2015.03.023
- Altimus, C. M., Güler, A. D., Alam, N. M., Arman, A. C., Prusky, G. T., Sampath, A. P., & Hattar, S., (2010), Rod photoreceptors drive circadian photoentrainment across a wide range of light intensities., *Nat. Neurosci.* *13*9, 1107–12, doi:10.1038/nn.2617, arXiv: 296
- Amedi, A., Malach, R., Hendler, T., Peled, S., & Zohary, E., (2001), Visuo-haptic object-related activation in the ventral visual pathway., *Nat. Neurosci.* *4*3, 324–30, doi:10.1038/85201
- Amedi, A. [A.], Raz, N., Pianka, P., Malach, R., & Zohary, E., (2003), Early 'visual' cortex activation correlates with superior verbal memory performance in the blind, *Nat. Neurosci.* *6*7, 758–766, doi:10.1038/nm1072
- Amunts, K. [K.], Schleicher, A., & Zilles, K., (2007), Cytoarchitecture of the cerebral cortex-More than localization, *Neuroimage*, *37*4, 1061–1065, doi:10.1016/j.neuroimage.2007.02.037
- Amunts, K. [K.], Schleicher, A., Bürgel, U., Mohlberg, H., Uylings, H. B. M., & Zilles, K., (1999), Broca's region revisited: Cytoarchitecture and intersubject variability, *J. Comp. Neurol.* *412*2, 319–341, doi:10.1002/(SICI)1096-9861(19990920)412:2<319::AID-CNE10>3.0.CO;2-7
- Anurova, I., Renier, L. A., De Volder, A. G., Carlson, S., Rauschecker, J. P., Ptito, M., ... Rauschecker, J. P., (2014), Relationship Between Cortical Thickness and Functional Activation in the Early Blind., *Cereb. Cortex*, *47*1, [Epub ahead of print], doi:10.1093/cercor/bhu009

-
- Arendt, D. & Wittbrodt, J., (2001), Reconstructing the eyes of Urbilateria., *Philos. Trans. R. Soc. Lond. B. Biol. Sci.* 356 1414, 1545–1563, doi:10.1098/rstb.2001.0971
- Arendt, D. [Detlev], (2003), Evolution of eyes and photoreceptor cell types, *Int. J. Dev. Biol.* 477-8, 563–571.
- Arendt, D. [Detlev], (2008), The evolution of cell types in animals: emerging principles from molecular studies., *Nat. Rev. Genet.* 9 11, 868–882, doi:10.1038/nrg2416
- Arendt, D. [Detlev], Denes, A. S., Jekely, G., & Tessmar-Raible, K., (2008), The evolution of nervous system centralization, *Philos. Trans. R. Soc. B Biol. Sci.* 363 1496, 1523–1528, doi:10.1098/rstb.2007.2242
- Arendt, D. [Detlev], Tessmar-Raible, K., Snyman, H., Dorresteyn, A. W., & Wittbrodt, J., (2004), Ciliary photoreceptors with a vertebrate-type opsin in an invertebrate brain., *Science*, 306 5697, 869–71, doi:10.1126/science.1099955
- Asteriti, S., Gargini, C., & Cangiano, L., (2014), Mouse rods signal through gap junctions with cones., *Elife*, 3, e01386, doi:10.7554/eLife.01386
- Audo, I., Meunier, S., Mohand-Saïd, S., & Sahel, J.-A., (2012), Rétinites pigmentaires, In S. Y. Cohen & A. Gaudric (Eds.), *Rétine* (pp. 128–153), Paris: Lavoisier.
- Authié, C. N., Berthoz, A., Sahel, J.-A., & Safran, A. B., (2016), Adaptive gaze strategies for locomotion with constricted visual field, *IOVS*, in press.
- Baker, C. I. [Chris I.], Dilks, D. D., Peli, E., & Kanwisher, N., (2008), Reorganization of visual processing in macular degeneration: Replication and clues about the role of foveal loss, *Vision Res.* 48 18, 1910–1919, doi:10.1016/j.visres.2008.05.020
- Baker, C. I. [Chris I.], Peli, E., Knouf, N., & Kanwisher, N. G., (2005), Reorganization of visual processing in macular degeneration., *J. Neurosci.* 25 3, 614–618, doi:10.1523/JNEUROSCI.3476-04.2005
- Balavoine, G., (2003), The Segmented Urbilateria: A Testable Scenario, *Integr. Comp. Biol.* 43 1, 137–147, doi:10.1093/icb/43.1.137
- Banissy, M. J., Tester, V., Muggleton, N. G., Janik, A. B., Davenport, A., Franklin, A., ... Ward, J., (2013), Synesthesia for color is linked to improved color perception but reduced motion perception., *Psychol. Sci.* 24 12, 2390–7, doi:10.1177/0956797613492424
- Barone, P., Batardiere, A., Knoblauch, K., & Kennedy, H., (2000), Laminar distribution of neurons in extrastriate areas projecting to visual areas V1 and V4 correlates with the hierarchical rank and indicates the operation of a distance rule., *J. Neurosci.* 20 9, 3263–81.
- Barrett, K. C., Ashley, R., Strait, D. L., & Kraus, N., (2013), Art and science: how musical training shapes the brain., *Front. Psychol.* 4 October, 713, doi:10.3389/fpsyg.2013.00713

-
- Bartolomeo, P., Bachoud-Lévi, A. C., & Thiebaut de Schotten, M., (2014), The anatomy of cerebral achromatopsia: A reappraisal and comparison of two case reports, *Cortex*, *56*, 138–144, doi:10.1016/j.cortex.2013.01.013
- Baseler, H. A., Brewer, A. A., Sharpe, L. T., Morland, A. B., Jägle, H., & Wandell, B. a., (2002), Reorganization of human cortical maps caused by inherited photoreceptor abnormalities., *Nat. Neurosci.* *5* 4, 364–370, doi:10.1038/nm817
- Baseler, H. A., Gouws, A., Haak, K. V., Racey, C., Crossland, M. D., Tufail, A., ... Morland, A. B., (2011), Large-scale remapping of visual cortex is absent in adult humans with macular degeneration., *Nat. Neurosci.* *14* 5, 649–655, doi:10.1038/nm.2793
- Baylor, B., Lamb, T., & Yau, K., (1979), Responses of retinal rods to single photons, *J. Physiol.* *288* 1, 613–634, doi:10.1113/jphysiol.1979.sp012716
- Bedny, M., Pascual-Leone, A., Dodell-Feder, D., Fedorenko, E., & Saxe, R., (2011), Language processing in the occipital cortex of congenitally blind adults., *Proc. Natl. Acad. Sci. U. S. A.* *108* 11, 4429–4434, doi:10.1073/pnas.1014818108
- Bedny, M., Pascual-Leone, A., Dravida, S., & Saxe, R., (2012a), A sensitive period for language in the visual cortex: Distinct patterns of plasticity in congenitally versus late blind adults, *Brain Lang.* *122* 3, 162–170, doi:10.1016/j.bandl.2011.10.005
- Bedny, M., Pascual-Leone, A., Dravida, S., & Saxe, R., (2012b), A sensitive period for language in the visual cortex: distinct patterns of plasticity in congenitally versus late blind adults., *Brain Lang.* *122* 3, 162–170, doi:10.1016/j.bandl.2011.10.005
- Berencsi, A., (2005), The functional role of central and peripheral vision in the control of posture, *24*, 689–709, doi:10.1016/j.humov.2005.10.014
- Biswal, B., Yetkin, F. Z., Haughton, V. M., & Hyde, J. S., (1995), Functional connectivity in the motor cortex of resting human brain using echo-planar MRI., *Magn. Reson. Med.* *34* 4, 537–541, doi:10.1002/mrm.1910340409
- Blasdel, G. G. & Lund, J. S., (1983), Termination of afferent axons in macaque striate cortex., *J. Neurosci.* *3* 7, 1389–1413.
- Bloomfield, S. A. & Volgyi, B., (2009), The diverse functional roles and regulation of neuronal gap junctions in the retina, *Nat Rev Neurosci*, *10* 7, 495–506, doi:nrn2636 [pii]r10.1038/nrn2636
- Bock, A. S., Binda, P., Benson, N. C., Bridge, H., Watkins, K. E., & Fine, I., (2015), Resting-State Retinotopic Organization in the Absence of Retinal Input and Visual Experience, *J. Neurosci.* *35* 36, 12366–12382, doi:10.1523/JNEUROSCI.4715-14.2015
- Bock, A. & Fine, I., (2014), Anatomical and functional plasticity in early blind individuals and the mixture of experts architecture., *Front. Hum. Neurosci.* *8* December, 971, doi:10.3389/fnhum.2014.00971

-
- Boucard, C. C., Hernowo, A. T., Maguire, R. P., Jansonius, N. M., Roerdink, J. B. T. M., Hooymans, J. M. M., & Cornelissen, F. W., (2009), Changes in cortical grey matter density associated with long-standing retinal visual field defects., *Brain*, *132 Pt 7*, 1898–1906, doi:10.1093/brain/awp119
- Boucart, M., Naili, F., Despretz, P., Defoort-Dhellemmes, S., & Fabre-Thorpe, M., (2010), Implicit and explicit object recognition at very large visual eccentricities: No improvement after loss of central vision, *Vis. cogn.* *186*, 839–858, doi:10.1080/13506280903287845
- Bourne, J. A. & Rosa, M. G. P., (2006), Hierarchical development of the primate visual cortex, as revealed by neurofilament immunoreactivity: Early maturation of the middle temporal area (MT), *Cereb. Cortex*, *163*, 405–414, doi:10.1093/cercor/bhi119
- Boussaoud, D., Ungerleider, L. G., & Desimone, R., (1990), Pathways for motion analysis: Cortical connections of the medial superior temporal and fundus of the superior temporal visual areas in the macaque, *J. Comp. Neurol.* *2963*, 462–495, doi:10.1002/cne.902960311
- Bridge, H., Cowey, A., Ragge, N., & Watkins, K., (2009), Imaging studies in congenital anophthalmia reveal preservation of brain architecture in 'visual' cortex, *Brain*, *13212*, 3467–3480, doi:10.1093/brain/awp279
- Bruner, E. & Iriki, A., (2016), Extending mind, visuospatial integration, and the evolution of the parietal lobes in the human genus, *Quat. Int.* *405*, 98–110, doi:10.1016/j.quaint.2015.05.019
- Bruner, E., Lozano, M., & Lorenzo, C., (2016), Visuospatial integration and human evolution: The fossil evidence, *J. Anthropol. Sci.* *94*, 81–97, doi:10.4436/jass.94025
- Buldyrev, I., Puthussery, T., & Taylor, W. R., (2012), Synaptic pathways that shape the excitatory drive in an OFF retinal ganglion cell, *J. Neurophysiol.* *1077*, 1795–1807, doi:10.1152/jn.00924.2011
- Burge, W. K., Griffis, J. C., Nenert, R., Elkhetafi, A., DeCarlo, D. K., ver Hoef, L. W., ... Visscher, K. M., (2016), Cortical thickness in human V1 associated with central vision loss, *Sci. Rep.* *6 September 2015*, 23268, doi:10.1038/srep23268, arXiv: 1011.1669
- Burton, H., (2003a), Dissociating Cortical Regions Activated by Semantic and Phonological Tasks: A fMRI Study in Blind and Sighted People, *J. Neurophysiol.* *903*, 1965–1982, doi:10.1152/jn.00279.2003
- Burton, H., (2003b), Visual cortex activity in early and late blind people., *J. Neurosci.* *2310*, 4005–4011.
- Burton, H., Snyder, A. Z., Conturo, T. E., Akbudak, E., Ollinger, J. M., & Raichle, M. E., (2002), Adaptive changes in early and late blind: a fMRI study of Braille reading., *J. Neurophysiol.* *871*, 589–607.

-
- Burton, H. [Harold], Snyder, A. Z., & Raichle, M. E., (2014), Resting state functional connectivity in early blind humans., *Front. Syst. Neurosci.* 8 April, 51, doi:10.3389/fnsys.2014.00051
- Butler, A., (2007), The dual elaboration hypothesis of the evolution of the dorsal thalamus, In J. Kaas & L. Krubitzer (Eds.), *Evol. nerv. syst.* (pp. 517–523), Amsterdam: Elsevier/ Academic Press.
- Butler, A., (2012), Evolution of the brain in vertebrates, In O. Lazareva, T. Shimizu, & E. Wasserman (Eds.), *How anim. see world* (Chap. Evolution, pp. 419–440), New York.
- Butt, O. H., Benson, N. C., Datta, R., & Aguirre, G. K., (2013), The Fine-Scale Functional Correlation of Striate Cortex in Sighted and Blind People, *J. Neurosci.* 33 41, 16209–16219, doi:10.1523/JNEUROSCI.0363-13.2013
- Butt, O. H., Benson, N. C., Datta, R., & Aguirre, G. K., (2015), Hierarchical and homotopic correlations of spontaneous neural activity within the visual cortex of the sighted and blind, *Front. Hum. Neurosci.* 9 February, 25, doi:10.3389/fnhum.2015.00025
- Caceres, A., Hall, D. L., Zelaya, F. O., Williams, S. C., & Mehta, M. A., (2009), Measuring fMRI reliability with the intra-class correlation coefficient, *Neuroimage*, 45 3, 758–768, doi:10.1016/j.neuroimage.2008.12.035
- Calabrèse, A., Bernard, J. B., Faure, G., Hoffart, L., & Castet, E., (2014), Eye movements and reading speed in macular disease: The shrinking perceptual span hypothesis requires and is supported by a mediation analysis, *Investig. Ophthalmol. Vis. Sci.* 55 6, 3638–3645, doi:10.1167/iovs.13-13408
- Calabro, F. J. & Vaina, L. M., (2012), Interaction of cortical networks mediating object motion detection by moving observers, *Exp. Brain Res.* 221 2, 177–189, doi:10.1007/s00221-012-3159-8
- Casagrande, V. A. [Vivien A] & Kaas, J. H. [Jon H], (1994), The Afferent, Intrinsic, and Efferent Connections of Primary Visual Cortex in Primates, In A. Peters & K. S. Rockland (Eds.), *Prim. vis. cortex primates* (pp. 201–259), doi:10.1007/978-1-4757-9628-5_5
- Caspers, J., Palomero-Gallagher, N., Caspers, S., Schleicher, A., Amunts, K., & Zilles, K., (2013), Receptor architecture of visual areas in the face and word-form recognition region of the posterior fusiform gyrus, *Brain Struct. Funct.* 220 1, 205–219, doi:10.1007/s00429-013-0646-z
- Caspers, J., Zilles, K., Eickhoff, S. B., Schleicher, A., Mohlberg, H., & Amunts, K., (2013), Cytoarchitectonical analysis and probabilistic mapping of two extrastriate areas of the human posterior fusiform gyrus, *Brain Struct. Funct.* 218 2, 511–526, doi:10.1007/s00429-012-0411-8

-
- Chen, J.-D., Lin, Y.-C., & Hsiao, S.-T., (2010), Obesity and high blood pressure of 12-Hour shift female clean-room workers, *Chronobiol. Int.* 272, 334–344, doi:10.3109/07420520903502242
- Chen, S. & Li, W., (2012), A color-coding amacrine cell may provide a blue-Off signal in a mammalian retina, *Nat. Neurosci.* 157, 954–956, arXiv: NIHMS150003
- Chen, W. W., Wang, N., Cai, S., Fang, Z., Yu, M., Wu, Q., . . . Gong, Q., (2013), Structural brain abnormalities in patients with primary open-angle glaucoma: a study with 3T MR imaging., *Invest. Ophthalmol. Vis. Sci.* 541, 545–554, doi:10.1167/iovs.12-9893
- Cheng, A., (1997), La main et l’esprit. In *Hist. la pensée chin.* (Chap. Zhuengzi à, pp. 117–120), Paris: Seuil.
- Cipolla-Neto, J., Amaral, F. G., Afeche, S. C., Tan, D. X., & Reiter, R. J., (2014), Melatonin, energy metabolism, and obesity: a review, *J. Pineal Res.* 564, 371–381, doi:10.1111/jpi.12137
- Clark, A., (2013), Re-Inventing Ourselves: The Plasticity of Embodiment, Sensing, and Mind, *Transhumanist Read. Class. Contemp. Essays Sci. Technol. Philos. Hum. Futur. June 2004*, 113–127, doi:10.1002/9781118555927.ch11
- Cohen, L. G., Weeks, R. A., Sadato, N., Celnik, P., Ishii, K., & Hallett, M., (1999), Period of susceptibility for cross-modal plasticity in the blind., *Ann. Neurol.* 454, 451–460.
- Collignon, O., Dormal, G., Albouy, G., Vandewalle, G., Voss, P., Phillips, C., & Lepore, F., (2013), Impact of blindness onset on the functional organization and the connectivity of the occipital cortex, *Brain*, 1369, 2769–2783, doi:10.1093/brain/awt176
- Collignon, O., Renier, L., Bruyer, R., Tranduy, D., & Veraart, C., (2006), Improved selective and divided spatial attention in early blind subjects, *Brain Res.* 10751, 175–182, doi:10.1016/j.brainres.2005.12.079
- Cunningham, S. I., Weiland, J. D., Bao, P., Lopez-Jaime, G. R., & Tjan, B. S., (2014), Correlation of vision loss with tactile-evoked V1 responses in retinitis pigmentosa., *Vision Res.* doi:10.1016/j.visres.2014.10.015
- Curcio, C. a., Sloan, K. R., Kalina, R. E., & Hendrickson, a. E., (1990), Human photoreceptor topography., *J. Comp. Neurol.* 292, 497–523, doi:10.1002/cne.902920402
- Cynader, M. & Berman, N., (1972), Receptive-field organization of monkey superior colliculus., *J. Neurophysiol.* 352, 187–201.
- Dacey, D. M., (2000), Parallel Pathways for Spectral Coding in Primate Retina, *Annu. Rev. Neurosci.* 231, 743–775, doi:10.1146/annurev.neuro.23.1.743
- Damoiseaux, J. S., Rombouts, S. A. R. B., Barkhof, F., Scheltens, P., Stam, C. J., Smith, S. M., & Beckmann, C. F., (2006), Consistent resting-state networks across healthy subjects, *Proc. Natl. Acad. Sci.* 10337, 13848–13853, doi:10.1073/pnas.0601417103
- Davies, W. I. L., Collin, S. P., & Hunt, D. M., (2012), Molecular ecology and adaptation of visual photopigments in craniates, *Mol. Ecol.* 2113, 3121–3158, doi:10.1111/j.1365-294X.2012.05617.x

-
- Dawson, D. A., Cha, K., Lewis, L. B., Mendola, J. D., & Shmuel, A., (2013), Evaluation and calibration of functional network modeling methods based on known anatomical connections, *Neuroimage*, *67*, 331–343, doi:10.1016/j.neuroimage.2012.11.006
- Dawson, D. A., Lam, J., Lewis, L. B., Carbonell, F., Mendola, J. D., & Shmuel, A., (2016), Partial Correlation-Based Retinotopically Organized Resting-State Functional Connectivity Within and Between Areas of the Visual Cortex Reflects More Than Cortical Distance, *Brain Connect.* *6* 1, 57–75, doi:10.1089/brain.2014.0331
- Dehaene, S. & Cohen, L., (2011), The unique role of the visual word form area in reading, *Trends Cogn. Sci.* *15* 6, 254–262, doi:10.1016/j.tics.2011.04.003
- Demb, J. B. & Singer, J. H., (2012), Intrinsic properties and functional circuitry of the AII amacrine cell., *Vis. Neurosci.* *29* 1, 51–60, doi:10.1017/S0952523811000368, arXiv: NIHMS150003
- Dennis, M., Spiegler, B. J., Juranek, J. J., Bigler, E. D., Snead, O. C., & Fletcher, J. M., (2013), Age, plasticity, and homeostasis in childhood brain disorders, *Neurosci. Biobehav. Rev.* *37* 10, 2760–2773, doi:10.1016/j.neubiorev.2013.09.010
- DeVries, S. H. [S H] & Baylor, D. A., (1995), An alternative pathway for signal flow from rod photoreceptors to ganglion cells in mammalian retina., *Proc. Natl. Acad. Sci. U. S. A.* *92* 23, 10658–62.
- Dilks, D. D., Baker, C. I., Peli, E., & Kanwisher, N., (2009), Reorganization of visual processing in macular degeneration is not specific to the "preferred retinal locus"., *J. Neurosci.* *29* 9, 2768–2773, doi:10.1523/JNEUROSCI.5258-08.2009
- Dilks, D. D., Serences, J. T., Rosenau, B. J., Yantis, S., & McCloskey, M., (2007), Human adult cortical reorganization and consequent visual distortion., *J. Neurosci.* *27* 36, 9585–9594, doi:10.1523/JNEUROSCI.2650-07.2007
- Donders, F. C., (1857), Beiträge zur pathologischen Anatomie des Auges, *Albr. von Graefes Arch. für Ophthalmol.* *3* 1, 139–165, doi:10.1007/BF02720685
- Dormal, G. & Collignon, O., (2011), Functional selectivity in sensory-deprived cortices., *J. Neurophysiol.* *105* 6, 2627–30, doi:10.1152/jn.00109.2011
- Dormal, G., Lepore, F., & Collignon, O., (2012), Plasticity of the dorsal "spatial" stream in visually deprived individuals., *Neural Plast.* doi:10.1155/2012/687659
- Dosenbach, N. U. F., Fair, D. a., Miezin, F. M., Cohen, A. L., Wenger, K. K., Dosenbach, R. A. T., ... Petersen, S. E., (2007), Distinct brain networks for adaptive and stable task control in humans, *Proc. Natl. Acad. Sci.* *104* 26, 11073–11078, doi:10.1073/pnas.0704320104
- Doty, R. W., (1983), Nongeniculate afferents to striate cortex in macaques, *J. Comp. Neurol.* *218* 2, 159–173, doi:10.1002/cne.902180204
- Dugas-Ford, J., Rowell, J. J., & Ragsdale, C. W., (2012), Cell-type homologies and the origins of the neocortex, *Proc. Natl. Acad. Sci.* *109* 42, 16974–16979, doi:10.1073/pnas.1204773109

-
- Duret, F., Issenhuth, M., & Safran, A. B., (1999), Combined use of several preferred retinal loci in patients with macular disorders when reading single words, *Vision Res.* *39*4, 873–879, doi:10.1016/S0042-6989(98)00179-5
- Eggers, E. D. & Lukasiewicz, P. D., (2011), Multiple pathways of inhibition shape bipolar cell responses in the retina., *Vis. Neurosci.* *28*1, 95–108, doi:10.1017/S095252381000209
- Essen, D. C. & Zeki, S. M., (1978), The topographic organization of rhesus monkey prestriate cortex., *J. Physiol.* *277*, 193–226.
- Euler, T. & Masland, R. H. [R H], (2000), Light-evoked responses of bipolar cells in a mammalian retina., *J. Neurophysiol.* *83*4, 1817–1829.
- Fahim, A. T., Khan, N. W., Zahid, S., Schachar, I. H., Branham, K., Kohl, S., . . . Jayasundera, T., (2013), Diagnostic fundus autofluorescence patterns in achromatopsia., *Am. J. Ophthalmol.* *156*6, 1211–1219.e2, doi:10.1016/j.ajo.2013.06.033
- Falchier, A., Clavagnier, S., Barone, P., & Kennedy, H., (2002), Anatomical evidence of multimodal integration in primate striate cortex., *J. Neurosci.* *22*13, 5749–5759, doi:20026562
- Fernandes, A. M., Fero, K., Driever, W., & Burgess, H. A., (2013), Enlightening the brain: Linking deep brain photoreception with behavior and physiology, *BioEssays*, *35*9, 775–779, doi:10.1002/bies.201300034
- Ferreira, S., Pereira, A. C., Quendera, B., Reis, A., Silva, E. D., & Castelo-Branco, M., (2016), Primary visual cortical remapping in patients with inherited peripheral retinal degeneration, *NeuroImage Clin.* *13*, 428–438, doi:10.1016/j.nicl.2016.12.013
- Feuda, R., Hamilton, S. C., McInerney, J. O., & Pisani, D., (2012), Metazoan opsin evolution reveals a simple route to animal vision, *Proc. Natl. Acad. Sci.* *109*46, 18868–18872, doi:10.1073/pnas.1204609109
- ffytche, D. H., (2005), Visual hallucinations and the Charles Bonnet syndrome., *Curr. Psychiatry Rep.* *7*3, 168–179.
- ffytche, D. H., (2007), Visual hallucinatory syndromes: past, present, and future, *Dialogues Clin. Neurosci.* *9*2, 173–189.
- Fitzpatrick, D., Usrey, W. M., Schofield, B. R., & Einstein, G., (1994), The sublaminar organization of corticogeniculate neurons in layer 6 of macaque striate cortex., *Vis. Neurosci.* *11*2, 307–315, doi:10.1017/S0952523800001656
- Fortenbaugh, F. C., Hicks, J. C., Hao, L., & Turano, K. A., (2007), Losing sight of the bigger picture: Peripheral field loss compresses representations of space, *Vision Res.* *47*19, 2506–2520, doi:10.1016/j.visres.2007.06.012
- Fortin, M., Voss, P., Lord, C., Lassonde, M., Pruessner, J., Saint-Amour, D., . . . Lepore, F., (2008), Wayfinding in the blind: Larger hippocampal volume and supranormal spatial navigation, *Brain*, *131*11, 2995–3005, doi:10.1093/brain/awn250

-
- Fox, M. D., Corbetta, M., Snyder, A. Z., Vincent, J. L., & Raichle, M. E., (2006), Spontaneous neuronal activity distinguishes human dorsal and ventral attention systems, *Proc. Natl. Acad. Sci.* *103* 26, 10046–10051, doi:10.1073/pnas.0604187103
- Fox, M. D., Snyder, A. Z., Vincent, J. L., Corbetta, M., Van Essen, D. C., & Raichle, M. E., (2005), From The Cover: The human brain is intrinsically organized into dynamic, anticorrelated functional networks, *Proc. Natl. Acad. Sci.* *102* 27, 9673–9678, doi:10.1073/pnas.0504136102
- Franceschetti, A., (1963), Über Tapeto-Retinale Degenerationen im Kindesalter. In *Entwicklung und fortschritt der augenkeilkd.* (pp. 107–120), Stuttgart: Enke Verlag.
- François, J. & Neetens, A., (1962), Vegetative Physiology and Biochemistry, In H. Davson (Ed.), *Eye* (3rd, Chap. Comparativ, Vol. 1, pp. 369–415), London: Academic Press Inc.
- Franze, K., Grosche, J., Skatchkov, S. N., Schinkinger, S., Foja, C., Schild, D., . . . Guck, J., (2007), Muller cells are living optical fibers in the vertebrate retina, *Proc. Natl. Acad. Sci.* *104* 20, 8287–8292, doi:10.1073/pnas.0611180104
- Fried, S. I., Münch, T. a., & Werblin, F. S., (2002), Mechanisms and circuitry underlying directional selectivity in the retina, *Nature*, *420* 6914, 411–414, doi:10.1038/nature01179
- Fries, W., (1990), Pontine projection from striate and prestriate visual cortex in the macaque monkey: an anterograde study., *Vis. Neurosci.* *4* 3, 205–16, doi:10.1017/S0952523800003357
- Giacomini, P. S., Levesque, I. R., Ribeiro, L., Narayanan, S., Francis, S. J., Pike, G. B., & Arnold, D. L., (2009), Measuring demyelination and remyelination in acute multiple sclerosis lesion voxels., *Arch Neurol*, *66* 3, 375–81, doi:10.1001/archneurol.2008.578
- Goldreich, D. & Kanics, I. M., (2003), Tactile acuity is enhanced in blindness., *J. Neurosci.* *23* 8, 3439–3445, doi:10.1097/WNR.0b013e32802b70f8
- Gollisch, T. & Meister, M., (2010), Eye Smarter than Scientists Believed: Neural Computations in Circuits of the Retina, *Neuron*, *65* 2, 150–164, doi:10.1016/j.neuron.2009.12.009
- Goodale, M. A. & Milner, A. D., (1992), Separate visual pathways for perception and action, *Trends Neurosci.* *15* 1, 20–25, doi:10.1016/0166-2236(92)90344-8
- Gougoux, F., Lepore, F., Lassonde, M., Voss, P., Zatorre, R. J., & Belin, P., (2004), Neuropsychology: Pitch discrimination in the early blind, *Nature*, *430* 6997, 309–309, doi:10.1038/430309a
- Gougoux, F., Zatorre, R. J., Lassonde, M., Voss, P., & Lepore, F., (2005), A functional neuroimaging study of sound localization: Visual cortex activity predicts performance in early-blind individuals, *PLoS Biol.* *3* 2, 0324–0333, doi:10.1371/journal.pbio.0030027

-
- Gould, S. J. & Lewontin, R. C., (1979), The spandrels of San Marco and the Panglossian paradigm: a critique of the adaptationist programme., *Proc. R. Soc. London. Ser. B, Biol. Sci.* 205 1161, 581–98, doi:10.1098/rspb.1979.0086
- Goyal, M. S., Hansen, P. J., & Blakemore, C. B., (2006), Tactile perception recruits functionally related visual areas in the late-blind., *Neuroreport*, 1713, 1381–1384, doi:10.1097/01.wnr.0000227990.23046.fe
- Graham, D. M., Wong, K. Y., Shapiro, P., Frederick, C., Pattabiraman, K., & Berson, D. M., (2008), Melanopsin ganglion cells use a membrane-associated rhabdomic phototransduction cascade, *J Neurophysiol*, 99 5, 2522–2532, doi:10.1152/jn.01066.2007
- Graham, J., (1982), Some topographical connections of the striate cortex with subcortical structures in *Macaca fascicularis*, *Exp. Brain Res.* 471, 1–14, doi:10.1007/BF00235880
- Greicius, M. D., Krasnow, B., Reiss, A. L., & Menon, V., (2003), Functional connectivity in the resting brain: A network analysis of the default mode hypothesis, *Proc. Natl. Acad. Sci.* 100 1, 253–258, doi:10.1073/pnas.0135058100
- Grimes, D. A. & Schulz, K. F., (2005), Compared to what? Finding controls for case-control studies, *Lancet*, 365 9468, 1429–1433, doi:10.1016/S0140-6736(05)66379-9
- Grimes, W. N., Zhang, J., Graydon, C. W., Kachar, B., & Diamond, J. S., (2010), Retinal Parallel Processors: More than 100 Independent Microcircuits Operate within a Single Interneuron, *Neuron*, 65 6, 873–885, doi:10.1016/j.neuron.2010.02.028
- Gutierrez, C. & Cusick, C. G., (1997), Area V1 in macaque monkeys projects to multiple histochemically defined subdivisions of the inferior pulvinar complex, *Brain Res.* 765 2, 349–356, doi:10.1016/S0006-8993(97)00696-3
- Hadzibeganovic, T., van den Noort, M., Bosch, P., Perc, M., van Kralingen, R., Mondt, K., & Coltheart, M., (2010), Cross-linguistic neuroimaging and dyslexia: a critical view., *Cortex.* 46 10, 1312–6, doi:10.1016/j.cortex.2010.06.011
- Hampson, M., Olson, I. R., Leung, H.-c., Skudlarski, P., & Gore, J. C., (2004), Changes in functional connectivity of human MT/V5 with visual motion input., *Neuroreport*, 15 8, 1315–1319, doi:10.1097/01.wnr.0000129997
- Hansen, T., Pracejus, L., & Gegenfurtner, K. R., (2009), Color perception in the intermediate periphery of the visual field., *J. Vis.* 9 4, 26.1–12, doi:10.1167/9.4.26
- Harting, J. K. [J. K.], Hall, W. C., Diamond, I. T., & Martin, G. F., (1973), Anterograde degeneration study of the superior colliculus in *Tupaia glis*: Evidence for a subdivision between superficial and deep layers, *J. Comp. Neurol.* 148 3, 361–386, doi:10.1002/cne.901480305
- Harting, J. K. [John K], Huerta, M. F., Frankfurter, A. J., Strominger, N. L., & Royce, G. J., (1980), Ascending pathways from the monkey superior colliculus: An autoradiographic analysis, *J. Comp. Neurol.* 192 4, 853–882, doi:10.1002/cne.901920414

-
- Hattar, S., (2002), Melanopsin-Containing Retinal Ganglion Cells: Architecture, Projections, and Intrinsic Photosensitivity, *Science (80-.)*. *295* 5557, 1065–1070, doi:10.1126/science.1069609
- Hayreh, S. S., (1963), The cilio-retinal arteries., *Br. J. Ophthalmol.* *47*, 71–89.
- Hecht, S., (1942), Energy, quant, and vision, *J. Gen. Physiol.* *25* 6, 819–840, doi:10.1085/jgp.25.6.819
- Heesy, C. P. & Hall, M. I., (2010), The nocturnal bottleneck and the evolution of mammalian vision, *Brain. Behav. Evol.* *75* 3, 195–203, doi:10.1159/000314278
- Hendry, S. H. & Yoshioka, T., (1994), A neurochemically distinct third channel in the macaque dorsal lateral geniculate nucleus, *Science (80-.)*. *264* 5158, 575–577, doi:10.1126/science.8160015
- Hendry, S. H. C. & Reid, R. C., (2000), The Koniocellular Pathway in Primate Vision, *Annu. Rev. Neurosci.* *23* 1, 127–153, doi:10.1146/annurev.neuro.23.1.127
- Hernowo, A. T., Prins, D., Baseler, H. a., Plank, T., Gouws, A. D., Hooymans, J. M. M., ... Cornelissen, F. W., (2014), Morphometric analyses of the visual pathways in macular degeneration., *Cortex.* *56*, 99–110, doi:10.1016/j.cortex.2013.01.003
- Hewes, G. W., Andrew, R. J., Carini, L., Choe, H., Gardner, R. A., Kortlandt, A., ... Wescott, R. W., (1973), Primate communication and the gestural origin of language [and comments and reply], *Curr. Anthropol.* *14*, 5–24, doi:10.1086/201401
- Hochel, M., Milán, E. G., Martín, J. L. M., González, A., García, E. D., Tornay, F., & Vila, J., (2009), Congruence or coherence? Emotional and physiological responses to colours in synaesthesia, *Eur. J. Cogn. Psychol.* *21* 5, 703–723, doi:10.1080/09541440802176292
- Holland, L. Z., Carvalho, J. E., Escrava, H., Laudet, V., Schubert, M., Shimeld, S. M., & Yu, J.-K., (2013), Evolution of bilaterian central nervous systems: a single origin? *Evodevo*, *4* 1, 1–20, doi:10.1186/2041-9139-4-27
- Horton, J. C. & Hoyt, W. F., (1991), The representation of the visual field in human striate cortex. A revision of the classic Holmes map., *Arch. Ophthalmol. (Chicago, Ill. 1960)*, *109* 6, 816–824, doi:10.1001/archophth.1991.01080060080030
- Hosoya, T., Baccus, S., & Meister, M., (2005), Dynamic predictive coding by the retina., *Nature*, *436* 7047, 71–77, doi:10.1038/nature03689
- Hubel, D. H. & Wiesel, T. N., (1963), Receptive fields of cells in striate cortex of very young, visually inexperienced kittens., *J. Neurophysiol.* *26*, 994–1002.
- Hunt, D. M. & Peichl, L. [Leo], (2014), S cones: Evolution, retinal distribution, development, and spectral sensitivity, *Vis. Neurosci.* *31* 2, 115–138, doi:10.1017/s0952523813000242
- Hutton, C., Draganski, B., Ashburner, J., & Weiskopf, N., (2009), A comparison between voxel-based cortical thickness and voxel-based morphometry in normal aging, *Neuroimage*, *48* 2, 371–380, doi:10.1016/j.neuroimage.2009.06.043

-
- Innocenti, G. M. & Price, D. J., (2005), Exuberance in the development of cortical networks., *Nat. Rev. Neurosci.* 6 12, 955–965, doi:10.1038/nrn1790
- Ioannidis, J. P. A., (2005), Contradicted and Initially Stronger Effects in Highly Cited Clinical Research, *JAMA*, 294 2, 218, doi:10.1001/jama.294.2.218
- Ismail, F. Y., Fatemi, A., & Johnston, M. V., (2016), Cerebral plasticity: Windows of opportunity in the developing brain., *Eur. J. Paediatr. Neurol.* 1–26, doi:10.1016/j.ejpn.2016.07.007
- Jacobs, G. H., Fenwick, J. C., Calderone, J. B., & Deeb, S. S., (1999), Human cone pigment expressed in transgenic mice yields altered vision., *J. Neurosci.* 19 8, 3258–3265.
- Jiang, J., Zhu, W., Shi, F., Liu, Y., Li, J., Qin, W., ... Jiang, T., (2009), Thick Visual Cortex in the Early Blind, *J. Neurosci.* 29 7, 2205–2211, doi:10.1523/JNEUROSCI.5451-08.2009
- Jones, B. W. [Bryan W.] & Marc, R. E. [Robert E.], (2005), Retinal remodeling during retinal degeneration, *Exp. Eye Res.* 81 2, 123–137, doi:10.1016/j.exer.2005.03.006
- Jones, B. W. [Bryan W.], Watt, C. B., Frederick, J. M., Baehr, W., Chen, C. K., Levine, E. M., ... Marc, R. E., (2003), Retinal remodeling triggered by photoreceptor degenerations, *J. Comp. Neurol.* 464 1, 1–16, doi:10.1002/cne.10703
- Jusuf, P. R., Haverkamp, S., & Grünert, U., (2005), Localization of glycine receptor alpha subunits on bipolar and amacrine cells in primate retina, *J. Comp. Neurol.* 488 2, 113–128, doi:10.1002/cne.20555
- Kaas, J. H. [J H] & Preuss, T. M., (1993), Archontan affinities as reflected in the visual system, In F. Szalay, M. Novacek, & M. McKeena (Eds.), *Mamm. phylogeny* (pp. 115–128), New York: Springer-Verlag.
- Kaas, J. H. [Jon H.], (2012), The evolution of neocortex in primates. In *Prog. brain res.* (Vol. 195, pp. 91–102), doi:10.1016/B978-0-444-53860-4.00005-2
- Kaas, J. H. [Jon H.], (2013a), The evolution of brains from early mammals to humans, *Wiley Interdiscip. Rev. Cogn. Sci.* 4 1, 33–45, doi:10.1002/wcs.1206
- Kaas, J. H. [Jon H.], (2013b), The evolution of the visual system in primates, In J. Werner & L. Chalupa (Eds.), *New vis. neurosci.* (pp. 1–26), Cambridge, Massachusetts: MIT Press.
- Kaas, J. H. [Jon H.], (2015), Blindsight: Post-natal potential of a transient pulvinar pathway, *Curr. Biol.* 25 4, R155–R157, doi:10.1016/j.cub.2014.12.053
- Kaas, J. H. [Jon H.], Gharbawie, O. a., & Stepniewska, I., (2011), The Organization and Evolution of Dorsal Stream Multisensory Motor Pathways in Primates, *Front. Neuroanat.* 5, 34, doi:10.3389/fnana.2011.00034
- Kanwisher, N., (2001), Faces and places: of central (and peripheral) interest., *Nat. Neurosci.* 4 5, 455–456, doi:10.1038/87399

-
- Kaplan, E., (2008), The P, M and K Streams of the Primate Visual System: What Do They Do for Vision? In *Senses a compr. ref.* (pp. 369–381), Elsevier, doi:10.1016/B978-012370880-9.00274-7
- Kaplan, E. [Ehud], (2014), The M, P and K pathways of the Primate Visual System revisited, In J. Werner & L. Chalupa (Eds.), *New vis. neurosci.* Cambridge, MA: Massachusetts Institute of Technology.
- Karten, H. J., (2013), Neocortical evolution: Neuronal circuits arise independently of lamination, *Curr. Biol.* 231, R12–R15, doi:10.1016/j.cub.2012.11.013
- Kastrup, O., Leonhardt, G., Kurthen, M., & Hufnagel, A., (2000), Cortical motor reorganization following early brain damage and hemispherectomy demonstrated by transcranial magnetic stimulation., *Clin. Neurophysiol.* 1118, 1346–52, doi:S1388-2457(00)00339-4[pii]
- Kawachi, I., Colditz, G. A., Stampfer, M. J., Willett, W. C., Manson, J. E., Speizer, F. E., & Hennekens, C. H., (1995), Prospective study of shift work and risk of coronary heart disease in women., *Circulation*, 9211, 3178–82.
- Kemp, T. S., (2006), The origin and early radiation of the therapsid mammal-like reptiles: A palaeobiological hypothesis, *J. Evol. Biol.* 194, 1231–1247, doi:10.1111/j.1420-9101.2005.01076.x
- Kim, J.-w., Yang, H.-j., Oel, A. P., Brooks, M. J., Jia, L., Plachetzki, D. C., ... Swaroop, A., (2016), Recruitment of Rod Photoreceptors from Short-Wavelength-Sensitive Cones during the Evolution of Nocturnal Vision in Mammals, *Dev. Cell*, 376, 520–532, doi:10.1016/j.devcel.2016.05.023
- Klein, D., Mok, K., Chen, J.-K., & Watkins, K. E., (2014), Age of language learning shapes brain structure: a cortical thickness study of bilingual and monolingual individuals., *Brain Lang.* 131, 20–24, doi:10.1016/j.bandl.2013.05.014, arXiv: 1301.4689
- Kröger, R. H. & Biehlmaier, O., (2009), Space-saving advantage of an inverted retina, *Vision Res.* 4918, 2318–2321, doi:10.1016/j.visres.2009.07.001
- Kryger, Z., Galli-Resta, L., Jacobs, G., & Reese, B., (1998), The topography of rod and cone photoreceptors in the retina of the ground squirrel, *Vis. Neurosci.* 1504, 685–691, doi:10.1017/S0952523898154081
- Kujala, T., Alho, K., Huotilainen, M., Ilmoniemi, R. J., Lehtokoski, A., Leinonen, A., ... Näätänen, R., (1997), Electrophysiological evidence for cross-modal plasticity in humans with early- and late-onset blindness, doi:10.1111/j.1469-8986.1997.tb02134.x
- Lachica, E. A. & Casagrande, V. A. [V. A.], (1992), Direct W-like geniculate projections to the cytochrome oxidase (CO) blobs in primate visual cortex: Axon morphology, *J. Comp. Neurol.* 3191, 141–158, doi:10.1002/cne.903190112

-
- Lamb, T. D. [Trevor D], (2013), Evolution of phototransduction, vertebrate photoreceptors and retina, *Prog. Retin. Eye Res.* 36, 52–119, doi:10.1016/j.preteyeres.2013.06.001
- Lamb, T. D. [Trevor D.], Collin, S. P., & Pugh, E. N., (2007), Evolution of the vertebrate eye: opsins, photoreceptors, retina and eye cup, *Nat. Rev. Neurosci.* 8 12, 960–976, doi:10.1038/nrn2283
- Large layer VI neurons of monkey striate cortex (Meynert cells) project to the superior colliculus., (1983), *Proc. R. Soc. London. Ser. B, Biol. Sci.* 219 1214, 53–59, doi:10.1098/rspb.1983.0058
- Larsson, J. & Heeger, D. J., (2006), Two retinotopic visual areas in human lateral occipital cortex., *J. Neurosci.* 26 51, 13128–13142, doi:10.1523/JNEUROSCI.1657-06.2006
- Lawlor, D. A., Smith, G. D., & Ebrahim, S., (2004), Commentary: The hormone replacement-coronary heart disease conundrum: Is this the death of observational epidemiology? *Int. J. Epidemiol.* 33 3, 464–467, doi:10.1093/ije/dyh124
- Lazzarino De Lorenzo, L. G., ffytche, D. H., Di Camillo, E., & Buiatti, T., (2014), The Dide-Botcazo syndrome: forgotten and misunderstood., *Cortex.* 56, 182–190, doi:10.1016/j.cortex.2013.01.011
- Lee, S. C. & Grünert, U., (2007), Connections of diffuse bipolar cells in primate retina are biased against S-cones, *J. Comp. Neurol.* 502 1, 126–140, doi:10.1002/cne.21284
- Lee, S. & Zhou, Z. J., (2006), The Synaptic Mechanism of Direction Selectivity in Distal Processes of Starburst Amacrine Cells, *Neuron*, 51 6, 787–799, doi:10.1016/j.neuron.2006.08.007
- Leichnetz, G. R., Spencer, R. F., Hardy, S. G. P., & Astruc, J., (1981), The prefrontal corticotectal projection in the monkey; An anterograde and retrograde horseradish peroxidase study, *Neuroscience*, 6 6, 1023–1041, doi:10.1016/0306-4522(81)90068-3
- Leventhal, A. G., Rodieck, R. W., & Dreher, B., (1981), Retinal ganglion cell classes in the Old World monkey: morphology and central projections, *Science (80-)*. 213 4512, 1139–1142, doi:10.1126/science.7268423
- Levi, D. M., (2005), Perceptual learning in adults with amblyopia: A reevaluation of critical periods in human vision, *Dev. Psychobiol.* 46 3, 222–232, doi:10.1002/dev.20050
- Lewis, T. L. & Maurer, D., (2005), Multiple sensitive periods in human visual development: Evidence from visually deprived children, *Dev. Psychobiol.* 46 3, 163–183, doi:10.1002/dev.20055
- Li, P., Legault, J., & Litcofsky, K. A., (2014), Neuroplasticity as a function of second language learning: anatomical changes in the human brain., *Cortex.* 58 June, 301–24, doi:10.1016/j.cortex.2014.05.001

-
- Lin, B., Martin, P. R., Solomon, S. G., & Grünert, U., (2000), Distribution of glycine receptor subunits on primate retinal ganglion cells: a quantitative analysis, *Eur. J. Neurosci.* *12* 12, 4155–4170, doi:10.1111/j.1460-9568.2000.01311.x
- Liu, Y., Yu, C., Liang, M., Li, J., Tian, L., Zhou, Y., ... Jiang, T., (2007), Whole brain functional connectivity in the early blind, *Brain*, *130* 8, 2085–2096, doi:10.1093/brain/awm121
- Livingstone, M. S. & Hubel, D. H., (1987), Connections between layer 4B of area 17 and the thick cytochrome oxidase stripes of area 18 in the squirrel monkey., *J. Neurosci.* *7* 11, 3371–3377.
- Lucas, S. G. & Luo, Z.-X., (1993), Adelobasileus from the Upper Triassic of West Texas : The oldest mammal, *J. Vertebr. Paleontol.* *13* 3, 309–334, doi:10.1080/02724634.1993.10011512
- Lucas-Lledó, J. I. & Lynch, M., (2009), Evolution of mutation rates: Phylogenomic analysis of the photolyase/cryptochrome family, *Mol. Biol. Evol.* *26* 5, 1143–1153, doi:10.1093/molbev/msp029
- Lund, J. S., Lund, R. D., Hendrickson, a. E., Bunt, a. H., & Fuchs, a. F., (1975), The origin of efferent pathways from the primary visual cortex, area 17, of the macaque monkey as shown by retrograde transport of horseradish peroxidase., *J. Comp. Neurol.* *164* 3, 287–303, doi:10.1002/cne.901640303
- Lynch, J. C., Graybiel, a. M., & Lobeck, L. J., (1985), The differential projection of two cytoarchitectonic subregions of the inferior parietal lobule of macaque upon the deep layers of the superior colliculus, *J Comp Neurol*, *235* 2, 241–254, doi:10.1002/cne.902350207
- Lyon, D. C. & Kaas, J. H. [Jon H.], (2002), Connectional Evidence for Dorsal and Ventral V3, and Other Extrastriate Areas in the Prosimian Primate, Galago garnetti, *Brain. Behav. Evol.* *59* 3, 114–129, doi:10.1159/000064159
- MacNeil, M. A., Heussy, J. K., Dacheux, R. F., Raviola, E., & Masland, R. H., (1999), The shapes and numbers of amacrine cells: Matching of photofilled with Golgi-stained cells in the rabbit retina and comparison with other mammalian species, *J. Comp. Neurol.* *413* 2, 305–326, doi:10.1002/(SICI)1096-9861(19991018)413:2<305::AID-CNE10>3.0.CO;2-E
- Malach, R., Reppas, J. B., Benson, R. R., Kwong, K. K., Jiang, H., Kennedy, W. a., ... Tootell, R. B., (1995), Object-related activity revealed by functional magnetic resonance imaging in human occipital cortex., *Proc. Natl. Acad. Sci. U. S. A.* *92* 18, 8135–8139, doi:10.1073/pnas.92.18.8135
- Malach, R. [Rafael], Levy, I., & Hasson, U., (2002), The topography of high-order human object areas, *Trends Cogn. Sci.* *6* 4, 176–184, doi:10.1016/S1364-6613(02)01870-3
- Malikovic, A., Amunts, K., Schleicher, A., Mohlberg, H., Kujovic, M., Palomero-Gallagher, N., ... Zilles, K., (2016), Cytoarchitecture of the human lateral occipital cortex:

-
- mapping of two extrastriate areas hOc4la and hOc4lp, *Brain Struct. Funct.* *221* 4, 1877–1897, doi:10.1007/s00429-015-1009-8
- Maltese, F., Adda, M., Bablon, A., Hraeich, S., Guervilly, C., Lehingue, S., . . . Papazian, L., (2016), Night shift decreases cognitive performance of ICU physicians., *Intensive Care Med.* *42* 3, 393–400, doi:10.1007/s00134-015-4115-4
- Marc, R. E. [Robert E] & Jones, B. W. [Bryan W], (2003), Retinal remodeling in inherited photoreceptor degenerations., *Mol. Neurobiol.* *28* 2, 139–147, doi:10.1385/MN:28:2:139
- Marc, R. E. [Robert E.], Jones, B. W., Watt, C. B., & Strettoi, E., (2003), Neural remodeling in retinal degeneration, *Prog. Retin. Eye Res.* *22* 5, 607–655, doi:10.1016/S1350-9462(03)00039-9
- Margulies, D. S., Böttger, J., Long, X., Lv, Y., Kelly, C., Schäfer, A., . . . Villringer, A., (2010), Resting developments: a review of fMRI post-processing methodologies for spontaneous brain activity, *Magn. Reson. Mater. Physics, Biol. Med.* *23* 5-6, 289–307, doi:10.1007/s10334-010-0228-5
- Masland, R. H. [Richard H.], (2012), The Neuronal Organization of the Retina, *Neuron*, *76* 2, 266–280, doi:10.1016/j.neuron.2012.10.002
- Masuda, Y., Dumoulin, S. O., Nakadomari, S., & Wandell, B. A., (2008), V1 Projection Zone Signals in Human Macular Degeneration Depend on Task, not Stimulus, *Cereb. Cortex*, *18* 11, 2483–2493, doi:10.1093/cercor/bhm256
- Masuda, Y., Horiguchi, H., Dumoulin, S. O., Furuta, A., Miyauchi, S., Nakadomari, S., & Wandell, B. a., (2010), Task-dependent V1 responses in human retinitis pigmentosa., *Invest. Ophthalmol. Vis. Sci.* *51* 10, 5356–5364, doi:10.1167/iovs.09-4775
- Maunsell, J. H. & van Essen, D. C., (1983), The connections of the middle temporal visual area (MT) and their relationship to a cortical hierarchy in the macaque monkey., *J. Neurosci.* *3* 12, 2563–2586.
- Mavranakans, N. A., Dang-Burgener, N. P. L., Lorincz, E. N., Landis, T., & Safran, A. B., (2009), Perceptual distortion in homonymous paracentral scotomas., doi:10.1097/WNO.0b013e318198ca37
- McCarthy, J. D. & Caplovitz, G. P., (2014), Color synesthesia improves color but impairs motion perception, *Trends Cogn. Sci.* *18* 5, 224–226, doi:10.1016/j.tics.2014.02.002
- McKeefry, D. J., Burton, M. P., & Morland, A. B., (2010), The contribution of human cortical area V3A to the perception of chromatic motion: A transcranial magnetic stimulation study, *Eur. J. Neurosci.* *31* 3, 575–584, doi:10.1111/j.1460-9568.2010.07095.x
- McKyton, A. & Zohary, E., (2007), Beyond retinotopic mapping: The spatial representation of objects in the human lateral occipital complex, *Cereb. Cortex*, *17* 5, 1164–1172, doi:10.1093/cercor/bhl027

-
- Merabet, L. B., Hamilton, R., Schlaug, G., Swisher, J. D., Kiriakopoulos, E. T., Pitskel, N. B., ... Pascual-Leone, A., (2008), Rapid and Reversible Recruitment of Early Visual Cortex for Touch, *PLoS One*, *3* 8, e3046, doi:10.1371/journal.pone.0003046
- Merabet, L. B., Maguire, D., Warde, A., Alterescu, K., Stickgold, R., & Pascual-Leone, A., (2004), Visual hallucinations during prolonged blindfolding in sighted subjects., *J. Neuroophthalmol.* *24* 2, 109–113.
- Merabet, L. B. & Pascual-Leone, A., (2010), Neural reorganization following sensory loss: the opportunity of change., *Nat. Rev. Neurosci.* *11* 1, 44–52, doi:10.1038/nrn2758
- Meunier, I. & Puech, B., (2012), Maladie de Stargardt (Stargardt disease), In S. Y. Cohen & A. Gaudric (Eds.), *Rétine* (Chap. Dystrophie, pp. 26–48), Paris: Lavoisier.
- Mohlberg, H., Eickhoff, S., Schleicher, A., Zilles, K., & Amunts, K., (2012), A new processing pipeline and release of cytoarchitectonic probabilistic maps – JuBrain. In *Ohbm*, Peking.
- Mollon, J. & Jordan, G., (1988), Eine evolutionäre Interpretation des menschlichen Farbensiehens, *Die Farbe*, *35* 36, 139–170.
- Morland, A. B., Baseler, H. A., Hoffmann, M. B., Sharpe, L. T., & Wandell, B. A., (2001), Abnormal retinotopic representations in human visual cortex revealed by fMRI., *Acta Psychol. (Amst)*. *107* 1-3, 229–247, doi:http://dx.doi.org/10.1016/S0001-6918(01)00025-7
- Müller, B. & Peichl, L., (1989), Topography of cones and rods in the tree shrew retina., *J. Comp. Neurol.* *282* 4, 581–594, doi:10.1002/cne.902820409
- Münch, T. a., da Silveira, R. A., Siebert, S., Viney, T. J., Awatramani, G. B., & Roska, B., (2009), Approach sensitivity in the retina processed by a multifunctional neural circuit., *Nat. Neurosci.* *12* 10, 1308–1316, doi:10.1038/nn.2389
- Murphy, K., Birn, R. M., Handwerker, D. A., Jones, T. B., & Bandettini, P. A., (2009), The impact of global signal regression on resting state correlations: Are anti-correlated networks introduced? *Neuroimage*, *44* 3, 893–905, doi:10.1016/j.neuroimage.2008.09.036
- Murphy, W. J., Pevzner, P. A., & O’Brien, S. J., (2004), Mammalian phylogenomics comes of age, *Trends Genet.* *20* 12, 631–639, doi:10.1016/j.tig.2004.09.005
- Nassi, J. J. & Callaway, E. M., (2009), Parallel processing strategies of the primate visual system, *Nat. Rev. Neurosci.* *10* 5, 360–372, doi:10.1038/nrn2619
- Nathans, J., (1999), The Evolution and Physiology of Human Review Color Vision: Insights from Molecular Genetic Studies of Visual Pigments, *Neuron*, *24*, 299–312, doi:10.1016/S0896-6273(00)80845-4
- Nava, E. & Röder, B., (2011), Adaptation and maladaptation insights from brain plasticity., *Prog. Brain Res.* *191*, 177–194, doi:10.1016/B978-0-444-53752-2.00005-9
- Niemeyer, W. & Starlinger, I., (1981), Do The Blind Hear Better-Investigations on Auditory (Audiology 1981).pdf.

-
- Nieuwenhuys, R., Voogd, J., & van Huijzen, C., (2008), Visual system. In *Hum. cent. nerv. syst.* (Forth, pp. 751–790), Berlin: Springer Berlin Heidelberg.
- Nilsson, D.-E. & Arendt, D. [Detlev], (2008), Eye Evolution: The Blurry Beginning, *Curr. Biol.* 18 23, R1096–R1098, doi:http://dx.doi.org/10.1016/j.cub.2008.10.025
- Noppeney, U., Friston, K. J., Ashburner, J., Frackowiak, R., & Price, C. J., (2005), Early visual deprivation induces structural plasticity in gray and white matter, *Curr Biol.* 15 13, R488–R490, doi:10.1016/j.cub.2005.06.053
- Northcutt, R. G., (2002), Understanding Vertebrate Brain Evolution, *Integr. Comp. Biol.* 42 4, 743–756, doi:10.1093/icb/42.4.743
- Ogren, M. & Hendrickson, A., (1976), Pathways between striate cortex and subcortical regions in *Macaca mulatta* and *Saimiri sciureus*: Evidence for a reciprocal pulvinar connection, *Exp. Neurol.* 53 3, 780–800, doi:10.1016/0014-4886(76)90155-2
- O’Hare, F., Bentley, S. A., Wu, Z., Guymer, R. H., Luu, C. D., & Ayton, L. N., (2015), Charles Bonnet Syndrome in Advanced Retinitis Pigmentosa, *Ophthalmology*, 122 9, 1951–1953, doi:10.1016/j.ophtha.2015.03.006
- Okano, T., Kojima, D., Fukada, Y., Shichida, Y., & Yoshizawa, T., (1992), Primary structures of chicken cone visual pigments: vertebrate rhodopsins have evolved out of cone visual pigments., *Proc. Natl. Acad. Sci. U. S. A.* 89 13, 5932–6, doi:10.1073/pnas.89.13.5932
- Olivo, G., Gaia, O., Melillo, P., Coccozza, S., Sirio, C., D’Alterio, F. M., . . . Quarantelli, M., (2015), Cerebral Involvement in Stargardt’s Disease: A VBM and TBSS Study., *Invest. Ophthalmol. Vis. Sci.* 56 12, 7388–7397, doi:10.1167/iovs.15-16899
- Olveczky, B. P., Baccus, S. A., & Meister, M., (2003), Segregation of object and background motion in the retina., *Nature*, 423 6938, 401–408, doi:10.1038/nature01652
- Orban, G. A., Claeys, K., Nelissen, K., Smans, R., Sunaert, S., Todd, J. T., . . . Vanduffel, W., (2006), Mapping the parietal cortex of human and non-human primates, *Neuropsychologia*, 44 13, 2647–2667, doi:10.1016/j.neuropsychologia.2005.11.001
- Osterberg, G., (1935), Topography of the layer of rods and cones in the human retina., *Nyt Nord. Forl.*
- Pandit, A. S., Expert, P., Lambiotte, R., Bonnelle, V., Leech, R., Turkheimer, F. E., & Sharp, D. J., (2013), Traumatic brain injury impairs small-world topology, *Neurology*, 80 20, 1826–1833, doi:10.1212/WNL.0b013e3182929f38
- Pang, J.-j., Gao, F., Paul, D. L., & Wu, S. M., (2012), Rod, M-cone and M/S-cone inputs to hyperpolarizing bipolar cells in the mouse retina, *J. Physiol.* 590 4, 845–854, doi:10.1113/jphysiol.2011.224113
- Park, H. J., Lee, J. D., Kim, E. Y., Park, B., Oh, M. K., Lee, S., & Kim, J. J., (2009), Morphological alterations in the congenital blind based on the analysis of cortical thickness and surface area, *Neuroimage*, 47 1, 98–106, doi:10.1016/j.neuroimage.2009.03.076

-
- Pascual-Leone, A., Amedi, A., Fregni, F., & Merabet, L. B., (2005), The plastic human brain cortex., *Annu. Rev. Neurosci.* *28* 1, 377–401, doi:10.1146/annurev.neuro.27.070203.144216
- Pascual-Leone, A. & Hamilton, R., (2001), Chapter 27 The metamodal organization of the brain, *Prog. Brain Res.* *134*, 427–445, doi:10.1016/S0079-6123(01)34028-1
- Peichl, L. [Leo], (2005), Diversity of mammalian photoreceptor properties: Adaptations to habitat and lifestyle? *Anat. Rec. - Part A Discov. Mol. Cell. Evol. Biol.* *287* 1, 1001–1012, doi:10.1002/ar.a.20262
- Peirson, S. N., Halford, S., & Foster, R. G., (2009), The evolution of irradiance detection: melanopsin and the non-visual opsins., *Philos. Trans. R. Soc. B*, *364* 1531, 2849–2865, doi:10.1098/rstb.2009.0050
- Pereira-Pedro, A. S. & Bruner, E., (2016), Sulcal pattern, extension, and morphology of the precuneus in adult humans, *Ann. Anat. - Anat. Anzeiger*, *208*, 85–93, doi:10.1016/j.aanat.2016.05.001
- Perkel, D. J., Bullier, J., & Kennedy, H., (1986), Topography of the afferent connectivity of area 17 in the macaque monkey: a double-labelling study., *J. Comp. Neurol.* *253* 3, 374–402, doi:10.1002/cne.902530307
- Pisani, D., Mohun, S. M., Harris, S. R., McInerney, J. O., & Wilkinson, M., (2006), Molecular evidence for dim-light vision in the last common ancestor of the vertebrates, *Curr. Biol.* *16* 9, 318–319, doi:10.1016/j.cub.2006.03.090
- Pitzalis, S., Fattori, P., & Galletti, C., (2012), The functional role of the medial motion area V6., *Front. Behav. Neurosci.* *6* January, 91, doi:10.3389/fnbeh.2012.00091
- Plank, T., Frolo, J., Brandl-Rühle, S., Renner, A. B., Hufendiek, K., Helbig, H., & Greenlee, M. W., (2011), Gray matter alterations in visual cortex of patients with loss of central vision due to hereditary retinal dystrophies, *Neuroimage*, *56* 3, 1556–1565, doi:10.1016/j.neuroimage.2011.02.055
- Plasticity in the vestibulo-ocular reflex, (1981), *Ann. Rev. Neurosci.* *4*, 273–299.
- Plummer, T., (2004), Flaked stones and old bones: Biological and cultural evolution at the dawn of technology, *Yearb. Phys. Anthropol.* *47*, 118–164, doi:10.1002/ajpa.20157
- Poort, J., Raudies, F., Wannig, A., Lamme, V. A. F., Neumann, H., & Roelfsema, P. R., (2012), The role of attention in figure-ground segregation in areas V1 and V4 of the visual cortex, *Neuron*, *75* 1, 143–156, doi:10.1016/j.neuron.2012.04.032
- Prins, D., Hanekamp, S., & Cornelissen, F. W., (2016), Structural brain MRI studies in eye diseases: are they clinically relevant? A review of current findings., *Acta Ophthalmol.* *94* 2, 113–21, doi:10.1111/aos.12825
- Prins, D., Plank, T., Baseler, H. A., Gouws, A. D., Beer, A., Morland, A. B., ... Cornelissen, F. W., (2016), Surface-Based Analyses of Anatomical Properties of the Visual Cortex in Macular Degeneration, *PLoS One*, *11* 1, e0146684, doi:10.1371/journal.pone.0146684

-
- Ptito, M., Schneider, F. C. G., Paulson, O. B., & Kupers, R., (2008), Alterations of the visual pathways in congenital blindness, *Exp. Brain Res.* *187*1, 41–49, doi:10.1007/s00221-008-1273-4
- Puelles, L. & Rubenstein, J. L., (2003), Forebrain gene expression domains and the evolving prosomeric model, *Trends Neurosci.* *26* 9, 469–476, doi:10.1016/S0166-2236(03)00234-0
- Qin, W., Liu, Y., Jiang, T., & Yu, C., (2013), The Development of Visual Areas Depends Differently on Visual Experience, *PLoS One*, *8* 1, 1–10, doi:10.1371/journal.pone.0053784
- Qin, W., Xuan, Y., Liu, Y., Jiang, T., & Yu, C., (2015), Functional Connectivity Density in Congenitally and Late Blind Subjects, *Cereb. Cortex*, *25* 9, 2507–2516, doi:10.1093/cercor/bhu051
- Qiu, F. T., Sugihara, T., & von der Heydt, R., (2007), Figure-ground mechanisms provide structure for selective attention., *Nat. Neurosci.* *10* 11, 1492–1499, doi:10.1038/nn1989
- Rahman, S. A. & Shah, V. S., (2016), Retinitis Pigmentosa, In C. A. Medina, J. H. Townsend, & A. D. Singh (Eds.), *Man. retin. dis. - a guid. to diagnosis manag.* (pp. 85–91), Switzerland: Springer International Publishing.
- Ralph, C. L., (1975), The pineal gland and geographical distribution of animals, *Int. J. Biometeorol.* *19* 4, 289–303, doi:10.1007/BF01451040
- Reich, L., Szwed, M., Cohen, L., & Amedi, A., (2011), A ventral visual stream reading center independent of visual experience, *Curr. Biol.* *21* 5, 363–368, doi:10.1016/j.cub.2011.01.040
- Reislev, N. L., Kupers, R., Siebner, H. R., Ptito, M., & Dyrby, T. B., (2016), Blindness alters the microstructure of the ventral but not the dorsal visual stream., *Brain Struct. Funct.* *221* 6, 2891–903, doi:10.1007/s00429-015-1078-8
- Renier, L. A., Anurova, I., De Volder, A. G., Carlson, S., VanMeter, J., & Rauschecker, J. P., (2010), Preserved functional specialization for spatial processing in the middle occipital gyrus of the early blind., *Neuron*, *68* 1, 138–148, doi:10.1016/j.neuron.2010.09.021
- Reymond, L., (1987), Spatial visual acuity of the falcon, *Falco berigora*: A behavioural, optical and anatomical investigation, *Vision Res.* *27* 10, 1859–1874, doi:10.1016/0042-6989(87)90114-3
- Reynolds, J. H. & Desimone, R., (2003), Interacting roles of attention and visual salience in V4, *Neuron*, *37* 5, 853–863, doi:10.1016/S0896-6273(03)00097-7
- Rezak, M. & Benevento, L. A., (1979), A comparison of the organization of the projections of the dorsal lateral geniculate nucleus, the inferior pulvinar and adjacent lateral pulvinar to primary visual cortex (area 17) in the macaque monkey, *Brain Res.* *167* 1, 19–40, doi:10.1016/0006-8993(79)90260-9

-
- Ribelayga, C., Cao, Y., & Mangel, S. C., (2008), The Circadian Clock in the Retina Controls Rod-Cone Coupling, *Neuron*, *59* 5, 790–801, doi:10.1016/j.neuron.2008.07.017
- Ricciardi, E. & Pietrini, P., (2011), New light from the dark, *Curr. Opin. Neurol.* *24* 4, 357–363, doi:10.1097/WCO.0b013e328348bdbf
- Rockland, K. S. [Kathleen S.] & Ojima, H., (2003), Multisensory convergence in calcarine visual areas in macaque monkey, *Int. J. Psychophysiol.* *50* 1-2, 19–26, doi:10.1016/S0167-8760(03)00121-1
- Rockland, K. S. [Kathleen S], Saleem, K. S., & Tanaka, K., (1994), Divergent feedback connections from areas V4 and TEO in the macaque, *Vis. Neurosci.* *11* 03, 579–600, doi:10.1017/S0952523800002480
- Roe, A. W., Chelazzi, L., Connor, C. E., Conway, B. R., Fujita, I., Gallant, J. L., ... Vanduffel, W., (2012), Toward a Unified Theory of Visual Area V4, *Neuron*, *74* 1, 12–29, doi:10.1016/j.neuron.2012.03.011
- Rokem, A., Takemura, H., Bock, A. S., Scherf, K. S., Behrmann, M., Wandell, B. A., ... Pestilli, F., (2017), The visual white matter: The application of diffusion MRI and fiber tractography to vision science, *J. Vis.* *17* 2, 4, doi:10.1167/17.2.4
- Rosa, M. G., Casagrande, V. A., Preuss, T., & Kaas, J. H., (1997), Visual field representation in striate and prestriate cortices of a prosimian primate (*Galago garnetti*)., *J. Neurophysiol.* *77* 6, 193–217.
- Roska, B. & Werblin, F., (2003), Rapid global shifts in natural scenes block spiking in specific ganglion cell types, *Nat Neurosci*, *6* 6, 600–608, doi:10.1038/nn1061\rnn1061[pii]
- Sabbah, N., Authié, C. N., Sanda, N., Mohand-Said, S., Sahel, J. A., & Safran, A. B., (2014), Importance of eye position on spatial localization in blind subjects wearing an argus II retinal prosthesis, *Investig. Ophthalmol. Vis. Sci.* *55* 12, 8259–8266, doi:10.1167/iovs.14-15392
- Sabbah, N., Authié, C. N., Sanda, N., Mohand-Saïd, S., Sahel, J. A., Safran, A. B., ... Amedi, A., (2016), Increased functional connectivity between language and visually deprived areas in late and partial blindness, *Neuroimage*, *136*, 162–173, doi:10.1016/j.neuroimage.2016.04.056
- Sadato, N., Okada, T., Honda, M., & Yonekura, Y., (2002), Critical period for cross-modal plasticity in blind humans: a functional MRI study., *Neuroimage*, *16* 2, 389–400, doi:10.1006/nimg.2002.1111
- Sadato, N., Okada, T., Kubota, K., & Yonekura, Y., (2004), Tactile discrimination activates the visual cortex of the recently blind naive to Braille: A functional magnetic resonance imaging study in humans, *Neurosci. Lett.* *359* 1-2, 49–52, doi:10.1016/j.neulet.2004.02.005

-
- Safran, a. B., Achard, O., Duret, F., & Landis, T., (1999), The "thin man" phenomenon: a sign of cortical plasticity following inferior homonymous paracentral scotomas., *Br. J. Ophthalmol.* *83* 2, 137–142, doi:10.1136/bjo.83.2.137
- Safran, A. B. [A B] & Landis, T., (1996), Plasticity in the adult visual cortex: implications for the diagnosis of visual field defects and visual rehabilitation., *Curr. Opin. Ophthalmol.* *7* 6, 53–64.
- Safran, A. B. [Avinoam B], Duret, F., Issenhuth, M., & Mermoud, C., (1999), Full text reading with a central scotoma: pseudo regressions and pseudo line losses, *Br. J. Ophthalmol.* *83* 12, 1341–1347, doi:10.1136/bjo.83.12.1341
- Safran, A. B. [Avinoam B.], Lupolover, Y., & Berney, J., (1984), Macular reflexes in optic atrophy, *Am. J. Ophthalmol.* *98* 4, 494–498, doi:10.1016/0002-9394(84)90138-7
- Sahel, J.-A., Marazova, K., & Audo, I., (2015), Clinical Characteristics and Current Therapies for Inherited Retinal Degenerations, *Cold Spring Harb. Perspect. Med.* *5* 2, a017111–a017111, doi:10.1101/cshperspect.a017111
- Santhouse, a. M., (2000), Visual hallucinatory syndromes and the anatomy of the visual brain, *Brain*, *123* 10, 2055–2064, doi:10.1093/brain/123.10.2055
- Saszik, S. & DeVries, S. H. [S. H.], (2012), A Mammalian Retinal Bipolar Cell Uses Both Graded Changes in Membrane Voltage and All-or-Nothing Na⁺ Spikes to Encode Light, *J. Neurosci.* *32* 1, 297–307, doi:10.1523/JNEUROSCI.2739-08.2012
- Schernhammer, E. S. [Eva S.], Laden, F., Speizer, F. E., Willett, W. C., Hunter, D. J., Kawachi, I., & Colditz, G. A., (2001), Rotating night shifts and risk of breast cancer in women participating in the nurses' health study, *J. Natl. Cancer Inst.* *93* 20, 1563–1568, doi:10.1093/jnci/93.20.1563
- Schernhammer, E. S. [Eva S], Speizer, F. E., Walter, C., Hunter, D. J., Fuchs, C. S., Colditz, G. a., . . . Colditz, G. a., (2003), Night-shift work and risk of colorectal cancer in the nurses' health study, *J Natl. Cancer Inst.* *95* 11, 825–828, doi:10.1093/jnci/95.11.825
- Schlosser, G. & Wagner, G. P. (Eds.). (2004), *Modularity in developpement and evolution*, The University of Chicago Press.
- Schmid, M. C., Schmiedt, J. T., Peters, A. J., Saunders, R. C., Maier, A., & Leopold, D. A., (2013), Motion-sensitive responses in visual area V4 in the absence of primary visual cortex., *J. Neurosci.* *33* 48, 18740–18745, doi:10.1523/JNEUROSCI.3923-13.2013
- Schmierer, K., Scaravilli, F., Altmann, D. R., Barker, G. J., & Miller, D. H., (2004), Magnetization transfer ratio and myelin in postmortem multiple sclerosis brain, *Ann. Neurol.* *56* 3, 407–415, doi:10.1002/ana.20202
- Schmolesky, M., (2007), The Primary Visual Cortex by Matthew Schmolesky, In H. Kolb, E. Fernandez, & R. Nelson (Eds.), *Webvision* (<http://webvision.med.utah.edu/book/part-ix-psychop>), Salt Lake City.

-
- Schoth, F., Burgel, U., Dorsch, R., Reinges, M. H. T., & Krings, T., (2006), Diffusion tensor imaging in acquired blind humans, *Neurosci. Lett.* *398* 3, 178–182, doi:10.1016/j.neulet.2005.12.088
- Schwab, I. R., (2012), *Evolutions's Witness*, New York: Oxford University Press.
- Sereno, M. I., Dale, a. M., Reppas, J. B., Kwong, K. K., Belliveau, J. W., Brady, T. J., ... Tootell, R. B., (1995), Borders of multiple visual areas in humans revealed by functional magnetic resonance imaging., *Science*, *268* 5212, 889–893.
- Sher, A. & DeVries, S. H. [Steven H], (2012), A non-canonical pathway for mammalian blue-green color vision, *Nat. Neurosci.* *15* 7, 952–953, doi:10.1038/nn.3127
- Shipp, S. & Zeki, S., (1989), The Organization of Connections between Areas V5 and V1 in Macaque Monkey Visual Cortex, *Eur. J. Neurosci.* *1* 4, 309–332, doi:10.1111/j.1460-9568.1989.tb00798.x
- Shu, N., Liu, Y., Li, J., Li, Y., Yu, C., & Jiang, T., (2009), Altered Anatomical Network in Early Blindness Revealed by Diffusion Tensor Tractography, *PLoS One*, *4* 9, e7228, doi:10.1371/journal.pone.0007228
- Singh, A. & Sørensen, T. L., (2012), The prevalence and clinical characteristics of Charles Bonnet Syndrome in Danish patients with neovascular age-related macular degeneration, *Acta Ophthalmol.* *90* 5, 476–480, doi:10.1111/j.1755-3768.2010.02051.x
- Sinke, C., Neufeld, J., Zedler, M., Emrich, H. M., Bleich, S., Münte, T. F., & Szycik, G. R., (2014), Reduced audiovisual integration in synesthesia - Evidence from bimodal speech perception, *J. Neuropsychol.* *81*, 94–106, doi:10.1111/jnp.12006
- Smallwood, P. M., Olveczky, B. P., Williams, G. L., Jacobs, G. H., Reese, B. E., Meister, M., & Nathans, J., (2003), Genetically engineered mice with an additional class of cone photoreceptors: implications for the evolution of color vision., *Proc. Natl. Acad. Sci. U. S. A.* *100* 20, 11706–11711, doi:10.1073/pnas.1934712100
- Smith, S. M. [Stephen M], Fox, P. T., Miller, K. L., Glahn, D. C., Fox, P. M., Mackay, C. E., ... Beckmann, C. F., (2009), Correspondence of the brain's functional architecture during activation and rest., *Proc. Natl. Acad. Sci. U. S. A.* *106* 31, 13040–13045, doi:10.1073/pnas.0905267106
- Smith, S. M. [Stephen M.], Miller, K. L., Salimi-Khorshidi, G., Webster, M., Beckmann, C. F., Nichols, T. E., ... Woolrich, M. W., (2011), Network modelling methods for FMRI., *Neuroimage*, *54* 2, 875–891, doi:10.1016/j.neuroimage.2010.08.063
- Sokunbi, M. O., Fung, W., Sawlani, V., Choppin, S., Linden, D. E. J., & Thome, J., (2013), Resting state fMRI entropy probes complexity of brain activity in adults with ADHD, *Psychiatry Res. - Neuroimaging*, *214* 3, 341–348, doi:10.1016/j.psychres.2013.10.001
- Soucy, E., Wang, Y., Nirenberg, S., Nathans, J., & Meister, M., (1998), A novel signaling pathway from rod photoreceptors to ganglion cells in mammalian retina, *Neuron*, *21* 3, 481–493, doi:10.1016/S0896-6273(00)80560-7

-
- Spreng, R. N., Stevens, W. D., Chamberlain, J. P., Gilmore, A. W., & Schacter, D. L., (2010), Default network activity, coupled with the frontoparietal control network, supports goal-directed cognition., *Neuroimage*, *53* 1, 303–317, doi:10.1016/j.neuroimage.2010.06.016
- Stargardt, K., (1909), Über familiäre, progressive degeneration in der maculagegend des auges., *Albr. von Graefes Arch Klin Ophthalmol.* *71* 71, 534–550.
- Steiper, M. E. & Seiffert, E. R., (2012), Evidence for a convergent slowdown in primate molecular rates and its implications for the timing of early primate evolution, *Proc. Natl. Acad. Sci.* *109* 16, 6006–6011, doi:10.1073/pnas.1119506109
- Straka, H., Fritzsche, B., & Glover, J. C., (2014), Connecting ears to eye muscles: Evolution of a 'Simple' reflex arc, *Brain. Behav. Evol.* *83* 2, 162–175, doi:10.1159/000357833
- Striem-Amit, E. & Amedi, A. [Amir], (2014), Visual cortex extrastriate body-selective area activation in congenitally blind people "Seeing" by using sounds, *Curr. Biol.* *24* 6, 687–692, doi:10.1016/j.cub.2014.02.010
- Striem-Amit, E., Dakwar, O., Reich, L., & Amedi, A., (2012), The large-scale organization of "visual" streams emerges without visual experience, *Cereb. Cortex*, *22* 7, 1698–1709, doi:10.1093/cercor/bhr253
- Striem-Amit, E., Ovidia-Caro, S., Caramazza, A., Margulies, D. S., Villringer, A., & Amedi, A., (2015), Functional connectivity of visual cortex in the blind follows retinotopic organization principles, *Brain*, *138* 6, 1679–1695, doi:10.1093/brain/awv083
- Suzuki, W., Saleem, K. S., & Tanaka, K., (2000), Divergent backward projections from the anterior part of the inferotemporal cortex (area TE) in the macaque, *J. Comp. Neurol.* *422* 2, 206–228, doi:10.1002/(SICI)1096-9861(20000626)422:2<206::AID-CNE5>3.0.CO;2-0
- Swaroop, A., Kim, D., & Forrest, D., (2010), Transcriptional regulation of photoreceptor development and homeostasis in the mammalian retina., *Nat. Rev. Neurosci.* *11* 8, 563–576, doi:10.1038/nrn2880
- Szentagothai, J., (1950), The elementary vestibulo-ocular reflex arc., *J. Neurophysiol.* *13* 6, 395–407.
- Szikra, T., Trenholm, S., Drinnenberg, A., Jüttner, J., Raics, Z., Farrow, K., . . . Roska, B., (2014), Rods in daylight act as relay cells for cone-driven horizontal cell-mediated surround inhibition., *Nat. Neurosci.* *17* 12, 1728–1735, doi:10.1038/nn.3852
- Tagliazucchi, E., von Wegner, F., Morzelewski, A., Brodbeck, V., & Laufs, H., (2012), Dynamic BOLD functional connectivity in humans and its electrophysiological correlates., *Front. Hum. Neurosci.* *6*, doi:10.3389/fnhum.2012.00339
- Tamietto, M. & Morrone, M. C., (2016), Visual Plasticity: Blindsight Bridges Anatomy and Function in the Visual System., *Curr. Biol.* *26* 2, R70–R73, doi:10.1016/j.cub.2015.11.026

-
- Tan, D. X., Manchester, L. C., Fuentes-Broto, L., Paredes, S. D., & Reiter, R. J., (2011), Significance and application of melatonin in the regulation of brown adipose tissue metabolism: Relation to human obesity, *Obes. Rev.* *12*3, 167–188, doi:10.1111/j.1467-789X.2010.00756.x
- Taylor, J. C., Wiggett, A. J., & Downing, P. E., (2007), Functional MRI analysis of body and body part representations in the extrastriate and fusiform body areas., *J. Neurophysiol.* *98*3, 1626–1633, doi:10.1152/jn.00012.2007
- Temme, L. A., Maino, J. H., & Noell, W. K., (1985), Eccentricity perception in the periphery of normal observers and those with retinitis pigmentosa., *Am. J. Optom. Physiol. Opt.* *62*11, 736–743, doi:10.1097/00006324-198511000-00003
- Terakita, A., (2005), Protein family review The opsins, *Genome Biol.* 1–9, doi:10.1186/gb-2005-6-3-213
- Thiebaut de Schotten, M., Urbanski, M., Batrancourt, B., Levy, R., Dubois, B., Cerliani, L., & Volle, E., (2016), Rostro-caudal Architecture of the Frontal Lobes in Humans, *Cereb. Cortex.* 1–15, doi:10.1093/cercor/bhw215
- Tomaszczyk, J. C., Green, N. L., Frasca, D., Colella, B., Turner, G. R., Christensen, B. K., & Green, R. E. A., (2014), Negative neuroplasticity in chronic traumatic brain injury and implications for neurorehabilitation., *Neuropsychol. Rev.* *24*4, 409–427, doi:10.1007/s11065-014-9273-6
- Troncoso, X., Macknik, S., & Martinez-Conde, S., (2011), Vision’s first steps: anatomy, physiology and perception in the retine, lateral geniculate nucleus and early visual cortical areas. In *Vis. prosthetics* (Springer, pp. 23–57), Boston.
- Tsukamoto, Y., Morigiwa, K., Ueda, M., & Sterling, P., (2001), Microcircuits for night vision in mouse retina., *J. Neurosci.* *21*21, 8616–8623.
- Turano, K. a., Gerguschat, D. R., Stahl, J. W., & Massof, R. W., (1999), Perceived visual ability for independent mobility in persons with retinitis pigmentosa, *Investig. Ophthalmol. Vis. Sci.* *40*5, 865–877.
- Turano, K. A., Massof, R. W., & Quigley, H. A., (2002), A self-assessment instrument designed for measuring independent mobility in RP patients: generalizability to glaucoma patients., *Invest. Ophthalmol. Vis. Sci.* *43*9, 2874–2881.
- Ungerleider, L. G. & Desimone, R., (1986), Projections to the superior temporal sulcus from the central and peripheral field representations of V1 and V2, *J. Comp. Neurol.* *248*2, 147–163, doi:10.1002/cne.902480202
- Van Dijk, K. R., Sabuncu, M. R., & Buckner, R. L., (2012), The influence of head motion on intrinsic functional connectivity MRI, *Neuroimage*, *59*1, 431–438, doi:10.1016/j.neuroimage.2011.07.044
- van Leeuwen, T. M., den Ouden, H. E. M., & Hagoort, P., (2011), Effective connectivity determines the nature of subjective experience in grapheme-color synesthesia., *J. Neurosci.* *31*27, 9879–9884, doi:10.1523/JNEUROSCI.0569-11.2011

-
- Vanduffel, W., (2002), Extracting 3D from Motion: Differences in Human and Monkey Intraparietal Cortex, *Science (80-.).* 298 5592, 413–415, doi:10.1126/science.1073574
- Vigh, B., Manzano, M. J., Zádori, A., Frank, C. L., Lukáts, A., Röhlich, P., . . . Dávid, C., (2002), Nonvisual photoreceptors of the deep brain, pineal organs and retina., *Histol. Histopathol.* 172, 555–90.
- Vigh, B. [Béla] & Vigh-Teichmann, I., (1998), Actual problems of the cerebrospinal fluid-contacting neurons, *Microsc. Res. Tech.* 41 1, 57–83, doi:10.1002/(SICI)1097-0029(19980401)41:1<57::AID-JEMT6>3.0.CO;2-R
- Vincent, J. L., Kahn, I., Snyder, A. Z., Raichle, M. E., & Buckner, R. L., (2008), Evidence for a Frontoparietal Control System Revealed by Intrinsic Functional Connectivity, *J. Neurophysiol.* 100 6, 3328–3342, doi:10.1152/jn.90355.2008
- Volgyi, B. [B.], (2004), Convergence and Segregation of the Multiple Rod Pathways in Mammalian Retina, *J. Neurosci.* 24 49, 11182–11192, doi:10.1523/JNEUROSCI.3096-04.2004
- Voogdt, J., Nieuwenhuys, R., van Dongen, P., & Ten Donkelaar, H., (1998), Mammals, In R. Nieuwenhuys, Ten Donkelaar HJ, & V. Nicholson (Eds.), *Cent. nerv. syst. vertebr.* (1st, pp. 1637–2097), Berlin: Springer Berlin Heidelberg.
- Voss, P., Gougoux, F., Lassonde, M., Zatorre, R. J., & Lepore, F., (2006), A positron emission tomography study during auditory localization by late-onset blind individuals., *Neuroreport*, 17 4, 383–388, doi:10.1097/01.wnr.0000204983.21748.2d
- Voss, P., Gougoux, F., Zatorre, R. J., Lassonde, M., & Lepore, F., (2008), Differential occipital responses in early- and late-blind individuals during a sound-source discrimination task, *Neuroimage*, 40 2, 746–758, doi:10.1016/j.neuroimage.2007.12.020
- Voss, P., Pike, B. G., & Zatorre, R. J., (2014), Evidence for both compensatory plastic and disuse atrophy-related neuroanatomical changes in the blind, *Brain*, 137 4, 1224–1240, doi:10.1093/brain/awu030
- Voss, P. & Zatorre, R. J., (2012), Occipital cortical thickness predicts performance on pitch and musical tasks in blind individuals, *Cereb. Cortex*, 22 11, 2455–2465, doi:10.1093/cercor/bhr311
- Wandell, B. a., Dumoulin, S. O., & Brewer, A. a., (2007), Visual field maps in human cortex., *Neuron*, 56 2, 366–383, doi:10.1016/j.neuron.2007.10.012
- Wang, D., Qin, W., Liu, Y., Zhang, Y., Jiang, T., & Yu, C., (2013), Altered White Matter Integrity in the Congenital and Late Blind People, *Neural Plast.* 2013 1, 1–8, doi:10.1155/2013/128236
- Wang, D., Qin, W., Liu, Y., Zhang, Y., Jiang, T., & Yu, C., (2014), Altered resting-state network connectivity in congenital blind., *Hum. Brain Mapp.* 35 6, 2573–2581, doi:10.1002/hbm.22350

-
- Wang, J., Zhou, T., Qiu, M., Du, A., Cai, K., Wang, Z., . . . Chen, L., (1999), Relationship between ventral stream for object vision and dorsal stream for spatial vision: An fMRI+ERP study, *Hum. Brain Mapp.* *84*, 170–181, doi:10.1002/(SICI)1097-0193(1999)8:4<170::AID-HBM2>3.0.CO;2-W
- Wang, K., Jiang, T., Yu, C., Tian, L., Li, J., Liu, Y., . . . Li, K., (2008), Spontaneous activity associated with primary visual cortex: A resting-state fMRI study, *Cereb. Cortex*, *183*, 697–704, doi:10.1093/cercor/bhm105
- Warner, C. E., Kwan, W. C., Wright, D., Johnston, L. A., Egan, G. F., & Bourne, J. A., (2015), Preservation of vision by the pulvinar following early-life primary visual cortex lesions, *Curr. Biol.* *254*, 424–434, doi:10.1016/j.cub.2014.12.028
- Wässle, H. & Boycott, B. B., (1991), Functional architecture of the mammalian retina., *Physiol. Rev.* *712*, 447–480.
- Wässle, H. [Heinz], (1999), No Title, *Nature*, *3976719*, 473–475, doi:10.1038/17216
- Wässle, H. [Heinz], (2004), Parallel processing in the mammalian retina, *Nat. Rev. Neurosci.* *510*, 747–757, doi:10.1038/nrn1497
- Weiner, K. S. & Grill-Spector, K., (2011), Not one extrastriate body area: Using anatomical landmarks, hMT+, and visual field maps to parcellate limb-selective activations in human lateral occipitotemporal cortex, *Neuroimage*, *564*, 2183–2199, doi:10.1016/j.neuroimage.2011.03.041
- Westheimer, G. & McKee, S. P., (1975), Visual acuity in the presence of retinal-image motion, *J. Opt. Soc. Am.* *657*, 847–850, doi:10.1364/JOSA.65.000847
- Westlye, L. T., Walhovd, K. B., Dale, A. M., Bjørnerud, A., Due-Tønnessen, P., Engvig, A., . . . Fjell, A. M., (2010), Differentiating maturational and aging-related changes of the cerebral cortex by use of thickness and signal intensity, *Neuroimage*, *521*, 172–185, doi:10.1016/j.neuroimage.2010.03.056
- Willstutter, R., (1906), Zur Kenntniss der Zusammensetzung des Chlorophylls, *Justus Liebigs Ann. Chem.* *3501-2*, 48–82.
- Wittich, W., Faubert, J., Watanabe, D. H., Kapusta, M. A., & Overbury, O., (2011), Spatial judgments in patients with retinitis pigmentosa, *Vision Res.* *511*, 165–173, doi:10.1016/j.visres.2010.11.003
- Wolburg, H., Liebner, S., Reichenbach, A., & Gerhardt, H., (1999), The pecten oculi of the chicken: a model system for vascular differentiation and barrier maturation, *Int. Rev. Cytol.* *187*, 111–159.
- y Cajal, S. R., (1893), La rétine des vertébrés, *Cellule*, *9*, 119–257.
- Yao, Y., Lu, W. L., Xu, B., Li, C. B., Lin, C. P., Waxman, D., & Feng, J. F., (2013), The increase of the functional entropy of the human brain with age., *Sci. Rep.* *32853*, doi:10.1038/srep02853

-
- Yokoyama, S., (1997), Molecular Genetic Basis of Adaptive Selection : Examples from Color Vision in Vertebrates, *Annu. Rev. Genet.* 31 1, 315–336, doi:10.1146/annurev.genet.31.1.315
- Yokoyama, S. & Yokoyama, R., (1996), Adaptive Evolution of Photoreceptors and Visual Pigments in Vertebrates, *Annu. Rev. Ecol. Syst.* 27 1, 543–567, doi:10.1146/annurev.ecolsys.27.1.543
- Yu, C., Liu, Y., Li, J., Zhou, Y., Wang, K., Tian, L., . . . Li, K., (2008), Altered functional connectivity of primary visual cortex in early blindness, *Hum. Brain Mapp.* 29 5, 533–543, doi:10.1002/hbm.20420
- Yu, L., Xie, B., Yin, X., Liang, M., Evans, A. C., Wang, J., & Dai, C., (2013), Reduced Cortical Thickness in Primary Open-Angle Glaucoma and Its Relationship to the Retinal Nerve Fiber Layer Thickness, *PLoS One*, 8 9, 1–7, doi:10.1371/journal.pone.0073208
- Yu, L., Yin, X., Dai, C., Liang, M., Wei, L., Li, C., . . . Wang, J., (2014), Morphologic changes in the anterior and posterior subregions of V1 and V2 and the V5/MT+ in patients with primary open-angle glaucoma, *Brain Res.* 1588, 135–143, doi:10.1016/j.brainres.2014.09.005
- Zeharia, N., Hertz, U., Flash, T., & Amedi, A., (2015), New Whole-Body Sensory-Motor Gradients Revealed Using Phase-Locked Analysis and Verified Using Multivoxel Pattern Analysis and Functional Connectivity, *J. Neurosci.* 35 7, 2845–2859, doi:10.1523/JNEUROSCI.4246-14.2015
- Zeki, S., (2003), The Processing of Kinetic Contours in the Brain, *Cereb. Cortex*, 13 2, 189–202, doi:10.1093/cercor/13.2.189
- Zeki, S. & fytche, D., (1998), The Riddoch syndrome: Insights into the neurobiology of conscious vision, *Brain*, 121 1, 25–45, doi:10.1093/brain/121.1.25
- Zhang, D., Snyder, A. Z., Fox, M. D., Sansbury, M. W., Shimony, J. S., & Raichle, M. E., (2008), Intrinsic Functional Relations Between Human Cerebral Cortex and Thalamus, *J. Neurophysiol.* 100 4, 1740–1748, doi:10.1152/jn.90463.2008
- Zhang, N. & Chen, W., (2006), A dynamic fMRI study of illusory double-flash effect on human visual cortex, *Exp. Brain Res.* 172 1, 57–66, doi:10.1007/s00221-005-0304-7
- Zilles K, A. K., (2010), Centenary of Brodmann’s map — conception and fate, *Nat. Rev. Neurosci.* 11 2, 139–145, doi:10.1038/nrn2776
- Zilles, K. & Amunts, K. [Katrin], (2015), Anatomical Basis for Functional Specialisation, In K. Uludag, K. Ugurbil, & L. Berliner (Eds.), *Fmri from nucl. spins to brain funct.* (pp. 27–66), New York: Springer.

PART VI

Annexes

*Annexe I: "Increased optic nerve
radiosensitivity following optic
neuritis"*

Nicolae Sanda, MD
Francoise Heran, MD
Nicolas Daly-Schweitzer,
MD, PhD
Jose-Alain Sahel, MD,
PhD
Avinoam Bezael Safran,
MD

INCREASED OPTIC NERVE RADIOSENSITIVITY FOLLOWING OPTIC NEURITIS

Radiation-induced optic neuropathy (RION) is a late complication of radiotherapy, resulting in severe visual loss.¹ We report a RION case following radiation therapy delivered at a dose widely considered as innocuous, occurring on a background of previous isolated optic neuritis. Increased brain sensitivity to radiation has been observed in patients with multiple sclerosis (MS),²⁻⁴ but we are not aware of previously reported cases solely involving the optic nerves (ONs). This aspect deserves consideration when defining therapeutic strategies.

Case report. A 69-year-old woman with medical history of bilateral sequential optic neuritis 22 and 12 years previously in the right eye (RE) and left eye (LE), respectively, presented with progressive bilateral visual loss. Her visual acuity (VA) before visual loss was 0.7 in the RE and 0.8 in the LE. MS diagnosis based on 2010 McDonald criteria was ruled out by clinical course and multiple MRIs. Two years before presentation, a left maxillary sinus cystic adenoid carcinoma was diagnosed ($T_{4a}N_0M_0$) and treated by surgery and external 6 MV fractionated radiotherapy. The right ON received an average dose of 19.9 Gy, while the left ON received an average dose of 5.3 Gy. Total dose per daily fraction was <0.2 Gy.

The patient noted progressive painless bilateral visual loss evolving over 4 months, starting 12 months after completion of the radiotherapy, and decided to consult. VA was 0.1 in the RE and 0.5 in the LE. Relative afferent pupillary defect and optic disc pallor were noted in the RE and a significant corticonuclear cataract in the LE. RE visual field was constricted and in addition showed a markedly reduced sensitivity in the central area. LE presented a diffuse reduction in sensitivity that was attributed to cataract (Humphrey perimetry mean deviation -3.34 dB $P < 2\%$, pattern SD 1.53 dB).

MRI performed to explore the anterior visual pathway showed T2 hyperintensity and postgadolinium T1 enhancement of the intracranial part of the right ON and of the right half of the chiasm (figure). In addition, nonspecific hyperintense T2 white matter lesions were noted. They were identical to those noted on successive MRI performed after the first episode of inflammatory optic neuropathy.

Careful analysis of the images ruled out local or distant recurrence of the maxillary tumor.

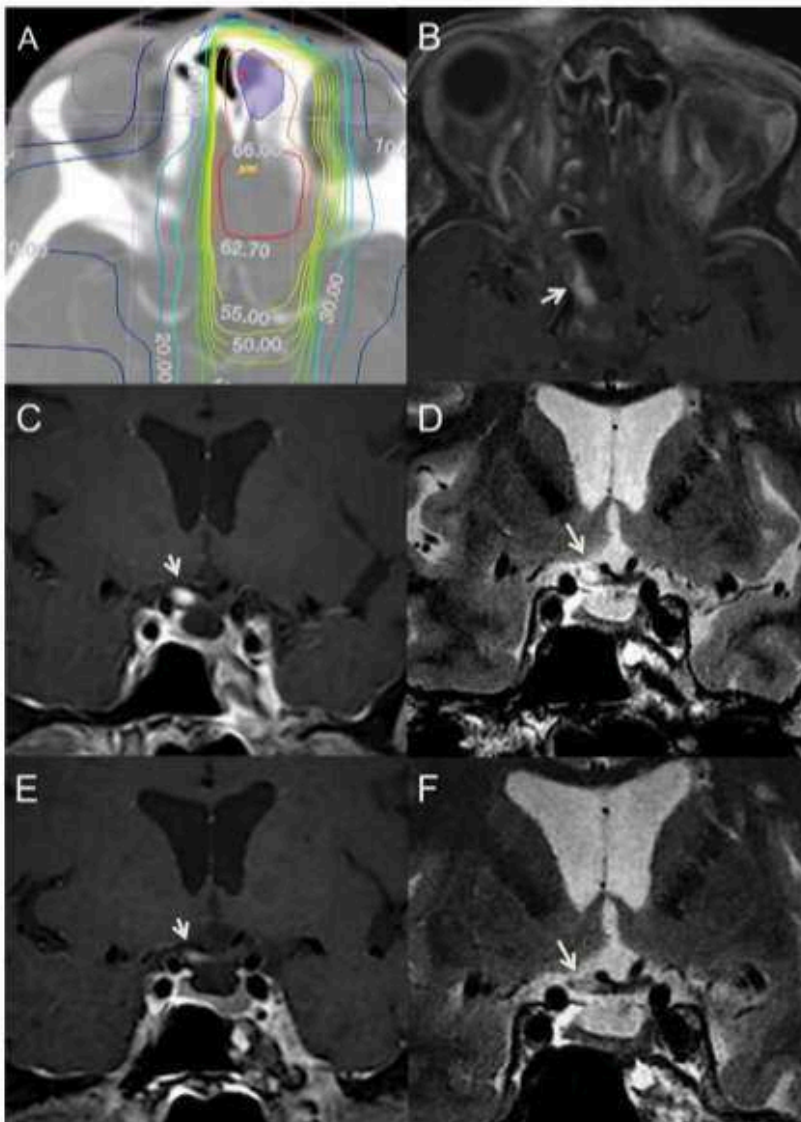
CSF showed no oligoclonal immunoglobulin G (IgG) bands, elevated IgG index, or carcinomatous cell. Erythrocyte sedimentation rate, C-reactive protein, angiotensin-converting enzyme, as well as whole-body scan were unremarkable. Except for LE phacoemulsification that was refused by the patient, attending physicians advised no treatment and attentive follow-up was organized. RE VA progressed to light perception over an 8-month period, while LE VA stabilized at 0.4.

Discussion. The vision loss in this case started 12 months after the radiotherapy and was produced by optic neuropathy in the RE and cataract in the LE. However, minimal optic neuropathy in the LE could not be excluded.

The lavish localized contrast enhancement of the intracranial part of the right ON was highly suggestive of RION. Infiltrative, inflammatory, and tumoral etiologies were considered, although no clinical findings favored such hypotheses. The severity of the visual loss, its irreversible course, the timing between the radiation exposure and symptom onset, and major and stable MRI enhancement strongly supported the diagnosis of RION. Applied radiation, however, was much below doses considered potentially neurotoxic. Total doses of 50–63 Gy are reportedly associated with a 5% risk of RION occurrence at 5 years, while doses less than 50 Gy are considered to encompass a negligible risk.^{1,4} Fraction doses higher than 1.8–2 Gy are also associated with increased risk.^{1,5} Nevertheless, low doses of radiation may affect cell-to-cell communication mechanisms or tissue-level homeostatic processes.⁶

It is probable that the unexpected radiosensitivity of the patient's ON was due to former episodes of optic neuritis, as several studies have demonstrated that patients with MS^{3,4} or compressive optic neuropathy^{1,7} show a lower threshold for radiation-induced neurotoxicity. It is conceivable that the damage of the ONs following demyelination was more extensive on the right than on the left ON, thus explaining the particular radiosensitivity of this structure. This suggestion is supported by the VA values, slightly worse in the RE than in the LE 3 months prior to radiation therapy. Data concerning the severity of visual impairment at the time of previous optic neuritis episodes were unavailable.

Figure Dose distribution plan and MRI



(A) Dose distribution plan: right optic nerve (ON) average dose 19.9 Gy (median 19.1 Gy, minimal 9.6 Gy, maximal 53.8 Gy for a 0.1 cm³ volume); left ON average dose 53 Gy (median 59.2 Gy, minimal 21.4 Gy, maximal 67.5 Gy for a 0.2 cm³ volume). Initial MRI (B, C, D): the intracranial right ON segment and the right half of the optic chiasm (arrows) show enlargement, lavish T1 gadolinium enhancement (B, C), and T2 hyperintensity. Follow-up MRI (E, F) 3 months later shows (arrows) atrophy of the right ON and the right part of the optic chiasm (E, F), reduced but persistent gadolinium enhancement (E), and moderate T2 hyperintensity (F). Strong initial gadolinium enhancement of an enlarged ON and its remote persistence (for months) coupled with subsequent optic atrophy are in the appropriate clinical context, highly suggestive of radiation-induced optic neuropathy.

Increased ON radiosensitivity following inflammatory disorders^{1,4} deserves a particular consideration and warrants more precise determination of radiation values potentially deleterious in such conditions.

From the Institut de la Vision/Université Pierre et Marie Curie (N.S., J.-A.S., A.B.S.); CHNO des Quinze-Vingts (N.S., J.-A.S., A.B.S.), Paris; Foch Hospital (N.S.), Suresnes; Fondation Ophtalmologique Adolphe de Rothschild (F.H.), Paris; Institut Gustave Roussy (N.D.-S.), Villejuif, France; and Geneva University School of Medicine (A.B.S.), Switzerland.

Author contributions: N. Sanda: drafting/revising the manuscript for content, including medical writing for content; study concept or design; acquisition, analysis or interpretation of data. F. Heran: drafting/revising the manuscript for content, including medical writing for content; analysis or interpretation of data. N. Daly-Schweitzer: analysis or interpretation of data. J.A. Sabat: drafting/revising the manuscript for content, including medical writing for content. A.B. Safran: critical revision of the manuscript for important intellectual content, study concept, acquisition and interpretation of data.

Study funding: No targeted funding reported.

Disclosure: The authors report no disclosures relevant to the manuscript. Go to Neurology.org for full disclosures.

Received August 7, 2013. Accepted in final form January 8, 2014.

Correspondence to Dr. Sanda: n.sanda@hopital-foch.org

© 2014 American Academy of Neurology

1. Danesh-Meyer HV. Radiation-induced optic neuropathy. *J Clin Neurosci* 2008;15:95–100.
2. Miller RC, Lachance DH, Lucchinetti CF, et al. Multiple sclerosis, brain radiotherapy, and risk of neurotoxicity: the Mayo Clinic experience. *Int J Radiat Oncol Biol Phys* 2006;66:1178–1186.
3. Peterson K, Rosenblum MK, Powers JM, Alvord E, Walker RW, Posner JB. Effect of brain irradiation on demyelinating lesions. *Neurology* 1993;43:2105–2112.
4. Daniels TB, Pollock BE, Miller RC, Lucchinetti CF, Leavitt JA, Brown PD. Radiation-induced optic neuritis after pituitary adenoma radiosurgery in a patient with multiple sclerosis: case report. *J Neurooncol* 2009;93:263–267.
5. Bhandare N, Monme AT, Morris CG, Bharti MT, Mendenhall WM. Does altered fractionation influence the risk of radiation-induced optic neuropathy? *Int J Radiat Oncol Biol Phys* 2005;62:1070–1077.
6. Brechignac F, Paquet F. Radiation-induced risks at low dose: moving beyond controversy towards a new vision. *Radiat Environ Biophys* 2013;52:299–301.
7. Siddiqui JD, Loeffler JS, Murphy MA. Radiation optic neuropathy after proton beam therapy for optic nerve sheath meningioma. *J Neuroophthalmol* 2013;33:165–168.

*Annexe II: "A neurological disorder
presumably underlies painter
Francis Bacon distorted world
depiction"*



A neurological disorder presumably underlies painter Francis Bacon distorted world depiction

Avinoam B. Safran^{1,2*}, Nicolae Sanda^{1,3} and José-Alain Sahel¹

¹ Sorbonne Universités, UPMC Univ Paris 06, UMR_S 968, Institut de la Vision, INSERM, U968, CNRS, UMR_7210, Paris, France

² Neurosciences, Geneva University School of Medicine, Geneva, Switzerland

³ Neurology Department, Hôpital Foch, Paris, France

*Correspondence: avinoam.safran@unige.ch

Edited by:

Baingio Pinna, University of Sassari, Italy

Reviewed by:

Claus-Christian Carbon, University of Bamberg, Germany

Simone Gori, University of Padua, Italy

Keywords: Francis bacon, illusions, central metamorphopsia, dysmorphopsia, vision, art, neurological disorder

A commentary on

The “Visual Shock” of Francis Bacon an essay in neuroesthetics

by Zeki, S., and Ishizu, T. (2013). *Front. Hum. Neurosci.* 7:850. doi: 10.3389/fnhum.2013.00850

We read with interest the remarkable paper by Zeki and Ishizu (2013), on Francis Bacon’s subverted representation of the body. On that occasion, we wish to share the results of an observation we recently made on Bacon’s depicted deformities (Safran et al., 2012, ARVO poster,) that led us to consider Bacon’s paintings to be the reflexion of a rare central perception disorder called dysmorphopsia (Kölmel, 1993) (see **Figure 1**). This conclusion was supported by Bacon’s own detailed description of a perceptual phenomenon of dynamic distortion, progressively changing in magnitude and pattern, which he consistently experienced upon steady fixation.

Bacon’s comments on his perceptual experience are found in published interviews (Russell, 1979; Sylvester, 1980; Clair et al., 1996; Peppiatt, 2008). In his discussions with renown art critic Jean Clair, Bacon reportedly stated: “When I am watching you talking—I don’t know what it is - I see a kind of image, which constantly changes: the movement of your mouth, of the head, somehow; it keeps changing all the time. I attempted to trap this thing in the portraits.” (Clair et al., 1996, p 29). Another distinguished critic, David Sylvester, further quoted him

as saying “[...] in my case, with this disruption all the time of the image—or distortion, or whatever you like to call it—it’s an elliptical way of coming to the appearance of that particular body... And it needs a sort of magic to coagulate color and form so that it gets the equivalent of appearance, the appearance that you see at any moment, because so-called appearance is only retrieved for one moment as that appearance. (Sylvester, 1980, pp. 116–117). Still according to Sylvester, Bacon also acknowledged “I’m just trying to make images as accurately off my nervous system as I can. I don’t even know what half of them mean” (Sylvester, 1980, p. 82).

Gross image distortion is a rare clinical manifestation of disordered higher visual function. It presents as episodes of dynamic, ever-changing deformities, a condition referred to as dysmorphopsia (Kölmel, 1993) or (central) metamorphopsia (ffytche and Howard, 1999). Usually, the image initially appears normal but undergoes illusionary transformation if looked at for any length of time. Visages appear distorted, contracted or expanded, often in a dynamic manner (Kölmel, 1993; ffitche and Howard, 1999); image may appear “cut up” and displaced (ffytche and Howard, 1999). It was associated with occipito-parietal (Trojano et al., 2009) and callosal (Cho et al., 2011) lesions. Dysmorphopsia might represent a variant of the “thin man phenomenon” (Safran et al., 1999), a perceptual distortion phenomenon occurring around focal field defects (Mavrakanas et al., 2009), as suggested by Ganssaugue et al. (2012).

Striking similarities to Bacon’s portraits are found in drawings produced by a patient with a parasagittal parieto-occipital meningioma, and right inferior homonymous defect (Mooney et al., 1965). This patient also experienced abnormal percepts featuring persons who demonstrated continuously changing distortions, similar to those described by Bacon. He stated the following: “[...] everything was always moving [...]. The girl would start normal enough but rapidly her lips would get coarser, her mouth more open and her teeth long and pointed. [...] men’s faces going through similar contortions, very red and shiny under a fishlike eye, the lower part of the lid dragged down, showing a very bloodshot white” (Mooney et al., 1965).

Dysmorphic percepts apparently occurred over virtually the whole duration of his painting activities. With one exception, all 131 Bacon portraits assembled in the volume by Kundera (1996) were produced between 1961 and 1989, and showed consistent abnormalities in face depiction. Similar deformities were noted in other paintings, created from 1959 up to 1991 (Peppiatt, 2008). Previously (1949–1957), Bacon depicted distorted faces where salient abnormalities repeatedly consisted of frightening wide open mouth and large, pointed teeth (Russell, 1979; Sylvester, 1980; Kundera, 1996). Remarkably that specific deformity is one of the commonest features reported individual suffering from dysmorphopsia (Mooney et al., 1965; ffitche and Howard, 1999). Over the years, deformities in



FIGURE 1 | Francis Bacon—Self-portrait 1971. Centre Georges Pompidou, Paris, France.
© The Estate of Francis Bacon/All rights reserved/ADAGP, Paris 2014.

Bacon's portraits increased in forms and roughness.

The origin of Bacon's visual percepts is unknown. Painter's creativity has been ascribed to catalyzing effects of psychological disturbances generated by unhappy childhood (Peppiatt, 2008; Zeki and Ishizu, 2013). It is conceivable that cerebral injury had been caused during his childhood by violent blows reportedly inflicted by his father (Peppiatt, 2008). Moreover, Bacon suffered from asthma (Falliers, 1996). Cerebral hypoxic-ischemic lesions could have occurred during asthmatic attacks, which were reported to be "so severe that Bacon would lie in bed for days, blue in the face, struggling for each breath" (Peppiatt, 2008, p. 11). In addition, since Bacon has been prescribed morphine and stramonium to ease his bronchial spasms (Peppiatt, 2008), toxic factors (Vella-Brincat and Macleod, 2007; Glatstein et al., 2012) might be considered, although unlikely as not associated with pronounced systemic manifestations; in addition, distorted percepts upon sustained fixation consistently occurred over decades (Sylvester, 1980).

Influence on Bacon by fellow artists has been suggested (Sylvester, 1980, Peppiatt, 2008). Bacon was impressed by Picasso's

fluidity of lines and inventiveness, which he discovered in 1927 at Rosenberg's Gallery. Bacon considered Picasso as the artist having come closer than anyone to "the core of what feeling is about" (Peppiatt, 2008, p. 46). Although most of works presented at Rosenberg's gallery were classical in style, and included no cubist compositions, it is conceivable that Bacon saw in some of the forms elaborated by Picasso a resemblance to his own perceptions, as also did other subjects affected by dysmorphopsia (Mooney et al., 1965; ffytche and Howard, 1999). He then felt that there was a way to transpose on canvas the reality—the very one reality that his senses presented him: "[...] I thought afterwards, well, perhaps I could draw as well" (Peppiatt, 2008, p. 46).

Bacon detailed description of distorted percepts point out the organic element in the grounds of his art. It might contribute to clarify Bacon's "enigma" (Peppiatt, 2008), and assist art analysts to revisit foundations of Bacon's major contribution to twentieth century painting. Furthermore, Bacon's observational and artistic talents provide us with invaluable insights into the perceptual phenomena of dysmorphopsia.

REFERENCES

- Cho, J. Y., Moon, S. Y., Hong, K. S., Cho, Y. J., Kim, S. C., Hwang, S. I., et al. (2011). Teaching neuroImages: unilateral prosopometamorphopsia as a dominant hemisphere-specific disconnection sign. *Neurology* 76, e110. doi: 10.1212/WNL.0b013e31821d74a0
- Clair, J., Eschapaspe, M., Malchus, P. (1996). "Entretien avec Jean Clair, 1971," in *Francis Bacon: Entretiens* (Paris: Ed. Carré), 25–40.
- ffytche, D. H., and Howard, R. J. (1999). The perceptual consequences of visual loss: 'positive' pathologies of vision. *Brain* 122, 1247–1260.
- Falliers, C. J. (1996). Asthma in the life of a modern british painter. Francis bacon (1909-1992). *J. Asthma* 33, 349–350.
- Ganssaugue, M., Papageorgiou, E., and Schiefer, U. (2012). Facial dysmorphopsia: a notable variant of the "thin man" phenomenon? *Graefes Arch. Clin. Exp. Ophthalmol.* 250, 1491–1497. doi: 10.1007/s00417-012-1958-z
- Glatstein, M. M., Alabdulrazzaq, F., Garcia-Bournissen, F., and Scolnik, D. (2012). Use of physostigmine for hallucinogenic plant poisoning in a teenager: case report and review of the literature. *Am. J. Ther.* 19, 384–388. doi: 10.1097/MJT.0b013e3181f0cbb4
- Kölmel, H. W. (1993). Visual illusions and hallucinations. *Baillieres Clin. Neurol.* 2, 243–264.
- Kundera, M. (1996). *Francis Bacon: Portraits et Autoportraits*. Paris: Les Belles Lettres.
- Mavrankanas, N. A., Dang-Burgener, N. P., Lorincz, E. N., Landis, T., and Safran, A. B. (2009). Perceptual distortion in homonymous paracentral scotomas. *J. Neuroophthalmol.* 29, 37–42. doi: 10.1097/WNO.0b013e318198ca37
- Mooney, A. J., Carey, P., Ryan, M., and Bofin, P. (1965). Parasagittal parieto-occipital meningioma. With visual hallucinations. *Am. J. Ophthalmol.* 59, 197–205.
- Peppiatt, M. (2008). *Francis Bacon Anatomy of an Enigma*. London: Constable & Robinson Ltd.
- Russell, J. (1979). *Francis Bacon*. 2nd Edn. London; New York, NY: Thames & Hudson.
- Safran, A. B., Achard, O., Duret, F., and Landis, T. (1999). The "thin man" phenomenon: a sign of cortical plasticity following inferior homonymous paracentral scotomas. *Br. J. Ophthalmol.* 83, 137–142.
- Safran, A. B., Sanda, N., and Sahel, J. A. (2012). Francis Bacon's distorted representation of faces presumably reflects occipital dysfunction. *Invest. Ophthalmol. Vis. Sci.* 53, E-Abstract 4846.
- Sylvester, D. (1980). *Interviews with Francis Bacon*. London: Thames & Hudson Ltd.
- Trojano, L., Conson, M., Salzano, S., Manzo, V., and Grossi, D. (2009). Unilateral left prosopometamorphopsia: a neuropsychological case study. *Neuropsychology* 47, 942–948. doi: 10.1016/j.neuropsychologia.2008.12.015
- Vella-Brincat, J., and Macleod, A. D. (2007). Adverse effects of opioids on the central nervous systems of palliative care patients. *J. Pain Palliat. Care Pharmacother.* 21, 15–25. doi: 10.1080/J354v21n01_05

Zeki, S., and Ishizu, T. (2013). The “Visual Shock” of Francis Bacon: an essay in neuroesthetics. *Front. Hum. Neurosci.* 7:850. doi: 10.3389/fnhum.2013.00850

Conflict of Interest Statement: The authors declare that the research was conducted in the absence of any commercial or financial relationships that could be construed as a potential conflict of interest.

Received: 01 April 2014; accepted: 14 July 2014; published online: 29 August 2014.

Citation: Safran AB, Sanda N and Sahel J-A (2014) A neurological disorder presumably underlies painter Francis Bacon distorted world depiction. Front. Hum. Neurosci. 8:581. doi: 10.3389/fnhum.2014.00581

This article was submitted to the journal Frontiers in Human Neuroscience.

Copyright © 2014 Safran, Sanda and Sahel. This is an open-access article distributed under the terms of the Creative Commons Attribution License (CC BY). The use, distribution or reproduction in other forums is permitted, provided the original author(s) or licensor are credited and that the original publication in this journal is cited, in accordance with accepted academic practice. No use, distribution or reproduction is permitted which does not comply with these terms.

Annexe III: "Importance of eye position on spatial localization in blind subjects wearing an Argus II retinal prosthesis"

Importance of Eye Position on Spatial Localization in Blind Subjects Wearing an Argus II Retinal Prosthesis

Norman Sabbah,¹⁻⁴ Colas N. Authié,¹⁻⁴ Nicolae Sanda,¹⁻⁴ Saddek Mohand-Said,¹⁻⁴ José-Alain Sahel,¹⁻⁶ and Avinoam B. Safran^{1-4,7}

¹Sorbonne Universités, UPMC Université Paris 06, UMR S968, Institut de la Vision, Paris, France

²INSERM, U968, Institut de la Vision, Paris, France

³CNRS, UMR 7210, Institut de la Vision, Paris, France

⁴Centre Hospitalier National d'Ophthalmologie des Quinze-Vingts, INSERM-DHOS CIC 1423, Paris, France

⁵Institute of Ophthalmology, University College of London, United Kingdom

⁶Fondation Ophthalmologique Adolphe de Rothschild, Paris, France

⁷Department of Clinical Neurosciences, Geneva University School of Medicine, Geneva, Switzerland

Correspondence: Avinoam B. Safran, Institut de la Vision, Unité Mixte de Recherche S 968, Paris, France; avinoam.safran@unige.ch.

Submitted: August 6, 2014

Accepted: November 4, 2014

Citation: Sabbah N, Authié CN, Sanda N, Mohand-Said S, Sahel J-A, Safran AB. Importance of eye position on spatial localization in blind subjects wearing an Argus II retinal prosthesis. *Invest Ophthalmol Vis Sci.* 2014;55:8259-8266. DOI:10.1167/iov.14-15392

PURPOSE. With a retinal prosthesis connected to a head-mounted camera (camera-connected prosthesis [CC-P]), subjects explore the visual environment through head-scanning movements. As eye and camera misalignment might alter the spatial localization of images generated by the device, we investigated if such misalignment occurs in blind subjects wearing a CC-P and whether it impacts spatial localization, even years after the implantation.

METHODS. We studied three subjects blinded by retinitis pigmentosa, fitted with a CC-P (Argus II) 4 years earlier. Eye/head movements were video recorded as subjects tried to localize a visual target. Pointing coordinates were collected as subjects were requested to orient their gaze toward predetermined directions, and to point their finger to the corresponding perceived spot locations on a touch screen. Finally, subjects were asked to give a history of their everyday behavior while performing visually controlled grasping tasks.

RESULTS. Misaligned head and gaze directions occurred in all subjects during free visual search. Pointing coordinates were collected in two subjects and showed that median pointing directions shifted toward gaze direction. Reportedly all subjects were unable to accurately determine their eye position, and they developed adapted strategies to perform visually directed movements.

CONCLUSIONS. Eye position affected perceptual localization of images generated by the Argus II prosthesis, and consequently visuomotor coordination, even 4 years following implantation. Affected individuals developed strategies for visually guided movements to attenuate the impact of eye and head misalignment. Our observations provide indications for rehabilitation procedures and for the design of upcoming retinal prostheses. (ClinicalTrials.gov number: NCT00407602.)

Keywords: retinal prostheses, eye movements, spatial localization

Retinitis pigmentosa (RP) is a potentially blinding degenerative disease of the retina. The condition results in the destruction of photoreceptors, but characteristically spares other retinal neurons.¹

Various biologic and bioelectronic approaches have been proposed to restore some vision in individuals blinded by RP.^{2,5} Particular interest has been generated by the development of retinal prostheses.⁴ These devices are designed to electrically stimulate preserved cells in the inner retina and thus to produce a neural signal that is eventually conveyed by optic nerves to the brain, where visual percepts are generated.⁵

Clinical trials with retinal prostheses have brought promising results.⁶ Subjects fitted with such systems can identify windows and doors; some of them are able to count fingers and even to read short sentences presented on a computer screen.⁶⁻⁸ Moreover, retinal prostheses provide invaluable

visual information to perform visually directed movements, such as following a layout on the ground or seizing objects.⁹⁻¹¹

According to their underlying technology, retinal prostheses can be categorized into two general groups. One comprises devices consisting of a photodiode array placed close to the retina,^{1,2} receiving and converting light into electrical impulses. The other comprises systems including a microcamera fitted to a glass frame,⁶ which records pixelated visual information that is eventually converted into an electronic signal; this is then sent to a microelectrode implant fixed onto the retina. With both techniques, the produced electrical signals stimulate preserved retinal cells (essentially retinal bipolar and ganglion cells), which start processing the signal and forward it along anterior visual pathways to the brain, where visual percepts are generated.⁵

Over currently available photovoltaic-based systems, camera-connected devices demonstrate the benefits of providing

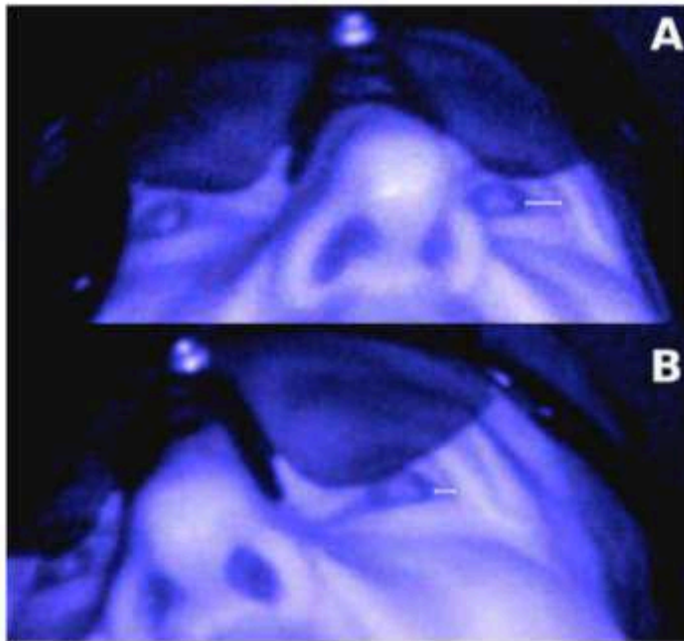


FIGURE 1. Subject 1. Vestibulo-ocular reflex observed during search head movements. (A) Before head rotation, eyes are oriented rightward; (B) following head rotation to the right, gaze remains stable in space. Note that, in the left eye, distance (*ubite line*) between the limbus and temporal canthus is reduced in (B) compared with (A).

For data analysis, pointed locations were grouped according to associated gaze directions. A Mann-Whitney test with Bonferroni correction for multiple comparisons was applied between each pointing group for values measured along horizontal and vertical axes, respectively.

Subject’s Appreciation of His Visual Localization Abilities, and Perceived Gaze Position

The tested subject was asked to describe the strategy used in everyday life for localizing and then seizing an object, using the information provided by the implant, and to indicate whether he perceived his gaze orientation.

RESULTS

Subject 1

Misalignment of Head and Gaze Directions During Visual Search. Camera recordings demonstrated that during visual search in the head-free condition, contraversive eye movements (i.e., vestibulo-ocular reflex [VOR]) occurred upon head rotations (Fig. 1). Moreover, it was observed that finger

pointing was occasionally performed while the CC-P-fitted eye and camera were misaligned.

Effect of Gaze Orientation on Target Localization.

When subject 1 was for the first time requested to shift gaze toward a determined direction while keeping head stable, he was unable to carry out the task, and instead turned both eyes and head in a conjugate manner. After several attempts, however, he succeeded in volitionally dissociating gaze and head directions and performing the task. Subject 1 performed the requested finger pointing within the limits of the screen.

Median pointing directions were shifted toward the gaze direction (Mann-Whitney tests $P < 0.01$, see Table 1 and Fig. 2). Thus, with left gaze, pointing coordinates were significantly shifted to the left of the center. Conversely, with right gaze, pointing coordinates were significantly shifted to the right. With up and down gaze, locations were respectively significantly shifted upward and downward of the center.

Independently of this effect of gaze direction, it appeared that the pointing locations of grouped right, center, and left gaze conditions were significantly shifted downward (when compared to the central target position, Mann-Whitney tests $U = 23, n = 30, P < 0.01$). Also, the pointing locations of grouped up, center, and down conditions were significantly shifted rightward (Mann-Whitney tests $U = 462, n = 30, P < 0.01$, see Fig. 2).

Subject’s Appreciation of His Visual Localization Abilities, and Perceived Gaze Position.

Subject 1 reported that in everyday life, to accurately localize and then seize an object using the implant image, he first attempted to get the target image in the viewing field, then performed successive small head movements, either horizontally or vertically. If he had not accomplished these preliminary oscillatory head movements, he reportedly failed to grasp the object. Moreover, the subject indicated that he only roughly perceived where his gaze was directed.

Subject 2

Misalignment of Head and Gaze Directions During Visual Search. Camera recordings showed that during head-free visual search, head rotations induced reflexive contraversive eye movements (Fig. 3; Supplementary Video S1). Moreover, misaligned head and gaze directions were also observed when the subject detected and intended to point to the target on the screen (Fig. 4; Supplementary Video S2).

Effect of Gaze Orientation on Target Localization.

From the start, subject 2 was able to direct his gaze toward the directions indicated by the examiner. He performed the requested finger-pointing task within the limits of the screen.

In 7 out of 50 trials, subject 2 did not press firmly enough on the screen when indicating the perceived location, and the corresponding results could not be recorded and taken into account.

Median pointing directions were shifted toward the gaze direction (Mann-Whitney tests $P < 0.01$, see Table 2 and Fig.

TABLE 1. Subject 1: Finger-Pointing Coordinates Grouped by Gaze Direction Compared to Those Obtained With Gaze Directed to the Center

Pointing Coordinates	Condition 1	Condition 2	Statistics
Horizontal	Right gaze	Gaze to the center	$U = 99, n1 = n2 = 10, P = 0.0002$
	Left gaze	Gaze to the center	$U = 100, n1 = n2 = 10, P = 0.0001$
Vertical	Up gaze	Gaze to the center	$U = 100, n1 = n2 = 10, P = 0.0018$
	Down gaze	Gaze to the center	$U = 100, n1 = n2 = 10, P = 0.0001$

Values recorded along the horizontal axis and those recorded along the vertical are considered independently. *U*, Mann-Whitney values; *n1*, first condition sample size; *n2*, second condition sample size; *P*, statistical significance.

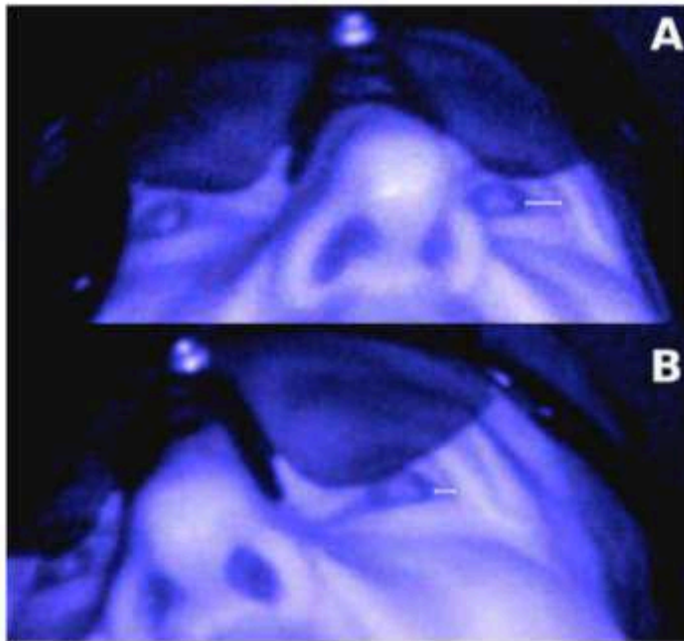


FIGURE 1. Subject 1. Vestibulo-ocular reflex observed during search head movements. (A) Before head rotation, eyes are oriented rightward; (B) following head rotation to the right, gaze remains stable in space. Note that, in the left eye, distance (*ubite line*) between the limbus and temporal canthus is reduced in (B) compared with (A).

For data analysis, pointed locations were grouped according to associated gaze directions. A Mann-Whitney test with Bonferroni correction for multiple comparisons was applied between each pointing group for values measured along horizontal and vertical axes, respectively.

Subject’s Appreciation of His Visual Localization Abilities, and Perceived Gaze Position

The tested subject was asked to describe the strategy used in everyday life for localizing and then seizing an object, using the information provided by the implant, and to indicate whether he perceived his gaze orientation.

RESULTS

Subject 1

Misalignment of Head and Gaze Directions During Visual Search. Camera recordings demonstrated that during visual search in the head-free condition, contraversive eye movements (i.e., vestibulo-ocular reflex [VOR]) occurred upon head rotations (Fig. 1). Moreover, it was observed that finger

pointing was occasionally performed while the CC-P-fitted eye and camera were misaligned.

Effect of Gaze Orientation on Target Localization.

When subject 1 was for the first time requested to shift gaze toward a determined direction while keeping head stable, he was unable to carry out the task, and instead turned both eyes and head in a conjugate manner. After several attempts, however, he succeeded in volitionally dissociating gaze and head directions and performing the task. Subject 1 performed the requested finger pointing within the limits of the screen.

Median pointing directions were shifted toward the gaze direction (Mann-Whitney tests $P < 0.01$, see Table 1 and Fig. 2). Thus, with left gaze, pointing coordinates were significantly shifted to the left of the center. Conversely, with right gaze, pointing coordinates were significantly shifted to the right. With up and down gaze, locations were respectively significantly shifted upward and downward of the center.

Independently of this effect of gaze direction, it appeared that the pointing locations of grouped right, center, and left gaze conditions were significantly shifted downward (when compared to the central target position, Mann-Whitney tests $U = 23, n = 30, P < 0.01$). Also, the pointing locations of grouped up, center, and down conditions were significantly shifted rightward (Mann-Whitney tests $U = 462, n = 30, P < 0.01$, see Fig. 2).

Subject’s Appreciation of His Visual Localization Abilities, and Perceived Gaze Position.

Subject 1 reported that in everyday life, to accurately localize and then seize an object using the implant image, he first attempted to get the target image in the viewing field, then performed successive small head movements, either horizontally or vertically. If he had not accomplished these preliminary oscillatory head movements, he reportedly failed to grasp the object. Moreover, the subject indicated that he only roughly perceived where his gaze was directed.

Subject 2

Misalignment of Head and Gaze Directions During Visual Search. Camera recordings showed that during head-free visual search, head rotations induced reflexive contraversive eye movements (Fig. 3; Supplementary Video S1). Moreover, misaligned head and gaze directions were also observed when the subject detected and intended to point to the target on the screen (Fig. 4; Supplementary Video S2).

Effect of Gaze Orientation on Target Localization.

From the start, subject 2 was able to direct his gaze toward the directions indicated by the examiner. He performed the requested finger-pointing task within the limits of the screen.

In 7 out of 50 trials, subject 2 did not press firmly enough on the screen when indicating the perceived location, and the corresponding results could not be recorded and taken into account.

Median pointing directions were shifted toward the gaze direction (Mann-Whitney tests $P < 0.01$, see Table 2 and Fig.

TABLE 1. Subject 1: Finger-Pointing Coordinates Grouped by Gaze Direction Compared to Those Obtained With Gaze Directed to the Center

Pointing Coordinates	Condition 1	Condition 2	Statistics
Horizontal	Right gaze	Gaze to the center	$U = 99, n1 = n2 = 10, P = 0.0002$
	Left gaze	Gaze to the center	$U = 100, n1 = n2 = 10, P = 0.0001$
Vertical	Up gaze	Gaze to the center	$U = 100, n1 = n2 = 10, P = 0.0018$
	Down gaze	Gaze to the center	$U = 100, n1 = n2 = 10, P = 0.0001$

Values recorded along the horizontal axis and those recorded along the vertical are considered independently. *U*, Mann-Whitney values; *n1*, first condition sample size; *n2*, second condition sample size; *P*, statistical significance.

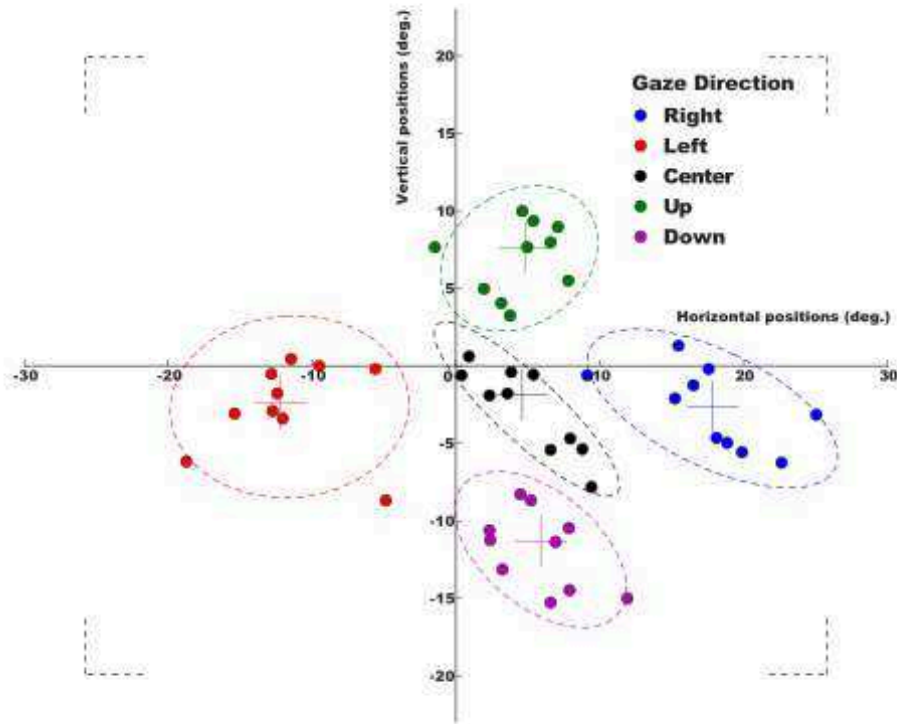


FIGURE 2. Subject 1. Coordinates of pointing locations, colored according to gaze directions. Colored crosses indicate respective median pointing positions for each tested gaze direction, and dashed ellipses indicate confidence intervals (2 SD). Dotted corners show the limits of the screen.

5), except for the down gaze condition. Thus, along the horizontal axis, as with subject 1, left gaze pointing coordinates were significantly shifted to the left, and right gaze pointing locations were significantly shifted to the right of the center. However, along the vertical axis, the pointing location was not affected for the down gaze condition.

Independently of this effect of gaze direction, it appeared that the pointing locations of grouped right, center, and left gaze conditions were significantly shifted downward (when compared to the central target position, Mann-Whitney tests $U = 400, n = 31, P < 0.01$). In addition, the pointing locations of grouped up, center, and down conditions were significantly shifted rightward (Mann-Whitney tests $U = 258, n = 23, P < 0.01$, see Fig. 5).

Subject's Appreciation of His Visual Localization Abilities, and Perceived Gaze Position. In everyday life, in order to localize an object using the implant-generated image and to then seize that item, subject 2 reportedly first searched the target through rather ample head scans. Then, when the target had been perceived, he performed smaller horizontal head movements to more precisely pinpoint target location. The subject added that he proceeded this way because if he directed his hand as soon as he perceived the object, he would consistently fail to reach it.

He further indicated that he did not perceive accurately where his eyes were directed, except when he drove his eyes



FIGURE 3. Subject 2. Vestibulo-ocular reflex observed following search head movements. (A) Before head rotation, both head and eyes are oriented forward; (B) after head rotation to the left, gaze remains directed forward, being stabilized in space by VOR. Note that, in the right eye, distance (white line) between the limbus and temporal canthus is reduced in (B) compared with (A) (see Supplementary Video S1).



FIGURE 4. Subject 2. Misaligned head and right (CC-P fitted, viewing) eye directions at the time the subject just detected and was intending to point to the target on the screen (see Supplementary Video S2).

TABLE 2. Subject 2: Finger-Pointing Coordinates Grouped by Gaze Direction Compared to Those Obtained With Gaze Directed to the Center

Pointing Coordinates	Condition 1	Condition 2	Statistics
Horizontal	Right gaze	Gaze to the center	$U = 100, n1 = n2 = 10, P = 0.0012$
	Left gaze	Gaze to the center	$U = 99, n1 = n2 = 10, P = 0.0024$
Vertical	Up gaze	Gaze to the center	$U = 100, n1 = 8, n2 = 10, P = 0.0005$
	Down gaze	Gaze to the center	$U = 42, n1 = 5, n2 = 10, P = 0.3996$

Values recorded along the horizontal axis and those recorded along the vertical axis are considered independently. *U*, Mann-Whitney values; *n1*, first condition sample size; *n2*, second condition sample size; *P*, statistical significance.

to a very eccentric position, as he then experienced a feeling of intraorbital tension.

Subject 3

Misalignment of Head and Gaze Directions During Visual Search. During search head movements, subject 3 showed VOR contraversive ocular movements (Fig. 6; Supplementary Video S3). Moreover, video recording demonstrated the occurrence of camera and eye misalignment at the time the subject detected the stimulus and was about to reach it (Fig. 7; Supplementary Video S4).

Effect of Gaze Orientation on Target Localization. Subject 3 was unable to carry out the requested tasks. During both training and evaluation phases, he was incapable of volitionally dissociating eye and head orientations in a dependable manner. Very rarely, he did succeed in shifting only his eyes laterally, but then his gaze swiftly drifted back to the primary position before he was able to point to the perceived target.

Subject's Appreciation of His Own Visual Localization Abilities, and Perceived Gaze Position. Subject 3 was unable to describe any strategy used in his everyday life to reliably reach an object perceived with his prosthetic device. He added that he could not perceive the position of his eyes.

DISCUSSION

Our results demonstrated that in two of the three subjects fitted with a camera-connected retinal prosthesis, (1) periods of head and gaze misalignment occurred during head-free visual search; (2) the perceptual location of the image was affected by gaze position and, consequently, the conflict between head (i.e., camera) and gaze information affected visuomotor coordination even 4 years after implantation; and (3) adaptive strategies were developed to partly overcome that inconvenience. The third subject (subject 3) was unable to consistently perform some requested tasks and therefore could not be adequately investigated.

Impact of gaze direction on visual localization has been investigated in healthy individuals. Gauthier and colleagues^{14,15} showed that occluding one eye and then deviating that eye induced a hand-pointing error to a visual target seen by the uncovered eye. They noted that the perceived target location was shifted in the direction to which the manipulated eye was deviated. The same authors later obtained similar results by rotating instead of deviating the eye.¹⁶ They suggested that proprioceptors in the deviated eye muscles were responsible for location misjudgment.^{14,16} Goodwin and colleagues²⁰ produced an illusion of visual target movement by vibrating extraocular muscles in a sighted individual; and again the phenomenon was ascribed to the activation of proprioceptive

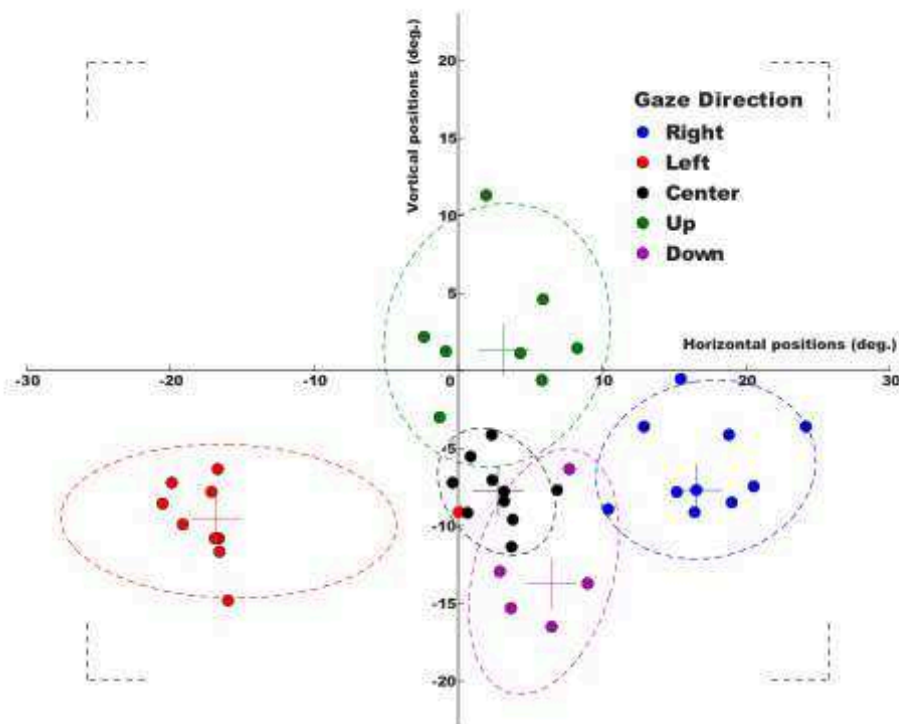


FIGURE 5. Subject 2. Coordinates of pointing locations, colored according to gaze directions. Colored crosses indicate respective median pointing positions for each tested gaze direction, and dashed ellipses indicate confidence intervals (2 SD). Dotted corners show the limits of the screen.

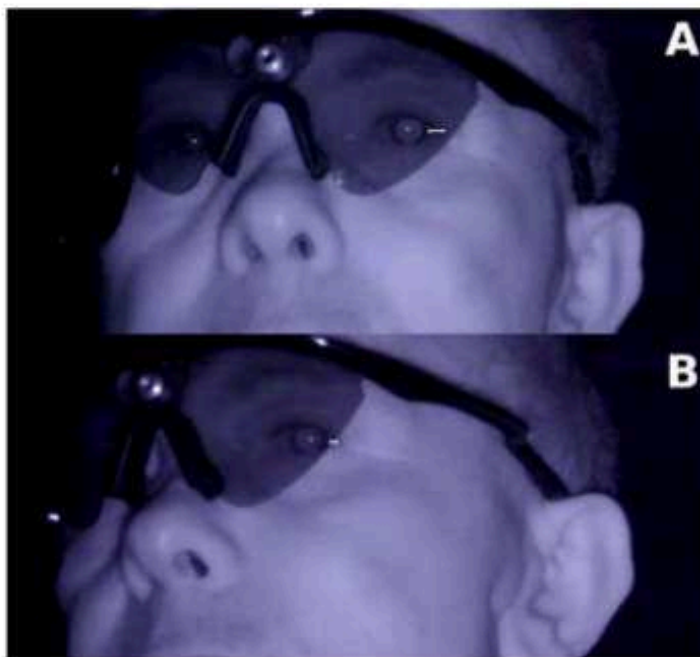


FIGURE 6. Subject 3. Vestibulo-ocular reflex observed following search head movements. (A) Before head rotation. (B) After head rotation to the right, eyes perform a contraversive leftward movement, as shown by the fact that in the left eye, distance (white line) between the limbus and temporal canthus is reduced in (B) compared with (A). Note, however, that VOR gain is less than 1, as in (B), corneal light reflex is slightly shifted to the right compared with (A). Gaze does not exhibit a noteworthy shift when compared to the magnitude of head rotation (see Supplementary Video S3).

receptors, leading the individual to misjudge target location. Similar localization errors have been observed in clinical conditions. Lewis and Zee²¹ reported altered visuospatial perception in a patient with trigeminal-oculomotor synkinesis trying to point to visual targets, a phenomenon also attributed to proprioceptive disturbances.

An additional mechanism known as efference copy, which takes into account the message generated by the cerebral command to modify gaze direction, is also considered to contribute to perceptual integration of gaze direction, hence to perceptual localization of the image.^{22,23}

We therefore assume that in our testing procedure, when asking tested subjects to shift gaze, both proprioceptive information and efference copy contributed to perceived gaze direction and hence to visual localization process.

During head-free visual search, we distinctly observed periods of camera and gaze misalignment (Figs. 1, 3, 4, 6, 7; Supplementary Videos S1–S4). At least some of them appeared to be generated by VOR upon head/camera scans. In healthy subjects, VOR is intended to stabilize gaze in space during head rotations, and consequently to stabilize the visual percept of the environment. In spite of its apparent uselessness when visual function is lost, VOR still occurs in individuals with late-acquired blindness, although VOR gain is then reduced as compared to the gain in sighted subjects.²⁴ The importance of vestibular function in the process of visuospatial localization is well illustrated by the occurrence, in vestibular disorders, of illusory oscillatory movements of the image (so-called oscillopsia) related to changes of eye position in space.²⁵

It was therefore expected that VOR would be observed in our subjects and was conceivable that occurrence of such eye movements could impact visual localization. Obviously, it would be interesting to measure the effects of such reflexive ocular movements on spatial localization. However, quantify-



FIGURE 7. Subject 3. Camera and right (CC-P fitted) eye are misaligned at the time the subject detected the stimulus and was about to reach it (see Supplementary Video S4).

ing VOR and correlating eye deviation with the degree of bias in spatial perception was not feasible in our study as a result of limitations in available eye-tracking systems. Infrared eye trackers require a calibration procedure that cannot be properly performed in blind individuals,²⁶ and the use of magnetic search coils is not acceptable in subjects wearing a retinal prosthesis, as the conjunctiva of affected individuals is vulnerable.⁶ We therefore decided to video record eye and head movements. This procedure demonstrated that ocular/camera misalignment periods obviously occurred during both target search and finger-pointing preparation, and has shed some light on the nature of the oculomotor mechanisms involved. However, due to the irregularity of head movements and occasional periods of eye masking, for example, by blinks, video recordings did not enable us to determine the proportion of time when misalignment was obvious.

Subjects' reports on strategies used when searching an object using the CC-P and eventually attempting to seize it were most informative with regard to the presumed effect of contraversive eye movements following head rotation. Indeed, both subjects 1 and 2 indicated that their grasping attempts were consistently misdirected if performed as soon as the object was detected. In such a condition, before taking hold of the seen object, they would perform several back and forth head turns, regressive in amplitude, before attempting to seize the item.

We therefore believe that in our subjects, ocular rotation—opposite to the search head movement by dissociating eye and head (i.e., camera) directions—provoked a misestimation of the image position. Subsequent regressive back and forth head turns presumably contributed to bringing gaze closer to its primary position, aligned with the camera direction, thus providing more accurate information on the image position in space. It is, however, also conceivable that these to-and-fro head movements were conducted also to optimize delineation of the image perceived in the seeing window offered by the retinal implant,²⁷ as well as to refresh the visual percept generated by the prosthesis, which often swiftly fades upon stable fixation.²⁸

Noteworthy observations were additionally made when subjects were first requested to shift gaze to a prescribed direction while keeping their heads stable.

The cause of the slight global downward and rightward bias observed in our patients is speculative. To optimize perceptual spatial localization of the information provided by the prosthesis, following implantation surgery the patients underwent a rehabilitation procedure consisting of the following two phases. First, a computerized processing developed by the

manufacturer (Second Sight Medical Products) allowed aligning the center of the field of view of the camera with the field of view processed by the retinal prosthesis. Second, the patients were trained to keep their gaze in primary position and perform pointing tasks to random visual targets recorded by the head-mounted camera, being informed after each trial by auditory feedback on errors observed. They thus progressively improved accuracy in their visuomotor coordination. The global bias observed in the pointing task conducted in our study possibly reflected a slightly shifted system positioning (e.g., retinal prosthesis position in the retina, camera settings) or a trend of patient's resting gaze position to shift in such conditions. However, importantly, this slight global shift does not question the significance of our observations regarding the effect of gaze/camera misalignment on spatial localization.

Two of the tested subjects (subjects 1 and 3) were found to be initially incapable of complying with the request, and instead turned both eyes and head toward the indicated direction. After several attempts, however, they both eventually succeeded in voluntarily dissociating gaze and head directions. In contrast, the third individual (subject 2) showed no apparent difficulty in performing, from the start, the requested isolated ocular movement. It is conceivable that the reinforced coupling of eye and head positions expressed, on the one hand, in subjects 1 and 3 by the relative difficulty of voluntarily dissociating them and, on the other hand, in subjects 1 and 2 by to-and-fro regressive head turns following visual search, might represent adaptive processes in the motor control, preventing the occurrence of erroneous image localization. While the former would contribute to preventing the dissociation of eye and head directions, the latter would help in realigning them when dissociated.

Since implantation was performed 4 years prior to our study, subjects were repeatedly advised to keep their gaze straight ahead, thus avoid dissociating eye and head movements, which was presumed to generate distorted spatial orientation. That training might have contributed to the development of the adaptive process observed here, although our findings showed that the individuals investigated were unable to indicate their eye position, or at best only roughly, and consequently to precisely control gaze direction. The lack of gaze direction control could be another argument to explain the dissociation of gaze and head positions when subjects were about to detect and reach a target during visual search. Moreover, these subjects demonstrated VOR, dissociating eye and head positions in an uncontrolled manner. These findings show the limits of adaptive processes that could be developed by the subjects after 4 years of training.

When gaze was laterally directed, two of the tested subjects (subjects 1 and 2) were able to maintain eccentric eye position, whereas the remaining one (subject 3) could not prevent his eyes from rapidly drifting back to the primary, straight-ahead position. As a result, perceptual image shift according to gaze changes could not be evaluated in this subject. This observation is in accordance with previous studies reporting that late blinds commonly exhibit difficulties in maintaining an eccentric gaze position.¹⁷

Our findings demonstrate, for the first time quantitatively, the importance of eye and camera axis alignment for blind individuals fitted with a camera-connected retinal prosthesis. They also identify conditions that contribute to achieving this alignment, those breaking it, and the adaptive strategies developed to manage situations when information provided on spatial image localization is conflicting, 4 years after implantation.

This study was conducted with a limited patient population, since the Argus II is an innovative retinal prosthetic device implanted in only few patients in the world. However,

these observations can have a significant impact with regard to optimization of the functional rehabilitative procedures of affected individuals. Moreover, in the design of future generations of CC-P, these issues should be addressed. From that perspective, a suggestion has been to develop devices including a head-mounted wide-angle camera showing part of the image contingent to gaze direction, or using a microcamera implanted in the eye.^{13,29}

Acknowledgments

The authors thank Alexandre Leseigneur, OD, and Céline Chaumette, OD, for their assistance during test performance; Johan Lebrun, engineer, for computer programming; Gregoire Cosandey, PhD, Avi Caspi, PhD, Jessy Dorn, PhD, Brian Coley, PhD, Mark Wexler, PhD, and William H. Seiple, PhD, for valuable discussion; and Katia Marazova, MD, PhD, and Anne-Fleur Barfuss, PhD, for editorial assistance.

Presented in part at the annual meeting of the Association for Research in Vision and Ophthalmology, Orlando, Florida, United States, May 2014.

Supported by French state funds managed by the Agence Nationale de la Recherche (ANR) within the Investissements d'Avenir program (ANR-11-IDEX-0004-02) and by a grant from Humanis. This work was performed within the framework of the Labex LIFESENSES (ANR-10-LABX-65). The authors alone are responsible for the content and writing of the paper.

Disclosure: N. Sabbah, None; C.N. Authié, None; N. Sanda, None; S. Mohand-Said, None; J.-A. Sahel, Pixium Vision (C), GenSight Biologics (C), Sanofi-Fovea (C), Genesignal (C); A.B. Safran, None

References

- Santos A. Preservation of the inner retina in retinitis pigmentosa. *Arch Ophthalmol*. 1997;115:511.
- Busskamp V, Picaud S, Sahel JA, Roska B. Optogenetic therapy for retinitis pigmentosa. *Gene Ther*. 2012;19:169-175.
- Sahel JA, Léveillard T, Picaud S, et al. Functional rescue of cone photoreceptors in retinitis pigmentosa. *Graefes Arch Clin Exp Ophthalmol*. 2013;251:1669-1677.
- Chader GJ, Weiland J, Humayun MS. Artificial vision: needs, functioning, and testing of a retinal electronic prosthesis. *Prog Brain Res*. 2009;175:317-332.
- Humayun MS, de Juan E, Dagnelie G, et al. Visual perception elicited by electrical stimulation of retina in blind humans. *Arch Ophthalmol*. 1996;114:40-46.
- Humayun M, Dorn J, Da Cruz L. Interim results from the international trial of Second Sight's visual prosthesis. *Ophthalmology*. 2012;119:779-788.
- Da Cruz L, Coley BF, Dorn J, et al. The Argus II epiretinal prosthesis system allows letter and word reading and long-term function in patients with profound vision loss. *Br J Ophthalmol*. 2013;97:632-636.
- Zrenner E, Bartz-Schmidt KU, Benav H, et al. Subretinal electronic chips allow blind patients to read letters and combine them to words. *Proc Biol Sci*. 2011;278:1489-1497.
- Humayun MS, Dorn JD, Ahuja AK, et al. Preliminary 6 month results from the Argus II epiretinal prosthesis feasibility study. *Conf Proc IEEE Eng Med Biol Soc*. 2009;2009:4566-4568.
- Ahuja AK, Dorn JD, Caspi A, et al. Blind subjects implanted with the Argus II retinal prosthesis are able to improve performance in a spatial-motor task. *Br J Ophthalmol*. 2011;95:539-543.
- Barry MP, Dagnelie G; Argus II Study Group. Use of the Argus II retinal prosthesis to improve visual guidance of fine hand movements. *Invest Ophthalmol Vis Sci*. 2012;53:5095-5101.

12. Stingl K, Bartz-Schmidt KU, Besch D, et al. Artificial vision with wirelessly powered subretinal electronic implant alpha-IMS. *Proc Biol Sci*. 2013;280:20130077.
13. Stiles NRB, Nasiatka PJ, Hauer MC, Weiland JD, Humayun MS, Tanguay AR. An intraocular camera for retinal prostheses: restoring sight to the blind. In: Serpenguzel A, Poon A, eds. *Optical Processes in Microparticles and Nanostructures, Advanced Series in Applied Physics*. Vol 6. Singapore: World Scientific; 2011:385-429.
14. Gauthier GM, Nommay D, Vercher JL. Ocular muscle proprioception and visual localization of targets in man. *Brain*. 1990;113:1857-1871.
15. Gauthier GM, Nommay D, Vercher JL. The role of ocular muscle proprioception in visual localization of targets. *Science*. 1990;249:58-61.
16. Gauthier GM, Vercher JL, Zee DS. Changes in ocular alignment and pointing accuracy after sustained passive rotation of one eye. *Vision Res*. 1994;34:2613-2627.
17. Leigh RJ, Zee DS. Eye movements of the blind. *Invest Ophthalmol Vis Sci*. 1980;19:328-331.
18. Cohen ED. Prosthetic interfaces with the visual system: biological issues. *J Neural Eng*. 2007;4:R14-R31.
19. Lee DS, Lee JS, Oh SH, et al. Cross-modal plasticity and cochlear implants. *Nature*. 2001;409:149-150.
20. Goodwin GM, McCloskey DI, Matthews PB. Proprioceptive illusions induced by muscle vibration: contribution by muscle spindles to perception? *Science*. 1972;175:1382-1384.
21. Lewis RF, Zee DS. Abnormal spatial localization with trigeminal-oculomotor synkinesis. Evidence for a proprioceptive effect. *Brain*. 1993;116:1105-1118.
22. Bridgeman B. A review of the role of efference copy in sensory and oculomotor control systems. *Ann Biomed Eng*. 1995;23:409-422.
23. von Helmholtz H. *Handbuch der physiologischen Optik*. Leipzig: Leopold Voss; 1866:874.
24. Sherman KR, Keller EI. Vestibulo-ocular reflexes of adventitiously and congenitally blind adults. *Invest Ophthalmol Vis Sci*. 1986;27:1154-1159.
25. Jeong S-H, Oh Y-M, Hwang J-M, Kim JS. Emergence of diplopia and oscillopsia due to Heimann-Bielschowsky phenomenon after cataract surgery. *Br J Ophthalmol*. 2008;92:1402.
26. Schneider RM, Thurtell MJ, Eisele S, Lincoff N, Bala E, Leigh RJ. Neurological basis for eye movements of the blind. *PLoS One*. 2013;8:e56556.
27. Pérez Fornos A, Sommerhalder J, Rappaz B, Safran AB, Pelizzone M. Simulation of artificial vision, III: do the spatial or temporal characteristics of stimulus pixelization really matter? *Invest Ophthalmol Vis Sci*. 2005;46:3906-3912.
28. Pérez Fornos A, Sommerhalder J, Da Cruz L, et al. Temporal properties of visual perception on electrical stimulation of the retina. *Invest Ophthalmol Vis Sci*. 2012;53:2720-2731.
29. Caspi A, Arup A, Cosendai G, Greenberg R, Safran AB, Sahel JA. Retinal prosthesis: steering the line of sight with eye movements. Paper presented at: *36th Annual International Conference of the IEEE Engineering in Medicine and Biology Society*; August 26-30, 2014; Chicago, IL. Submission 2647.

*Annexe IV: "Color synesthesia.
Insight into perception, emotion
and consciousness"*



Color synesthesia. Insight into perception, emotion, and consciousness

Avinoam B. Safran^{a,b} and Nicolae Sanda^{a,c}

Purpose of review

Synesthesia is an extraordinary perceptual phenomenon, in which individuals experience unusual percepts elicited by the activation of an unrelated sensory modality or by a cognitive process. Emotional reactions are commonly associated. The condition prompted philosophical debates on the nature of perception and impacted the course of art history. It recently generated a considerable interest among neuroscientists, but its clinical significance apparently remains underevaluated. This review focuses on the recent studies regarding variants of color synesthesia, the commonest form of the condition.

Recent findings

Synesthesia is commonly classified as developmental and acquired. Developmental forms predispose to changes in primary sensory processing and cognitive functions, usually with better performances in certain aspects and worse in others, and to heightened creativity. Acquired forms of synesthesia commonly arise from drug ingestion or neurological disorders, including thalamic lesions and sensory deprivation (e.g., blindness). Cerebral exploration using structural and functional imaging has demonstrated distinct patterns in cortical activation and brain connectivity for controls and synesthetes. Artworks of affected painters are most illustrative of the nature of synesthetic experiences.

Summary

Results of the recent investigations on synesthesia offered a remarkable insight into the mechanisms of perception, emotion and consciousness, and deserve attention both from neuroscientists and from clinicians.

Keywords

cerebral disorders, color, consciousness, emotion, perception, synesthesia, vision

INTRODUCTION

Synesthesia is an extraordinary perceptual phenomenon, in which the world is experienced in unusual ways. In this condition, a particular stimulation in a given sensory modality (e.g., touch) or cognitive process (e.g., computing) automatically triggers additional experiences in one or several other unstimulated domains (e.g., vision, emotion) [1]. An illustrative presentation of the condition would be that of a given person in whom hearing the sound of a trumpet consistently elicits the vision of brightly colored triangles dancing in front of his eyes, in association with a sensation of pressure on his arms, letting him feel uncomfortable to sit still. Stimuli generating additional unusual experiences are termed ‘inducers’, whereas internally produced synesthetic percepts are termed ‘concurrents’ [2].

Synesthetic experiences have had over the centuries far-reaching sociocultural implications. They prompted philosophical debates on the nature of perception, consciousness and even talent and creativity, and significantly impacted the course

of art history, notably at the turn of the 20th Century [3–6]. Moreover, favored by the emergence of sophisticated tools for functional brain exploration, they have generated a considerable interest among neuroscientists [6,7]. Clinical significance of synesthesia, however, is still largely underevaluated.

Although some synesthetic phenomena express the presence of a disease, developmental synesthesia as a rule is considered an individual cognitive

^aSorbonne Universités, UPMC Univ Paris 06, UMR_S 968, Institut de la Vision, INSERM, U968, CNRS, UMR_7210, Paris, France, ^bDepartment of Clinical Neurosciences, Geneva University School of Medicine, Geneva, Switzerland and ^cNeurology Department, Hôpital Foch, Suresnes, Paris, France

Correspondence to Avinoam B. Safran, MD, 17 rue Moreau, Paris, F-75012, France. E-mail: avinoam.safran@unige.ch

Curr Opin Neurol 2015, 28:36–44

DOI:10.1097/WCO.0000000000000169

This is an open-access article distributed under the terms of the Creative Commons Attribution-NonCommercial-NoDerivatives 4.0 License, where it is permissible to download and share the work provided it is properly cited. The work cannot be changed in any way or used commercially.

KEY POINTS

- Persons presenting with synesthesia commonly avoid mentioning their unusual percepts and even tend to close on themselves in psychological distress.
- Developmental synesthesia predisposes to changes in primary sensory processing and cognitive functions, and heightened creativity.
- Affected individuals demonstrate distinct patterns in cerebral activation and connectivity, compared with nonsynesthetes.
- Acquired forms of synesthesia are commonly related to drug ingestion or neurological conditions.

variant in the normal population [8]. Unfortunately, the astonishing features of these percepts have too often led the entourage of affected persons, including physicians, to wrongfully consider them as confabulators, drug users, or schizophrenics [7]. In this regard, the following history reported by Vincent Van Gogh is representative. While in 1885 the painter was taking piano lessons, his teacher noticed that he was continually relating the sounds of the piano keys with specific colors; considering then that his pupil was insane, the teacher sent him away [9]. It is therefore understandable that synesthetes (i.e., persons affected by synesthesia) commonly avoid mentioning their percepts and even tend to close on themselves in psychological distress [10–12]. For that very reason, scientific studies probably underestimate synesthesia prevalence in the general population.

SYNESTHESIA VARIANTS

Synesthesia is commonly classified as developmental and acquired. Developmental synesthesia appears to be the most frequent type of this condition, with a 4.4% estimated prevalence rate [13]. It can run in families and demonstrate Mendelian transmission [14]. Different forms of synesthesia can be observed in the same person or in the same family [15]. The condition is occasionally associated with autism spectrum disorders, like Asperger syndrome [16].

The following criteria have been proposed to help establishing a diagnosis of developmental synesthesia: induced percepts should be elicited by a specific stimulus, they should be automatically generated, and typically have percept-like qualities [8,17,18]. Usually, pairings of inducers and concurrents are specific (i.e., a particular stimulus consistently triggers the same synesthetic percept). They

tend to be stable over time in a given individual, although this has recently been challenged by the finding that synesthetic ability can disappear over time [19[¶]].

Acquired forms of synesthesia have also been reported, essentially associated with neurologic disorders or following psychotropic drug ingestion [20–23]. In contrast to its developmental counterpart, acquired synesthesia does not demonstrate either idiosyncrasy or automaticity or stability [3,24[¶]].

So far, over 60 types of synesthetic phenomena have been described. The apparently most common form (with a 64.4% prevalence among synesthetes) is grapheme–color synesthesia, in which achromatic letters or digits automatically trigger an idiosyncratic color perceptual experience (e.g., the letter ‘m’ induces blue color percepts) [25,26] (Fig. 1 [27]). The second most prevalent form is time unit (e.g., Monday, January)–color synesthesia (22.4%), followed by musical sound–color synesthesia (18.50%) [26,28] (Figs 2 and 3 [29,30]). Inducers and concurrents also include smells, tastes, temperatures, personalities and emotions [26], and can be multiple during a single synesthetic experience. Thus, percepts induced by grapheme–color synesthesia are occasionally accompanied by shape, texture, movement features, and even nonvisual percepts such as smells and tastes, particularly emotions [31,32]. Synesthetic colors generated in grapheme–color synesthesia are determined by systematic rules rather than randomly occurring, and based on the psycholinguistic mechanisms of language processing. The same occurs with both Latin characters and Chinese ideograms [33,34[¶]].

An additional type of colored synesthetic experience was recently described and termed ‘swimming-style color synesthesia’. It is characterized by the generation of specific colored percepts upon conceptual representation of swimming in a particular style (i.e., breast, backstroke, crawl, and butterfly) [35,36]. This phenomenon could be triggered by either presenting a picture of a swimming individual or asking the tested individual to think about a given swimming style. It was speculated that this synesthetic type was caused by overactivity in the mirror neuron system responding to the specific representation [37].

Synesthetic experiences are labeled ‘lower’ when triggered by elementary perceptual processes (e.g., texture) or ‘higher’ when involving a higher cognitive process (e.g., semantic, computing) [7,38,39]. Synesthetes who experience the atypical percepts in an internal space (‘in the mind’s eye’, as they sometimes describe it) have been categorized into ‘associators’, whereas those for whom the additional,

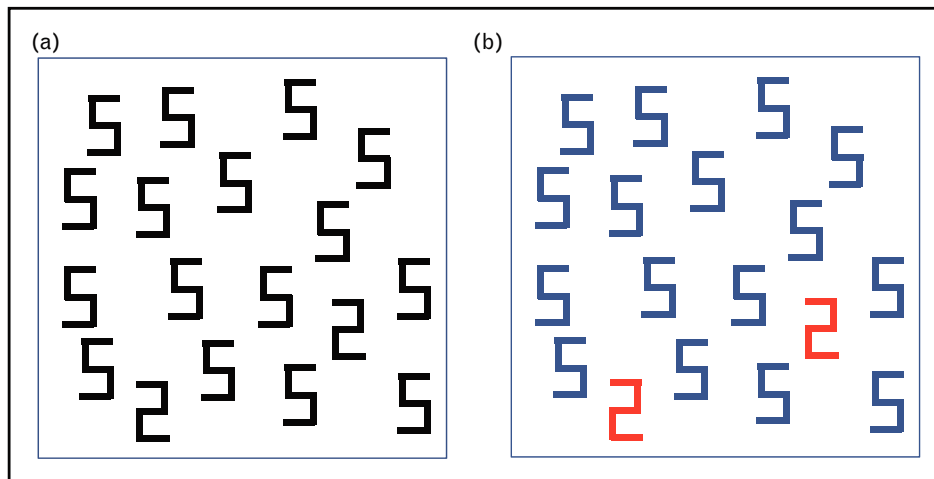


FIGURE 1. Visual segregation test demonstrating improved digit identification performances by grapheme–color synesthetes. (a) Pattern presented to the tested individuals and (b) same pattern as perceived by a grapheme–color synesthete. To identify digits ‘2’, a person with regular visual perception must perform a systematic search; in contrast, for a grapheme–color synesthete, who links a specific color with a given number, digits ‘2’ instantly pop-out. Adapted with permission [27].

atypical percept appears to be ‘out there’, overlaying the actual, external surrounding, are designated as ‘projectors’ [40,41].

PAINTERS’ COMPREHENSION OF SYNESTHESIA

Painters commonly demonstrate unique skills in the observation of visual phenomena, in which

depiction offers an invaluable source of information for neuroscientists investigating visual function in health and disease [42–46]. Regarding our understanding of synesthesia, painters’ contribution is particularly precious. Among this population, the prevalence of synesthesia was found higher than in general population; in addition, their percepts are frequently represented in their artworks [47]. Indeed, synesthete prevalence among fine art students was estimated to be 23% [48]. Among art students, prevalence of grapheme–color synesthesia alone was reported to be 7%, compared to 2% in controls [49].

Interestingly, synesthetes’ personality profile favors their involvement in creative, artistic activities [50]. Recently evaluated by a structured measure of personality (the ‘Big Five Inventory’) and by

FIGURE 2. ‘Vision’ 1996, by Carol Steen, private collection, represents a synesthetic visual experience elicited in this synesthetic painter by a needle puncture during an acupuncture session [29]. Reproduced with permission.

FIGURE 3. ‘Kondo’s Trumpet’ 2010, by Carol Steen, private collection, depicts the synesthetic visual experience elicited by the timbre of that trumpet [30]. Reproduced with permission.

questionnaires assessing empathy, synesthetes exhibited higher levels of 'Openness to Experience', considered to be related to imagination and artistic tendencies, and higher levels of 'Fantasizing', conceptually related to 'Openness' [51[¶]]. Moreover, grapheme–color synesthetes show a distinct cognitive style, with a preference for processing information in both verbal and vivid imagery styles [52[¶]].

The peculiar world perception decisively impacted the artistic work of numerous 'synesthetic' artists. Thus, Kandinsky's nonfigurative paintings and theory of synesthesia [53], prompted by his experience of extraordinary visions of lines and colors elicited by the sound of musical instruments, paved the way to abstract art and thus marked a turning point in history of art [47]. A recent analysis of Kandinsky's works using the Implicit Association Test found no implicit association between the original color–form combinations, and authors concluded that these are probably not a universal property of the visual system [44].

Most informative indications on the character of percepts commonly observed by synesthetic painters, as well as on the compulsive manner they depict their visions, were provided by Carol Steen, a remarkable synesthetic painter [54]. She emphasized that synesthetes' internal world differs tremendously from what is commonly perceived by others. For instance, colors can be perceived intensely bright, 'similar to sunlight streaming through a stained glass window'. Noteworthy, she felt that the 'overwhelming beauty of what she has seen' powerfully compelled her to capture and reproduce her visions, and that 'urgency to paint needed to be expressed'. To depict the brightness of colors perceived, synesthetic painters reportedly often apply with speed, pure, unmixed oil paint, or watercolor straight from the tube. Faithfully representing their perceptions may require breaking some long-standing rules, a feature that – as underlined by Carol Steen – characterizes modern art. The artist also specified that her visions were never representational nor figurative. This is apparently typical of many synesthetes' experiences, and probably explains why synesthetic artwork commonly looks abstract, even though it is a 'realistic' depiction of the artist's perceptions [54].

EMOTIONAL DIMENSION OF SYNESTHESIA

Emotional reactions play a prominent role in synesthetic processes. They are commonly experienced in such conditions [32,55], acting as either inducer, concurrent, or modulator [32,56]. A conflict between the actual color of a stimulus and synesthetically induced percepts can generate discomfort, whereas

'pleasantness' is experienced when synesthetic and actual stimulus features match. Some synesthetes indicate that all disagreeable events generate same color, specific for the given individual. Saturation of evoked colors is susceptible to be altered by mood [32]. In some personality–color type of synesthesia, viewing known faces elicits emotionally mediated color percepts, presenting either as colored faces or colored auras around heads [1,32,57] (Figs 4 and 5 [58]), conceivably as a result of cross-activation between right, face recognition area and neighboring V4 color cortex [7,59]. In this regard, the following delightful dedication by Julia Simner, a prominent expert in synesthesia, is illustrative: 'For my two children: the blue one (Indigo) and the brown one (Tommy Bruno)' [60]. In the so-called 'ordinal linguistic personification' synesthesia, letters have emotional valences, as well as a sex and personality [61,62]. Sexual arousal also triggers synesthetic experiences in some 2% of individuals [26]. These perceptual phenomena mainly consist of colored shapes, less commonly of flavors, smells, sounds, or temperatures, and are associated with a higher degree of trance and loss of environmental boundaries [63].

FIGURE 4. 'I and the Village' 1911, by Marc Chagall. Museum of Modern Art, New York, USA. Reproduced with permission, © Adagp, Paris 2014. Over decades, Chagall repeatedly depicted using intense green or blue colors, the faces of central characters in his paintings [58]. This most probably reflected a variant of personality–color synesthesia.

FIGURE 5. 'Half-Past Three' ('The Poet') 1911, by Marc Chagall. Philadelphia Museum of Art, The Louise and Walter Arensberg Collection, Philadelphia, PA, USA. Reproduced with permission, © Adagp, Paris 2014. For comments, see the legend of Fig. 4.

Cerebral structures processing emotion are altered in developmental synesthetes. MRI exploration of associator grapheme-color synesthetes recently brought further evidence of structural changes in emotional areas both at cortical and at subcortical levels [64[■]]. Acquired cerebral disorders are also susceptible to cause emotional synesthetic percepts. Thus, a patient who had sustained a posterolateral thalamus hemorrhage [24[■]] experienced blue photisms, intense extracorporeal sensation, and 'orgasmic' ecstasy when hearing brass instruments, or severe disgust sensations when reading words printed in blue characters. Occurrence, expression, and the underlying mechanisms of affect-related forms of synesthesia have recently been reconsidered [56].

IMPACT OF SYNESTHESIA ON COGNITIVE FUNCTIONS

Synesthetic experiences impact the cognitive functions to a larger extent than believed in the past [65,66[■],67,68]. Constitutional synesthesia

predisposes to better performances in certain aspects and worse in others. Although having better color perception compared with nonsynesthetes [69,70], synesthetes present impaired motion [66[■],67] and speech perception [71]. Speech perception deficit could be a consequence of the impaired motion perception, namely the biological movement of lips or of a much wider deficit in multisensory integration [71]. In grapheme-color and tone-color synesthetes, increased gray matter volume in the left posterior fusiform gyrus and decreased gray matter volume of the anterior part of the same gyrus and in the left MT/V5 support these hypotheses [72]. Improved perception can occur within both inducing stimulus and concurrent domains [68]. Memory was also found enhanced when using synesthetic percepts [25,73].

Improved performances depend partly on preconscious mechanisms, operating early in sensory processing [74]. Thus, a recent investigation using pictures containing hidden letters found that grapheme-color projectors recognized the letters faster than nonsynesthetes; interestingly, tested individuals noted that concurrent colors were generated before conscious letter recognition [75[■]]. Grapheme-color synesthesia even allows computing via synesthetically perceived colors [68] and as expected, emotional experience modulates synesthetes' performances [55].

CEREBRAL DISORDERS CAUSING SYNESTHESIA

Acquired forms of synesthesia have been related to a variety of neurological conditions, including migraine [76,77], multiple sclerosis – radiologically isolated syndrome [34[■]], posthypnotic suggestion [78], and drug ingestion [20,79]. In recent years, secondary synesthesia has been reported following thalamic stroke [24[■],80–83]: two of these affected individuals experienced colored synesthetic percepts [24[■],83]. Thalamic insult may induce large-scale reorganization of the brain, modify the balance between excitatory and inhibitory connections in high-order visual areas, and favor the development of synesthesia [80].

Sensory deprivation favors the occurrence of synesthetic phenomena. With blind people, non-visual stimuli tend to elicit various percepts in the suppressed sensory modality, including colored photisms [84,85] presumably by cross-modal activation of the deafferented cortex [86]. Sound-induced photisms in visually affected people are a well recognized phenomenon [87]. Six late-blind individuals were recently reported experiencing colored phenomena when hearing or thinking

about letters, numbers, and time-related terms [88,89]. In one of these individuals, touching Braille characters induced colored photisms. A patient of ours, blinded by bilateral arteritic anterior ischemic optic neuropathy, reported perceiving colored photisms when brushing his teeth or hearing a hand clap (personal observation). We also recently observed an unusual case of a late-blind individual suffering from retinitis pigmentosa who volunteered consistently ‘seeing’ his limbs when moving them, a phenomenon presumably related to cross-modal activation of his visual cortex by proprioceptive inputs [90].

Brain lesions disrupting canonical networks and sensory input to associative areas are also susceptible to induce synesthetic-like hallucinatory syndromes. A right monophthalm patient with right parosmia reported intricate visual and olfactory hallucinations following a right occipitotemporal stroke [91]. The patient described seeing people with strong odors. The presumed mechanism of these hallucinations was the disinhibition of the connections from the visual association areas to perirhinal and parahippocampal gyri [92].

ARTIFICIALLY ELICITED SYNESTHESIA

Sensory substitution devices (SSDs) have been developed to provide blind individuals with information on their visual surrounding. They convey visual information through another sensory modality, like audition [93]. Visual-to-auditory SSDs proceed by online translation of camera-captured views into sounds, which represent the visual features of the scene [93,94]. Users of such devices commonly claim to ‘see’ the objects figured by sounds, and therefore sensory substitution has been considered a kind of synthetic synesthesia [93]. Interestingly, functional magnetic resonance imaging (fMRI) investigations using a visual-to-auditory SSD, both in blindfolded healthy individuals [95] and in congenitally blind individuals [96], showed activation of visual areas. Whether – and to what extent – SSD users also perceive the auditory stimulus as a sound is debated [97,98].

Sensory substitution, however, differs in some respect from the naturally occurring synesthesia. Indeed, intended to reliably figure the visual surrounding, percepts elicited by SSDs are elaborated, whereas regular synesthetic phenomena exhibit essentially idiosyncratic features [8]. Further, in contrast to SSD-provoked synesthetic experiences, in developmental synesthesia, inducers do not conform to sensorimotor contingencies of the concurrent modality [98].

NEURAL FOUNDATIONS OF SYNESTHESIA

Assumptions have been made on the mechanisms underlying synesthesia, including hyperconnectivity between cortical areas [99], reduced level of feedback from inhibitory cerebral structures [2], learned association in early life [100], and a normal perceptual mechanism incompletely suppressed in synesthetes [17]. Neurocognitive models have been elaborated [101–105].

In recent years, brain-imaging studies brought further evidence that synesthetes connect more inside and between sensory regions and less with remote areas, especially the frontal cortex. Indeed, these individuals exhibit increased intranetwork connectivity in medial visual, auditory and intraparietal networks, and internetworks connectivity between the medial and lateral visual networks, the right frontoparietal network and between the lateral visual and auditory networks. In contrast, nonsynesthetes have more intranetwork connections within frontoparietal network [106]. When presented with inducers, synesthetes exhibit a clustering pattern of activated brain areas uniting more visual regions, whereas nonsynesthetes activate particularly frontal and parietal regions [107] (Fig. 6).

Involvement of the bottom-up and top-down mechanisms has further been considered [105,108–111]. The bottom-up model stipulates that the concurrent representation is prompted by the inducer representation via overrepresented and overactive horizontal connections, whereas the top-down model proposes that the inducer stimulates the concurrent percept via an input from a convergent, higher order integrator [2].

Using dynamic causal modeling, Van Leeuwen *et al.* [106] have shown that projectors exhibited effective connectivity patterns involving a bottom-up mechanism, whereas associators used a top-down mechanism. However, a recent electroencephalographic (EEG) study found evidence favoring the top-down disinhibited feedback model as the core of the synesthetic phenomenon [112]. Reduction of long-range couplings in the theta frequency band could facilitate the top-down feedback. An fMRI study demonstrated that, in contrast with projectors, associators’ synesthetic experience was related to areas linked to memory processes, including hippocampus and parahippocampal gyrus [113,114].

THALAMUS AND DEVELOPMENTAL SYNESTHESIA

It was suggested that congenital alterations in thalamic circuitry might be responsible for

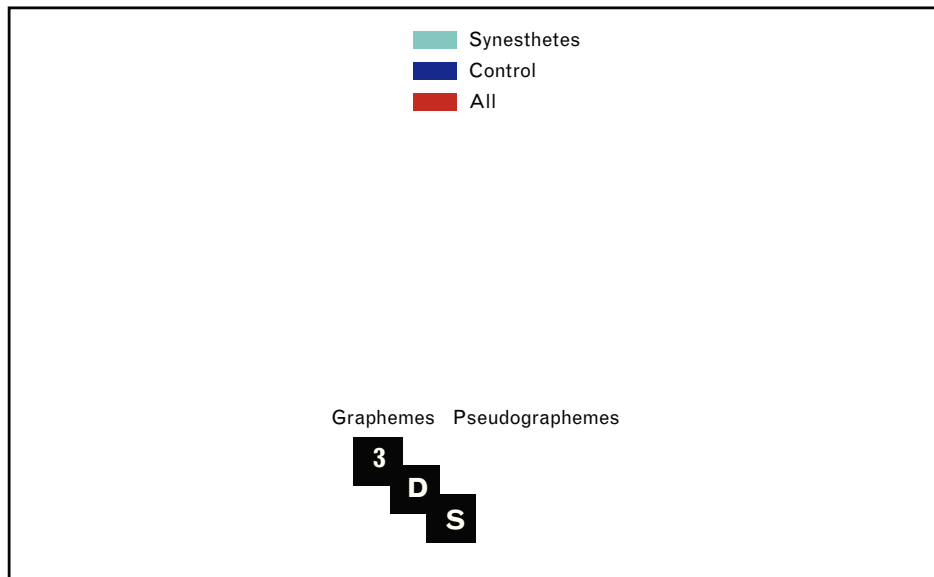


FIGURE 6. Cerebral activation revealing distinct activity patterns for controls and synesthetes during grapheme and pseudo-grapheme presentation. Synesthetes demonstrate the most significant activity in the bilateral posterior inferior temporal gyri. Reproduced with permission [107¹¹].

atypical cortical morphology and connections, found with different synesthetic phenotypes [64¹¹,115]. Cytoarchitectonic maturation of the primary sensory areas and the development of their specific connections are highly dependent on the thalamic input [116]. Enucleation in pre-natal macaque drastically alters the equivalents of V1 and V2 visual cortices, and induces rich non-canonical connections with somatosensory, auditory, and frontal areas [117], resembling transient fetal connections [118]. Thus, the visual cortex ends up treating other types of information. Likewise, congenitally blind humans exhibit occipital cortex activation following auditory or somatosensory stimulation [96¹¹]. It is therefore conceivable that in developmental synesthesia, congenitally anomalous sensory input leads to abnormal synaptic pruning and differences in brain connectivity. In grapheme–color synesthetes, low white matter densities in pulvinar, medial and lateral ventral posterior nuclei, and low fractional anisotropy in medial dorsal and ventral anterior nuclei suggest a constitutional disconnection and hypoconnection between thalamus and cerebral cortex [64¹¹]. The concerned white matter tracts project to the left prefrontal cortex and bilateral temporal and posterior parietal cortex, regions that in synesthetes are distinct both in structure and function. Secondary synesthesia after thalamic stroke also support the involvement of thalamic output in synesthetic phenomena [24¹¹,80–83].

CONCLUSION

Over the last few years, substantial advances have been made in the understanding of synesthesia, and hence more globally in the comprehension of perception and consciousness. Fortunately, awareness of this condition in the societal environment also significantly improved, finally allowing synesthetes to feel relieved by the so badly needed recognition of their particular situation. In a near future, in addition to the expected deepening of the explorations undertaken, elaborating a more comprehensive definition of synesthesia would be welcomed. Currently used criteria are rather restrictive for a condition that is quite polymorphic in nature. This process, however, is customary in the history of medicine, which consists of initially establishing a restricted definition to encapsulate the core of the condition and then broadening it, taking into account the numerous subtle presentations encountered.

Acknowledgements

The authors thank Katia Marazova, MD, PhD, for editorial assistance.

Financial support and sponsorship

Funding: This study was supported in part by grants from LABEX and Humanis.

Conflicts of interest

There are no conflicts of interest.

REFERENCES AND RECOMMENDED READING

Papers of particular interest, published within the annual period of review, have been highlighted as:

- of special interest
- of outstanding interest

1. Hochel M, Milán EG, Martín JLM, *et al.* Congruence or coherence? Emotional and physiological responses to colours in synaesthesia. *Eur J Cogn Psychol* 2009; 21:703–723.
 2. Grossenbacher PG, Lovelace CT. Mechanisms of synesthesia: cognitive and physiological constraints. *Trends Cogn Sci* 2001; 5:36–41.
 3. Sinke C, Neufeld J. Synaesthesia: a conceptualization ('synthesis') phenomenon. Philosophical and neurobiological aspects. *Theor Hist Sci* 2013; 10:37–54.
 4. Auvray M, Deroy O. How do synesthetes experience the world? In: Matthen M, editor. *Oxford handbook of the philosophy of perception*. New York: Oxford University Press, Inc; in press.
 5. Sagiv N, Frith C. Synesthesia and consciousness. In: Simner J, Hubbard EM, editors. *Oxford handbook of synesthesia*. Oxford: Oxford University Press; 2013. pp. 924–940.
 6. Hubbard EM. Synesthesia and functional imaging. In: Simner J, Hubbard E, editors. *Oxford handbook of synesthesia*. Oxford: Oxford University Press; 2013. pp. 475–499.
 7. Ramachandran VS, Hubbard EM. Synaesthesia – a window into perception, thought and language. *J Conscious Stud* 2001; 8:3–34.
 8. Ward J. Synesthesia. *Annu Rev Psychol* 2013; 64:49–75.
 9. Voskuil PHA, Van Gogh's disease in the light of his correspondence. In: Bogousslavsky J, Dieguez S, editors. *Frontiers of neurology and neuroscience*. Basel: Karger AG; 2013. pp. 116–125.
 10. Zedler M, Rehme M. Synesthesia: a psychosocial approach. In: Simner J, Hubbard E, editors. *Oxford handbook of synesthesia*. Oxford: Oxford University Press; 2013. pp. 459–472.
 11. Van Campen C. The discovery of synesthesia in childhood. *Theor Hist Sci* 2013; 10:195–206.
 12. Day S. Synesthesia: a first-person perspective. In: Simner J, Hubbard EM, editors. *Oxford handbook of synesthesia*. Oxford: Oxford University Press; 2013. pp. 903–923.
 13. Simner J, Mulvenna C, Sagiv N, *et al.* Synaesthesia: the prevalence of atypical cross-modal experiences. *Perception* 2006; 35:1024–1033.
 14. Brang D, Ramachandran VS. Survival of the synesthesia gene: why do people hear colors and taste words? *PLoS Biol* 2011; 9:e1001205.
 15. Jackson TE, Sandramouli S. Auditory–olfactory synesthesia coexisting with auditory–visual synesthesia. *J Neuroophthalmol* 2012; 32:221–223.
 16. Neufeld J, Roy M, Zapf A, *et al.* Is synesthesia more common in patients with Asperger syndrome? *Front Hum Neurosci* 2013; 7:847.
 17. Cytowic RE. *Synesthesia: a union of the senses* – second edition. Cambridge, MA: A Bradford Book; 2002.
 18. Mattingley JB. Attention, automaticity, and awareness in synesthesia. *Ann N Y Acad Sci* 2009; 1156:141–167.
 19. Simner J, Bain AE. A longitudinal study of grapheme–color synesthesia in childhood: 6/7 years to 10/11 years. *Front Hum Neurosci* 2013; 7:603.
- The authors observed the development of child synesthetes over 4 years and found that in some individuals, synesthesia apparently died out over time or developed more slowly in some individuals over others. This demonstrated that synesthetic phenomena are not as consistent over time as previously thought.
20. Brogaard B. Serotonergic hyperactivity as a potential factor in developmental, acquired and drug-induced synesthesia. *Front Hum Neurosci* 2013; 7:657.
 21. Luke DP, Terhune DB. The induction of synaesthesia with chemical agents: a systematic review. *Front Psychol* 2013; 4:753.
 22. Terhune DB, Song SM, Duta MD, Cohen Kadosh R. Probing the neurochemical basis of synaesthesia using psychophysics. *Front Hum Neurosci* 2014; 8:89.
 23. Van Hout MC. Nod and wave: an Internet study of the codeine intoxication phenomenon. *Int J Drug Policy* 2014. [Epub ahead of print]
 24. Schweizer TA, Li Z, Fischer CE, *et al.* From the thalamus with love: a rare window into the locus of emotional synesthesia. *Neurology* 2013; 81:509–510.
- The authors for the first time report a case of acquired emotional synesthesia after focal thalamic lesion.
25. Brang D, Rouw R, Ramachandran VS, Coulson S. Similarly shaped letters evoke similar colors in grapheme–color synesthesia. *Neuropsychologia* 2011; 49:1355–1358.
 26. Day S. Types of synesthesia. *Synesthesia* 2014. Available at <http://www.day-syn.com>. [Accessed October 2014].
 27. Ramachandran VS, Hubbard EM. Hearing colors, tasting shapes. *Sci Am* 2003; 288:52–59.
 28. Day S. Some demographic and socio-cultural aspects of synesthesia. In: Robertson LC, Sagiv N, editors. *Synesthesia: perspectives from cognitive neuroscience*. New York: Oxford University Press, Inc; 2005. pp. 11–33.
 29. Steen C. Visions shared. A firsthand look into synesthesia and art. *Leonardo* 2001; 34:203–208.
 30. McDonald F. Synesthesia: bringing out the contours. *Aust Art Rev* 2006. Available at http://www.synesthesia.info/Steen-Australian_Art_Review.pdf. [Accessed 12 October 2014]
 31. Tyler C. Varieties of synesthetic experience. In: Robertson LC, Sagiv N, editors. *Synesthesia: perspectives from cognitive neuroscience*. New York: Oxford University Press, Inc; 2005. pp. 34–44.
 32. Ward J. Emotionally mediated synaesthesia. *Cogn Neuropsychol* 2004; 21:761–772.
 33. Hung W-Y, Simner J, Shillcock R, Eagleman DM. Synaesthesia in Chinese characters: the role of radical function, position. *Conscious Cogn* 2014; 24:38–48.
 34. Simner J, Carmichael DA, Hubbard EM, *et al.* Rates of white matter hyperintensities compatible with the radiological profile of multiple sclerosis within self-referred synesthete populations. *Neurocase* (in press).
- The study reported an apparent statistical link between synesthesia and multiple sclerosis – radiologically isolated syndrome.
35. Nikolić D, Jürgens UM, Rothen N, *et al.* Swimming-style synesthesia. *Cortex* 2011; 47:874–879.
 36. Rothen N, Nikolić D, Jürgens UM, *et al.* Psychophysiological evidence for the genuineness of swimming-style colour synaesthesia. *Conscious Cogn* 2013; 22:35–46.
 37. Mroczko-Wasowicz A, Werning M. Synesthesia, sensory–motor contingency, and semantic emulation: how swimming style–color synesthesia challenges the traditional view of synesthesia. *Front Psychol* 2012; 3: 279.
 38. Meier B. Semantic representation of synaesthesia. *Theor Hist Sci* 2013; 10:125–134.
 39. Mroczko-Wasowicz A, Nikolic D. Semantic mechanisms may be responsible for developing synesthesia. *Front Hum Neurosci* 2014; 8:509.
 40. Dixon MJ, Smilek D, Merikle PM. Not all synesthetes are created equal: projector versus associator synaesthetes. *Cogn Affect Behav Neurosci* 2004; 4:335–343.
 41. Mohr C. Synesthesia in space versus in the 'mind's eye': how to ask the right questions. In: Simner J, Hubbard E, editors. *Oxford handbook of synesthesia*. Oxford: Oxford University Press; 2013. pp. 440–458.
 42. Cavanagh P. The artist as neuroscientist. *Nature* 2005; 434:301–307.
 43. Blanke O, Forucchi L, Dieguez S. Don't forget the artists when studying perception of art. *Nature* 2009; 462:984.
 44. Makin ADJ, Wuerger SM. The IAT shows no evidence for Kandinsky's color–shape associations. *Front Psychol* 2013; 4:616.
 45. Zeki S. Neurobiology and the humanities. *Neuron* 2014; 84:12–14.
 46. Safran AB, Sanda N, Sahel J-A. A neurological disorder presumably underlies painter Francis Bacon distorted world depiction. *Front Hum Neurosci* 2014; 8:581.
 47. Van Campen C. Synesthesia in the visual arts. In: Simner J, Hubbard E, editors. *Oxford handbook of synesthesia*. Oxford: Oxford University Press; 2013. pp. 631–646.
 48. Domino G. Synesthesia and creativity in fine arts students: an empirical look. *Creat Res J* 1989; 2:17–29.
 49. Rothen N, Meier B. Higher prevalence of synaesthesia in art students. *Perception* 2010; 39:718–720.
 50. Ward J, Thompson-Lake D, Ely R, Kaminski F. Synaesthesia, creativity and art: what is the link? *Br J Psychol* 2008; 195:2008; 99:127–141.
 51. Banissy MJ, Holle H, Cassell J, *et al.* Personality traits in people with synesthesia: do synesthetes have an atypical personality profile? *Personal Individ Differ* 2013; 54:828–831.
- The authors found that, relative to matched controls, synaesthetes reported higher levels of imagination, artistic tendencies, and 'fantasizing'.
52. Meier B, Rothen N. Grapheme–color synaesthesia is associated with a distinct cognitive style. *Front Psychol* 2013; 4:632.
- The authors reported that grapheme–color synesthetes showed higher ratings on verbal and vivid imagery style dimensions.
53. Kandinsky W. *Concerning the spiritual in art*. London: Constable and Co Ltd; 1914.
 54. Steen C, Berman G. Synesthesia and the artistic process. In: Simner J, Hubbard E, editors. *Oxford handbook of synesthesia*. Oxford: Oxford University Press; 2013. pp. 671–691.
 55. Perry A, Henik A. The emotional valence of a conflict: implications from synesthesia. *Front Psychol* 2013; 4:978.
 56. Dael N, Sierro G, Mohr C. Affect-related synesthesias: a prospective view on their existence, expression and underlying mechanisms. *Front Psychol* 2013; 4:754.
 57. Cytowic RE, Eagleman D. Wednesday is indigo blue: discovering the brain of synesthesia. Cambridge, MA: MIT Press; 2009.
 58. Salzman M. The fiancée with a blue face by Marc Chagall (1887–1985). *Neurosurgery* 2007; 61:1322–1324.
 59. Hubbard EM, Brang D, Ramachandran VS. The cross-activation theory at 10. *J Neuropsychol* 2011; 5:152–177.
 60. Simner J, Hubbard E. *Oxford handbook of synesthesia*. Oxford: Oxford University Press; 2013.
 61. Simner J, Holenstein E. Ordinal linguistic personification as a variant of synesthesia. *J Cogn Neurosci* 2007; 19:694–703.

62. Smilek D, Malcolmson KA, Carriere JSA, *et al.* When '3' is a jerk, 'E' is a king: personifying inanimate objects in synesthesia. *J Cogn Neurosci* 2007; 19:981–992.
63. Nielsen J, Kruger THC, Hartmann U, *et al.* Synaesthesia and sexuality: the influence of synaesthetic perceptions on sexual experience. *Front Psychol* 2013; 4:751.
64. Melerio H, Peña-Melián Á, Ríos-Lago M, *et al.* Grapheme–color synesthetes show peculiarities in their emotional brain: cortical and subcortical evidence from VBM analysis of 3D-T1 DTI data. *Exp Brain Res* 2013; 227:343–353.
- This study demonstrates morphological differences in thalamocortical connections in synesthetes as well as increased gray matter volume in brain regions involved in emotional processing. It provides morphological evidence about the importance of emotion in synesthetic phenomena.
65. Motttron L, Bouvet L, Bonnel A, *et al.* Veridical mapping in the development of exceptional autistic abilities. *Neurosci Biobehav Rev* 2013; 37:209–228.
66. Banissy MJ, Tester V, Muggleton NG, *et al.* Synesthesia for color is linked to improved color perception but reduced motion perception. *Psychol Sci* 2013; 24:2390–2397.
- This study showed that synesthesia for color is linked to facilitated color sensitivity, but decreased motion sensitivity.
67. McCarthy JD, Caplovitz GP. Color synesthesia improves color but impairs motion perception. *Trends Cogn Sci* 2014; 18:224–226.
68. McCarthy JD, Barnes LN, Alvarez BD, Caplovitz GP. Two plus blue equals green: grapheme–color synesthesia allows cognitive access to numerical information via color. *Conscious Cogn* 2013; 22:1384–1392.
69. Cohen Kadosh R, Gertner L, Terhune DB. Exceptional abilities in the spatial representation of numbers and time: insights from synesthesia. *Neuroscientist* 2012; 18:208–215.
70. Brang D, Miller LE, McQuire M, *et al.* Enhanced mental rotation ability in time-space synesthesia. *Cogn Process* 2013; 14:429–434.
71. Sinke C, Neufeld J, Zedler M, *et al.* Reduced audiovisual integration in synesthesia – evidence from bimodal speech perception. *J Neuropsychol* 2014; 8:94–106.
72. Banissy MJ, Stewart L, Muggleton NG, *et al.* Grapheme–color and tone–color synesthesia is associated with structural brain changes in visual regions implicated in color, form, and motion. *Cogn Neurosci* 2012; 3:29–35.
73. Witthoft N, Winawer J. Learning, memory, and synesthesia. *Psychol Sci* 2013; 24:258–265.
74. Rothen N, Scott RB, Meador AD, *et al.* Synesthetic experiences enhance unconscious learning. *Cogn Neurosci* 2013; 4:231–238.
75. Ramachandran VS, Seckel E. Synesthetic colors induced by graphemes that have not been consciously perceived. *Neurocase* (in press).
- In pictures that contained hidden letters, grapheme–color projector synesthetes recognized the letters faster and reported that the colors were evoked before conscious letter recognition, suggesting that in some synesthetes colors are evoked pre-consciously early in sensory processing.
76. Podoll K, Robinson D. Auditory–visual synaesthesia in a patient with basilar migraine. *J Neurol* 2002; 249:476–477.
77. Alstadhaug KB, Benjaminsen E. Synesthesia and migraine: case report. *BMC Neurol* 2010; 10:121.
78. Terhune DB, Cardena E, Lindgren M. Disruption of synaesthesia by posthypnotic suggestion: an ERP study. *Neuropsychologia* 2010; 48:3360–3364.
79. Sinke C, Halpern JH, Zedler M, *et al.* Genuine and drug-induced synesthesia: a comparison. *Conscious Cogn* 2012; 21:1419–1434.
80. Ro T, Farnè A, Johnson RM, *et al.* Feeling sounds after a thalamic lesion. *Ann Neurol* 2007; 62:433–441.
81. Beauchamp MS, Ro T. Neural substrates of sound–touch synesthesia after a thalamic lesion. *J Neurosci* 2008; 28:13696–13702.
82. Naumer MJ, van den Bosch JFF. Touching sounds: thalamocortical plasticity and the neural basis of multisensory integration. *J Neurophysiol* 2009; 102:7–8.
83. Fornazzari L, Fischer CE, Ringer L, Schweizer TA. 'Blue is music to my ears': multimodal synesthesias after a thalamic stroke. *Neurocase* 2012; 18:318–322.
84. Niccolai V, van Leeuwen TM, Blakemore C, Stoerig P. Synaesthetic perception of colour and visual space in a blind subject: an fMRI case study. *Conscious Cogn* 2012; 21:889–899.
85. Armel K, Ramachandran VS. Acquired synesthesia in retinitis pigmentosa. *Neurocase* 1999; 5:293–296.
86. Merabet LB, Pascual-Leone A. Neural reorganization following sensory loss: the opportunity of change. *Nat Rev Neurosci* 2010; 11:44–52.
87. Jacobs L, Karpik A, Bozian D, Gøthgen S. Auditory–visual synesthesia: sound-induced photisms. *Arch Neurol* 1981; 38:211–216.
88. Steven MS, Hansen PC, Blakemore C. Activation of color-selective areas of the visual cortex in a blind synesthete. *Cortex* 2006; 42:304–308.
89. Steven MS, Blakemore C. Visual synaesthesia in the blind. *Perception* 2004; 33:855–868.
90. Safran AB, Sabbah N, Sanda N, Sahel JA. The blind man who saw his hands. ■ Cross-modal plasticity revisited. In: The Association for the Research in Vision and Ophthalmology (ARVO); 2014 Annual Meeting; Poster no: 4147. A patient blinded as a result of retinitis pigmentosa volunteered that he visually perceived the shape of his hands when waving them; the visual synesthetic percept was presumably elicited by proprioceptive inputs.
91. Gubernick D, Ameli P, Teng Q, *et al.* Visual–olfactory hallucinatory synesthesia: the Charles Bonnet Syndrome with olfactory hallucinations. *Cortex* 2014; 50:204–207.
92. Ninomiya T, Sawamura H, Inoue K-I, Takada M. Multisynaptic inputs from the medial temporal lobe to V4 in macaques. *PLoS One* 2012; 7:e52115.
93. Suslick KS. Synesthesia in science and technology: more than making the unseen visible. *Curr Opin Chem Biol* 2012; 16:557–563.
94. Proulx MJ. Synthetic synaesthesia and sensory substitution. *Conscious Cogn* 2010; 19:501–503.
95. Striem-Amit E, Cohen L, Dehaene S, Amedi A. Reading with sounds: sensory substitution selectively activates the visual word form area in the blind. *Neuron* 2012; 76:640–652.
96. Striem-Amit E, Amedi A. Visual cortex extrastriate body-selective area activation in congenitally blind people 'seeing' by using sounds. *Curr Biol* 2014; 24:687–692.
- This study demonstrates the presence of selective activation of extrastriate body area in congenitally blind while detecting body shapes with a sensory substitution device, supporting the view that brain has a sensory independent, task-selective organization.
97. Ortiz T, Poch J, Santos JM, *et al.* Recruitment of occipital cortex during sensory substitution training linked to subjective experience of seeing in people with blindness. *PLoS One* 2011; 6:e23264.
98. Ward J, Wright T. Sensory substitution as an artificially acquired synaesthesia. *Neurosci Biobehav Rev* 2014; 41:26–35.
99. Ramachandran VS, Hubbard EM. Psychophysical investigations into the neural basis of synaesthesia. *Proc Biol Sci* 2001; 268:979–983.
100. Calkins M. Synesthesia. *J Psychol* 1895; 7:90–107.
101. Harvey JP. Sensory perception: lessons from synesthesia: using synesthesia to inform the understanding of sensory perception. *Yale J Biol Med* 2013; 86:203–216.
102. Froese T. Steps toward an inactive account of synesthesia. *Cogn Neurosci* 2014; 5:126–127.
103. O'Regan JK, Degenaar J. Predictive processing, perceptual presence, sensorimotor theory. *Cogn Neurosci* 2014; 5:130–131.
104. Rouw R, Ridderinkhof KR. The most intriguing question in synesthesia research. *Cogn Neurosci* 2014; 5:128–130.
105. Van Leeuwen TM. Constructing priors in synesthesia. *Cogn Neurosci* 2014; 5:124–126.
106. Van Leeuwen TM, den Ouden HEM, Hagoort P. Effective connectivity determines the nature of subjective experience in grapheme–color synesthesia. *J Neurosci* 2011; 31:9879–9884.
107. Tomson SN, Narayan M, Allen GI, Eagleman DM. Neural networks of colored sequence synesthesia. *J Neurosci* 2013; 33:14098–14106.
- This study demonstrates hodological differences between synesthetes and non-synesthetes. Synesthetes cluster more in visual areas and nonsynesthetes in frontal and parietal areas. These clustering patterns may provide an explanation for the different cognitive performances associated with synesthetic phenotype.
108. Hubbard EM. Neurophysiology of synesthesia. *Curr Psychiatry Rep* 2007; 9:193–199.
109. Hubbard EM. A real red-letter day. *Nat Neurosci* 2007; 10:671–672.
110. Brogaard B, Vanni S, Silvanto J. Seeing mathematics: perceptual experience and brain activity in acquired synesthesia. *Neurocase* 2013; 19:566–575.
111. Brogaard B, Marlow K, Rice K. The long-term potentiation model for grapheme–color binding in synesthesia. In: Bennett D, Hill C, editors. *Sensory integration and the unity of consciousness*. Cambridge, MA: MIT Press; in press.
112. Volberg G, Karmann A, Birkner S, Greenlee MW. Short- and long-range neural synchrony in grapheme–color synesthesia. *J Cogn Neurosci* 2013; 25:1148–1162.
- This study provides electrophysiological arguments that favor the top-down disinhibited model as the core of synesthetic phenomena.
113. Rouw R, Scholte HS. Neural basis of individual differences in synesthetic experiences. *J Neurosci* 2010; 30:6205–6213.
114. Rouw R, Scholte HS. Increased structural connectivity in grapheme–color synesthesia. *Nat Neurosci* 2007; 10:792–797.
115. Mitchell KJ. Synesthesia and cortical connectivity – a neurodevelopmental perspective. In: Simner J, Hubbard EM, editors. *Oxford handbook of synesthesia*. Oxford: Oxford University Press; 2013. pp. 530–550.
116. Dehay C, Kennedy H. Cell-cycle control and cortical development. *Nat Rev Neurosci* 2007; 8:438–450.
117. Rakic P, Suñer I, Williams RW. A novel cytoarchitectonic area induced experimentally within the primate visual cortex. *Proc Natl Acad Sci USA* 1991; 88:2083–2087.
118. Price DJ, Kennedy H, Dehay C, *et al.* The development of cortical connections. *Eur J Neurosci* 2006; 23:910–920.

*Annexe V: "Impact of thrombolysis
in acute stroke without occlusion:
an observational comparative study"*

Impact of thrombolysis in acute ischaemic stroke without occlusion: an observational comparative study

N. Ajili^a, J. P. Decroix^a, C. Preda^b, J. Labreuche^c, D. Lopez^a, Y. Bejot^d, P. Michel^e, M. Sévin-Allouet^f, I. Sibon^g, S. Vergnet^g, A. Wang^a, N. Sanda^a, M. Mazighi^h, F. Bourdain^a and B. Lapergue^a

^aDivision of Neurology, Stroke Centre, Foch Hospital, University Versailles Saint-Quentin en Yvelines, Suresnes; ^bLaboratoire de Mathématiques Paul Painlevé, UMR CNRS 8524, Lille; ^cDepartment of Biostatistics, Lille University Medical Centre, Lille; ^dDepartment of Neurology, University Hospital and Medical School of Dijon, Dijon, France; ^eNeurology Service, Centre Hospitalier Universitaire Vaudois and University of Lausanne, Lausanne, Switzerland; ^fDepartment of Neurology, Nantes University Hospital, Nantes; ^gUniversité Bordeaux 2, CHU Bordeaux, Pole de Neurosciences Cliniques, Unité neuro-vasculaire, Bordeaux; and ^hDepartment of Neurology and Stroke Centre, Lariboisière Hospital, Paris, France

Keywords:

arterial occlusion,
ischaemic stroke,
outcome, thrombolysis

Received 22 September 2015
Accepted 4 April 2016

*European Journal of
Neurology* 2016, **0**: 1–7

doi:10.1111/ene.13042

Background and purpose: The impact of intravenous recombinant tissue plasminogen activator (IV-rtPA) in patients with acute ischaemic stroke (AIS) but no arterial occlusion is currently a matter of debate. This study aimed to assess functional outcome of such patients with respect to IV-rtPA use.

Methods: A retrospective case–control analysis was performed comparing the outcome of AIS patients without arterial occlusion with or without IV-rtPA use. Patients were selected from prospective consecutive observational registries of five European university hospitals. The primary study outcome was excellent outcome at 3 months after stroke, as defined by a modified Rankin Scale (mRS) 0–1.

Results: A total of 488 patients without arterial occlusion documented by angiography were included in the present study; 300 received IV-rtPA and 188 did not. No between-group difference was found for excellent outcome before and after adjustment for baseline characteristics (adjusted odds ratio for no IV-rtPA use 0.79, 95% confidence interval 0.51–1.24, $P = 0.31$). Similar results were found for favourable outcome (defined as a 90-day mRS of 0–2) whereas a higher rate of early neurological improvement was found in IV-rtPA-treated patients (adjusted odds ratio 1.99; 95% confidence interval 1.29–3.07, $P = 0.002$). Sensitivity analyses yielded similar results.

Conclusions: Our study suggests that AIS patients without visible arterial occlusion treated with IV-rtPA may have no better outcome at 3 months than those untreated. However, only a randomized controlled trial would provide a definitive answer about the impact of rtPA in acute stroke patients without occlusion. Until then, these patients should be treated by rtPA as recommended.

Introduction

The efficacy of intravenous recombinant tissue plasminogen activator (IV-rtPA) in the setting of acute ischaemic stroke (AIS) was demonstrated in trials

Correspondence: B. Lapergue, Division of Neurology, Stroke Centre, Foch Hospital, University Versailles Saint-Quentin en Yvelines, Suresnes, France (tel.: +33 1 46 25 73 43; fax: +33 1 46 25 27 24; e-mail: b.lapergue@hopital-foch.org).

where intracranial arterial status was not studied [1]. As the rationale for IV-rtPA benefit is based on intracranial artery recanalization, the absence of arterial occlusion documented on vascular imaging in AIS patients raises the question of their eligibility for reperfusion therapy [2]. The benefit/risk balance is a significant issue in the daily practice of physicians managing AIS patients. Indeed, 30% of AIS patients treated with rtPA have no occlusion at admission

[2,3], and any benefit of fibrinolysis is hampered by a 10-fold increase in haemorrhagic transformation, with devastating consequences (7.7% of symptomatic intracerebral haemorrhage) [1]. Two recent studies on the impact of thrombolysis in cerebral infarction without occlusion showed opposing results [4,5]. Here, our aim was to assess the outcome of AIS patients without arterial occlusion with respect to IV-rtPA use.

Methods

Study design and data sources

A collaborative retrospective analysis was performed of observational data from five European university hospitals to assess the impact of IV-rtPA use in AIS patients without visible arterial occlusion. In all centres, data were prospectively collected using a structured questionnaire and approved by local institutional review boards. There were four participating centres in France (Bordeaux, Foch, Dijon and Nantes University Hospitals) and one in Switzerland (Lausanne University Hospital). In Lausanne University Hospital, data were extracted from the Acute Stroke Registry and Analysis of Lausanne (ASTRAL), which is a published ongoing prospective registry of AIS patients admitted within 24 h of symptom onset [6]. A subset of 236 included patients from the ASTRAL registry has been used in a previous publication testing the influence of arterial occlusion on favourable outcome after IV-rtPA use [5] but without focusing on lacunar subgroups. In this centre, all patients eligible for IV-rtPA treatment, as assessed by a vascular neurologist within 4.5 h (3 h before August 2008), received conventional IV-rtPA treatment. In Foch University Hospital, data were extracted from an unpublished ongoing prospective registry of AIS patients admitted within 6 h of symptom onset. In this centre, all patients eligible for IV-rtPA treatment, as assessed by a vascular neurologist within 4.5 h, received conventional IV-rtPA treatment when arterial occlusion was documented by angiography; in cases of no documented occlusion, patients received appropriate antithrombotic medication. In the remaining three participating centres, data were extracted from a local registry of consecutive patients having undergone conventional IV-rtPA treatment [7].

The study was considered and approved as observational by the internal review board (Comité de protection des personnes, CPP Ile de France VIII, 10 July 2013). Patient databases were approved by the locally competent ethics committees and the 'Comité consultatif sur le traitement de l'information en matière de

recherche dans le domaine de santé' of the individual participating centres.

Data collection

Patients were eligible for inclusion in this study if they (i) were admitted to hospital within 4.5 h, (ii) had no arterial occlusion documented by magnetic resonance angiography (MRA) or computed tomography angiography (CTA) at admission, (iii) had an admission National Institutes of Health Stroke Scale (NIHSS) score >4 , (iv) had a pre-stroke modified Rankin Scale (mRS) <3 and (v) had available information on mRS at 3 months.

No arterial occlusion was documented on CT or MR angiograms at presentation, before IV-rtPA therapy. This variable was prospectively collected after adjudication by a senior neuroradiologist and a vascular neurologist in each case.

Data from individual patients were extracted from the observational data sources using a standardized form with predefined variables and were compiled at the coordinating centre (Foch University Hospital, Suresnes, France). The following variables were collected: age, sex, time between symptom onset (or from when the patient was last seen in a normal condition) and admission, medical history including main vascular risk factors (hypertension, diabetes mellitus, current smoking, prior stroke history) and antithrombotic treatment, clinical measures at admission (systolic and diastolic blood pressure, glucose level, heart rate, NIHSS score, pre-stroke mRS), NIHSS at 24 h, functional outcome assessed by the mRS at 3 months, symptomatic intracerebral haemorrhage (defined as a haemorrhage on the follow-up CT/MRI scan associated with an increase of ≥ 4 points in NIHSS score) [8] and lacunar stroke aetiology according to the TOAST classification. The mRS at 3 months was recorded either at the outpatient stroke clinic visit in an unblinded manner or by a structured telephone interview by mRS-certified medical personnel in a manner blinded to treatment type and recanalization [9].

Outcome definitions

The primary study outcome was excellent, defined by a 90-day mRS of 0–1. Secondary outcomes included a favourable outcome (defined as a 90-day mRS of 0–2), early neurological improvement (ENI) (defined as an NIHSS score of 0–1 at 24 h or a decrease of ≥ 4 points in NIHSS score at 24 h), 90-day all-cause mortality and symptomatic intracerebral haemorrhage.

Statistical analysis

Quantitative variables are expressed as means (standard deviation) in the case of normal distribution or medians (interquartile range, IQR) otherwise. Categorical variables are expressed as percentages (count). Normality of distributions was assessed using histograms and the Shapiro–Wilk test. Bivariate comparisons between IV-rtPA-treated and non-IV-rtPA-treated patients were made using chi-squared tests for qualitative variables (Fisher's exact test was used when the expected cell frequency was <5) and Student's *t* test for continuous variables (Mann–Whitney *U* test was used for non-Gaussian distributions). Comparisons in efficacy outcomes (excellent outcome, favourable outcome and ENI) were further adjusted for baseline between-group differences (at $P < 0.10$ in bivariate analyses) using logistic regression models. Unadjusted and adjusted odds ratios (ORs) for reaching each outcome were calculated using non-IV-rtPA-treated patients as the control group. Our first analyses covered the whole study group. Further analyses were stratified according to lacunar stroke aetiology; heterogeneity in IV-rtPA treatment effects across non-lacunar and lacunar subgroups were tested by formal interaction tests.

Two sensitivity analyses were performed. As a first sensitivity analysis, the main analysis was repeated after excluding the patients with a pre-stroke mRS ≥ 1 . A secondary sensitivity analysis was performed using

a propensity score adjustment approach [10]. A propensity score was calculated using a non-parsimonious multivariable logistic regression model, with IV-rtPA use as the dependent variable and all of the characteristics listed in Table 1 as covariates [10].

Finally, a meta-analysis was performed pooling the two existing previous studies [4,5] with our study results (after excluding the 236 overlapping participants in the Medlin *et al.* [5] publication). From the two previous studies the fully adjusted effect size [OR associated with IV use with its 95% confidence interval (CI)] for favourable outcome (available in both studies) was extracted. The adjusted effect sizes were combined using the inverse variance weighted fixed-effects model; heterogeneity between studies was quantified by calculation of the I^2 statistic.

Statistical testing was done at the two-tailed α level of 0.05. Data were analysed using the SAS software version 9.3 (SAS Institute, Cary, NC, USA).

Results

A total of 488 patients without arterial occlusion documented by angiography admitted from five European university hospitals were included in the present study; amongst them, 300 received IV-rtPA and 188 did not. The baseline characteristics of patients are shown in Table 1. IV-rtPA-treated patients less frequently had antithrombotic medications, prior stroke history, pre-stroke mRS ≥ 1 , lacunar stroke aetiology, had lower

Table 1 Baseline characteristics in control and IV-rtPA-treated groups

Variable	Control group	IV-rtPA-treated group	<i>P</i>
Number of patients	188	300	
Age, years, mean \pm SD	69.5 \pm 14.0	67.6 \pm 14.3	0.16
Men	128 (68.1)	195 (65.0)	0.48
Medical history			
Hypertension	114 (60.6)	164 (54.7)	0.19
Diabetes	32 (17.0)	46 (15.3)	0.62
Hypercholesterolaemia	70 (37.2)	95 (34.7)	0.57
Current smoking	52 (28.9)	74 (24.8)	0.32
Antithrombotic therapy	84 (44.7)	102 (34.0)	0.018
Prior stroke history	37 (19.7)	37 (12.4)	0.029
Clinical measures			
Blood glucose, mg/dl, median (IQR)	117 (101–142)	114 (100–137)	0.60
Heart rate, beats/min, mean \pm SD	82 \pm 18	82 \pm 16	0.84
Systolic BP, mmHg, mean \pm SD	162 \pm 30	157 \pm 26	0.086
Diastolic BP, mmHg, mean \pm SD	90 \pm 18	85 \pm 16	0.003
NIHSS score, median (IQR)	7 (6–10)	8 (6–12)	<0.001
Pre-stroke Rankin ≥ 1	76 (40.4)	60 (20.0)	<0.001
Lacunar stroke	45 (24.2)	38 (12.8)	0.001
Time to admission, min, mean \pm SD	131 \pm 76	108 \pm 63	<0.001

BP, blood pressure; IQR, interquartile range; IV, intravenous; NIHSS, National Institutes of Health Stroke Scale; rtPA, recombinant tissue plasminogen activator. Values are expressed as numbers (percentages) unless otherwise indicated.

blood pressure values and a lower time from symptom onset to admission than non-IV-rtPA-treated patients (all $P < 0.05$). However, IV-rtPA-treated patients had one point difference in baseline NIHSS than non-IV-rtPA-treated patients [median (IQR): 8 (6–12) vs. 7 (6–10), $P < 0.001$].

Amongst 488 patients without occlusion included in the study, 188 were not treated by IV-rtPA. The details are 50 (27%) because of local protocol of treatment indicating no fibrinolysis in the case of no documented arterial occlusion; 19 (10%) were on oral anticoagulants and 119 (63%) were assessed after the time window for rtPA treatment of 3 h until the ECASS-III trial publication in 2008 or after 4.5 h after 2008.

Excellent outcome (our primary outcome) was achieved in 50% ($n = 242$) of patients overall, with no significant difference between the two groups ($P = 0.82$). A similar result was found when considering favourable outcome, whereas IV-rtPA-treated patients had significantly better ENI than non-IV-rtPA-treated patients (Figs 1 and S1). After adjustment for baseline between-group differences, the increased probability of ENI for IV-rtPA-treated patients remained significant, with an adjusted OR of 1.99 (95% CI 1.29–3.07, $P = 0.002$).

When the analysis was stratified according to lacunar and non-lacunar stroke aetiology, a significant heterogeneity was found in the IV-rtPA effect size for ENI (Fig. 1). The adjusted OR of ENI for IV-rtPA-treated relative to non-IV-rtPA-treated patients was 0.53 (95% CI 0.16–1.75, $P = 0.30$) in lacunar stroke

patients and 2.52 (95% CI 1.56–4.09, $P < 0.001$) in non-lacunar stroke patients. Although the heterogeneity test did not reach the significance level for functional outcome, a detrimental effect of IV-rtPA was found in lacunar stroke patients only, whereas a trend towards a higher rate of favourable outcome in IV-rtPA-treated patients was found in non-lacunar stroke patients only.

Both sensitivity analyses (Fig. S2) yielded similar results.

Twenty-three deaths occurred in each group, with a non-significant between-group difference (8% in the IV-rtPA-treated group versus 12% in the non-IV-rtPA group; $P = 0.09$). Symptomatic intracerebral haemorrhage occurred in 6% of IV-rtPA-treated patients ($n = 18$) and in 3% of controls ($P = 0.18$). Death and symptomatic intracerebral haemorrhage occurred more frequently in non-lacunar stroke patients; only three deaths and two cases of symptomatic intracerebral haemorrhage occurred in lacunar stroke patients.

Finally, in a meta-analysis combining the three existing studies (including our result after excluding overlapping patients), the impact of IV use on favourable outcome was not significant; the combined adjusted OR was 1.43 (95% CI 0.51–3.99; $P = 0.50$; $I^2 = 20\%$) (Fig. 2).

Discussion

Our study suggests that AIS patients without visible arterial occlusion treated with IV-rtPA may have a no

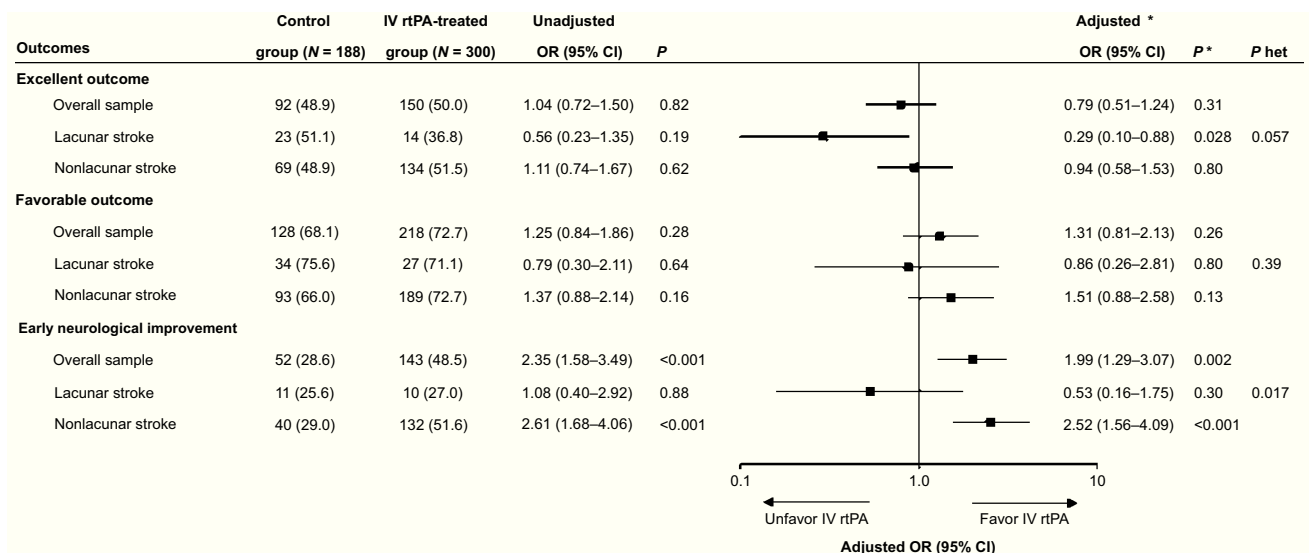


Figure 1 Clinical efficacy outcomes in IV-rtPA-treated and control groups, overall and according to lacunar stroke subtype. *Adjusted for antithrombotic therapy, prior stroke history, admission systolic blood pressure, diastolic blood pressure, National Institutes of Health Stroke Scale, pre-stroke Rankin ≥ 1 , lacunar stroke aetiology and time to admission from symptom onset. P values for heterogeneity between lacunar and non-lacunar stroke (P het) are reported. CI, confidence interval; IV, intravenous; OR, odds ratio; rtPA, recombinant tissue plasminogen activator.

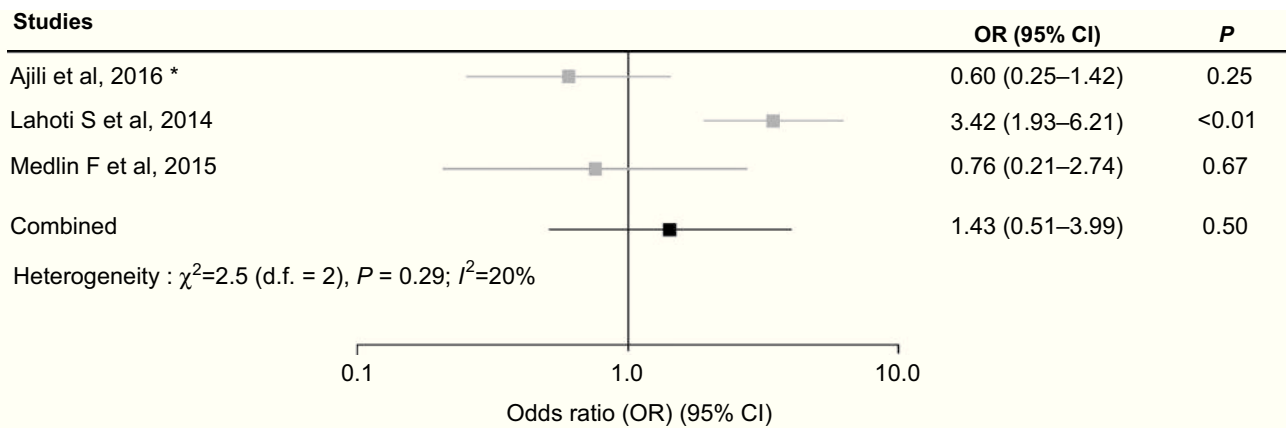


Figure 2 Meta-analysis pooling the available adjusted odds ratios (ORs) of favourable outcome. *This paper; calculated after excluding the 236 overlapping participants in the Medlin *et al.* publication.

better outcome at three months than those untreated. However, they have better early neurological improvement without evidence of safety concerns.

Acute ischaemic stroke patients without arterial occlusion are commonly admitted to stroke centres, and such a situation may result from either a spontaneous recanalization before vascular imaging in 17% [3] or a lacunar infarction in up to 30% of patients [2]. Our results are consistent with the hypothesis that IV-rtPA may not benefit AIS patients without arterial occlusion as suggested by previous reported studies [5,11,12]. The issue of IV-rtPA benefit according to the occlusion status in AIS was first debated after *post hoc* subgroup analysis from the NINDS trial [13]. Recently, Medlin *et al.* [5] reported, in 272 AIS patients with no/minimal arterial occlusion, no improved outcome in IV-rtPA-treated patients compared to those who did not undergo thrombolysis (adjusted OR 0.76; 95% CI 0.21–2.74).

Interestingly, Lahoti *et al.* [4] reported opposite findings with a benefit of IV-rtPA amongst 256 stroke patients without arterial occlusion. In the latter study, high ORs for favourable outcome (3.42, 95% CI 2.05–7.03) [4] were observed, which contrasts with the non-significant OR observed in our study (1.25, 95% CI 0.84–1.86) or the OR from Medlin *et al.* [5] (0.71, 95% CI 0.21–2.74). It cannot be excluded that these discrepancies may be explained by differences in the patients' baseline characteristics. Besides, Lahoti *et al.*'s study did not adjust for confounding factors, such as pre Rankin score, onset to admission time, which may have potentially affected their results [4]. Nevertheless, in meta-analysis combining these results, the combined adjusted OR for favourable outcome was not significant (pooled OR 1.43; 95% CI 0.51–3.99) (Fig. 2).

In the present study, the effect of IV-rtPA also differed according to stroke aetiology. Indeed, although there was no significant benefit of IV-rtPA on the overall sample of 488 patients whatever the outcomes (Fig. 1), adjusted OR of ENI for IV-rtPA-treated patients was 2.52 (95% CI 1.56–4.09, $P < 0.001$) in non-lacunar stroke patients but not for those with lacunar stroke, in a stratified analysis.

A trend for the benefit of IV-rtPA on favourable outcome was seen only for non-lacunar stroke (adjusted OR 1.51; 95% CI 0.88–2.58). Lahoti *et al.* [4] found the same result when they stratified according to lacunar and non-lacunar stroke aetiology. IV-rtPA increased the rates of excellent or favourable outcome in the non-lacunar group but not in the lacunar group [4].

Several hypotheses may explain the difference of IV-rtPA according to lacunar or non-lacunar stroke patients. It could be speculated that cardioembolic stroke or extra/intra-cranial atherosclerosis stroke (i.e. non-lacunar stroke patients) may be more sensitive to IV-rtPA than lacunar stroke. Although the lacunar group sample was limited ($n = 83$), a detrimental effect of IV-rtPA was found on excellent outcome (adjusted OR 0.29; 95% CI 0.10–0.88). The detrimental effect of IV-rtPA found in lacunar stroke patients was not associated with an increased risk of intracerebral haemorrhage, despite the presence of small vessel disease usually associated with such AIS. It can be hypothesized that high blood pressure management may play a role in this detrimental effect in lacunar stroke, as suggested in a *post hoc* analysis of the SCAST trial [14]. rtPA-treated stroke patients require a lower blood pressure target such as systolic blood pressure <185 mmHg and diastolic blood pressure <110 mmHg. This lower blood pressure target may impact lacunar versus non-lacunar stroke

differently. This point must be evaluated in further prospective trials.

However, the debated definition of lacunar stroke as suggested elsewhere [15], together with the small sample size of lacunar patients in our study, make it difficult to draw any definite conclusion from these findings. These differences between lacunar and non-lacunar subgroups should be interpreted with extreme caution since only a small number of patients with lacunar strokes were included in our cohort.

The increased probability of early improvement for IV-rtPA-treated patients was driven by non-lacunar stroke patients. Amongst non-lacunar stroke patients, the discrepancy between a significantly improved ENI and the lack of benefit on an excellent outcome at 3 months may be explained by the fact that patients without occlusion have spontaneously a better 3 month prognosis (rate of favourable outcome 68.1%; Fig. S1).

None of the previous rtPA trials in AIS routinely assessed or controlled for arterial pathology. However, recent data were published from the International Stroke Trial (IST-3) [16]. Amongst 3035 patients enrolled in IST-3, 342 were classified as lacunar arterial cerebral infarction (LACI, subtype defined by the Oxfordshire Community Stroke Project classification, thus without occlusion). Amongst lacunar patients, the adjusted OR of the effect of rtPA on functional outcome at 6 months was 1.17 (0.70–1.94). Besides, in the LACI subgroup of IST-3, eight (5%) patients suffered from symptomatic intracerebral haemorrhage versus none in the control group. These results confirm the trend observed in our study of the absence of beneficial effect of rtPA on the mRS and a non-significant increase of symptomatic intracerebral haemorrhage (rtPA-treated group, 6% vs. 3%).

But, the test of heterogeneity was not significant ($P = 0.867$) suggesting that the global beneficial effect (adjusted ordinal analysis of Oxford Handicap score) of rtPA in IST-3 may be applicable to lacunar patients.

In our study, MRA or CTA were used according to local protocols. Furthermore, the presence of a small distal occlusion cannot be ruled out in some cases, especially with CTA. Indeed, the sensitivity of CTA and MRA for detecting distal branch occlusions is limited [17].

The present study has several limitations. First, our findings are derived from observational non-randomized analyses which are subject to well-known limitations. The first is the potential for confounding factors by measured or unmeasured variables, which cannot be ruled out. However, the findings were

consistent after several methods of adjustment and sensitivity analyses (Fig. S2).

Secondly, the analysis of IV-rtPA effect amongst a stroke population with no occlusion and good outcome exposes a risk of lack of power. However, our study included the largest reported series of stroke patients without arterial occlusion studied in the acute phase of ischaemic stroke ($n = 488$). A *post hoc* power analysis was performed using the observed excellent outcome rate (60%). With 80% power, an OR of 2.3 could be detected with our study sample. For these reasons, the present findings can be considered as hypothesis-generating.

Although IV-rtPA-treated patients without visible occlusion did not have a better outcome at 3 months than without rtPA, a better ENI is shown in non-lacunar patients. Taking this into account could reduce cost by shortening the duration of hospitalization and decreasing the length of rehabilitation.

Besides, our observations support that there are no safety concerns in using IV-rtPA in patients without occlusion and that IV-rtPA may have some beneficial effects (faster recovery, a trend towards fewer deaths).

Further randomized controlled trials, analysis of prospective registry data and cost/effectiveness study analysis are warranted to address the level of efficacy of IV thrombolysis treatment in AIS without occlusion. Our conclusion is that only a randomized controlled trial would provide a definitive answer about the impact of rtPA in acute stroke patients without occlusion. Until then, these patients should be treated by rtPA as recommended.

Acknowledgements

We thank Mary Osborne-Pellegrin for help in editing the final draft of the manuscript.

Disclosure of conflicts of interest

The authors declare no financial or other conflicts of interest.

Supporting Information

Additional Supporting Information may be found in the online version of this article:

Figure S1. Distribution of modified Rankin Score at 90 days in control and IV-rtPA-treated groups.

Figure S2. Sensitivity analyses for comparison in clinical efficacy outcomes between control and IV-rtPA-treated groups. (A) Sensitivity analysis excluding

patients with a pre-stroke Rankin ≥ 1 . (B) Sensitivity analysis after adjusting for propensity score[†].

References

1. Wardlaw JM, Murray V, Berge E, *et al.* Recombinant tissue plasminogen activator for acute ischaemic stroke: an updated systematic review and meta-analysis. *Lancet* 2012; **379**: 2364–2372.
2. Bejot Y, Catteau A, Caillier M, *et al.* Trends in incidence, risk factors, and survival in symptomatic lacunar stroke in Dijon, France, from 1989 to 2006: a population-based study. *Stroke* 2008; **39**: 1945–1951.
3. Kassem-Moussa H, Graffagnino C. Nonocclusion and spontaneous recanalization rates in acute ischemic stroke: a review of cerebral angiography studies. *Arch Neurol* 2002; **59**: 1870–1873.
4. Lahoti S, Gokhale S, Caplan L, *et al.* Thrombolysis in ischemic stroke without arterial occlusion at presentation. *Stroke* 2014; **45**: 2722–2727.
5. Medlin F, Amiguet M, Vanacker P, Michel P. Influence of arterial occlusion on outcome after intravenous thrombolysis for acute ischemic stroke. *Stroke* 2015; **46**: 126–131.
6. Michel P, Odier C, Rutgers M, *et al.* The Acute Stroke Registry and Analysis of Lausanne (ASTRAL): design and baseline analysis of an ischemic stroke registry including acute multimodal imaging. *Stroke* 2010; **41**: 2491–2498.
7. Lainay C, Benzenine E, Durier J, *et al.* Hospitalization within the first year after stroke: the Dijon Stroke Registry. *Stroke* 2015; **46**: 190–196.
8. Hacke W, Kaste M, Bluhmki E, *et al.* Thrombolysis with alteplase 3 to 4.5 hours after acute ischemic stroke. *N Engl J Med* 2008; **359**: 1317–1329.
9. Bruno A, Shah N, Lin C, *et al.* Improving modified Rankin Scale assessment with a simplified questionnaire. *Stroke* 2010; **41**: 1048–1050.
10. D'Agostino RB Jr. Propensity score methods for bias reduction in the comparison of a treatment to a non-randomized control group. *Stat Med* 1998; **17**: 2265–2281.
11. Sylaja PN, Dzialowski I, Puetz V, *et al.* Does intravenous rtPA benefit patients in the absence of CT angiographically visible intracranial occlusion? *Neurol India* 2009; **57**: 739–743.
12. Shobha N, Bhatia R, Boyko M, *et al.* Outcomes in acute ischemic strokes presenting with disabling neurologic deficits without intracranial vascular occlusion. *Int J Stroke* 2011; **6**: 392–397.
13. Ingall TJ, O'Fallon WM, Asplund K, *et al.* Findings from the reanalysis of the NINDS tissue plasminogen activator for acute ischemic stroke treatment trial. *Stroke* 2004; **35**: 2418–2424.
14. Hornslien AG, Sandset EC, Igland J, *et al.* Effects of candesartan in acute stroke on vascular events during long-term follow-up: results from the Scandinavian Candesartan Acute Stroke Trial (SCAST). *Int J Stroke* 2015; **10**: 830–835.
15. Potter GM, Marlborough FJ, Wardlaw JM. Wide variation in definition, detection, and description of lacunar lesions on imaging. *Stroke* 2011; **42**: 359–366.
16. Lindley RI, Wardlaw JM, Whiteley WN, *et al.* Alteplase for acute ischemic stroke: outcomes by clinically important subgroups in the Third International Stroke Trial. *Stroke* 2015; **46**: 746–756.
17. Demchuk AM, Menon BK, Goyal M. Comparing vessel imaging: noncontrast computed tomography/computed tomographic angiography should be the new minimum standard in acute disabling stroke. *Stroke* 2016; **47**: 273–281.

Annexe VI: "Increased functional connectivity between language and visually deprived areas in late and partial blindness"



Contents lists available at ScienceDirect

NeuroImage

journal homepage: www.elsevier.com/locate/ynimg

Increased functional connectivity between language and visually deprived areas in late and partial blindness

Norman Sabbah^{a,b,c,d,*}, Colas N. Authié^{a,b,c,d}, Nicolae Sanda^{a,b,c,d}, Saddek Mohand-Saïd^{a,b,c,d},
José-Alain Sahel^{a,b,c,d,f,g}, Avinoam B. Safran^{a,b,c,d,h}, Christophe Habas^{a,b,c,e}, Amir Amedi^{a,b,c,i,j,k,**}

^a Sorbonne Universités, UPMC Université Paris 06, UMR S968, Institut de la Vision, Paris, F-75012, France

^b INSERM, U968, Institut de la Vision, Paris F-75012, France

^c CNRS, UMR 7210, Institut de la Vision, Paris F-75012, France

^d Centre d'investigation clinique, Centre Hospitalier National d'Ophtalmologie des Quinze-Vingts, INSERM-DHOS CIC 1423, Paris F-75012, France

^e Centre de neuroimagerie, Centre Hospitalier National d'Ophtalmologie des Quinze-Vingts, Paris F-75012, France

^f Institute of Ophthalmology, University College of London, United Kingdom

^g Fondation Ophtalmologique Adolphe de Rothschild, Paris, France

^h Department of Clinical Neurosciences, Geneva University School of Medicine, Geneva, Switzerland

ⁱ Department of Medical Neurobiology, The Institute for Medical Research Israel–Canada, Faculty of Medicine, The Hebrew University of Jerusalem, Jerusalem 91220, Israel

^j The Edmond and Lily Safra Center for Brain Sciences (ELSC), The Hebrew University of Jerusalem, Jerusalem 91220, Israel

^k The Cognitive Science Program, The Hebrew University of Jerusalem, Jerusalem 91220, Israel

ARTICLE INFO

Article history:

Received 17 December 2015

Revised 12 April 2016

Accepted 22 April 2016

Available online xxx

Keywords:

Adult brain plasticity
Critical periods
Cerebral reorganization
Resting-state fMRI
Retinitis pigmentosa
Brain connectivity
Language
Vision

ABSTRACT

In the congenitally blind, language processing involves visual areas. In the case of normal visual development however, it remains unclear whether later visual loss induces interactions between the language and visual areas. This study compared the resting-state functional connectivity (FC) of retinotopic and language areas in two unique groups of late visually deprived subjects: (1) blind individuals suffering from retinitis pigmentosa (RP), (2) RP subjects without a visual periphery but with preserved central “tunnel vision”, both of whom were contrasted with sighted controls. The results showed increased FC between Broca's area and the visually deprived areas in the peripheral V1 for individuals with tunnel vision, and both the peripheral and central V1 for blind individuals. These findings suggest that FC can develop in the adult brain between the visual and language systems in the completely and partially blind. These changes start in the deprived areas and increase in size (involving both foveal and peripheral V1) and strength (from negative to positive FC) as the disease and sensory deprivation progress. These observations support the claim that functional connectivity between remote systems that perform completely different tasks can change in the adult brain in cases of total and even partial visual deprivation.

© 2016 Elsevier Inc. All rights reserved.

Introduction

Functional magnetic resonance imaging studies have shown that the relationship between the language and visual areas varies depending on the presence or absence of visual function. For instance, during an abstract word recall task, sighted individuals exhibited strong visual area deactivation alongside activation of language specific regions (Azulay et al., 2009). In congenitally blind subjects, however, most groups

have reported strong activation of the early visual cortex in addition to the classical language areas (e.g. Broca's area) during both verbal memory (Amedi et al., 2003; Azulay et al., 2009) and language-related verb generation tasks (Amedi et al., 2003; Burton et al., 2002a, 2003). Activations of visual areas also play a functional role in both semantic memory and generation tasks, in that blind individuals showing strong recruitment of V1 also demonstrated superior performance in such processes (Amedi et al., 2003; Raz et al., 2005). Furthermore, language-related early visual cortex activity was shown to make a key contribution to this task in congenitally blind but not in sighted individuals. This is one of the very few examples of a causal relationship indicative of cross-modal plasticity in the blind (Amedi et al., 2004). Bedny et al.'s recent study using a variety of well-controlled language tasks showed that activity in the visual (essentially left) areas actually reflected complex language processing in the congenitally blind. They suggested that there was a critical period for this recruitment, as no such activation was found in the late blind (Bedny et al., 2011, 2012).

Abbreviations: FC, functional connectivity; RP, retinitis pigmentosa; fMRI, functional magnetic resonance imaging; rs-fMRI, resting-state functional magnetic resonance imaging.

* Correspondence to: N. Sabbah, Institut de la vision, UMR S968, 17 rue Moreau 75012, Paris, France.

** Correspondence to: A. Amedi, Department of Medical Neurobiology, Faculty of Medicine, The Hebrew University of Jerusalem, Jerusalem 91220, Israel.

E-mail addresses: norman.sabbah@gmail.com (N. Sabbah), amira@ekmd.huji.ac.il (A. Amedi).

<http://dx.doi.org/10.1016/j.neuroimage.2016.04.056>

1053-8119/© 2016 Elsevier Inc. All rights reserved.

Please cite this article as: Sabbah, N., et al., Increased functional connectivity between language and visually deprived areas in late and partial blindness, NeuroImage (2016), <http://dx.doi.org/10.1016/j.neuroimage.2016.04.056>

Anatomically, the semantic processing of the occipital cortex is likely supported by the inferior frontal–occipital fasciculus (IFOF), namely its superficial layer and the posterior component of the deep layer (Sarubbo et al., 2013). Congenitally but not late blind individuals exhibit altered IFOF, decreased structural global connectivity efficiency and increased local connectivity efficiency both in occipital and frontal lobes (Li et al., 2013; Shu et al., 2009; Reisleve et al., 2016). These structural changes, together with the above mentioned functional and behavioral data point to early absence of visual input altering brain structure to serve specific tuned-up non-visual functions of occipital cortex. Do only congenitally blind individuals develop this type of early visual cortex recruitment for language and memory? Or can it also occur in the late blind? This issue goes beyond the field of blindness to the wider question of whether this processing can only occur during critical or sensitive periods in childhood or whether some traces and mechanisms for this ability are present even in the adult brain (Bavelier and Neville, 2002; Bedny et al., 2012; Sadato et al., 2002). This has implications for rehabilitation, especially in the context of stroke since the loss of a specialized area requires another area to take over the missing function (Pascual-Leone et al., 2005). It also remains unclear whether visual deprivation needs to be complete for such plasticity to emerge or whether some changes can start even in the presence of residual vision (Cunningham et al., 2015). Finally, little is known about the large-scale anatomical and functional changes that might support such radical brain plasticity.

The current literature provides somewhat conflicting observations on these questions. Burton et al. (2002a, 2002b) found that when listening to words, both congenitally and late blind subjects exhibited bilateral activation of the visual cortex regions in addition to language and auditory areas (Burton et al., 2002a). By contrast, Bedny et al. (2012) found that only the congenitally blind – and not the late blind – showed an increased response in V1 to heard sentences as compared to backwards speech. They concluded that recruitment of the visual cortex for language processing depends critically on the age of blindness onset (Bedny et al., 2012). Thus, even in very recent research it remains unclear whether visual cortex activation by language is affected by previous visual experience in the blind. The picture in the effect of partial blindness on adult brain plasticity and visual input is even more limited and debated.

The analysis of resting-state functional connectivity constitutes a rich, efficient approach to studying brain function, brain large-scale connectivity and brain plasticity (Fox and Greicius, 2010; Guerra-Carrillo et al., 2014; Smith et al., 2009) as illustrated in the human connectome project (Hodge et al., 2015). These temporal correlations were shown to echo the co-activation between brain regions found in task-based fMRI studies (Buckner et al., 2013; Dosenbach et al., 2007). Of course like any method, rs-fMRI also has some limitations, which are discussed in depth in the discussion (see [Limitations and methodological considerations](#) section). Nevertheless, rs-fMRI is sensitive enough to detect interactions between specific language regions such as Broca's area and the visual cortex. Several teams found specific increased functional connectivity between the inferior frontal triangular gyrus (part of BA 44, 45, 47) including Broca's area and several occipital visual areas in the congenitally blind as compared to sighted subjects (Liu et al., 2007; Heine et al., 2015). Striem-Amit et al. (2015) recently studied the same type of population and found that central V1 was more tightly connected to language areas whereas peripheral V1 was linked to spatial attention and control networks in the congenitally blind as compared to a sighted group (Striem-Amit et al., 2015). Butt et al. (2013) also analyzed the brain resting-state in a heterogeneous population of blind subjects, and suggested that long-range FC between Broca's area and V1 could be explained by age at blindness onset; however, variability in visual conditions (e.g. age onset of vision loss, cause of the disease, visual field location of the scotoma before blindness) combined with the limited number of subjects in each condition constrained data interpretation (Butt et al., 2013). The type of condition has also been considered

by other authors (Bedny et al., 2012; Watkins et al., 2012), who have argued that retina versus optic nerve disorders or gradual versus sudden loss of vision may differentially affect the reorganization of the visual cortex.

Hence, analyzing the functional resting-state connectivity in visually affected individuals categorized into clinically well-defined homogeneous groups in terms of the etiology of blindness might provide valuable indications whether partial or total late deprivation of vision affects the functional links between Broca's area and the visual cortex. The current work was conducted with clinically homogeneous groups of subjects suffering from retinitis pigmentosa, a retinal degenerative condition that causes particularly structured defects initially involving the visual field periphery (and sparing the central “tunnel vision” area), and eventually leading to complete blindness.

Beyond its theoretical contribution, this study has important clinical implications. Late blind patients suffering from RP are the group most expected to benefit from visual restoration such as retinal prosthesis (Ayton et al., 2014; Stingl et al., 2013; Weiland and Humayun, 2014). The existence of cross-modality plasticity mechanisms in RP subjects has only been investigated in a few studies (Cunningham et al., 2015; Masuda et al., 2010) using other methodologies that the ones employed here. Given that there is some evidence of maladaptive cross-modal plasticity in deaf patients following cochlear implantation (Lee et al., 2001; Striem-Amit et al., 2011a), there is a crucial need to better understand the reorganization following progressive RP visual loss to overcome this potential issue in the context of sight restoration.

The present study thus used brain resting-state to characterize the functional connectivity between Broca's area and sub-regions of the visual cortex in: (1) individuals suffering from RP who still retain central “tunnel vision” – the RP tunnel vision group; and (2) individuals with more severe RP so that now there is not even tunnel vision, and visual loss covers the entire visual field, leading to blindness (please note that such patients might still occasionally have faint light perception but zero form vision, as in advanced disease most individuals report some visual fluctuation, described as “good days and bad days” (see Heckenlively, 1988) – the RP blind group (3) sighted individuals – the sighted control group. The following specific questions were explored:

- (1) What is the pattern of functional connectivity between Broca's area and visual areas in the sighted? Does this pattern show negative FC as might be predicted based on the deactivation (negative BOLD) in V1 to language and memory tasks (Azulay et al., 2009)?
- (2) Do Broca's and visual areas exhibit a different pattern of functional connectivity in the RP blind (e.g. reversal to positive FC)?
- (3) What is the functional connectivity of these same regions for RP tunnel vision subjects? Is a complete lack of visual input necessary for the development of such changes?
- (4) Does this pattern vary according to the topography of the visual retinotopic areas; e.g. does the peripheral visual cortex show a different pattern of connectivity than the foveal across groups, as might be predicted by the fact that at the tunnel vision stage, the disease affects more peripheral than central areas of the visual field?

Materials and methods

Subjects and ethics

The sample was made up of 35 subjects divided into 3 groups. Subjects were matched for age, and no subject had any reported neurological or psychiatric antecedents (Table 1).

- 11 retinitis pigmentosa (RP) tunnel vision subjects (four women; eight right-handed), presenting a residual central visual field limited to a 10–20° diameter (as evaluated by Goldmann III/4 kinetic perimetry), with a best-corrected visual acuity equal or superior to

Table 1
Subjects' clinical data. B: RP blind subjects, TV: RP tunnel vision subjects. S: sighted control subjects. N: Normal visual field, i.e. 130°–140° in horizontal diameter. Blindness duration: number of years since the subjects lost any form vision in all parts of their visual field but might still keep some bare light perception. BLP: Bare light perception. NLP: No light perception.

Subject	Sex	Age	Cause of blindness	Light perception	Left eye visual acuity (logmar)	Right eye visual acuity (logmar)	Left eye visual field diameter (°)	Right eye visual field diameter (°)	Blindness duration (years)	Handedness	Braille
B1	F	29	Retinitis pigmentosa	NLP	None	None	0	0	8	R	Yes
B2	F	57	Retinitis pigmentosa	BLP	None	None	0	0	17	R	Yes
B3	F	31	Retinitis pigmentosa	BLP	None	None	0	0	10	R	Yes
B4	H	62	Retinitis pigmentosa	BLP	None	None	0	0	19	R	Yes
B5	H	44	Retinitis pigmentosa	BLP	None	None	0	0	14	R	No
B6	H	56	Retinitis pigmentosa	BLP	None	None	0	0	7	R	Yes
B7	H	44	Retinitis pigmentosa	BLP	None	None	0	0	4	R	No
B8	F	60	Retinitis pigmentosa	BLP	None	None	0	0	15	R	Yes
B9	F	47	Retinitis pigmentosa	BLP	None	None	0	0	12	R	No
B10	H	59	Retinitis pigmentosa	BLP	None	None	0	0	6	R	No
B11	F	62	Retinitis pigmentosa	BLP	None	None	0	0	6	R	No
TV1	H	28	Retinitis pigmentosa	–	0	0.15	15	15	–	L/R	No
TV2	H	55	Retinitis pigmentosa	–	0	0.1	10	15	–	R	No
TV3	F	62	Retinitis pigmentosa	–	0.3	0.2	10	10	–	R	No
TV4	H	62	Retinitis pigmentosa	–	0.1	0.1	10	10	–	R	No
TV5	F	43	Retinitis pigmentosa	–	0.1	0.1	15	15	–	L	No
TV6	H	60	Retinitis pigmentosa	–	0.3	0.2	10	10	–	L/R	No
TV7	F	37	Retinitis pigmentosa	–	0.3	0.3	12	12	–	R	No
TV8	H	29	Retinitis pigmentosa	–	0.4	0.2	10	10	–	R	No
TV9	F	29	Retinitis pigmentosa	–	0	0	15	15	–	R	No
TV10	H	59	Retinitis pigmentosa	–	0.3	0.3	7	10	–	R	No
TV11	H	63	Retinitis pigmentosa	–	0.5	0.6	20	20	–	R	No
S1	F	42	–	–	0	0	N	N	–	R	No
S2	H	58	–	–	0	0	N	N	–	R/L	No
S3	H	31	–	–	0	0	N	N	–	R	No
S4	F	54	–	–	0	0	N	N	–	R	No
S5	F	28	–	–	0	0	N	N	–	R	No
S6	F	36	–	–	0	0	N	N	–	R	No
S7	F	59	–	–	0	0	N	N	–	R	No
S8	F	61	–	–	0	0	N	N	–	R	No
S9	H	57	–	–	0	0	N	N	–	R	No
S10	H	59	–	–	0	0	N	N	–	R	No
S11	F	63	–	–	0	0	N	N	–	R	No
S12	F	54	–	–	0	0	N	N	–	R	No
S13	H	56	–	–	0	0	N	N	–	R	No

20/40 (measured by EDTRS charts). Ages ranged from 28 to 63 years (mean: 47.9, median: 55.0). None read Braille.

- 11 RP blind subjects (six women; all right-handed), as defined by a complete loss of the entire visual field that might be accompanied by some form of bare light perception. Ages ranged from 29 to 62 years (mean: 50.1, median: 56). Six were Braille readers.
- 13 Sighted controls (eight women; 12 right-handed), with unremarkable routine ophthalmological examinations (normal visual acuity and visual field, as evaluated by Goldmann III/4 kinetic perimetry). Ages ranged from 28 to 63 years (mean: 49.2, median: 54.0). None read Braille.

The Ethics Committee (Comité de protection des personnes, Ile de France V, and Agence Nationale de Sécurité du Médicament et des Produits de Santé) approved the experimental protocol (number 12873), and all subjects gave their written informed consent (according to the Declaration of Helsinki) before participating.

Functional imaging

fMRI was conducted on a whole-body 3T clinical imager (Sigma Horizon) by using an 8-channel head coil. In each scanning sequence, 32 contiguous axial T2*-weighted gradient-echo echo-planar images (TE/TR, 93/3000 ms; FOV, 240 × 240 mm; matrix, 64 × 64; voxel size, 3.75 × 3.75 × 4 mm; thickness, 4 mm; interslice spacing, 0 mm; NEX, 1) were recorded to encompass the entire brain. 180 volumes were acquired including 4 “dummy” volumes obtained at the start of the session. The scan duration was 9.25 min for the echo planar imaging

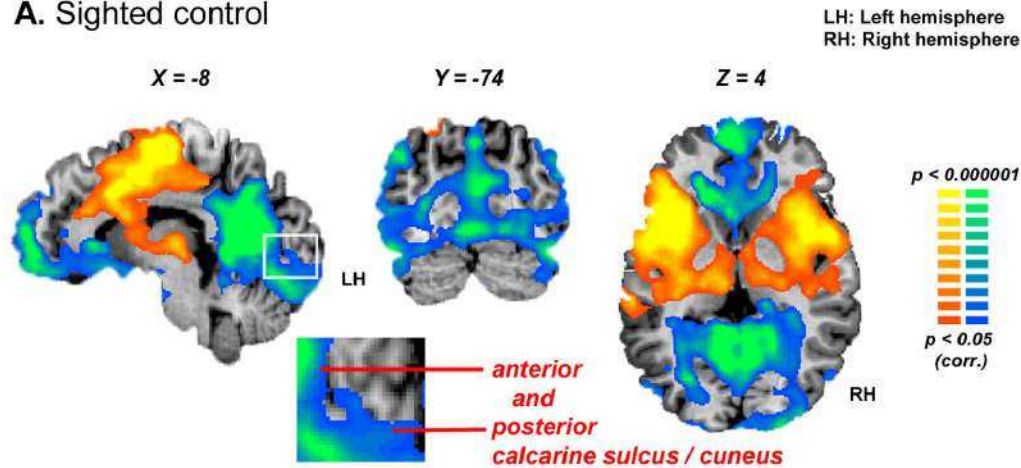
sequence. Off-line, T2*-weighted images were co-registered and overlaid on the corresponding anatomic T1-weighted gradient-echo images (TE/TR/flip angle, 3.9/9.5 ms/20°; FOV, 25.6 × 25.6 mm; matrix, 512 × 512; source voxel size, 1.2 × 0.5 × 0.5 mm converted to 1 × 1 × 1 mm; thickness, 1.2 mm; interslice spacing, 1.2 mm). During the scan, subjects were supine in the magnetic resonance imaging scanner and wore earplugs to compensate for the noisy environment. Subjects were instructed to keep their eyes closed. No explicit task was required.

fMRI preprocessing

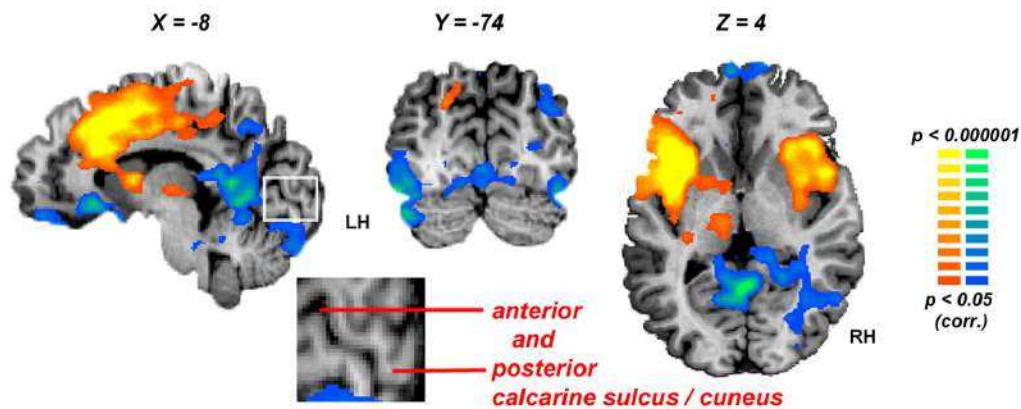
fMRI data were preprocessed using the BrainVoyager QX 2.8 software package (Brain Innovation, Maastricht, Netherlands) and complementary software written in MATLAB R2009a (MathWorks, USA). Preprocessing of functional scans included: slice-time correction, 3D motion correction (no head motion exceeded 2 mm in any direction; which means movements are maximum in the order of magnitude of one functional voxel only as voxels size was: 3.75 × 3.75 × 4 mm) in order to control and remove artifacts, band-pass filtering between 0.01 and 0.1 Hz to regress non-relevant frequencies (e.g. breathing, pulse), voxel-to-voxel linear regression (Cole et al., 2010) of spurious signal from the white matter and ventricles regions anatomically defined for each subject, normalization in the Talairach coordinate system in the volume (Talairach and Tournoux, 1988), and spatial smoothing with a Gaussian filter kernel of 6 mm full-width-at-half-maximum. We did not include global signal removing because of the potential introduction of false negative correlations (see Murphy et al., 2009). For the between groups comparison we tested and found no significant

Within-group FC analysis seeded from Broca's area (calcarine sulcus/cuneus)

A. Sighted control



B. RP tunnel vision



C. RP blind

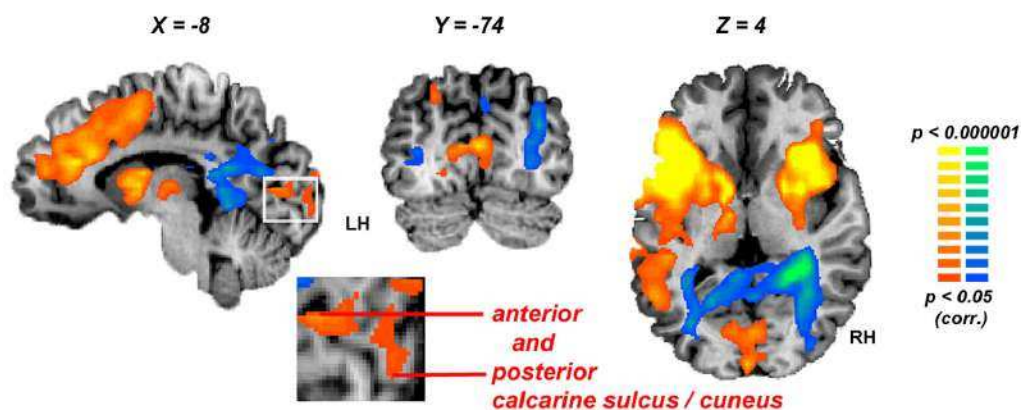


Fig. 1. Within-group analysis of functional connectivity seeded from Broca's area. The maps are shown in fMRI full-slice view (neurological convention) for (A) Sighted controls, (B) RP tunnel vision, (C) RP blind subjects. Colors depict the magnitude of the FC of Broca's area localizer and the rest of the brain: yellow-orange for positive FC and green-blue for negative FC. X, Y, Z are in Talairach coordinates. In all groups, the inferior frontal Broca's area is functionally connected to the anterior cingulate, left supramarginal gyrus (e.g. Wernicke's area), subcortical regions (e.g. bilateral insula, thalamus), superior temporal auditory regions and bilateral fronto-parietal regions. (A) The sighted control subjects show a strong negative FC of Broca's area with major ventral and dorsal visual areas (i.e. along the calcarine sulcus/lingual, cuneus, inferior occipital, middle occipital, parahippocampal, retrosplenial, fusiform, and inferior temporal gyri) and medial part of the superior frontal gyrus. (B) RP tunnel vision subjects show almost no negative FC of Broca's area with calcarine sulcus/cuneus but still preserve a negative FC with the inferior occipital, middle occipital, lingual, parahippocampal, retrosplenial, fusiform, and inferior temporal gyri. (C) RP blind subjects show positive FC of Broca's area with the calcarine sulcus/cuneus and lose almost all negative functional connectivity with the other extrastriate visual areas.

difference (or even a trend) in the extent (mm) of head movement between the three groups (ANOVAs: $p > 0.05$ for each direction: X, Y, Z, translations, X, Y, Z, rotations; see Supplementary Table S1). These data were confirmed by repeating the GLM analysis (see [Seed ROI definition and analysis](#) section) including the head movement predictors (control analysis; see Supplementary Fig. S1). Including these movement predictors in the GLM did not change the main results.

Seed ROI definition and analysis

For each subject, a seed region-of-interest (ROI) consisting of a 5 mm-radius sphere was located in Broca's area (BA45, pars triangularis; Talairach coordinates: $-39, 17, 11$; see (Burton et al., 2002a; Sarubbo et al., 2013)) which served to extract the blood-oxygen level-dependent time-course of this region (Burton et al., 2003). The average time-course for each subject was calculated, z-transformed and used as individual predictors in a group random-effect analysis based on the general linear model (GLM) (see Fig. 1; Friston et al., 1999). To establish a contrast among groups, a between-subject random effect ANOVA was performed with a significance level of $p < 0.05$, corrected for multiple comparisons using cluster-size thresholding (Forman et al., 1995; Goebel et al., 2006; Striem-Amit et al., 2015) implemented in BrainVoyager using the Monte Carlo simulation approach (see Figs. 2 and 3). This method takes the data contiguity of neighboring voxels directly into account and corrects for the false-positive rate of continuous clusters (a set-level statistical inference correction; corrected to $p < 0.05$).

External functional localizers

External functional localizers were used to define the seed ROI from visual localizers (left hemisphere foveal V1, peripheral V1). Each of these localizers was extracted from a group of sighted controls and analyzed in normalized Talairach space using a random effect GLM, which enabled generalization of the findings to the population (see details below; Friston et al., 1999).

To define the primary visual cortex seeds, 13 control subjects were scanned in a standard phase-encoded retinotopic mapping procedure, with ring (eccentricity mapping) and wedge (polar mapping) stimuli to establish the visual retinotopic mapping (Engel et al., 1994; Sereno et al., 1995; Striem-Amit et al., 2015; Wandell et al., 2007; Wandell and Winawer, 2011) delivered during the two separate experiments. The stimuli were projected via an LCD screen positioned over the subject's forehead and watched through a tilted mirror. In Experiment 1 an annulus was projected, expanding from 0° to 34° of the subject's visual field in 30 s, repeated 10 times. Experiment 2 included a wedge with a polar angle of 22.5° that rotated around the fixation point, and completed a cycle in 30 s repeated 20 times. Both the annulus in Experiment 1 and the wedge in Experiment 2 contained a flickering (6 Hz) radial checkerboard pattern with respect to standard retinotopic procedures (Engel et al., 1994) for the mapping of field maps. In both cases, there was a 30 s mute period before and after the visual stream for baseline. Group phase analysis was conducted on the two experiments as done in other studies from our group (Hertz and Amedi, 2010; Striem-Amit et al., 2011b) resulting in group maps of eccentricity and angle mapping. Angle mapping was then used to define the borders of V1, and the two maps were used to segregate it according to eccentricity (center or periphery of the visual field), laterality (left or right parts of the visual field).

The external functional definition of the early visual cortex was further used to calculate the within-subject correlation between Broca's area and left posterior or anterior calcarine sulcus and cuneus (localizers for the left fovea and the periphery of V1 respectively). Individual average time-courses from ROIs were sampled from each participant. The Pearson correlation coefficient between the time-courses of the two ROIs (within each subject) was calculated (see Fig. 4). ANOVA and Sheffe post-hoc analyses were also performed to test for differences

between the groups ($p < 0.05$). Then, non-parametric Wilcoxon rank sum tests were run on the same data to control for the effect of Braille reading skills in segregated populations of RP blind subjects (see Supplementary Table S2).

To evaluate the effect of age, blindness duration and Braille reading skills (see Supplementary Table S2) on the FC between Broca's area and the extrastriate areas of RP blind subjects, 5 mm-radius spheres were defined according to the most significant foci exhibiting positive FC at the within-group level (i.e. left inferior occipital gyrus, $-24 - 89 - 18$; left middle occipital gyrus $-26 - 89 4$; left fusiform gyrus $-24 - 62 - 7$; left parahippocampal gyrus $-24 - 39 - 8$; see Fig. 3). Then, non-parametric Wilcoxon rank sum and Pearson tests were performed on the correlation coefficients of Broca's area and each of these extrastriate regions in segregated populations of the RP blind subjects (Braille reader vs. non-Braille readers; see Supplementary Table S2).

To summarize, the resting-state data were analyzed by several complementary methods and levels. First, ROI-based seed functional connectivity analysis was performed on the rs-fMRI data to investigate the functional connectivity between the seeded Broca's area and the rest of the brain within each group (see Fig. 1). Next, ANOVAs and post-hoc tests were carried out to compare functional maps between groups (see Figs. 2-4; Table 2). FC coefficients between specific ROIs such as Broca's area and the anterior and posterior regions of the calcarine sulcus were also calculated for each group (see Fig. 4). ANOVAs and post-hoc tests were then performed on the mean z-score correlation coefficients to compare the groups. Finally, non-parametric Wilcoxon rank sum tests and Pearson tests were performed on the level of correlation of Broca's area and both the striate and extrastriate visual areas to control for the effects of age, duration of blindness and Braille reading skills in RP blind subjects (see Supplementary Table S2).

Results

In all groups, the data showed that Broca's area was functionally connected to the anterior cingulate, left supramarginal gyrus (Wernicke's area), the precentral gyrus (e.g. primary motor area), and the subcortical (e.g. bilateral insula, thalamus), auditory (e.g. A1) and frontoparietal regions (see Fig. 1).

In the sighted control within-group analysis, there was strong negative FC between Broca's area and early and high order visual areas as well as the medial part of the superior frontal gyrus. These included the major ventral and dorsal visual areas along the calcarine sulcus (corresponding to Brodmann Area 17/Visual area V1 – Primary visual cortex), cuneus, inferior occipital, lingual, parahippocampal, retrosplenial, fusiform, and inferior temporal gyri (see Fig. 1A).

The RP tunnel vision within-group analysis revealed almost no negative FC between Broca's area and the calcarine sulcus and cuneus but still preserved negative FC with the inferior occipital, lingual, parahippocampal, retrosplenial, fusiform, and inferior temporal gyri (see Fig. 1B).

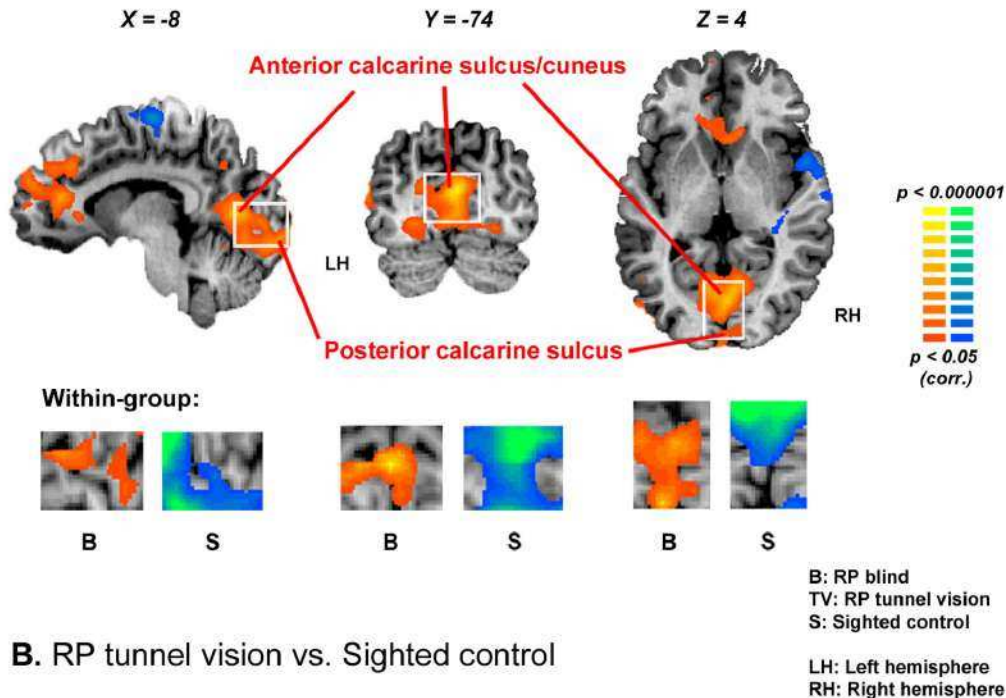
The RP blind group showed a complete reversal of the level of FC between Broca's area and the early visual cortex. The data showed positive FC between Broca's area and the calcarine sulcus/cuneus, but almost all the negative FC with other visual areas was lost (see Fig. 1C).

In the RP blind subjects compared to the sighted controls, between-group analyses revealed a significantly increased level of FC between Broca's area and parts of the calcarine sulcus, cuneus, lingual, left fusiform, left inferior occipital, left parahippocampal, left inferior temporal and medial part of the superior frontal gyri (see Figs. 2A and 3A; for Talairach coordinates of all the peaks for these contrasts see Table 2).

Increased FC between Broca's area and the anterior calcarine sulcus/cuneus as well as the medial part of the superior frontal gyrus was found for the RP tunnel vision subjects compared to the sighted controls (see Fig. 2B; for Talairach coordinates of all the peaks for these contrasts see Table 2).

Between-groups FC analysis seeded from Broca's area (calcarine sulcus/cuneus)

A. RP blind vs. Sighted control



B. RP tunnel vision vs. Sighted control

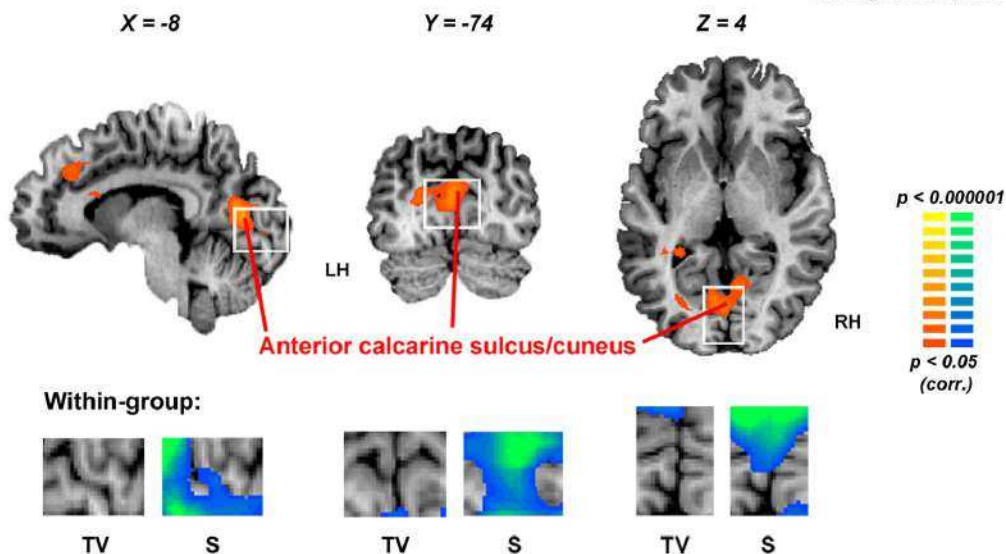


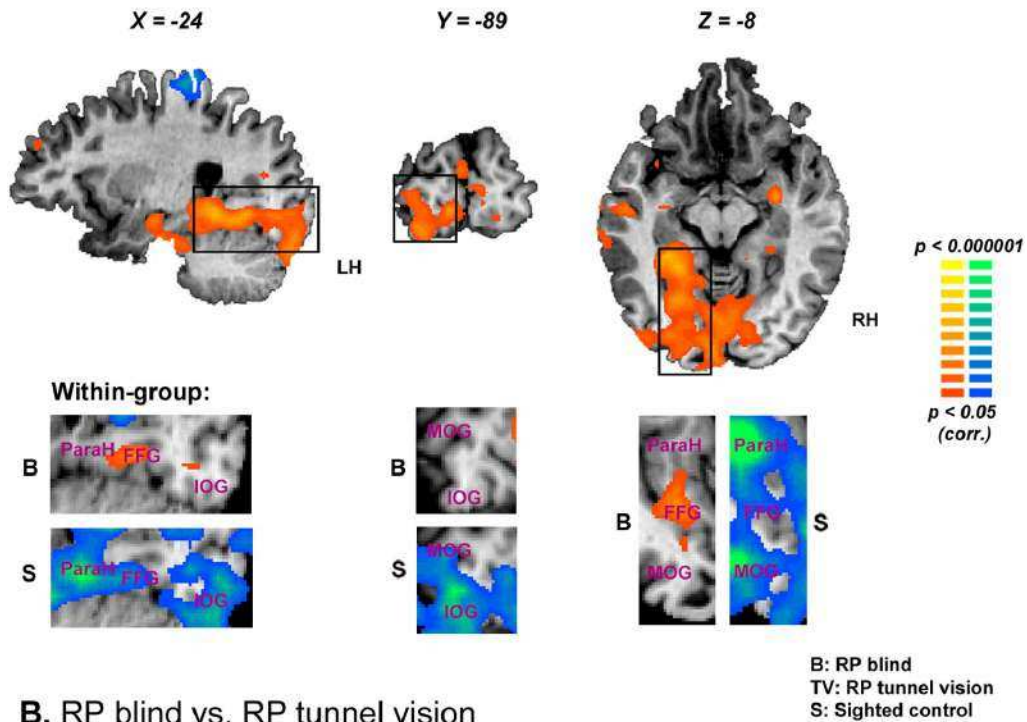
Fig. 2. Between-groups analysis of functional connectivity seeded from Broca's area (focus on calcarine sulcus/cuneus differences). The maps are shown in fMRI full-slice view (neurological convention) for (A) RP blind subjects or (B) RP tunnel vision subjects compared to the sighted control subjects. Colors depict the magnitude of the difference between groups of the FC of Broca's area localizer and the rest of the brain: yellow-orange for increased FC (away from zero) and green-blue for decreased FC (toward zero). X, Y, Z are Talairach coordinates. (A) Increased functional connectivity was found in RP blind subjects compared to sighted control subjects between Broca's area and the calcarine sulcus (Brodmann area 17) delineated in white as well as the cuneus, lingual, fusiform, inferior occipital, parahippocampal and medial part of the superior frontal gyri. (B) Increased functional connectivity was found in RP tunnel vision subjects compared to the sighted control subjects between Broca's area and the anterior calcarine sulcus/Cuneus (Brodmann areas 17–18) and the medial part of the superior frontal gyrus. As between-groups differences could result from positive or (and) negative functional connectivity at the group level, we show the within-group maps for selected regions with a blow-up at the bottom of each figure. Yellow-orange and green-blue represent positive and negative functional connectivity respectively with Broca's area for each group. S: sighted controls. TV: RP tunnel vision. FB: RP blind.

Compared to the RP tunnel vision subjects, the RP blind subjects showed increased FC between Broca's area and specific extrastriate areas such as the left middle occipital, inferior occipital and parahippocampal gyri (see Fig. 3B, Table 2).

In terms of correlation coefficients between ROIs, there was a group main effect for both the left anterior (ANOVA: $F(2,32) = 13.6$ $p < 0.0001$) and posterior (ANOVA: $F(2,32) = 5.78$ $p < 0.01$) calcarine sulcus and Broca's area (see Fig. 4). Post-hoc tests showed (1) a

Between-groups FC analysis seeded from Broca's area (extrastriate areas)

A. RP blind vs. Sighted control



B. RP blind vs. RP tunnel vision

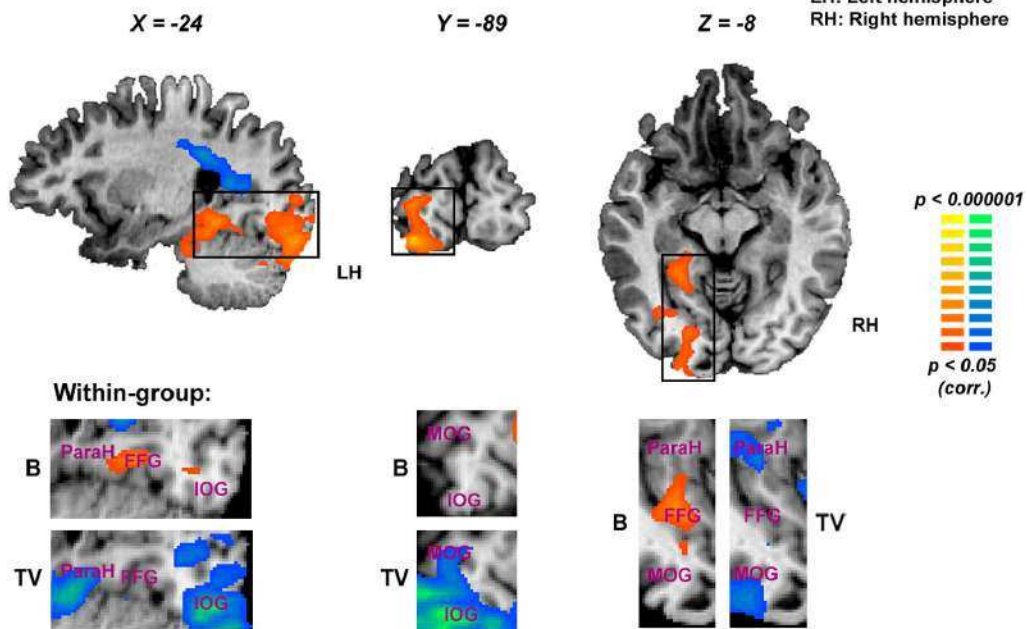


Fig. 3. Between-groups analysis of functional connectivity seeded from Broca's area (focus on extrastriate area differences). The maps are shown in fMRI full-slice view (neurological convention) for RP blind subjects compared to (A) sighted control subjects or (B) RP tunnel vision subjects. Colors depict the magnitude of the difference between groups of the FC of Broca's area localizer and the rest of the brain: yellow-orange for increased FC (away from zero) and green-blue for decreased FC (toward zero). X, Y, Z are Talairach coordinates. (A) Increased functional connectivity was found in RP blind compared to the sighted control subjects between Broca's area and the left fusiform (FFG), parahippocampal (ParaH), inferior (IOG) and middle (MOG) occipital gyri (delineated in black). (B) Increased functional connectivity was found in RP blind subjects compared to RP tunnel vision subjects between Broca's area and the parahippocampal, inferior and middle occipital gyri (delineated in black). As between-groups differences could result from positive or (and) negative functional connectivity at the group level, we show the within-group maps for selected regions with a blow-up at the bottom of each figure. Yellow-orange and green-blue represent positive and negative functional connectivity respectively with Broca's area for each group. S: sighted controls. TV: RP tunnel vision. FB: RP blind.

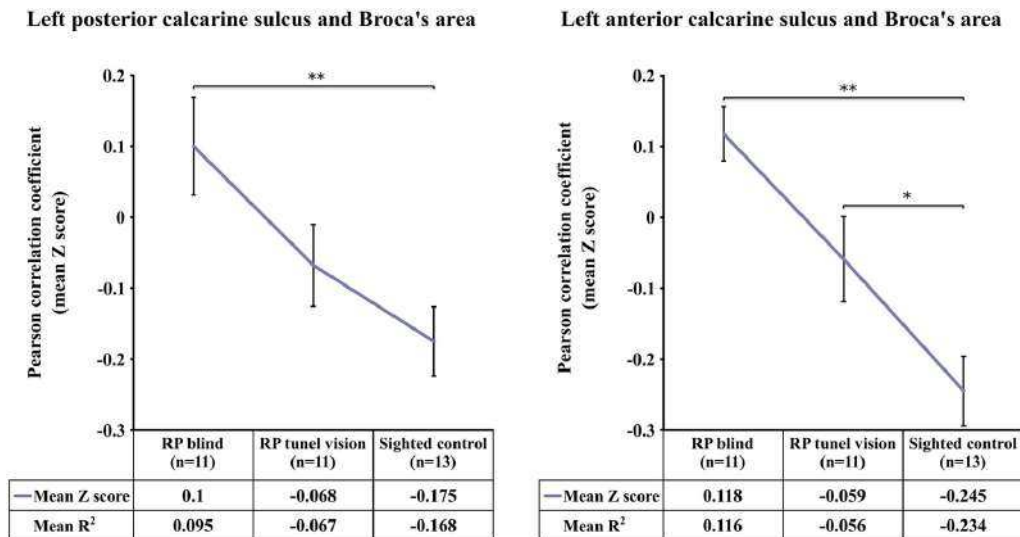


Fig. 4. Correlations between Broca's area and specific parts of the calcarine sulcus across populations (RP blind, RP tunnel vision, sighted control subjects). Correlations (R^2 Pearson test; mean z-score) of Broca's area with (A) left anterior or (B) left posterior calcarine sulcus was calculated for each group. Bars indicate between-subject standard error. (A) There was a group main effect for the correlation between the left anterior calcarine sulcus and Broca's area (ANOVA: $F(2,32) = 13.59$ $p < 0.0001$). Post-hoc tests (Scheffe) revealed significant differences between the RP blind and sighted control subjects' correlation coefficients ($** p < 0.01$), and between RP tunnel vision and sighted control subjects ($* p < 0.05$). (B) There was a main effect for the correlation between the groups for the left posterior calcarine sulcus and Broca's area (ANOVA: $F(2,32) = 5.78$ $p < 0.01$). Post-hoc tests (Scheffe) only revealed significant differences between the RP blind and the sighted control correlation coefficients ($** p < 0.01$). For each group, mean R^2 coefficients before Z transformation are mentioned.

statistically significant difference for both the anterior and posterior regions of the calcarine sulcus and Broca's area between the RP blind and the sighted control subjects ($p < 0.01$; see Fig. 4A–B), and (2) a statistically significant difference solely for the anterior regions of the calcarine sulcus and Broca's area in the RP tunnel vision subjects and the sighted controls ($p < 0.05$; see Fig. 4A).

In the RP blind subjects, Pearson tests revealed no effect for age or blindness duration on the FC between Broca's area and the anterior calcarine sulcus/cuneus (age: $R(9) = 0.32$ $p > 0.05$; blindness duration: $R(9) = 0.24$ $p > 0.05$), posterior calcarine sulcus/cuneus (age: $R(9) = 0.49$ $p > 0.05$; blindness duration: $R(9) = -0.14$ $p > 0.05$), left inferior occipital gyrus (age: $R(9) = -0.024$ $p > 0.05$; blindness duration: $R(9) = 0.18$ $p > 0.05$), left fusiform gyrus (age: $R(9) = 0.51$ $p > 0.05$; blindness duration: $R(9) = 0.094$ $p > 0.05$), and left parahippocampal gyrus (age: $R(9) = 0.23$ $p > 0.05$; blindness duration: $R(9) = -0.12$ $p > 0.05$).

Discussion

In this rs-fMRI study, we explored the FC between Broca's area (BA45, pars triangularis of the inferior frontal gyrus) and visual areas in sighted subjects as well as in two groups of subjects suffering from late onset retinitis pigmentosa (RP), one with tunnel vision (partial blind) and the other RP blind (covering the entire visual field). These groups exhibited negative, null and positive FC patterns respectively (see Fig. 1). Furthermore, in comparison to the sighted controls, both groups of RP subjects presented increased FC between Broca's area and regions of the calcarine sulcus and cuneus that are specifically deprived according to the evolution of their condition (i.e. the anterior part (peripheral V1) for the RP tunnel vision subjects, and both anterior and posterior part of V1 for the RP blind subjects; see Figs. 2 and 4, Table 2). Finally, compared to both the sighted control and the RP tunnel vision subjects, the RP blind showed increased FC between Broca's area and specific extrastriate areas including the left parahippocampal, fusiform, inferior and middle occipital gyri (see Fig. 3, Table 2).

Negative functional connectivity between Broca's area and visual areas in the sighted control group

Several studies support the claim that negative correlations reflect a true reduction in neuronal processing (Behzadi et al., 2007; Chai et al.,

2014; Fox et al., 2005; Guerra-Carrillo et al., 2014; Logothetis et al., 2009; Shmuel et al., 2002, 2006; Shulman et al., 1997; Zeharia et al., 2012).

In the current study, Broca's area in the sighted control group exhibited strong negative FC with the entire calcarine sulcus/cuneus (i.e. V1) and both the ventral and dorsal extrastriate visual areas. This is in agreement with a fMRI study which reported that in a verbal memory retrieval task, sighted subjects showed activation of classical language areas (including Broca's area) coupled with strong deactivation of visual areas including V1 calcarine sulcus and cuneus (Azulay et al., 2009). These study argued that a balance between activation and deactivation is required to filter out irrelevant information and enable an attentional focus on internal representations. This may imply that the negative FC we observed between language/control at rest (i.e. the intrinsic system) and visual (i.e. the extrinsic system) networks could reflect a functional competition that prevents visual inputs from disturbing language processing (for reviews of extrinsic and intrinsic systems see (Fox et al., 2005; Golland et al., 2007, 2008)). Broca's area in the sighted control group also showed negative FC with the medial part of the superior frontal gyrus. We assume based on its anatomical location (talairach coordinates: $-1, 47, -4$; see Fox et al., 2005), that it is part of the default-mode network. In healthy subjects, default-mode network regions are well known to be deactivated in a set of functional tasks (e.g. language), and activated in rest conditions, and would contribute to the emergence of spontaneous inner-oriented thoughts (Greicius et al., 2003; Raichle et al., 2001).

Differences in Broca's area functional connectivity to the calcarine sulcus/cuneus in the three groups

The results help clarify whether the pattern of connectivity can help to support language recruitment in visual areas in subjects with late visual deficits or partial visual deficits like tunnel vision. Burton et al. argued that recruitment can occur in both early and late blind subjects, and that it may be related to the learning of Braille reading (Burton et al., 2002a). More recently, Bedny et al. (2012) only found language-related activation of V1 in early but not in late blind participants (Bedny et al., 2012). They argued that the V1 activation observed in the late blind in previous studies reflects attention or preparation mechanisms and concluded that the recruitment of the visual cortex for

Table 2
Peaks of functional connectivity differences between groups (seed region-of-interest: Broca's area). Peaks X, Y, Z: Talairach coordinates. P values corrected for multiple comparisons. LH: Left hemisphere. RH: Right hemisphere. BA: Brodmann areas.

Contrast peaks	Peak X	Peak Y	Peak Z	t value	p value	BA
RP blind > Sighted control						
LH Anterior calcarine sulcus/cuneus	−2	−71	9	5.58	0.000	17
LH Posterior calcarine sulcus/lingual gyrus	−4	−83	−12	4.13	0.000	18
LH Inferior occipital gyrus	−28	−89	−18	4.05	0.000	18
LH Middle/inferior occipital gyrus	−31	−86	−3	3.80	0.001	18
LH Fusiform gyrus	−25	−62	−9	4.57	0.000	37
LH Parahippocampal gyrus	−31	−38	−9	5.18	0.000	37
LH Inferior temporal gyrus	−52	−14	−18	4.61	0.000	38
LH Anterior cingulate/medial part of the superior frontal gyrus	−13	37	18	5.49	0.000	24/10
RH Anterior calcarine sulcus/cuneus	2	−71	9	6.30	0.000	17
RH Posterior calcarine sulcus/cuneus	8	−89	0	2.84	0.008	17
RH Inferior temporal gyrus	23	1	−33	3.15	0.004	38
Medial part of the superior frontal gyrus	2	46	33	5.06	0.000	9
Sighted control > RP blind						
LH Postcentral gyrus	−25	−32	63	−4.46	0.000	5
LH Precentral gyrus	−7	−17	60	−3.87	0.001	4
RH Superior parietal lobe	17	−50	45	−5.66	0.000	7
RH Supramarginal gyrus	53	−32	39	−4.85	0.000	40
RH Cingulate gyrus	14	−35	30	−3.07	0.004	31
RH Precentral gyrus	14	−17	63	−4.41	0.000	4
RH Middle frontal gyrus	35	34	30	−3.98	0.000	9
RH Inferior frontal gyrus	53	1	18	−3.10	0.004	6
RH Superior temporal gyrus	38	−38	15	−4.03	0.000	39
RH Insula	29	1	15	−4.00	0.000	−
RH Thalamus	20	−17	18	−3.40	0.002	−
RP tunnel vision > Sighted control						
LH Anterior calcarine sulcus/cuneus	−4	−71	9	4.70	0.000	17
LH Anterior cingulate	−13	22	21	2.57	0.015	24
LH Superior frontal gyrus	−13	31	30	3.71	0.001	9
RH Anterior calcarine sulcus/cuneus	2	−68	9	4.12	0.000	17
RH Lingual gyrus	8	−65	9	3.91	0.000	17
Medial part of the superior frontal gyrus	11	49	21	3.06	0.004	10
Sighted control > RP tunnel vision						
RH Superior parietal lobe	30	−47	51	−2.50	0.018	7
RH Supramarginal gyrus	47	−35	30	−3.32	0.002	40
RP blind > RP tunnel vision						
LH Middle occipital gyrus	−28	−86	0	4.04	0.000	17
LH Inferior occipital gyrus	−28	−89	−18	5.18	0.000	18
LH Parahippocampal gyrus	−28	−41	−6	3.22	0.003	37
RP tunnel vision > RP blind						
LH Precuneus	−19	−26	33	−3.38	0.002	24
RH Superior parietal cortex	17	−47	45	−4.38	0.000	7
RH Primary motor cortex	23	−20	45	−3.04	0.005	4

language processing depends on the age of blindness onset (Bedny et al., 2012).

In the current study, the RP blind group exhibited positive Broca's area FC with parts of the calcarine sulcus/cuneus and increased FC of the same regions compared to the sighted controls (see Figs. 1C–2A), which completely reversed the picture of resting state functional connectivity found in the sighted. In the RP blind subjects, the entire visual field is lost, which is probably why the FC to Broca's area stretched from the anterior to the posterior deprived regions of the calcarine sulcus/cuneus (corresponding to early visual areas). However, no evidence for a FC difference was found between Broca's area and regions implicated in attentional mechanisms between groups. In contrast to the hypothesis put forward by Bedny et al. (2012), we suggest that our results might support the recruitment of the early visual areas by the language system, even in blind subjects with previous visual experience, or at least, that the basis for such recruitment emerges from the resting-state functional connectivity pattern. On the other hand, our data do not support the notion that this recruitment is tightly linked to the acquisition of Braille reading skills (Burton et al., 2002a, 2002b; Cunningham et al., 2015) since we did not find significant differences between Braille and non-Braille readers within the RP blind group (see Supplementary Table S2). Thus, the functional relevance of this connectivity still remains unclear. We also evaluated the effect of age and blindness duration, and found no correlation with the FC between

Broca and V1. Overall, these data suggest that there is no critical age for developing functional connectivity between Broca's area and early visual areas or for the complete reversal of their sign from negative FC in the sighted to positive in RP complete late blindness.

The data for the RP tunnel vision subjects were generally consistent with what was found for the RP blind in the sense that they support the hypothesis that recruitment for language processing is specific to visually deprived regions. They also demonstrate that these processes can not only occur in the blind but also in subjects with residual visual function.

The RP tunnel vision subjects showed a slight negative FC of Broca's area with the calcarine sulcus/cuneus (Brodmann area 17; see Fig. 1). However, when compared to the sighted subjects, the RP tunnel vision subjects presented increased FC between Broca's area and specific visually deprived regions (i.e., the anterior but not the posterior part of the calcarine sulcus/cuneus; see Figs. 2 and 4).

In sighted individuals, the anterior and posterior parts of the calcarine sulcus/cuneus code for peripheral and foveal representations of the visual field respectively (Serenio et al., 1995). In the RP tunnel vision subjects, however, the peripheral representation of the visual field is lost whereas the foveal field is preserved (Kalloniatis and Fletcher, 2004). Based on the inter-modality competition hypothesis (Azulay et al., 2009), and given the intra-group null FC for the tunnel vision group, in conjunction with their increased FC compared to the sighted,

we suggest that the language network develops functional connectivity with the sensory deprived early visual cortex and that this connectivity is limited by the remaining foveal vision input. Furthermore, the selective changes observed in the anterior V1 may be related to function re-allocation facilitated by the putative cross-modal abilities of this area (Eckert et al., 2008; Falchier et al., 2002; Wandell and Smirnakis, 2009). It would be worthwhile comparing RP tunnel vision subjects with other clinical conditions in which patients present with central vision loss (e.g. age-related macular degeneration, Stargardt disease) to test whether the posterior/foveal regions of V1 are also functionally connected to the language network.

Thus overall, these findings suggest that (1) dramatic changes occur in functional connectivity between the language and early visual areas of the adult brain that change the sign of the FC from negative to positive; (2) these changes occur even in a partial visual defect condition, though to a lesser extent; and (3) these changes presumably depend on the topography of the functionally deprived areas.

Differences in Broca's area functional connectivity to extrastriate areas in the three groups

RP blind subjects also exhibited increased FC between Broca's area and a set of extrastriate regions as compared to both RP tunnel vision and sighted subjects (see Fig. 3, Table 2) but not with the lateral occipital regions. Most of these regions have been identified in verb generation tasks on the late blind (Burton et al., 2002a, 2003). It was suggested that multisensory regions transfer language functions to tactile or auditory stimuli. Our results challenge this explanation for two main reasons: (1) we did not find any significant functional connectivity changes between Broca's area and these regions in Braille as compared to non-Braille readers (see Supplementary Table S2); (2) we did not find any significant difference in functional connectivity between the auditory and extrastriate visual areas across groups, as would be expected according to the auditory cross-modality hypothesis (Burton et al., 2002a).

These extrastriate visual areas have also been identified in verbal and semantic retrieval task studies in the congenitally blind (Amedi et al., 2003; Azulay et al., 2009; Noppeney et al., 2003; Raz et al., 2005). Hence increased FC between Broca's area and these extrastriate regions may reflect the lifting of inhibition of the visual association cortex to process verbal memory and semantic information. Nevertheless, the specific differences between the functional connectivity of these regions in RP blind compared to the RP tunnel vision subjects support the idea that complete vision loss is required for such changes to occur.

Preserved functional connectivity between Broca's area and the rest of the brain in the three groups

In all three groups, we identified regions that are regularly activated in functional language tasks and also belong to several intrinsically connected networks such as the language network (Bookheimer, 2002; Hagoort, 2005; Hampson et al., 2002; Johnson and Ojemann, 2000; Price, 2010; Yetkin et al., 1995) and the executive control network (Doucet et al., 2011; Spreng et al., 2010; Sundermann and Pfeleiderer, 2012; Vincent et al., 2008). These findings suggest that functional connectivity is useful in delineating networks for a given function, including language, and may imply that beyond the changes between Broca's and visual areas, the rest of the network is well preserved in cases of visual deprivation.

No sensitive period for the development of cross-modal plasticity at least as reflected by the rs-fMRI data

The massive changes observed in functional connectivity between language and visual areas in the late blind support the notion that some level of reorganization even in the calcarine sulcus/V1 can occur

in the adult brain. This change in connectivity was gradual and quite dramatic in term of the distance between these areas and the different functions they support. The fact that the tunnel vision subjects exhibited an intermediate pattern reinforces this idea and further suggests that it occurs not only after complete visual deprivation, but also in the context of partial visual loss. These observations strengthen arguments from the field of stroke rehabilitation where musical stimulation (Särkämö et al., 2008) as well as noninvasive stimulation devices (Di Pino et al., 2014) enhanced recovery in aphasia, probably by influencing the way information is processed in alternative networks. Taken together, these data imply that following input loss or damage to a certain network, the adult brain preserves the ability to functionally connect with other networks and to potentially optimize their performance. Nevertheless, the challenge of selecting the appropriate way to harness this functional connectivity for optimal behavioral recovery in such clinical conditions as stroke or visual restoration via retinal prostheses is still to be addressed. It is also not clear whether these changes are compensatory in nature or whether they simply underlie connections in the adult brain and furnish the 'raw material' for task-related compensatory plasticity.

Limitations and methodological considerations

Rs-fMRI is an invaluable sensitive tool to detect changes in brain connectivity (Fox and Greicius, 2010; Guerra-Carrillo et al., 2014; Smith et al., 2009). However, it should be mentioned that this method is subject to reliability problems induced by movement (a main confound) but also by mind wandering, or wakefulness state (Caceres et al., 2009; Tagliazucchi et al., 2012; van Dijk et al., 2012). This is why we took extra measures in order to control for head movement and verify that there was no significant difference in head movements between the groups. In our study, this method allowed us to delineate regions that are classically activated in functional language tasks and also belong to the intrinsic language network (Bookheimer, 2002; Hagoort, 2005; Hampson et al., 2002; Johnson and Ojemann, 2000; Price, 2010; Yetkin et al., 1995) supporting that our analysis is valid. Moreover, it allowed the identification of specific functional connectivity between Broca's area and V1. This result points toward probable plastic changes induced by visual loss. However, our approach does not allow a direct inference about the role of the increased FC between Broca's area and V1. Other approaches, such as language task-based fMRI (Burton et al., 2002a, 2003; Bedny et al., 2011, 2012) or transcranial magnetic resonance (Amedi et al., 2003) could provide complementary data to accurately establish the origin and the influence of this connectivity on processes that involve Broca's area. It should be noted that the limited availability of such relatively rare homogenous blind and tunnel vision subjects prevented us from extending the protocol to include these behavioral tasks or other interesting experiments such as retinotopy, at least not in this point of time. For instance, a retinotopy experiment in RP tunnel vision subjects would allow us to design seeds of different portions of V1 (i.e. underlying the projections of normal central and deprived peripheral visual field) and give an insight on the cross-modal FC changes occurring in their brain.

We should also specify that information on disease onset is lacking and therefore was not used as a covariate in our analysis. Indeed, in clinical practice, it is very hard to define the onset of RP because of fading and filling-in processes that could hide scotoma for years after the disease onset (see Pessoa and De Weerd, 2003).

As previously described in the discussion, several studies support that negative FC reflect a physiological neuronal processing (Behzadi et al., 2007; Chai et al., 2014; Fox et al., 2005; Guerra-Carrillo et al., 2014; Logothetis et al., 2009; Shmuel et al., 2002, 2006; Shulman et al., 1997; Zeharia et al., 2012) and may even have a role in cases of mental disorders (Whitfield-Gabrieli and Ford, 2012). Nevertheless, the interpretation of the negative correlation is subject to debate (Buckner et al., 2013). Indeed, several noise removal methods such as global signal regressions are believed to introduce false negative

correlations (see [Murphy et al., 2009](#)). These preprocessing methods were not used in our study, which give us some confidence in the data interpretation. Additionally, note that we did not record breathing or pulse during the scan but that their frequencies were regressed out by the bandpass filtering preprocessing step.

Conclusion

The findings presented here showed increased functional connectivity between language and visual areas, which strengthened with the progression of RP from tunnel vision to complete blindness. The data suggest that the changes observed between the language and the visual areas depend on the topography of the functionally deprived regions. These results contribute to the debate on claims concerning a sensitive period for the development of cross-modal mechanisms between language and visual areas, at least in the context of large-scale functional connectivity patterns between areas.

Future studies could address (1) the functional recruitment of foveal V1 for language processing in central visual deficits (e.g. in age macular degeneration and Stargardt disease), (2) the behavioral counterparts of the functional connectivity changes observed in the present study, and their applicability to visual restoration (e.g. using retinal prosthesis) and substitution (e.g. using sensory substitution devices) processes (3) the functional connectivity changes of different regions (as seed) of V1 and the rest of the brain across populations.

Supplementary data to this article can be found online at <http://dx.doi.org/10.1016/j.neuroimage.2016.04.056>.

Funding

This work was supported by a French State funding under the auspices of the Agence Nationale de la Recherche (ANR) within the Investissements d'Avenir program (ANR-11-IDEX-0004-02) and by a grant from Humanis. This work was conducted within the framework of the Labex LIFESENSES (ANR-10-LABX-65). This work was also supported by a European Research Council grant (grant number 310809 to AA), the James S. McDonnell Foundation scholar award (grant number 220020284 to AA).

Conflict of interest

Norman Sabbah, None; Colas Nils Authié, None; Nicolae Sanda, None; Saddek Mohand-Said, None; José-Alain Sahel, consultant for Pixium Vision, GenSight Biologics, Sanofi-Fovea, Genesignal; Avinoam B. Safran, None; Christophe Habas, None; Amir Amedi, None.

Acknowledgments

We thank Sami Abboud, Shachar Maidenbaum, Ella Striem-Amit, Ilan Goldberg, Céline Devisme and Anne-Fleur Barfuss who provided valuable input and help on this work.

References

- Amedi, A., Raz, N., Pianka, P., Malach, R., Zohary, E., 2003. Early "visual" cortex activation correlates with superior verbal memory performance in the blind. *Nat. Neurosci.* 6, 758–766. <http://dx.doi.org/10.1038/nn1072>.
- Amedi, A., Floel, A., Knecht, S., Zohary, E., Cohen, L.G., 2004. Transcranial magnetic stimulation of the occipital pole interferes with verbal processing in blind subjects. *Nat. Neurosci.* 7, 1266–1270. <http://dx.doi.org/10.1038/nn1328>.
- Ayton, L.N., Blamey, P.J., Guymer, R.H., Luu, C.D., Nayagam, D.A.X., Sinclair, N.C., Shivdasani, M.N., Yeoh, J., McCombe, M.F., Briggs, R.J., Opie, N.L., Villalobos, J., Dimitrov, P.N., Varsamidis, M., Petoe, M.A., McCarthy, C.D., Walker, J.G., Barnes, N., Burkitt, A.N., Williams, C.E., Shepherd, R.K., Allen, P.J., 2014. First-in-human trial of a novel suprachoroidal retinal prosthesis. *PLoS One* <http://dx.doi.org/10.1371/journal.pone.0115239>.
- Azulay, H., Striem, E., Amedi, A., 2009. Negative BOLD in sensory cortices during verbal memory: a component in generating internal representations? *Brain Topogr.* 21, 221–231. <http://dx.doi.org/10.1007/s10548-009-0089-2>.

- Bavelier, D., Neville, H.J., 2002. Cross-modal plasticity: where and how? *Nat. Rev. Neurosci.* 3, 443–452. <http://dx.doi.org/10.1038/nrn848>.
- Bedny, M., Pascual-Leone, A., Dodel-Feder, D., Fedorenko, E., Saxe, R., 2011. Language processing in the occipital cortex of congenitally blind adults. *Proc. Natl. Acad. Sci. U. S. A.* 108, 4429–4434. <http://dx.doi.org/10.1073/pnas.1014818108>.
- Bedny, M., Pascual-Leone, A., Dravida, S., Saxe, R., 2012. A sensitive period for language in the visual cortex: distinct patterns of plasticity in congenitally versus late blind adults. *Brain Lang.* 122, 162–170. <http://dx.doi.org/10.1016/j.bandl.2011.10.005>.
- Behzadi, Y., Restom, K., Liau, J., Liu, T.T., 2007. A component based noise correction method (CompCor) for BOLD and perfusion based fMRI. *NeuroImage* 37, 90–101. <http://dx.doi.org/10.1016/j.neuroimage.2007.04.042>.
- Bookheimer, S., 2002. Functional MRI of language: new approaches to understanding the cortical organization of semantic processing. *Annu. Rev. Neurosci.* 25, 151–188. <http://dx.doi.org/10.1146/annurev.neuro.25.112701.142946>.
- Buckner, R.L., Krienen, F.M., Yeo, B.T.T., 2013. Opportunities and limitations of intrinsic functional connectivity MRI. *Nat. Neurosci.* 16, 832–837. <http://dx.doi.org/10.1038/nn.3423>.
- Burton, H., Snyder, A., Diamond, J.B., Raichle, M.E., 2002a. Adaptive changes in early and late blind: a fMRI study of verb generation to heard nouns. *J. Neurophysiol.* 88, 3359–3371. <http://dx.doi.org/10.1152/jn.00129.2002>.
- Burton, H., Snyder, A.Z., Conturo, T.E., Akbudak, E., Ollinger, J.M., Raichle, M.E., 2002b. Adaptive changes in early and late blind: a fMRI study of braille reading. *J. Neurophysiol.* 87, 589–607.
- Burton, H., Diamond, J.B., McDermott, K.B., 2003. Dissociating cortical regions activated by semantic and phonological tasks: a fMRI study in blind and sighted people. *J. Neurophysiol.* 90, 1965–1982. <http://dx.doi.org/10.1152/jn.00279.2003>.
- Butt, O.H., Benson, N.C., Datta, R., Aguirre, G.K., 2013. The fine-scale functional correlation of striate cortex in sighted and blind people. *J. Neurosci.* 33, 16209–16219. <http://dx.doi.org/10.1523/JNEUROSCI.0363-13.2013>.
- Caceres, A., Hall, D.L., Zelaya, F.O., Williams, S.C.R., Mehta, M.A., 2009. Measuring fMRI reliability with the intra-class correlation coefficient. *NeuroImage* 45, 758–768. <http://dx.doi.org/10.1016/j.neuroimage.2008.12.035>.
- Chai, X.J., Ofen, N., Gabrieli, J.D.E., Whitfield-Gabrieli, S., 2014. Selective development of anticorrelated networks in the intrinsic functional organization of the human brain. *J. Cogn. Neurosci.* 26, 501–513. http://dx.doi.org/10.1162/jocn_a.00517.
- Cole, D.M., Smith, S.M., Beckmann, C.F., 2010. Advances and pitfalls in the analysis and interpretation of resting-state fMRI data. *Front. Syst. Neurosci.* 4, 8. <http://dx.doi.org/10.3389/fnsys.2010.00008>.
- Cunningham, S.I., Weiland, J.D., Bao, P., Lopez-Jaime, G.R., Tjan, B.S., 2015. Correlation of vision loss with tactile-evoked V1 responses in retinitis pigmentosa. *Vis. Res.* 111, 197–207. <http://dx.doi.org/10.1016/j.visres.2014.10.015>.
- Di Pino, G., Pellegrino, G., Assenza, G., Capone, F., Ferreri, F., Formica, D., Ranieri, F., Tombini, M., Ziemann, U., Rothwell, J.C., Di Lazzaro, V., 2014. Modulation of brain plasticity in stroke: a novel model for neurorehabilitation. *Nat. Rev. Neurol.* <http://dx.doi.org/10.1038/nrneurol.2014.162>.
- Dosenbach, N.U.F., Fair, D.A., Miezin, F.M., Cohen, A.L., Wenger, K.K., Dosenbach, R.A.T., Fox, M.D., Snyder, A.Z., Vincent, J.L., Raichle, M.E., Schlaggar, B.L., Petersen, S.E., 2007. Distinct brain networks for adaptive and stable task control in humans. *Proc. Natl. Acad. Sci. U. S. A.* 104, 11073–11078. <http://dx.doi.org/10.1073/pnas.0704320104>.
- Doucet, G., Naveau, M., Petit, L., Delcroix, N., Zago, L., Crivello, F., Jobard, G., Tzourio-Mazoyer, N., Mazoyer, B., Mellet, E., Joliot, M., 2011. Brain activity at rest: a multiscale hierarchical functional organization. *J. Neurophysiol.* 105, 2753–2763. <http://dx.doi.org/10.1152/jn.00895.2010>.
- Eckert, M.A., Kamdar, N., Chang, C.E., Beckmann, C.F., Greicius, M.D., Menon, V., 2008. A cross-modal system linking primary auditory and visual cortices: evidence from intrinsic fMRI connectivity analysis. *Hum. Brain Mapp.* 29, 848–857. <http://dx.doi.org/10.1002/hbm.20560>.
- Engel, S., Rumelhart, D., Wandell, B., Lee, A., Glover, G., Chichilnisky, E., Shadlen, M., 1994. fMRI of human visual cortex. *Nature* 369, 525. <http://dx.doi.org/10.1038/369525a0>.
- Falchier, A., Clavagnier, S., Barone, P., Kennedy, H., 2002. Anatomical evidence of multi-modal integration in primate striate cortex. *J. Neurosci.* 22, 5749–5759 (doi: 20026562).
- Forman, S.D., Cohen, J.D., Fitzgerald, M., Eddy, W.F., Mintun, M.A., Noll, D.C., 1995. Improved assessment of significant activation in functional magnetic resonance imaging (fMRI): use of a cluster-size threshold. *Magn. Reson. Med.* 33, 636–647.
- Fox, M.D., Greicius, M., 2010. Clinical applications of resting state functional connectivity. *Front. Syst. Neurosci.* 4, 19. <http://dx.doi.org/10.3389/fnsys.2010.00019>.
- Fox, M.D., Snyder, A.Z., Vincent, J.L., Corbetta, M., Van Essen, D.C., Raichle, M.E., 2005. The human brain is intrinsically organized into dynamic, anticorrelated functional networks. *Proc. Natl. Acad. Sci. U. S. A.* 102, 9673–9678. <http://dx.doi.org/10.1073/pnas.0504136102>.
- Friston, K.J., Holmes, A., Worsley, K.J., 1999. How many subjects constitute a study? *NeuroImage* 10, 1–5. <http://dx.doi.org/10.1006/nimg.1999.0439>.
- Goebel, R., Esposito, F., Formisano, E., 2006. Analysis of functional image analysis contest (FIAC) data with brainvoyager QX: from single-subject to cortically aligned group general linear model analysis and self-organizing group independent component analysis. *Hum. Brain Mapp.* 27, 392–401. <http://dx.doi.org/10.1002/hbm.20249>.
- Golland, Y., Bontin, S., Gelbard, H., Benjamini, Y., Heller, R., Nir, Y., Hasson, U., Malach, R., 2007. Extrinsic and intrinsic systems in the posterior cortex of the human brain revealed during natural sensory stimulation. *Cereb. Cortex* 17, 766–777. <http://dx.doi.org/10.1093/cercor/bhk030>.
- Golland, Y., Golland, P., Bontin, S., Malach, R., 2008. Data-driven clustering reveals a fundamental subdivision of the human cortex into two global systems. *Neuropsychologia* 46, 540–553. <http://dx.doi.org/10.1016/j.neuropsychologia.2007.10.003>.
- Greicius, M.D., Krasnow, B., Reiss, A.L., Menon, V., 2003. Functional connectivity in the resting brain: a network analysis of the default mode hypothesis. *Proc. Natl. Acad. Sci. U. S. A.* 100, 253–258. <http://dx.doi.org/10.1073/pnas.0135058100>.

- Guerra-Carrillo, B., Mackey, A.P., Bunge, S.A., 2014. Resting-state fMRI: a window into human brain plasticity. *Neuroscientist* 20, 522–533. <http://dx.doi.org/10.1177/1073858414524442>.
- Hagoort, P., 2005. On Broca, brain, and binding: a new framework. *Trends Cogn. Sci.* 9, 416–423. <http://dx.doi.org/10.1016/j.tics.2005.07.004>.
- Hampson, M., Peterson, B.S., Skudlarski, P., Gatenby, J.C., Gore, J.C., 2002. Detection of functional connectivity using temporal correlations in MR images. *Hum. Brain Mapp.* 15, 247–262. <http://dx.doi.org/10.1002/hbm.10022>.
- Heckenlively, J.T.R., 1988. *Good days, bad days. Retinitis Pigmentosa*. Lippincott, Philadelphia, p. 73.
- Heine, L., Bahri, M.A., Cavaliere, C., Soddu, A., Laureys, S., Ptito, M., Kupers, R., 2015. Prevalence of increases in functional connectivity in visual, somatosensory and language areas in congenital blindness. *Front. Neuroanat.* 9. <http://dx.doi.org/10.3389/fnana.2015.00086>.
- Hertz, U., Amedi, A., 2010. Disentangling unisensory and multisensory components in audiovisual integration using a novel multifrequency fMRI spectral analysis. *NeuroImage* 52, 617–632. <http://dx.doi.org/10.1016/j.neuroimage.2010.04.186>.
- Hodge, M.R., Horton, W., Brown, T., Herrick, R., Olsen, T., Hileman, M.E., McKay, M., Archie, K.a., Cler, E., Harms, M.P., Burgess, G.C., Glasser, M.F., Elam, J.S., Curtiss, S.W., Barch, D.M., Oostenveld, R., Larson-Prior, L.J., Ugurbil, K., Van Essen, D.C., Marcus, D.S., 2015. ConnectomeDB—sharing human brain connectivity data. *NeuroImage* <http://dx.doi.org/10.1016/j.neuroimage.2015.04.046>.
- Johnson, M.D., Ojemann, G.A., 2000. The role of the human thalamus in language and memory: evidence from electrophysiological studies. *Brain Cogn.* 42, 218–230. <http://dx.doi.org/10.1006/brcg.1999.1101>.
- Kalloniatis, M., Fletcher, E.L., 2004. *Retinitis pigmentosa: understanding the clinical presentation, mechanisms and treatment options*. *Clin. Exp. Optom.* 87, 65–80.
- Lee, D.S., Lee, J.S., Oh, S.H., Kim, S.K., Kim, J.W., Chung, J.K., Lee, M.C., Kim, C.S., 2001. Cross-modal plasticity and cochlear implants. *Nature* 409, 149–150. <http://dx.doi.org/10.1038/35051653>.
- Li, J., Liu, Y., Qin, W., Jiang, J., Qiu, Z., Xu, J., Yu, C., Jiang, T., 2013. Age of onset of blindness affects brain anatomical networks constructed using diffusion tensor tractography. *Cereb. Cortex* 23, 542–551. <http://dx.doi.org/10.1093/cercor/bhs034>.
- Liu, Y., Yu, C., Liang, M., Li, J., Tian, L., Zhou, Y., Qin, W., Li, K., Jiang, T., 2007. Whole brain functional connectivity in the early blind. *Brain* 130, 2085–2096. <http://dx.doi.org/10.1093/brain/awm121>.
- Logothetis, N.K., Murayama, Y., Augath, M., Steffen, T., Werner, J., Oeltermann, A., 2009. How not to study spontaneous activity. *NeuroImage* 45, 1080–1089. <http://dx.doi.org/10.1016/j.neuroimage.2009.01.010>.
- Masuda, Y., Horiguchi, H., Dumoulin, S.O., Furuta, A., Miyauchi, S., Nakadomari, S., Wandell, B.A., 2010. Task-dependent V1 responses in human retinitis pigmentosa. *Invest. Ophthalmol. Vis. Sci.* 51, 5356–5364. <http://dx.doi.org/10.1167/jovs.09-4775>.
- Murphy, K., Birn, R.M., Handwerker, D.A., Jones, T.B., Bandettini, P.A., 2009. The impact of global signal regression on resting state correlations: are anti-correlated networks introduced? *NeuroImage* 44, 893–905. <http://dx.doi.org/10.1016/j.neuroimage.2008.09.036>.
- Noppeney, U., Friston, K.J., Price, C.J., 2003. Effects of visual deprivation on the organization of the semantic system. *Brain* 126, 1620–1627. <http://dx.doi.org/10.1093/brain/awg152>.
- Pascual-Leone, A., Amedi, A., Fregni, F., Merabet, L.B., 2005. The plastic human brain cortex. *Annu. Rev. Neurosci.* 28, 377–401. <http://dx.doi.org/10.1146/annurev.neuro.27.070203.144216>.
- Pessoa, L., De Weerd, P. (Eds.), 2003. *Filling-in: From Perceptual Completion to Cortical Reorganization*. Oxford University Press, p. 98 (Chapter 5).
- Price, C.J., 2010. The anatomy of language: a review of 100 fMRI studies published in 2009. *Ann. N. Y. Acad. Sci.* 1191, 62–88. <http://dx.doi.org/10.1111/j.1749-6632.2010.05444.x>.
- Raichle, M.E., MacLeod, A.M., Snyder, A.Z., Powers, W.J., Gusnard, D.A., Shulman, G.L., 2001. A default mode of brain function. *Proc. Natl. Acad. Sci. U. S. A.* 98, 676–682. <http://dx.doi.org/10.1073/pnas.98.2.676>.
- Raz, N., Amedi, A., Zohary, E., 2005. V1 activation in congenitally blind humans is associated with episodic retrieval. *Cereb. Cortex* 15, 1459–1468. <http://dx.doi.org/10.1093/cercor/bhi026>.
- Reislev, N.L., Dyrby, T.B., Siebner, H.R., Kupers, R., Ptito, M., 2016. Simultaneous assessment of white matter changes in microstructure and connectedness in the blind brain. *Neural Plast.* 2016, 6029241. <http://dx.doi.org/10.1155/2016/6029241>.
- Sadato, N., Okada, T., Honda, M., Yonekura, Y., 2002. Critical period for cross-modal plasticity in blind humans: a functional MRI study. *NeuroImage* 16, 389–400. <http://dx.doi.org/10.1006/nimg.2002.1111>.
- Särkämö, T., Tervaniemi, M., Laitinen, S., Forsblom, A., Soinila, S., Mikkonen, M., Autti, T., Silvennoinen, H.M., Erkkilä, J., Laine, M., Peretz, I., Hietanen, M., 2008. Music listening enhances cognitive recovery and mood after middle cerebral artery stroke. *Brain* 131, 866–876. <http://dx.doi.org/10.1093/brain/awn013>.
- Sarubbo, S., De Benedictis, A., Maldonado, L.L., Basso, G., Duffau, H., 2013. Frontal terminations for the inferior fronto-occipital fascicle: anatomical dissection, DTI study and functional considerations on a multi-component bundle. *Brain Struct. Funct.* 218, 21–37. <http://dx.doi.org/10.1007/s00429-011-0372-3>.
- Sereno, M.I., Dale, A.M., Reppas, J.B., Kwong, K.K., Belliveau, J.W., Brady, T.J., Rosen, B.R., Tootell, R.B., 1995. Borders of multiple visual areas in humans revealed by functional magnetic resonance imaging. *Science* 268, 889–893.
- Shmuel, A., Yacoub, E., Pfeuffer, J., Van de Moortele, P.-F., Adriany, G., Hu, X., Ugurbil, K., 2002. Sustained negative BOLD, blood flow and oxygen consumption response and its coupling to the positive response in the human brain. *Neuron* 36, 1195–1210. [http://dx.doi.org/10.1016/S0896-6273\(02\)01061-9](http://dx.doi.org/10.1016/S0896-6273(02)01061-9).
- Shmuel, A., Augath, M., Oeltermann, A., Logothetis, N.K., 2006. Negative functional MRI response correlates with decreases in neuronal activity in monkey visual area V1. *Nat. Neurosci.* 9, 569–577. <http://dx.doi.org/10.1038/nn1675>.
- Shu, N., Liu, Y., Li, J., Li, Y., Yu, C., Jiang, T., 2009. Altered anatomical network in early blindness revealed by diffusion tensor tractography. *PLoS One* 4, 1–13. <http://dx.doi.org/10.1371/journal.pone.0007228>.
- Shulman, G.L., Fiez, J.a., Corbetta, M., Buckner, R.L., Miezin, F.M., Raichle, M.E., Petersen, S.E., 1997. Common blood flow changes across visual tasks: II. Decreases in cerebral cortex. *J. Cogn. Neurosci.* 9, 648–663. <http://dx.doi.org/10.1162/jocn.1997.9.5.648>.
- Smith, S.M., Fox, P.T., Miller, K.L., Glahn, D.C., Fox, P.M., Mackay, C.E., Filippini, N., Watkins, K.E., Toro, R., Laird, A.R., Beckmann, C.F., 2009. Correspondence of the brain's functional architecture during activation and rest. *Proc. Natl. Acad. Sci. U. S. A.* 106, 13040–13045. <http://dx.doi.org/10.1073/pnas.0905267106>.
- Spreng, R.N., Stevens, W.D., Chamberlain, J.P., Gilmore, A.W., Schacter, D.L., 2010. Default network activity, coupled with the frontoparietal control network, supports goal-directed cognition. *NeuroImage* 53, 303–317. <http://dx.doi.org/10.1016/j.neuroimage.2010.06.016>.
- Stingl, K., Bartz-Schmidt, K.U., Besch, D., Braun, A., Bruckmann, A., Gekeler, F., Greppmaier, U., Hipp, S., Hörtldörfer, G., Kernstock, C., Koitschev, A., Kusnyerik, A., Sachs, H., Schatz, A., Stingl, K.T., Peters, T., Wilhelm, B., Zrenner, E., 2013. Artificial vision with wirelessly powered subretinal electronic implant alpha-IMS. *Proc. Biol. Sci.* 280, 20130077. <http://dx.doi.org/10.1098/rspb.2013.0077>.
- Striem-Amit, E., Bubic, A., Amedi, A., 2011a. Mechanisms underlying plastic changes and rehabilitation following sensory loss in blindness and deafness. *The Neural Bases of Multisensory Processes*, pp. 395–422.
- Striem-Amit, E., Hertz, U., Amedi, A., 2011b. Extensive cochleotopic mapping of human auditory cortical fields obtained with phase-encoding fMRI. *PLoS One* 6, e17832. <http://dx.doi.org/10.1371/journal.pone.0017832>.
- Striem-Amit, E., Ovadia-Caro, S., Caramazza, A., Margulies, D.S., Villringer, A., Amedi, A., 2015. Functional connectivity of visual cortex in the blind follows retinotopic organization principles. *Brain* 138, 1679–1695. <http://dx.doi.org/10.1093/brain/awv083>.
- Sundermann, B., Pfeleiderer, B., 2012. Functional connectivity profile of the human inferior frontal junction: involvement in a cognitive control network. *BMC Neurosci.* 13, 119. <http://dx.doi.org/10.1186/1471-2202-13-119>.
- Tagliazucchi, E., Wegner, F.V., Morzelewski, A., Brodbeck, V., Laufs, H., von Wegner, F., Morzelewski, A., Brodbeck, V., Laufs, H., 2012. Dynamic BOLD functional connectivity in humans and its electrophysiological correlates. *Front. Hum. Neurosci.* 6, 339. <http://dx.doi.org/10.3389/fnhum.2012.00339>.
- Talairach, J., Tournoux, P., 1988. *Co-planar stereotaxic atlas of the human brain. 3-dimensional Proportional System: An Approach to Cerebral Imaging*. Thieme, New York.
- van Dijk, K.R.A., Sabuncu, M.R., Buckner, R.L., 2012. The influence of head motion on intrinsic functional connectivity MRI. *NeuroImage* 59, 431–438. <http://dx.doi.org/10.1016/j.neuroimage.2011.07.044>.
- Vincent, J.L., Kahn, I., Snyder, A.Z., Raichle, M.E., Buckner, R.L., 2008. Evidence for a frontoparietal control system revealed by intrinsic functional connectivity. *J. Neurophysiol.* 100, 3328–3342. <http://dx.doi.org/10.1152/jn.90355.2008>.
- Wandell, B.A., Smirnakis, S.M., 2009. Plasticity and stability of visual field maps in adult primary visual cortex. *Nat. Rev. Neurosci.* 10, 873–884. <http://dx.doi.org/10.1038/nrn2741>.
- Wandell, B.A., Winawer, J., 2011. Imaging retinotopic maps in the human brain. *Vis. Res.* 51, 718–737. <http://dx.doi.org/10.1016/j.visres.2010.08.004>.
- Wandell, B.A., Dumoulin, S.O., Brewer, A.A., 2007. Visual field maps in human cortex. *Neuron* 56, 366–383. <http://dx.doi.org/10.1016/j.neuron.2007.10.012>.
- Watkins, K.E., Cowey, A., Alexander, I., Filippini, N., Kennedy, J.M., Smith, S.M., Ragge, N., Bridge, H., 2012. Language networks in anophthalmia: maintained hierarchy of processing in “visual” cortex. *Brain* 135, 1566–1577. <http://dx.doi.org/10.1093/brain/aww067>.
- Weiland, J.D., Humayun, M.S., 2014. Retinal prosthesis. *IEEE Trans. Biomed. Eng.* 61, 1412–1424. <http://dx.doi.org/10.1109/TBME.2014.2314733>.
- Whitfield-Gabrieli, S., Ford, J.M., 2012. Default mode network activity and connectivity in psychopathology. *Annu. Rev. Clin. Psychol.* 8, 49–76. <http://dx.doi.org/10.1146/annurev-clinpsy-032511-143049>.
- Yetkin, F.Z., Hammelke, T.A., Swanson, S.J., Morris, G.L., Mueller, W.M., McAuliffe, T.L., Houghton, V.M., 1995. A comparison of functional MR activation patterns during silent and audible language tasks. *AJNR Am. J. Neuroradiol.* 16, 1087–1092.
- Zeharia, N., Hertz, U., Flash, T., Amedi, A., 2012. Negative blood oxygenation level dependent homunculus and somatotopic information in primary motor cortex and supplementary motor area. *Proc. Natl. Acad. Sci.* 109, 18565–18570. <http://dx.doi.org/10.1073/pnas.1119125109>.